Heinrich Heine
Universität Düsseldorf

Influence of HCV on the expression of intercellular communication signals by the host cell

Inaugural-Dissertation

Zur Erlangung des Doktorgrades der Mathematisch-Naturwissenschaftlichen Fakultät der Heinrich-Heine-Universität Düsseldorf

vorgelegt von

Kerstin Hermine Rufinatscha

aus Meran

Düsseldorf, Januar 2021

Aus der Klinik für Gastroenterologie, Hepatologie und Infektiologie
des Universitätsklinikums der Heinrich-Heine-Universität Düsseldorf

Gedruckt mit der Genehmigung der
Mathematisch-Naturwissenschaftlichen Fakultät der
Heinrich-Heine-Universität Düsseldorf

Berichterstatter:

1. Prof. Dr. Johannes G. Bode
2. Prof. Dr. Dieter Willbold

Tag der mündlichen Prüfung: 01.06.2021

Parts of this work have been published:

As part of the following publication:

Gröpper C*, **Rufinatscha K***, Schröder N*, Stindt S, Ehlting C, Albrecht U, Bock HH, Bartenschlager R, Häussinger D, Bode JG. HCV modifies EGF signalling and upregulates production of CXCR2 ligands: Role in inflammation and antiviral immune response. *J Hepatol.* 2018 Sep;69(3):594-602. doi: 10.1016/j.jhep.2018.04.005. Epub 2018 Apr 27.
***co-shared first authorship.**

Contribution: performance of experiments (Fig. Number thesis corresponds to Figure Nr. publication: Fig. 11A+B corresponds to Fig. S3 A+B; Fig. 12 corresponds to S7; Fig. 13 corresponds to Fig. S5; Fig. 14 corresponds to Fig. S4; Fig. 15D corresponds to 3H; Fig. 15E corresponds to Fig. 3J Fig. 16A corresponds to Fig. 3E; Fig. 17A corresponds to Fig. 3F; Fig. 17D corresponds to Fig. 3G), analysis and interpretation of data, proofreading of manuscript

As Abstracts at conferences:

HCV triggers the release of CXCR2 ligands via an EGF-driven circuit, **Kerstin Rufinatscha**, Christina Gröpper, Nadja Triller, Sabine Stindt, Christian Ehlting, Dieter Häussinger, Johannes Bode, deliver, Düsseldorf, 09/17, oral presenation

Hepatitis C Virus mediates induction of CXC chemokine expression in response to the inflammatory cytokines TNFα and IL-1β, **Kerstin Rufinatscha**, Christina Gröpper, Nadja Triller, Sabine Stindt, Christian Ehlting, Dieter Häussinger, Johannes Bode, German Association of the Study of the Liver (GASL), Hamburg, 01/2018, poster presentation

The Hepatitis C Virus modifies CXC chemokine expression induced by the inflammatory cytokines TNFα and IL-1β, **Kerstin Rufinatscha**, Sabine Stindt, Christian Ehlting, Dieter Häussinger, Johannes Bode, Signal Transduction Society (STS), Weimar, 11/2018, oral presentation

The influence of Hepatitis C Virus on the induction of CXC chemokine expression in response to the inflammatory cytokines TNFα and IL-1β, **Kerstin Rufinatscha**, Sabine Stindt, Jochen Dobner, Christian Ehlting, Dieter Häussinger, Johannes Bode, Falk Symposium, Heidelberg 02/2019, poster presentation

CXCR2 chemokine expression is influenced by the inflammatory cytokines TNFα and IL-1β during HCV infection, **Kerstin Rufinatscha**, Sabine Stindt, Jochen Dobner, Christian Ehlting, Dieter Häussinger, Johannes Bode, German Association of the Study of the Liver (GASL), Heidelberg, 02/2019, poster presentation

The Hepatitis C Virus induces CXC chemokine expression in response to the inflammatory cytokines TNFα and Il1β, **Kerstin Rufinatscha**, Sabine Stindt, Christian Ehlting, Jochen Dobner, Dieter Häussinger, Johannes Bode, Gesellschaft für Virologie (GfV), Düsseldorf, 03/2019, poster presenation

The Hepatitis C Virus influences CXC chemokine expression of infected host cells in response to Il1β, **Kerstin Rufinatscha**, Sabine Stindt, Jochen Dobner, Christian Ehlting, Dieter Häussinger, Johannes Bode, German Association of the Study of the Liver (GASL), Mainz, 02/2020, poster presenation

Content

List of figures

List of tables

List of abbreviations

+*ss*RNA	Positive-sense single-stranded RNA
A	Alanine
AKT	Protein kinase B
AP1	Activator protein 1
ApoE	Apolipoprotein E
ATF	Activating transcription factor
BSA	Bovine serum albumin
C	Cysteine
C/EBPβ	CCAAT/enhancer-binding protein
CARDIF	CARD adaptor inducing IFNβ
ChIP	Chromatin Immunoprecipitation
CLDN1	Claudin 1
CREB	cAMP response element-binding protein
CRISPR	Clustered regularly interspaced short palindromic repeats
CTL	Cytotoxic T lymphocyte
DD	Death domain
DMSO	Dimethyl sulfoxide
DNA	Desoxyribonucleic acid
DR	Death receptor
DSBs	Double strand breaks
ECMV	*Encephalomyocarditis virus*
EGF	Epidermal growth factor
EGFR	Epidermal growth factor receptor
ELISA	Enzyme linked immunosorbent assay
EphA2	Ephrin receptor A2
EPR	Epiregulin
ER	Endoplasmic reticulum
ERK	Extracellular signal-regulated kinase
FBS	Fetal bovine serum
GAB1	GRB2-associated binding protein 1
gag	Group specific antigens
GAGs	Glycosaminoglycans
GPCR	G-protein coupled receptors
GRB2	Growth factor receptor-bound protein 2
GT	Genotype
HB-EGF	Heparin-binding EGF-like growth factor
HCC	Hepatocellular carcinoma
HCV	*Hepatitis C Virus*
HCV_{cc}	Cell culture-derived HCV particle system

HCV_{pp}	HCV pseudoparticle system
HCV_{TCP}	Trans-complemented particle system
HeLA	Henrietta Lacks
HIV	*Human immunodeficiency virus*
HRP	Horse radish peroxidase
HSPGs	Heparan sulfate proteoglycan
IFN	Interferon
IKK	IκB kinase
IL	Interleukin
IL1R1	IL-1 receptor type 1
IRAK	IL-1 receptor-associated kinase
iRES	Internal ribosomal entry site
IRF	Interferon regulatory factor
JFH1	Japanese fulminant hepatitis 1
JNK	c-JUN N-terminal kinase
kb	Kilobases
LDL	Low density lipoprotein
LDLR	LDL receptor
LPS	Lipopolysaccharide
LUBAC	Linear ubiquitin chain assembly complex
LVPs	Lipoviroparticles
MAPK	Mitogen-activated protein kinase
MAVS	Mitochondrial antiviral signalling protein
MKK	MAPK kinase
MKKK	MAPK kinase kinase
MLV	*Murine leukaemia virus*
MYD88	Myeloid differentiation primary response gene 88
mRNA	*Messenger* RNA
mTNFα	Transmembrane tethered TNFα
NEAA	Non-essential-amino-acids
NFκB	Nuclear Factor κ-light chain enhancer of B-cells
NLRs	NOD-like receptors
NLRP3	NOD-like receptor family pyrin domain containing 3
NPC1L1	Niemann-Pick C1-like 1
NRG	Neuregulin
NS	Non-structural
ORF	Open reading frame
PCR	Polymerase chain reaction
PDK1	Phosphoinositide-dependent kinase 1
PEG-IFNα	Pegylated-IFNα
PI3K	Phosphatidylinositol-3 kinase

PIP	Phosphatidylinositol phosphate
PI_4KA	PI_4 kinase IIIα
PLCγ	Phospholipase C γ
pol	Polymerase
PPARγ	Peroxisome proliferator-activated receptor γ
PRR	Pattern recognition receptor
PtdIns	Phosphatidylinositol
PTEN	Phosphatase and tensin homolog
qRT-PCR	Quantitative real time PCR
RdRp	RNA-dependent RNA polymerase
RelA or p65	reticuloendotheliosis viral oncogene homolog A
RIG-I	Retinoic acid-inducible gene-I
RIPK1	Receptor-interacting protein kinase 1
RNA	Ribonucleic acid
ROS	Reactive oxygen species
rT	Reverse transcriptase
RT	Room temperature
S	Serine
SEM	Standard error of means
SH2	Src homology 2
SHC1	Src homology 2 domain containing transforming protein 1
siRNA	Small interfering RNA
SP	Specificity protein
SR-B1	Scavenger receptors class B type 1
*ss*RNA	Single-stranded RNA
sTNFα	Soluble TNFα
SV40	*Simian virus 40*
SVR	Sustained virologic response
T	Threonine
TAB	TGFβ-activated protein kinase-binding protein
TAK	Transforming growth factor β-activated kinase
TBS-T	Tris-buffered saline with Tween
TCPTP	T-cell protein tyrosine phosphatase
TGF	Transforming growth factor
TIR	Toll/Interleukin-1 receptor
TLR	Toll-like receptor
Tm	Melting temperature
TNF	Tumour necrosis factor α
TNFR	TNF receptor
TRADD	TNFR1-associated death domain
TRAF	Tumour necrosis factor-associated factor

TRIF	TIR domain-containing adapter-inducing IFNβ
UBC13	Ubiquitin-conjugating enzyme E2 N
UTR	Untranslated region
WHO	World health organisation
Y	Tyrosine

1 Introduction

1.1 *Hepatitis C Virus*

1.1.1 *Hepatitis C Virus*

According to the world health organisation (WHO), approximately 71 million people, meaning 1 % of the total world population, are currently chronically infected with the *hepatitis C virus* (HCV). In 2016, 399 000 people suffering from the consequences of a chronic HCV infection died (1). HCV has evolved several strategies to persist in the body, despite of ongoing replication without being cleared by the immune system over decades, even though the innate immune system is activated vigorously. HCV infection leads in 70-80% of infected people to a lifelong chronic infection (2). A chronic infection can result in mild inflammation or develop into severe inflammation of the liver. This inflammation can then lead to fibrosis and finally to cirrhosis or hepatocellular carcinoma (HCC) (3). One in four cases of liver cancer is attributed to HCV, rendering it the only known oncogenic positive stranded RNA virus today. Besides HCV, there are so far only six other viruses known which are oncogenic (4). After a decade of research regarding the formerly termed non-A non-B hepatitis agents, or as agents causing hepatitis, HCV has been described as such for the first time in 1989 from Choo and colleagues. They could demonstrate that HCV is a RNA virus, consisting of at least 10 000 nucleotides (5). In the 1990s it was confirmed that the genome of HCV is around 10 kilobases (kb) long. Additionally, it was established that HCV is a positive-sense single-stranded RNA (+*ss*RNA) virus with sequence similarities and some homologies to *Flaviviruses* and *Pestiviruses* (6). HCV was therefore classified as a *Flaviviridae* family member and was the first member of a new genus: *Hepacivirus*. The family *Flaviviridae* consists of four different genera termed: *Flavivirus*, *Pestivirus*, *Hepacivirus* and *Pegivirus*, containing 60 different species in total (7, 8). They all have in common that they are *ss*RNA viruses with a genome range of 9 to 13 kb, they replicate in vesicles derived from the endoplasmic reticulum (ER) in the cytoplasm, and are enveloped as 40 to 60 nm virions with a single core protein and two or three envelope proteins (9). Today, 14 different viruses belong to the genus *Hepacivirus* and the best categorized among them is HCV (10). Eight different genotypes (GTs) of HCV have been reported that differ from each other by 32-35% in nucleotide sequence. The different GTs can be divided into several subgenotypes that differ from each other by 20-25% in nucleotide sequence (11-13). Distribution of GTs is epidemiologically distinct. GT1 is the most common HCV GT worldwide and also the most widely distributed in Germany (14).

1.1.2 Viral proteins

HCV contains a 9.6 kb positive-strand RNA genome composed of a 5´ and a 3´ untranslated region (UTR), four structural proteins (core, E1, E2, p7) and five non-structural (NS) proteins (NS2, NS3/4A, NS4B, NS5A and the RNA-dependent RNA polymerase (RdRp) NS5B) (15). The genome consists of one large open reading frame (ORF) encoding one polyprotein (16) (Fig. 1). The 5`and 3` UTRs are highly structured RNA sequences which are essential for replication and RNA translation (15). The core protein forms the viral nucleocapsid and terminates with E1. E1 is cleaved from core via signal-peptide (SP) peptidase. Recent studies showed that SP-cleavage is dispensable for HCV budding but is required for infectivity and virus-particle secretion (17, 18). Interestingly, however, there is no accumulation of virus particles in the cell, which indicates that the number of newly formed viral particles is determined before they are secreted. The exact mechanisms are not yet known (18).

The core protein has been described to have an impact on host cellular functions by engaging several interactions with host proteins (19-22). It was reported to downregulate insulin-receptor substrate 1 protein levels via downregulation of peroxisome proliferator-activated receptor γ (PPARγ) (23). In another study, Wu *et al.* could show that phosphatase and tensin homolog (PTEN) interacts with the viral core protein. It binds to the R50 domain I of HCV core protein and inhibits HCV replication (24). Contrarily, it was demonstrated that PTEN is downregulated by HCV core protein on both messenger RNA (mRNA) expression and protein level (25, 26). Additionally, evidence was provided that protein kinase B (AKT) and nuclear Factor κ-light chain enhancer of B-cells (NFκB) are both activated in response to PTEN downregulation via HCV core protein (26).

The two envelope proteins E1 and E2 seem to have different roles during viral entry and assembly. They interact with each other and are both involved in the attachment of the virus to different receptors, in fusion processes and in viral assembly. They can interact with claudin 1 (CLDN1) as E1/E2 heterodimer, but the exact mechanism remains unclear (27). Furthermore, E1 binds apolipoprotein E (ApoE) and ApoB, which is critical for HCV cell entry (28). It was shown that the back layer domain, a specific domain of E2, induces conformational changes of E1 and thus enables the HCV membrane to fuse with the cellular membrane (29, 30).

The structural viral protein p7 can form an ion channel and is thus classified as viroporin. It acts during assembly, envelopment and secretion of viral proteins but is dispensable for replication. It modulates the formation of complexes between NS2, E2, NS3 and NS5A, allowing regulation of assembly events (31). Furthermore, it regulates the localization of the core protein at lipid droplets in anterograde direction, it modulates the envelopment of viral

particles and regulates the pH to guarantee the protection and secretion of infectious particles (31).

NS2 has cysteine protease activity responsible for NS2/3 cleavage. Hence, it separates itself from NS3 via cleavage and reaches then full function. Additionally, it was reported to be crucial for viral assembly (32).

The NS3/4A complex is a S protease that cleaves C-(S/A) peptide bonds, exhibits both helicase and protease activity and is responsible for processing the non-structural part of the polyprotein. The interaction between NS3 with NS4A was already demonstrated in the early 1990s. Here, NS4A is the activating subunit, while NS3 is the catalytic subunit (33-35). NS3/4A not only cleaves viral proteins, but it also cleaves several host proteins and intervenes in the host immune reaction (36). By disruption of the retinoic acid-inducible gene-I (RIG-I) signalling via proteolytic cleavage of CARD adaptor-inducing interferon (IFN) β/mitochondrial antiviral signalling protein (CARDIF/MAVS), it blocks the cellular IFN response to exogenous double-stranded RNA (37). Furthermore, NS3/4A cleaves the adaptor molecule Toll/Interleukin-1 receptor (TIR) domain-containing adaptor-inducing IFNβ (TRIF) and disrupts Toll-like receptor (TLR) 3 signalling (37). In addition, other host cell proteins, such as the T-cell protein tyrosine phosphatase (TCPTP) are cleaved by NS3/4A, resulting in activity enhancement of epidermal growth factor (EGF) receptor (EGFR) by phosphorylation (36).

NS4B is essential for the formation of the so-called “membranous web” in which the virus replicates (38). Both NS4B and NS5A are essential for viral replication and assembly (39).

NS5A can be phosphorylated to form two different isoforms, by basal phosphorylation (p65) or by hyperphosphorylation (p58). The two forms have different molecular masses (40, 41). NS4B is required for NS5A phosphorylation (42). When NS5A is phosphorylated, it switches from replication to assembly activity by stabilization of NS2 in dotted structures (43). At its amino terminus it contains an amphipathic α-helix which shows membrane association (44, 45). The further structure consists of three domains (46, 47).

NS5B represents the RdRp (48, 49) and exhibits RdRp activity even in the absence of other HCV specific viral proteins. It does not preferentially bind to the HCV 3`-end sequence when also other RNAs are present, which shows that the HCV RdRp not only catalyses synthesis of HCV-specific RNA (50, 51). In collaboration with other viral and host proteins NS5B synthesizes a negative strand of RNA. As other RdRps the catalytically active domain of NS5B contains the subdomains “fingers”, “palm” and “thumb” (52). The RdRp catalyses RNA via *de novo synthesis* of a single-stranded template as well as by primer extension from RNA duplexes or from a pre-annealed template (53, 54).

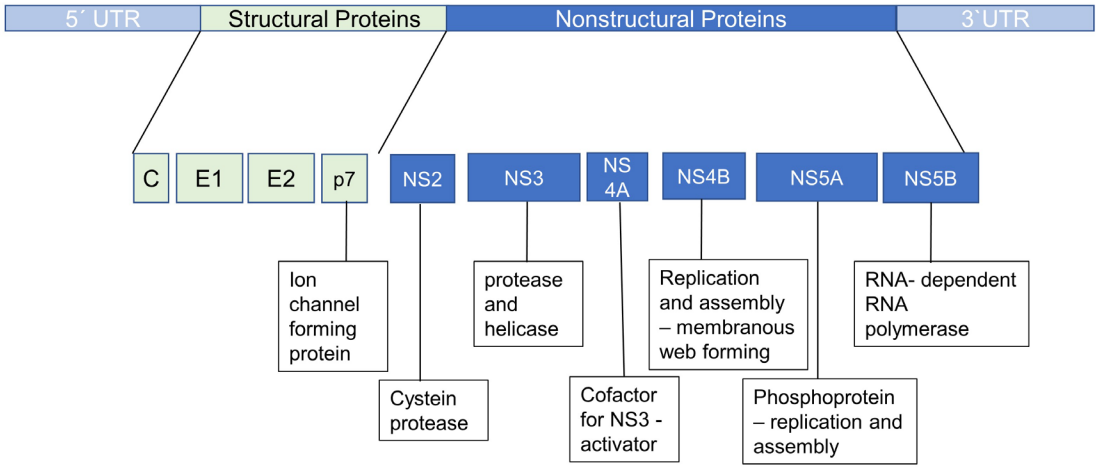

Fig. 1- Schematic depiction of the different HCV proteins. C = Core, E1 = Envelope 1, E2 = Envelope 2 and p7 are cleaved by host signal-peptide peptidases and belong to the structural components of the virus. The viral non-structural proteins NS2-NS5B are cleaved after processing from the viral proteins NS2/3 and NS3/4A itself. Modified according to Ashfaq, An overview of HCV molecular biology, replication and immune response, Virol J. , 20011 Apr 11;8:161 (55).

1.1.3 HCV - therapeutic aspects

Before the 1990s no treatment was available for HCV infection (56). Afterwards, interferon α (IFNα)-based regimens were the standard treatment for many years. The treatment had significant limitations, the efficacy was extremely low, dependent on the GT of the virus, and in many cases the therapy did not achieve eradication. Besides that, there were several side effects noticed (57).

In 1998 it was demonstrated that a treatment with pegylated-IFNα (PEG-IFNα), which is a long-acting interferon in combination with ribavirin (RBV) could enhance the cure rates, but also this treatment had many limitations similar to IFNα therapy and also the combination with RBV showed low efficacy and eradication of the virus was often not achieved (58). Only 40% of patients infected with HCV GT1 or GT6 could be cured by this treatment. Nevertheless, some advantages over IFNα therapy have been reported e. g. the sustained virologic response (SVR) was much higher in some GTs than before and the tolerability was enhanced, since the treatment was given only once a weak instead of three times (56). Due to the lack of other treatments, PEG-IFNα in combination with RBV remained the standard therapy until 2011.

In 2011, directed antiviral agents (DAAs) were licensed for treatment of patients infected with HCV GT1. Telaprevir and Boceprevir were termed first-wave or first-generation DAAs. Both act by inhibiting the viral NS3/4A protease. These protease inhibitors were used in combination with RBV and IFNα. The cost of these therapies was high and the SVR was at 60-75%. Therefore, further DAAs were needed.

In 2014, three new DAAs were available: sofosbuvir, which inhibits the RdRp NS5B, simeprevir, a second wave NS3/4A protease inhibitor, and daclatasvir, a NS5A inhibitor. Sofosbuvir was indicated in combination with RBV for GT2 and GT3, the SVR was around 80-95%. Sofosbuvir in combination with simeprevir or daclatasvir yielded a SVR of 93-100% in patients infected with HCV GT1 (59).

Today, a broad spectrum of different DAAs exists (60). The development of DAAs was only possible due to the development of suitable HCV cell culture systems. DAAs nowadays can cure >95% of HCV-infected patients, leading to the question whether further research regarding a curable disease is actually necessary. But there are certain challenges that cannot be combated with DAAs and therefore further research, in particular on the interference of HCV with its host cell, is more than appropriate. To underline this, some aspects should be mentioned. First, although the immune system is activated, the virus can often not be cleared and replicates at high levels. HCV is then often only recognized when the patient develops HCC or cirrhosis and these clinical issues, can no longer be cured with DAAs. Worldwide, HCV is most common in resource-limited countries. As DAAs are expensive, most patients in need of them cannot afford them. Clinically relevant antiviral resistance could occur in the future.

HCV itself infers no protective immunity. Hence, cured patients are not protected from reinfection with HCV. Thus, when not recognized at an early stage chronic HCV-induced hepatitis may result in the development of cirrhosis and cirrhosis-associated complications (4, 61).

1.1.4 Viral cell entry

HCV can only lead to chronic infection in humans, chimpanzees, and to a limited extent, in shrews (62, 63). This may be due to certain receptors that enable the virus to enter the cell and replicate there. There are numerous studies that try to explain the host specificity of HCV (64-66). However, the exact mechanism has not yet been fully explained. In recent studies it was demonstrated that HCV has the ability to replicate at low levels in the brain (67), but the main reservoir are hepatocytes, which express the full range of receptors needed for cell entry. Hepatocytes show a high polarity, adjacent membranes are separated from tight junctions and disconnect the apical-canicular from the basolateral-sinusoidal domain (68). HCV particles are strongly connected with lipoproteins forming a complex termed lipoviroparticle (LVP), those LVPs are transported into the space of Dissé where the virus can come in contact with the receptors needed for cell entry (69, 70). Several receptors are needed for viral entry. Viral entry can be roughly divided into three steps: the attachment to hepatocytes, receptor-mediated endocytosis and endosomal fusion (71). For attachment of the virus to the hepatocytes, the two binding factors glycosaminoglycans present on heparan sulfate proteoglycans (HSPGs) and the low density lipoprotein (LDL) receptor (LDLR) play a crucial role (72). For receptor-mediated endocytosis, the scavenger receptors class B type 1 (SR-B1) (73), tetraspanin (74), the tight junction proteins, CLDN1 and occludin are important (65, 75, 76). In addition, other receptors are also crucial for HCV entry, including EGFR, ephrin receptor A2 (EphA2) (77), transferrin receptor 1, and the cholesterol transporter Niemann-Pick C1-like 1 (NPC1L1) receptor (71, 78, 79). ApoE binds to LDLRs and appears to play a role in both HCV entry and assembly of infectious viral particles (80). HSPGs interact with ApoE and facilitate HCV attachment, while SR-B1 is relevant for VLDL uptake and also for the uptake of VLDLs associated with HCV LVPs (81). The viral envelope proteins E1 and E2 mediate viral entry by forming a non-covalent heterodimer where E2 binds to entry receptors prior to internalization (27). 40 % of total viral particles in the plasma are bound to triglyceride-rich lipoproteins containing ApoB, ApoE, ApoC1, C2 and C3 (82, 83). Studies suggest that CLDN1 directly binds to HCV E2 protein (27) and that during HCV entry CLDN1 and CD81 interact with each other forming a complex which is critical for HCV entry (84). EGFR does not interact directly with HCV but binding of HCV to the cell surface results in the colocalization of EGFR and CD81 (63, 85). Although the exact role of EGFR during viral cell entry is not yet known, EGFR has been reported to play a role at the interface between the colocalization of CD81 and CLDN1 and the clathrin-mediated endocytosis (CME) of HCV (63, 85) (Fig. 2).

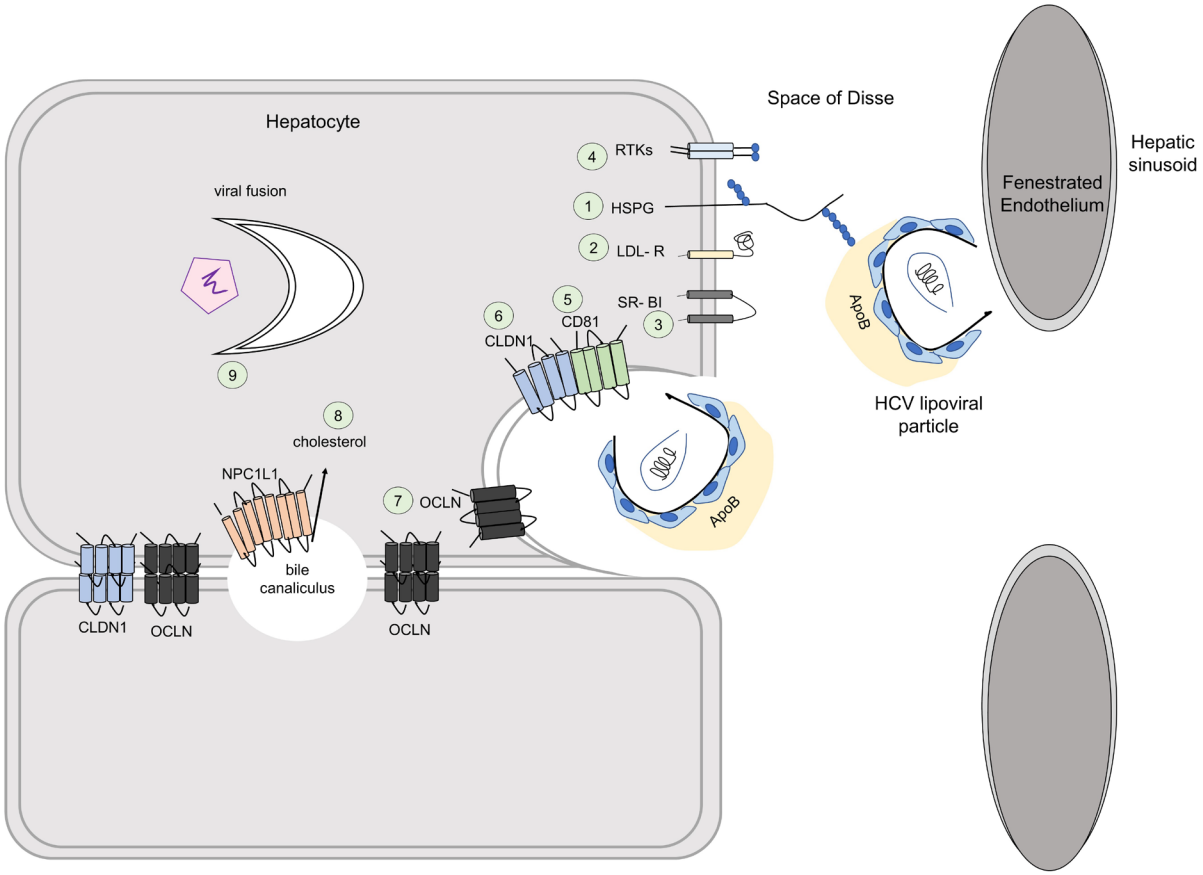

Fig. 2- Schematic depiction of the different cell entry factors of HCV. HCV particles circulate in the blood often associated with lipoproteins. In the first step (*1)* either E1/E2 binds to CLDN1/CD81 or ApoE binds to the heparan sulfate proteoglycan (HSPG) or to the LDLR (*2)*, SR-BI is also important for the binding of HCV via lipoproteins or E2 *(3)*. The receptor tyrosine kinases (RTKs) (*4)*, such as EGFR and EphA2 are important for the association between CD81 *(5)* and CLDN1 *(6)* and therefore contribute to HCV entry. The entry factor OCLN (*7)* is important for post entry steps of HCV and is a component of tight junctions along with CLDN1. The NPC1L1 (*8)* contributes to the cholesterol reabsorption from biliary secretion of cholesterol and is also a cofactor of HCV entry. The final step of HCV entry is the fusion of the host membrane (*9)* with the viral envelope. The nucleocapsid escapes the early endosome and viral RNA is translated in the cytoplasm. Modified according to Zeissel *et al.*, Hepatitis C Virus from Molecular Virology to Antiviral Therapy, page 90 (86).

1.1.5 HCV - cell culture systems

Four different cell culture systems exist to study different steps of viral infection.
The first available HCV cell culture system was the subgenomic replicon system generated by Lohmann *et al.* in 1999, where the NS proteins of the virus are stably expressed in Huh7 cells (87). These replicon cells can replicate but fail to produce viral particles because they have no structural proteins and are thus not infectious, while NS proteins are expressed. The first replicon system was generated by replacement of the encoding region of core to NS2 by two non-HCV sequences: a gene encoding for a reporter or a selection marker that gives resistance to the cytotoxic drug Geneticin (G418) and an additional internal ribosomal entry site (iRES) derived from *encephalomyocarditis virus* (ECMV). The iRES of ECMV serves for the synthesis of NS3 to NS5B, whereas the iRES of HCV serves for the synthesis of the selection marker. Huh7 cell lines are then transfected with both constructs. The first replicon systems were constructed containing HCV GT1b subgenomic replicon sequences (87, 88). In the beginning of these studies, only a few cells survived the G418 selection pressure, because the cells had to adapt to the cell culture conditions. Several adaptive mutations were noted in subgenomic replicon cells, whereas the 5´ and 3´ UTR showed no mutations. In the subgenomic replicon system Con1, several adaptive mutations were noted within the NS4B, NS5A and NS5B coding regions, upstream of the IFN sensitivity-determining region (89, 90).
Already in 2011, it was noted that HCV has evolved a mechanism to enhance PI_4 kinase IIIα (PI_4KA) activity (91). In 2016, it could be demonstrated that the level of PI_4KA in Huh7 cells is much higher compared to primary hepatocytes, leading to overactivation of PI_4KA after HCV infection due to a mechanism of HCV which enhance the levels of PI_4KA in the cell. An adaptive mutation leading to a loss of function of the PI_4KA amplification mechanism of HCV was found in the replicon systems, which shows that the overactivation of PI_4KA triggered by HCV infection prevents the cells from becoming infected. The adaptive mutation that led to the decreased activation of PI_4KA was crucial for the successful replication of HCV in Huh7 cells (92). Most GT1b isolates require only a single adaptive mutation for efficient replication in cell culture, whereas most of the other GTs require several adaptive mutations to replicate efficiently (93). With the knowledge of which adaptive mutations are essential for the survival of the virus in the cell culture system, it was possible to establish various subgenomic and full-length replication systems (89, 90, 94-97).
In 2003, the HCV pseudoparticle system (HCV_{pp}), which is often used to study HCV cell entry, was established (98, 99). Here, HEK293T cells are transfected with three plasmids containing retroviral group specific antigens (gag) and the desoxyribonucleic acid (DNA) polymerase (pol) gene of *murine leukaemia virus* (MLV) or *human immunodeficiency virus* (HIV), a reporter gene, and the envelope proteins of HCV E1 and E2. Particles containing the HCV proteins E1

and E2 on the surface are released into the cell culture media (100). Huh7 cells are then exposed to the cell culture medium containing those particles. Productive entry events can be recognized via the reporter gene which emits detectible light whenever cells display E1 and E2 in their envelope. Because HCV pseudoparticles carry the structural proteins of HCV, like HCV particles, they enter the cell via CME. HCV pseudoparticles do not replicate in the cell because they do not carry the RNA required for this. Therefore, only the HCV cell entry can be investigated via the HCV_{pp} (98, 100).

In 2005, fully permissive cell culture systems were described (101-103). The cloning of the HCV GT2a, isolated from a Japanese patient suffering a fulminant course of hepatitis termed Japanese fulminant hepatitis 1 (JFH1) (104), was crucial for the generation of the HCV_{cc}. Three groups reported independently from each other, but nearly at the same time that the wild-type JFH1 genome, or chimeras containing the JFH1 replicase genes NS3-NS5B and core to NS2 regions from other isolates, based on the same or other GTs, replicated efficiently in Huh7 cells. Since then, this specific HCV genome was used for the HCV_{cc} (100-103). In detail, Lindenbach *et al.* described for the first time in 2005 a HCV chimeric genome, were they used the NS3-NS5B proteins from JFH1 and the core to NS2 proteins from another GT2a isolate, the isolate J6 (strain J6/JFH1, JC1 was created) which is the HCV_{cc} strain used in the present work (101). Most of the chimeric genomes created contain the NS3-NS5B proteins from JFH1 due to their high efficiency which this is also the case for the chimeric genome created by Pietschmann *et al.* in 2006, where the NS3-NS5B proteins from JFH1 and the core-NS2 proteins from the GT1b Con1 isolate are used (105).

In 2008, the trans-complemented particle system (HCV_{TCP}) was described (15). Here, the HCV replicon RNA is transfected into a packaging cell line, which stably expresses the structural proteins of HCV. When naïve cells are transfected with the HCV_{TCP}, the particles replicate only once, because the HCV structural proteins are missing in the sequence of HCV_{TCP} (15).

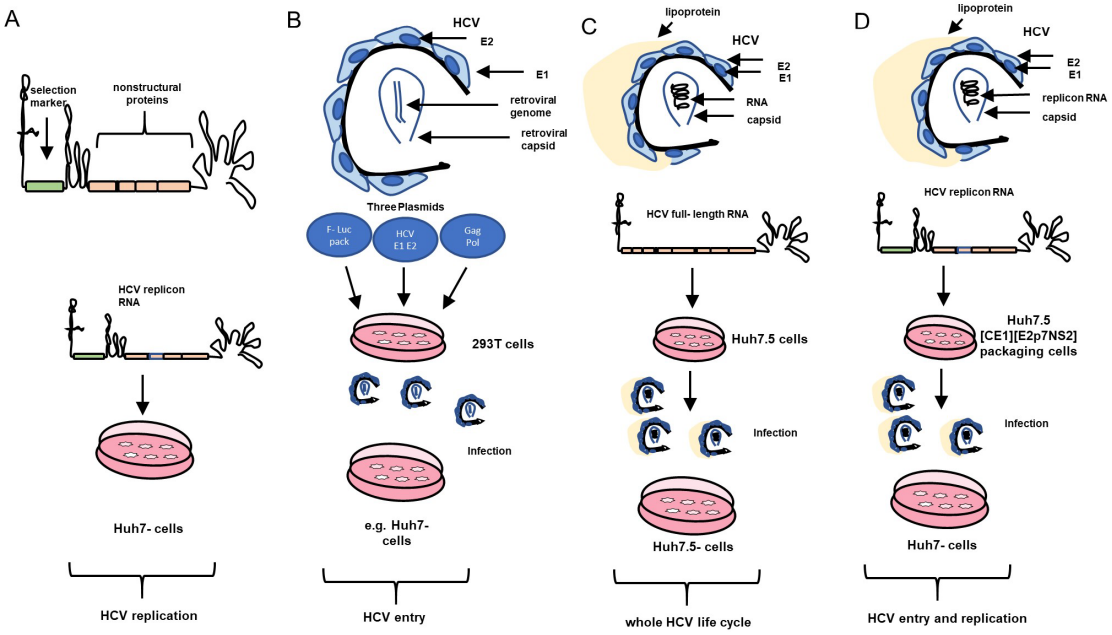

Fig. 3- Schematic depiction of the different HCV cell culture systems. A) HCV replicon system, B) HCV pseudoparticle (HCV_{pp}) system, C) cell culture-derived HCV particle system (HVC_{cc}) and D) HCV trans-complemented particle (HCV_{TCP}) system. Modified to Steinmann and Pietschmann, Hepatitis C Virus from Molecular Virology to Antiviral Therapy page 28, 2006 (100);

1.2 Interference of HCV with the host cell

When HCV enters the hepatocyte, it is recognized by pattern recognition receptors (PRRs) via presentation of pathogen-associated molecular patterns (106). One of those PRRs is the RIG-I. It recognizes HCV via its 3` UTR and structural intermediates during replication. The cascade which is switched on in turn involves the CARDIF/MAVS and several downstream molecules, such as the NFκB and the interferon regulatory factor (IRF) 3 (107, 108). MAVS, first described by Meylan *et al.* in 2005 is a RIG-I-interacting adaptor protein, which among others, leads to the activation of NFκB and IRF3. MAVS is cleaved by the HCV viral protease NS3/4A, resulting in its degradation (109).

Another PRR which recognizes HCV, is the TLR3. In contrast to RIG-I it recognizes only the double stranded structural intermediates of HCV during replication and results in upregulation of IRF3 and NFκB (110, 111).

NS3/4A is known to cleave several host cell proteins, thereby interfering in various cell signalling pathways of the host. Another example is the cleavage of TRIF which transmits signals from TLR3 (112). Important for this work is the cleavage of the TCPTP by the viral protein NS3/4A, since TCPTP is known to be one of the main endogenous negative regulators of EGFR (36) (described in more detail in chapter **1.3.1.2**).

HCV shows a high replication rate of 10^{12} -10^{14} particles/day. This high replication rate and the fact that RdRp has no proofreading function, leads to the presence of a multitude of quasispecies in the blood of a patient, allowing HCV to escape the $CD8^+$ T-cell response (113). $CD8^+$ cytotoxic T lymphocytes (CTL) pressure results in HCV quasispecies formation harbouring mutations in class I MHC epitopes that allows the virus to escape CTL control. It was seen that the quasispecies with those mutations are found predominantly in chimpanzees infected chronically with HCV, while chimpanzees that resolved HCV spontaneously were found to lack those mutations (114).

In this thesis the interference of HCV with EGF, as well as with the cytokines interleukin (IL)-1β and tumour necrosis factor (TNF) α signalling pathways was investigated. Therefore, the downstream signalling pathways of the EGFR and the cytokines IL-1β and TNFα will be described in more detail in the following chapters.

1.3 Interference of HCV with growth factors

1.3.1 ErbB family

The ErbB family consists of the EGFR (also termed as Heregulin (HER) 1 or ErbB1), ErbB2/HER2, ErbB3/HER3 and ErbB4/HER4 (Fig. 4). The ErbB family members play a role, among others, in the development and progression of cancer as well as in processes in development, homeostasis and pathologies. ErbB family members can be activated by several ligands including EGF, transforming growth factor alpha (TGFα), epiregulin (EPR), epigen and neuregulins 1-6 (NRG), some of which are specific for one receptor, while others have a broader binding pattern (115) (Fig. 4).

The EGFR is composed of a large extracellular ligand binding site, a transmembrane and a cytoplasmic region, which becomes phosphorylated at several Y residues after ligand binding (116-118) (Fig. 4).

The structure of ErbB2 is highly similar to that of EGFR (Fig. 4). Although it has no known ligand which binds directly to ErbB2, it is a RTK which acts as a co-receptor to the other ErbB receptors. It can form heterodimers with the other ErbB members and is the preferred binding partner for the EGFR compared to the other dimerization partners in response to EGF. Additionally, it decreases the dissociation of EGF from the EGFR which results in a longer receptor activation (119). Furthermore, the dimers formed with ErbB2 are more stable and less catalytically degraded (120).

As ErbB2, also ErbB3 shows high structural similarities to EGFR (Fig. 4). ErbB3 has long been assumed to lack catalytical activity itself, although it was known that it contains C-terminal Y residues, which can be phosphorylated after heterodimerization of ErbB3 with other ErbB receptors (120). In the last years it could be demonstrated that ErbB3 has a much weaker catalytic activity compared to EGFR, yet it can bind ATP and promotes *trans*-autophosphorylation (121). ErbB3 has got some ligand binding sites, such as for EPR, NRG1 and 2, which results in heterodimerization of the receptor (120). ErbB3 heterodimers activate PI3K signalling but they cannot activate the mitogen-activated protein kinase (MAPK) signalling, hence they are not interacting with growth factor receptor-bound protein 2 (GRB2), like EGFR is (122). In a recent publication, the authors demonstrated that ErbB3 also homodimerizes in response to ligand binding and that homodimers of ErbB3 can be monitored at the cell surface of the cell in the absence of ligands (123).

ErbB4 shows structural similarities to the other ErbB family members but it has some unique structures which for example results in enhanced cleavage of ErbB4 by metalloproteases at the cell surface. Several binding partners for ErbB4 exist, including EPR, NRG3 and 4 (120). EPR, heparin-binding epidermal growth factor-like factor (HB-EGF) and betacellulin are binding to the EGFR as well as to the ErbB4 receptor due to their high structural similarity. In

addition to the EGFR, also ErbB4 is recruiting and activating GRB2 and Shc. Additionally it recruits and activates signal transducer and activator of transcription 5 (122).

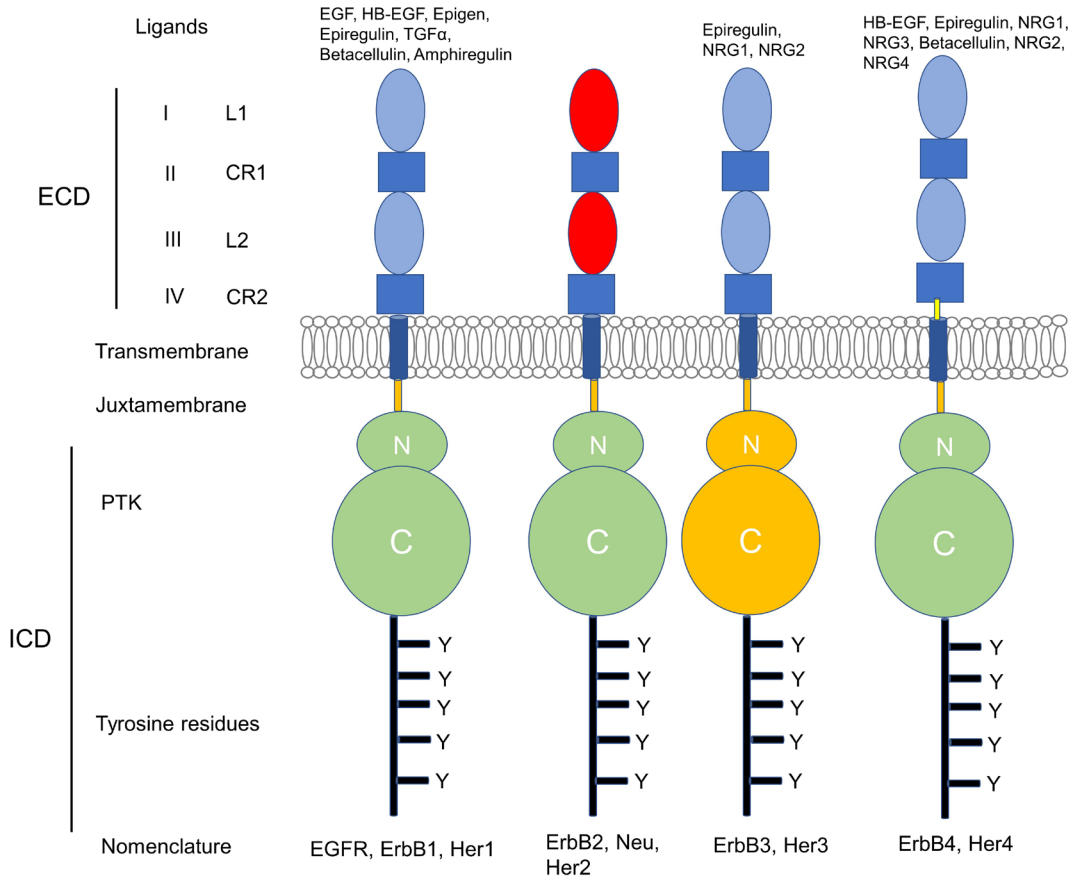

Fig. 4- Schematic depiction of the different ErbB receptors. The extracellular domain (ECD) of ErbB receptors consists of two leucin-rich and two cysteine-rich sub domains (L1; L2; CR1; CR2 respectively). ErbB2 has no known ligand. ErbB3 has weak protein tyrosine kinase (PTK) activity, therefore shown in orange. The intracellular domain (ICD) consists of a bilobal PTK indicated as N and C which is connected to the transmembrane domain via a short juxtamembrane sequence. The Y residues become phosphorylated on receptor activation. The ErbB4 receptor has a so called “stalk” region marked in yellow near to the transmembrane. EGF, HB-EGF, EPR, TGFα, betacellulin and amphiregulin are known to bind to the EGFR while EPR, NRG1 and 2 are binding to ErbB3 and HB-EGF, EPR, betacellulin, NRG1, 2, 3 and 4 are binding to ErbB4. The inactive domain of ErbB2 is depictured in red colour. Modified to Fuller *et al.*, J Mol Cell Cardiol. 2008 May;44(5):831-54 doi:10.1016/j.yjmcc.2008.02.278 (120) and to Steinkamp *et al.*, Mol Cell Biol. 2014 Mar;34(6):965-977 doi:10.1128/MCB.01605-13 (124).

1.3.1.1 EGFR - signalling cascade

The RTK EGFR is a glycosylated plasma membrane receptor with a molecular weight of 170 kDa, and is involved in different cellular processes like development, proliferation, differentiation, cell survival and motility (116-118). EGFR can be present as a monomeric structure on the cell surface or as preformed dimer. Dimerization of EGFR leads to rapid internalization of the receptor. The receptor can then be either lysosomally degraded or recycled back to the cell surface. Which path is preferred, is dependent on its phosphorylation status. Low concentration of EGF results in CME and a large portion of EGFR is recycled back to the plasma membrane, while a high concentration increases the rate of lysosomal degradation of the EGFR by internalization through clathrin-independent mechanisms (125). The binding of EGF to the binding site of the receptor leads either to rapid homo- or heterodimerization with itself or other members of the ErbB family (126). Both the monomeric and the dimeric form of EGFR binding EGF resulting in autophosphorylation of the EGFR, with the dimeric form binds EGF with higher affinity (126). Phosphorylation leads to conformational changes in the inner membrane domain of the EGFR and creates binding sites for GRB2, specifically to its Src homology 2 (SH2) domain, and additionally to SH2 domains from other downstream effector molecules (127). GRB2 binds directly to EGFR at Y1068, Y1086 and indirectly at Y1173. Here, GRB2 binds SH2-domain containing transforming protein 1 (SHC1), then the SH2 domain of SHC1 is binding directly to the EGFR at Y1173 or Y992 (128). GRB2, once bound to the phosphorylated residues of EGFR, builds with or without SHC1 a complex in which Ras exchange factor SOS is recruited and exchanges RAS-GDP for RAS-GTP, activating RAF1 which in turn activates the MAPKs. In general a MAPK kinase kinase (MKKK or MEKK or MAP3K), e. g. Raf, phosphorylates a downstream MAPK kinase (MKK or MEK or MAP2K), e. g. MEK1/2, which in turn phosphorylates and activates, e. g. the downstream MAPK extracellular signal-regulated kinase (ERK) 1/2 (129). MAPK protein phosphatases can inactivate MAPK by dephosphorylation of their S/T residues. Three MAPK signalling pathways are well investigated today: the ERK1/2, the c-JUN N-terminal kinase 1, 2 and 3 (JNK1/2/3) and the p38 MAPK α, β, δ and γ pathways. In a simplified model ERK1/2 is phosphorylated in response to growth factors, hormones and proinflammatory stimuli, while JNK1/2/3 and p38 MAPK α, β, δ and γ are activated in response to cellular and environmental as well as proinflammatory stimuli (130-132). The activation of the MAPKs results in a final activation of several transcription factors, such as NFκB, cAMP response element-binding protein (CREB) 1, or specificity protein (SP) (133-135) (Fig. 5).

Apart from MAPKs, also the phosphatidylinositol-3 kinase (PI3K) pathway can be switched on after a ligand binds to an ErbB receptor. PI3K is composed of the p85 subunit which binds to the ErbB specific docking sites and activates thereby the catalytic subunit p110, which in turn

activates the second messenger phosphatidylinositol 3, 4, 5-triphosphate (PtdIns 3, 4, 5 P3 (PIP_3)) via phosphorylation of PtdIns 4, 5 P2 (PIP_2) (136). EGFR has no direct binding site for the p85 subunit of PI3K, here GRB2-associated binding protein 1 (GAB1) is interconnected between the EGFR and PI3K (137). Next, AKT is recruited, its pleckstrin homology domain binds directly to PIP_3 and AKT gets phosphorylated at T308 and S473 by the 3-phosphoinositide-dependent protein kinase 1/2 (PDK1/2) (138). Precisely, when AKT is recruited, PH binds to PIP_3, to this end the residue T308 is unmasked and can be phosphorylated by PDK1. To fully activate AKT it has to be additionally phosphorylated at S473, this phosphorylation occurs either via autophosphorylation or by PDK2 (139, 140). AKT in turn activates several transcription factors, among them NFκB and CREB (141, 142) (Fig. 5). Those transcription factors activate, among others, the transcription of the chemokines *CXCL1, 2, 3* and *8* (143, 144). A third downstream signalling pathway can be activated immediately after EGF binding to EGFR: the phospholipase C γ (PLCγ) pathway. PLCγ is activated after binding to activated EGFR via its SH domain (145).

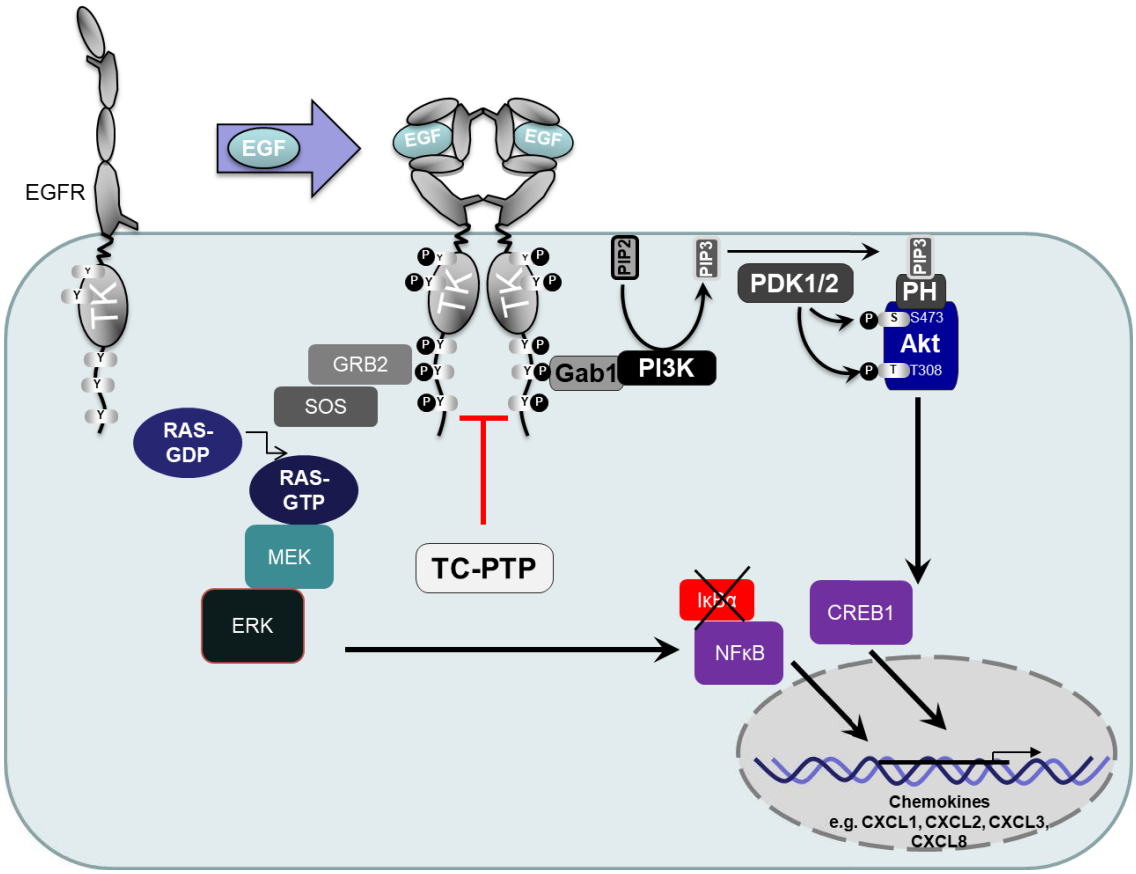

Fig. 5- Schematic depiction of EGFR downstream signalling pathways. EGF binds to the EGFR, which results in homo- or heterodimerization of the receptor. In response the Y residues of the receptor are autophosphorylated and GRB2, SOS and GAB1 are recruited to the receptor as described in 1.3.1. They further activate downstream targets, among others the MAPK and the PI3K signalling pathways. Modified according to Scaltriti and Baselga, The Epidermal Growth Factor Receptor Pathway: A Model for Targeted Therapy, Clinical Cancer Research, 2006 September 12;18 (146)

1.3.1.2 Growth factors and HCV

In 2011 Lupberger *et al.* described EGFR and EphA2 as two essential cofactors for HCV cell entry (77). In this context EGFR activates or modulates cell surface trafficking of CLDN1, CD81 or both to form CLDN1-CD81 complexes, which are necessary for HCV entry (77, 84). It was demonstrated that after binding of HCV_{cc} particles to human hepatocytes, EGFR is activated and in turn HCV_{cc} interacts with CD81, but not with CLDN-1. It was further shown that EGFR is internalized after ligand binding and colocalizes with CD81, suggesting that EGFR interacts with CD81 during HCV entry, which is known to be one of the essential HCV entry factors (84, 147).

Already in 2009, it could be demonstrated by Brenndörfer *et al.* that HCV degrades TCPTP by cleavage at two C-(S/A) peptide bonds that are located at position aa 123/124 (C/A) and aa 216/217 (C/S), via the viral protease NS3/4A, resulting in enhanced phosphorylation and therefore activation of EGFR and AKT (36). TCPTP is a well-known endogenous negative regulator of EGFR. In response to EGF, the nuclear form of TCPTP translocates to and accumulates in the cytoplasm. It then dephosphorylates the Y residues, important for the EGF-induced association with GRB2, which in response can no longer phosphorylate proteins of the downstream signalling pathways of EGFR like the MAPK RAS/RAF/MEK/ERK and the PI_3K (117, 148, 149).

In 2016 Stindt *et al.* demonstrated that HCV upregulates the EGFR and ErbB2 protein levels on the cell surface, whereas ErbB3 protein levels were downregulated. Additionally, they elucidated the mechanisms behind this and showed that ErbB3 protein levels are downregulated via SP1-induced upregulation of NRG1 and AKT activation in HCV-infected cells and this downregulation enhances the upregulation of EGFR and ErbB2 on the cell surface, showing a cross-regulation between the different ErbB receptors (150).

Besides EGF, also the vascular endothelial growth factor (VEGF) was reported to play an important role during HCV infection (151, 152). Interestingly, EGF stimulation of the cell results in an induction of *VEGF* mRNA expression in keratinocytes (151). VEGF is known to be critical in pathological angiogenesis and for HCV cell entry (152). HCV results in an upregulation of *VEGF* mRNA expression in primary hepatocytes and hepatoma cells, leading to a reduced polarity of the cells (153). HCV infection can result in the development of fibrosis, and the fibrosis status of the liver was reported to correlate with the VEGFA levels in the sera of patients, which are chronically infected with HCV (154).

1.4 Interference of HCV with cytokines

1.4.1 Cytokines

The term cytokine can refer to various growth factors, interleukins as well as tumour necrosis factors (TNF) and chemokines. Cytokines, as well as growth factors, prostaglandins, and interferons are proteins that are released by cells to communicate with other cells to maintain cellular homeostasis in response to several stressors. Often a single cytokine acts on several cells at the same time (pleiotropy). It is known that several cytokines can have both redundant and synergistic effects (155, 156). They have a plethora of functions, e. g. they are part of the stem cell development, embryonic development, progression of degenerative processes of aging, as well as response to infections (157).

During an infection, cytokines can be released from cells and the cascade released in this process subsequently leads to the recruitment of various regulatory immune cells to the site of inflammation (158). Cytokine production is associated with the regulation of several transcription factors such as IRFs, NFκB and AP-1 (159). In this manner, they react to inflammation, activate or reduce the immune response and respond to infection and trauma (160).

Two of the proinflammatory cytokines playing a role during HCV infection are described in this chapter in detail.

1.4.2 Interleukin-1

The IL-1 family comprises 11 family members, from which every single protein is encoded by a different gene (161). Their main function is to control infections by being major regulators of the innate immune system, they induce the mRNA expression of several genes and of themselves (162). Due to their strong and rapid activation, their control is of high relevance. They can be inactivated via different mechanisms, e. g. by control of receptors on the cell surface, by activation of the IL-1β-processing protease caspase 1 and by regulation of downstream signalling (161). The most studied representatives of the IL-1 family members are IL-1α and IL-1β (163). IL-1α is located in the nucleus where it acts as transcription factor and activate transcription of several genes such as *CXCL8* after binding of extracellular IL-1α to the IL-1 receptor type 1 (IL1R1) (163). It is constitutively present in mesenchymal and epithelial cells (164). IL-1β is synthesized as pro-IL-1β and has to be cleaved by caspase 1 to mature IL-1β, which is activated by the inflammasome a complex consisting of different PRRs depending on the inflammatory stimulus. During infection with an RNA virus the

inflammasome, which is often activated consists of the pro-caspase 1, NOD-like receptor (NLR) family pyrin domain containing 3 (NLRP3) and RIG-I (165-168).

1.4.2.1 Interleukin-1β signalling cascade

IL-1β was first purified in 1977 from rabbits after producing a monophasic fever, whereas the cDNA from human IL-1β was first cloned in 1984 (169, 170). IL-1β binds to the IL1R1, which is ubiquitously expressed, forming a trimeric complex with the IL-1 receptor accessory protein (IL-1RAcP) (171). The trimeric complex formation results in the recruitment of TIR like domains, leading to the recruitment of myeloid differentiation primary response gene 88 (MYD88), Toll-interacting protein as well as IL-1 receptor-associated kinase (IRAK) 4 resulting in the formation of a complex of these proteins (172). Next IRAK4, IRAK2 and IRAK1 are phosphorylated and in turn TNFR-associated factor (TRAF) 6 is recruited (173, 174). TRAF6 functions as ubiquitin E3 ligase, in concert with other ubiquitin ligases it attaches K63-linked polyubiquitin *chains* to IL-1β downstream signalling intermediates, e. g. to IRAK1, TGFβ-activated protein kinase-binding proteins (TAB) 2 and 3, as well as TGFβ-activated protein kinase, a member of the MAP3K family transforming growth factor β-activated kinase (TAK) 1 (175-178). As a result, ubiquitinated TAK1 associates with TRAF6 and another MAP3K MEKK3. TAK1 MEKK3 complex formation and oligomerization of TRAF6 lead to the activation of different downstream components of the IL-1β signalling pathway such as NFκB or the MAPKs JNK, ERK via MAP2K MEK and p38 (178-181). The activation of p38 occurs via phosphorylation of p38 at T180/Y182 (182) (Fig. 6).
JNK activation leads to the activation of c-Jun and in turn the activation of the activating transcription factor (ATF) 2 (183).
The NFκB complex consists of five different structural proteins, termed NFκB subunits, namely the subunits p50 (NFκB1), p52 (NFκB2), p65 (RelA), RelB and c-Rel, which have transcriptional activity (184). In case of activation of the NFκB complex they form hetero- or homodimers and translocate to the nucleus where they function as transcriptional activators or repressors for several genes (184). NFκB activation is rapid, meaning it can be activated within minutes, and does not require *de novo* protein synthesis (185).
NFκB is trapped in the cytoplasm by IkBα and can be released via phosphorylation and thereby degradation of IκBα by the IκB kinase (IKK) (Fig. 6). Once NFκB is released, its subunits translocate as homo- or heterodimers to the nucleus where they function as transcription factor and activate several genes such as *CCL2*, *CXCL1, 2, 3* and *8* but also *IL-1β* itself (162, 186-192). To activate transcription of several genes, NFκB recruits different coactivation factors such as CREB1, CCAAT/ enhancer-binding protein (C/EBPβ) and SP1 (193-195).

Interestingly, IL-1β transactivates the EGFR mediated by CXCL1 in dysplastic oral keratinocytes cells (196).

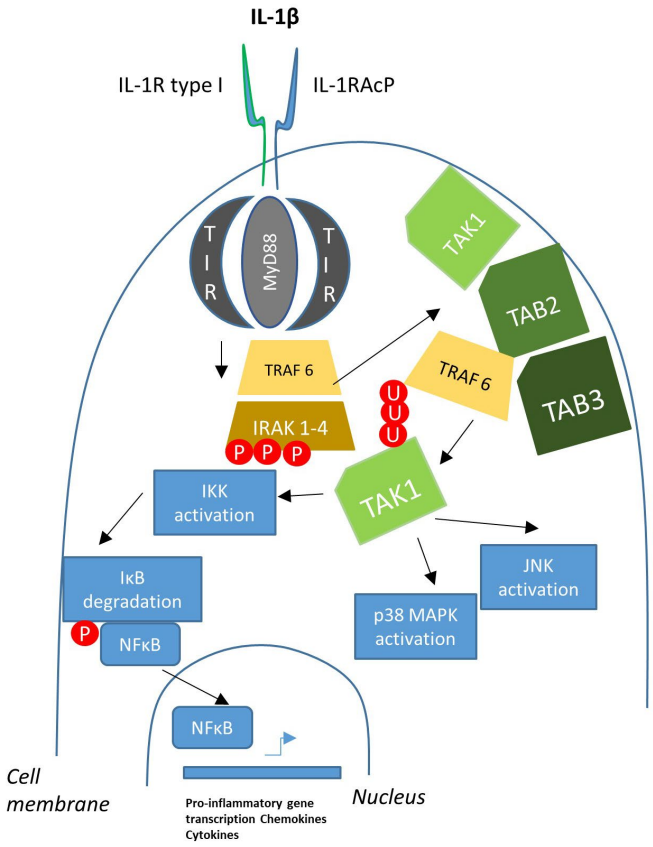

Fig. 6- Schematic depiction of the IL-1β signalling pathway. IL-1β binds to the IL-1R type I. The IL-1RAcP is then recruited and forms a heterodimer with the IL-1R type 1. MyD88 is recruited and recruits TIR. IRAK1-4 is recruited and phosphorylated, in turn TRAF6 is recruited. TRAF6 and IRAK1-4 dissociate to the plasma membrane where they associate with TAK1, TAB2 and TAB3. The complex then migrates back to the cytoplasm, TAK1 is subsequently phosphorylated, and TRAF6 ubiquitinated. Different pathways can be activated, including the IKK/IκB/NFκB and the MKK-MAPK/JNK/ERK signalling pathway. Modified to Sienstra *et al.* 2012, The inflammasome puts obesity in the danger zone, Cell Metab., 2012 Jan 4;15 (197)

1.4.2.2 Interference of HCV with Interleukin-1β

Patients chronically infected with HCV show higher IL-1β levels in the serum compared to healthy persons and higher IL-1β levels in liver tissue compared to patients suffering from HCC without HCV infection (198, 199). In patients infected chronically with HCV and having a narcotic drug consumption history, IL-1β, IL-6 and TNFα are highly enhanced (200). Increased serum levels of IL-1β after HCV infection are higher in patients chronically infected with HCV GT3 compared to GT1 (201).

In a cohort of 92 patients suffering from chronic HCV infection, those with an IL-1β gene polymorphism on the -31 T allele had a worse prognosis for the development of HCC (202). In addition to that IL-1β -551 T/T is associated with the development of HCC in patients chronically infected with HCV, although patients which spontaneously cleared HCV do not show polymorphism in the -551 allele of IL-1β (203, 204).

Although, HCV can neither infect Kupffer cells nor non-resident macrophages, they are nonetheless exposed to the virus in the liver. Therefore, Shrivastava *et. al* differentiated THP-1 cells via phorbol 12-myristate 13-acetate stimulation into macrophages which were exposed to HCV, supernatant was collected, and protein levels of different cytokines were examined. Additionally, they isolated human primary macrophages from PBMCs and exposed them to HCV. They demonstrated that HCV exposure of macrophages enhances the secretion of pro-IL-1β and pro-IL-18 mediated by NFκB (168).

In another study, it was shown via electrophoretic mobility shift assay (EMSA) and via immunohistochemistry that NFκB is activated in the liver tissue from patients chronically infected with HCV, as well as in HCV-core transfected HepG2 cells (205), constant activation of NFκB is observable in many solid tumours (206). In addition to that, activation of NFκB in response to HCV core-transfection was shown to result in downregulation of PTEN, which is known to be a negative regulator of AKT (26). Also AKT is known to be constantly activated in many tumours (207).

In 2013, Negash *et al.* collected liver samples from HCV-infected patients with mild inflammation (without fibrosis), percutaneous liver samples of HCV-infected patients which suffered from severe liver damage during transplantation as well as from the donor liver. By RNA-sequencing (RNAseq), they could demonstrate that HCV infection enhances, among others *IL-1β* mRNA expression. Furthermore, they co-stained liver sections from both control liver samples and samples from HCV-infected patients with both anti-IL-1β and anti-CD68 and showed that the staining of IL-1β was increased during HCV infection in Kupffer cells, while it was not enhanced in hepatocytes. In addition to that, they demonstrated that HCV activates the NLRP3 inflammasome, which in turn leads to an activation of pro-IL-1β via activation of caspase 1 (208).

HCV infection leads to the upregulation of IL-1β proteolytic activation and secretion in Huh7.5 cells infected with the JFH1 via recruitment of NLRP3 and another protein complex of the inflammasome apoptosis-associated speck-like protein containing a CARD (ASC) (209). The inflammasome complex formation leads to the proteolytic processing of pro-caspase 1 to caspase 1, which in turn activates IL-1β (209).

1.4.3.1 Tumour necrosis factor α

TNFα was first described in 1975 by Carswell *et al.* as a molecule that causes haemorrhagic necrosis in tumours in animals infected with *bacillus Calmette-Guérin* and treated with lipopolysaccharide (LPS) (210). TNFα is proinflammatory and plays a role in apoptosis, inflammation, cell proliferation and differentiation (211).

TNFα can be found as a soluble (sTNFα) and as a transmembrane form (mTNFα). The mTNFα form is the precursor of sTNFα and can be cleaved by the TNFα-converting enzyme. Both forms can bind to the TNF receptor 1 (TNFR1) and only the mTNFα form can bind to the TNF receptor 2 (TNFR2) (212). TNFR1 is ubiquitously expressed and plays a critical role in proinflammatory and proapoptotic processes, while TNFR2 is mainly expressed in lymphocytes and is responsible for their proliferation (212).

TNFR1 is described to be a death receptor (DR), containing death domains (DDs) in its cytoplasmic part (213). The DD is mainly responsible for signalling after ligand binding. It triggers necroptosis, apoptosis and activates NFκB signalling (214, 215). Binding of a ligand to TNFR1 leads to recruitment of TNFR1-associated death domains (TRADD) and receptor-interacting protein kinase 1 (RIPK1) (216, 217). After binding of TRADD and RIPK1 to TNFR1 TRAF2 homotrimers are recruited, these leads to recruitment of the E3 ligases cellular inhibitor of apoptosis protein (cIAP) 1 and 2 to the TNFR1 complex, where they attach K63-linked ubiquitin *chains* to the components of the TNFR1, e. g. RIPK1 (218, 219). This results in TAK1 recruitment via TAB2 and the inhibitor of IκB kinases complex (IKK), TAK1 then phosphorylates the IKK_2 subunit of IKK leading to the phosphorylation and degradation of IκBα and therefore to the release of NFκB (218, 219) (Fig. 7).

Interestingly, TNFα increases the protein levels of EGFR on the cell surface as well as intracellularly (220). Apart from activating the EGFR and NFκB, TNFα activates several MAPKs such as ERK, p38 and JNK. The MAPKK MEK activates herein the MAPK ERK (221, 222). JNK and p38 are activated by TRAF2 via activation of different MAP3Ks (222-224).

In addition to that, AKT, which is activated by PI3K downstream of binding of different ligands to RTKs such as EGFR, can contribute to the TNFα-induced NFκB transcriptional activity, although the exact mechanism is not elucidated yet (225).

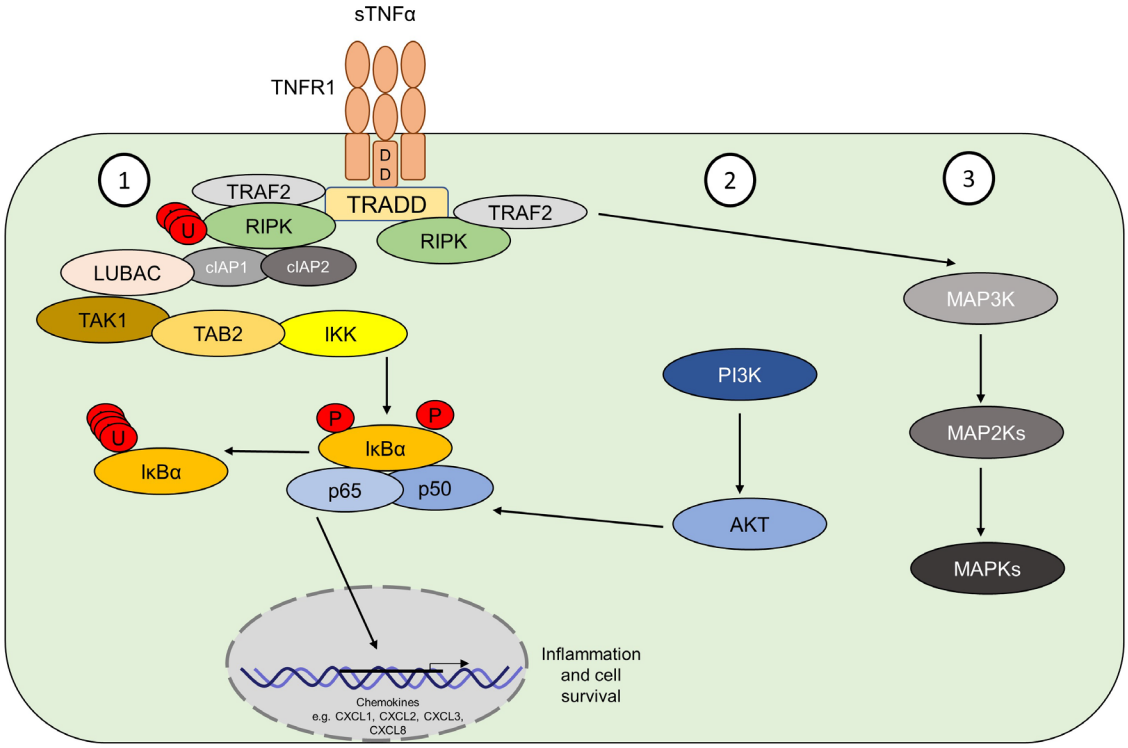

Fig. 7- Schematic depiction of the TNFα signalling pathway. TNFα binds to the TNFR1. The death domain (DD) of the receptor leads to the recruitment of TRADD and the RIPK. After binding of TRADD to TNFR1 and TRADD to RIPK, TRAF2 is recruited. **(1)** In turn the E3 ubiquitin ligases cIAP1 and cIAP2 are recruited. Thereafter, RIPK and the other proteins of the receptor complex are ubiquitinated which leads to the recruitment of LUBAC, TAK1, TAB2 and the IKK. IKK phosphorylates IκBα, the phosphorylation leads to the degradation of IκBα. The subunits p50 and p65 of NFκB are no longer trapped by IκBα in the cytoplasm and can translocate to the nucleus, where they function as transcription factors, resulting in an enhancement of different target genes, among others the chemokines CXCL1, 2, 3. **(2)** On the other hand, PI3K activates AKT in response to growth factor activation and in turn AKT contributes to the TNFα-mediated activation of p65. **(3)** Additionally, TNFα activates different MAPKs via TRAF2. Modified to Wajant *et al.*, TNFR1 induced activation of the classical NFκB pathway, FEBS J., 2011 Apr;278(6):862-76 (215) and Baud *et al.*, Signal transduction by tumor necrosis factor and its relatives, Trends Cell Biol., 2001 Sep;11(9):372-7 (222).

1.4.3.2 Interference of HCV with the tumour necrosis factor α

Patients chronically infected with HCV show significantly higher TNFα levels in the serum and the TNFα concentration is positively correlated with the severity of the infection (199, 226-228). Additionally, *TNFα* mRNA expression was found to be enhanced in the liver and mononuclear cells from patients chronically infected with HCV (229).

Transgenic mice expressing NS3/4A in the liver show lower levels of $CD4^+$ T-cells and type I/II dendritic cells in the liver compared to wild type mice (230, 231). In addition, they are protected from otherwise lethal TNFα and LPS-mediated liver damage via upregulation of NFκB activation and TNFα levels. The inhibition of p38 MAPK reverses this effect (230, 231). Besides, the resistance to LPS and TNFα-induced liver damage, the NS3/4A transgenic mice showed increased cytokine (IFNγ and IL-10) and chemokine levels (CCL3, CCL17, CCL22, CXCL9 and CXCL11) (232).

Another study demonstrated that Huh7 cells, which stably express NS5A show decreased activation of the apoptotic pathway induced after TNFα binding to the TNFR1 via caspase 8, although this is NFκB independent (233).

In 2015, it could be shown that TNFα is induced in Huh7 cells in response to HCV infection mediated by TLR7 and TLR8. Furthermore, it could be demonstrated that TNFα prevents the depletion of the interferon α/β receptor (IFNAR) 2 by HCV, meaning IFNAR2 can no longer bind IFN and activate downstream signalling pathways which would lead to an inflammatory activation (226).

Furthermore, HCV core enhances NFκB activation after TNFα stimulation of Huh7 cells independent of JNK, via a mechanism that has not been elucidated yet (234). In contrast to that, it was shown that the viral protein NS3 binds to LUBAC and renders it inactive, resulting in decreased activation of NFκB (235).

Core-transfected HepG2 cells have been shown to be resistant against TNFα-induced apoptosis due to NFκB activation. When the activation of NFκB is blocked by pyrrolidine dithiocarbamate, it has been shown that TNFα-induced apoptosis is reactivated (205).

1.5 Interference of HCV with Chemokines

1.5.1 Chemokines

Chemokines are responsible for the chemotactic migration of multiple leukocytes, such as haematopoietic precursors, mature leukocytes of the innate immune system as well as naïve, memory and effector lymphocytes belonging to the adaptive immune system (236). In addition, they are also known to stimulate other types of migratory behaviour including, but not limited to, haptotaxis and chemokinesis, as well as induction of cell adhesion and arrest. They play a central role in the homeostasis of the immune system (237), also they are important during embryonic development of the central nervous system and mediate angiogenetic effects, which is important e. g. during cancer development (238, 239). The classification of chemokines is determined by the arrangement of their C residues and their primary amino acid sequences (240). One chemokine monomer consists of a central three stranded β-sheet, a C-terminal α-helix and a short N-terminus which is important for receptor activation and is between 8 and 12kDa in size (241, 242). Four groups of chemokines exist and to which of them a distinct chemokine belongs is dependent on the position of the two Cs that are nearest to the N-terminus. While these Cs are directly adjacent in case of CC chemokines, CXC chemokines have another amino acid in between the two Cs, CX_3C has three amino acids between the two Cs and XC, of which two forms exist in humans and one in mice, has only one C after a random amino acid (240) (Fig. 8). Chemokine names include chemokine designation (CC, CXC, CX_3C or XC, where X may be any amino acid) followed by the letter L for ligands or R for receptors, followed by a number, dependent on when the gene was first isolated (237, 243). The receptors are seven transmembrane-domain G protein-coupled receptors (GPCRs) (244). In this work, the CXC ligands of the CXCR2 are of great interest and are thus described in further detail.

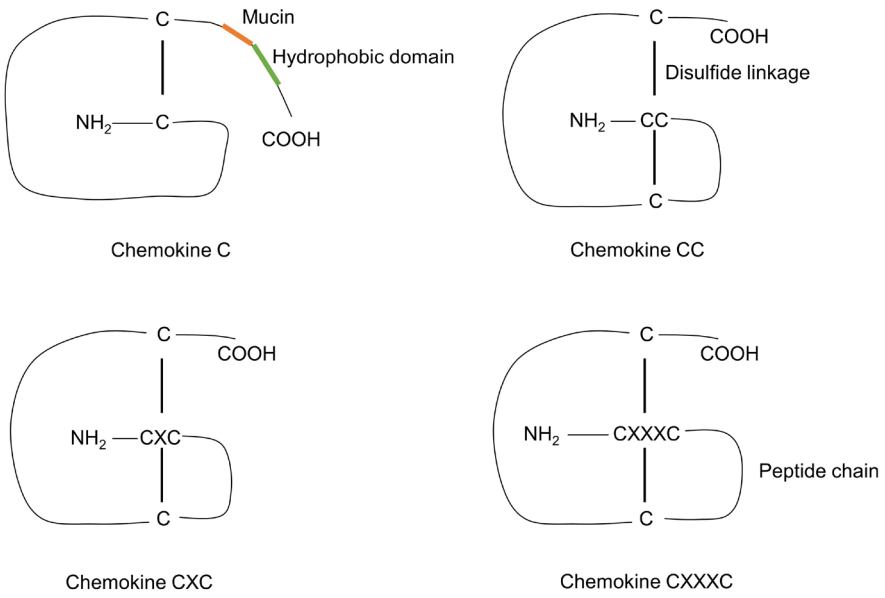

Fig. 8- Schematic depiction of the different structures from the four subtypes of chemokine ligands. C chemokines contain one C at the n-terminus, CC chemokines contain two Cs, CXC two Cs, which have another amino acid in between of the two Cs and CX_3C chemokines have three other amino acids in between the two Cs. Modified to Zhang *et al.* 2018, Function of chemokines in the perineural evasion of tumours, Int J Oncol. 2018 May;52(5):1369-1379 (240).

1.5.2 CXC ligands

CXC chemokines can be subdivided into two different groups dependent on whether the tripeptide glutamic acid-leucine-arginine (ELR) precedes the C (ELR^+) or not (ELR^-) (Tab. 1), of which the ELR^+ chemokines, among others CXCL1, 2, 3 and 8, mainly bind to the CXCR2 and are known to be angiogenic factors (245, 246). The receptor CXCR2 is the major receptor for ELR^+ CXC ligands and mediates angiogenesis. The CXCR2 is expressed in many cell types, including mast cells, monocytes, neutrophils, eosinophils and oligodendrocytes (247). CXC ligands are ubiquitously expressed (248). In the liver, hepatocytes, Kupffer cells, stellate cells, sinusoidal endothelial cells, biliary epithelial cells and infiltrating immune cells can release chemokines and are in turn responsible for the chemoattractant-induced migration of different immune cells to the liver (249-251). The infiltration of different immune cells can lead to chronic inflammation, liver injury or regeneration as well as to progression or resolution of fibrosis (252). Growth factors, other cytokines and cellular stressors lead to an enhanced expression of chemokines in hepatocytes (249-251). After liver injury, the chemokine ligands CXCL1, 2 and 8 play a crucial role, since their binding to the chemokine receptors CXCR2 and 1 ensures that monocytes and neutrophils migrate to the liver (253, 254). In 1987, IL-8 or CXCL8 was the first chemokine described as being a chemotactic proinflammatory human protein that recruits neutrophils after LPS stimulation of monocytes (255). *CXCL8* expression

is enhanced by different stimuli, such as the cytokines TNFα and IL-1β. The stimulation results in a 10-100-fold induction of *CXCL8* mRNA expression mediated by NFκB and activator-protein 1 (AP1) (256, 257). CXCL1, also known as GROα, shows both inflammatory and growth-regulatory functions (258). CXCL2/GROβ/MGSAβ and CXCL3/GROγ/MGSAγ show 90 and 86% identity at the deduced amino acids to CXCL1 (GROα) (258). CXCL1 and 2 mediate recruitment of neutrophil granulocytes to the site of infection (259). In addition to that, CXCL1 is essential for reactive oxygen species (ROS) formation at the site of infection to combat microbials in the tissue (260). CXCL1 signals via binding to either CXCR2 or to glycosaminoglycans (GAGs) on epithelial and endothelial cells (261). CXCL1 can be found in monomeric or dimeric forms whereas the dimeric form binds GAG with higher affinity (262). CXCL8 binds with high affinity to both receptors CXCR1 and 2 while CXCL1, 2, and 3 primarily bind to CXCR2 (263).

Tab. 1- ELR positive CXC chemokines and their corresponding receptors. All synonyms for the CXC ligands in humans and the binding affinities to their corresponding receptors are listed. The table was modified according to Yuan Cheng *et al.*, Potential roles and targeted therapy of the CXCLs/CXCR2 axis in cancer and inflammatory diseases, Biochim Biophys Acta Rev Cancer., 2019 April, 1871 (247).

Systemic name	**Synonyms**	**Receptors**	**Affinity to CXCR2 (nM, K_d)**
CXCL1	GROα MGSAα	CXCR2	5
CXCL2	GROβ MGSAβ MIP2α	CXCR2	4
CXCL3	GROγ MGSAγ MIP2β	CXCR2	1
CXCL5	ENA78	CXCR1, CXCR2	11
CXCL6	GCP2	CXCR2	N/A
CXCL7	NAP2	CXCR2	7
CXCL8	IL8	CXCR1, CXCR2	4

1.5.3 CC ligands

Today, there are 28 different CC chemokines described. CC chemokines bind to the CC receptors (CCRs), from which 10 different members are known until now (CCR1-10). CC chemokine release results in the recruitment of several immune cells, mainly monocytes and lymphocytes, but also basophils, eosinophils and neutrophils (264). Especially CCR2 chemokine ligands, such as CCL2, CCL7 and CCL12, specifically recruit monocytes and macrophages to the site of infection or to the damaged tissue (265-267). In addition to the

function of recruiting monocytes and macrophages, CCL2 is responsible for regulating adhesion molecules and the release of the proinflammatory cytokines IL-1β and IL-6 in monocytes (268). *CCL2* mRNA expression is enhanced in hepatocytes under different pathological conditions, among others non-alcoholic and alcoholic fatty liver disease (269, 270). CCR2 deficient mice do not develop liver fibrosis, because inflammatory $G1^{+}$ monocytes, which are suggested to be key players in the progression of liver fibrosis, are not recruited to the injured liver (271).

Tab. 2- CC chemokines and their corresponding receptors. All synonyms for the CC ligands in human and their corresponding receptors are listed. The table does not include all members of the CC ligand family. The table was modified according to Deshmane *et al.*, Monocyte Chemoattractant Protein-1 (MCP-1): An Overview, J. Interferon Cytokine Res., 2009 Jun; 29(6): 313-326 (272).

Systemic name	Synonym(s)	Receptor(s)
CCL1	I-309	CCR8
CCL2	MCP-1 MCAF TDCF	CCR2
CCL3	MIP-1α LD78α	CCR1 CCR5
CCL4	MIP-1β	CCR5
CCL5	RANTES	CCR1 CCR3 CCR5
CCL6	-	Unknown
CCL7	MCP-3	CCR1 CCR2 CCR5
CCL8	MCP-2	CCR1 CCR2 CCR3 CCR5
CCL12	-	CCR2

1.5.4 Interference of HCV with CXC and CC ligands

In most liver diseases, chemokines and their receptors are key players in activating the inflammatory response of the cell leading to recruitment of several immune cells to the affected organ (273).

Once HCV infects liver cells the immune system is activated and different cells such as neutrophils are recruited to the site of infection. This results in liver inflammation, liver damage, fibrosis, cirrhosis and HCC development (108). Two to five weeks after HCV infection, CXCR3

and CCR5-binding chemokines are detected in the peripheral blood of HCV-infected individuals, while antigen-specific intrahepatic T cells are detectable after eight to twelve weeks. Since CXCR3 are type 1 helper T cells (Th1)-associated, not the chemokine response of the cells, but the priming of T cells may be delayed during HCV infection (274).

Increased protein levels of CXCL1, 2, 3 and 8 in the sera of patients has already been described for various tumours and viral infections (247). Also in sera from HCV-infected patients, the CXCL8 protein levels are upregulated when compared to healthy control patients sera, correlating with the severity of liver inflammation (108).

Additionally, *CXCL8* mRNA expression, as well as CXCL8 protein levels are upregulated in Huh7 cells when they are transfected with the NS proteins NS4A, NS4B and NS5A of HCV (275).

Already in the late 1990ies, interference of HCV proteins with several cellular signalling pathways was demonstrated, because both NS5A and E2 HCV proteins inhibit the protein kinase R, which is an interferon-induced enzyme and is therefore important to activate the cellular immune response against viral invasion of the cell (276, 277). In studies further investigating the effects of the HCV protein NS5A, it was shown that NS5A upregulates *CXCL8* mRNA expression and CXCL8 protein levels resulting in the inhibition of IFNα-induced antiviral responses of the cell (278). TNFα stimulation of Henrietta Lacks (HeLA) cells resulted in an NFκB and AP1 mediated upregulation of *CXCL8* mRNA expression (278).

In addition, elevated TNFα as well as CXCL8 protein levels were observed in sera of patients chronically infected with HCV (279). Protein levels of CXCL8 are highly upregulated in patients not responding to IFN therapy, whereas the protein levels of CXCL8 in patients sera decreased after successful IFN therapy (279).

The transcription of *CXCL8* is not only induced in response to NS4A, NS4B and NS5A, but also activated in NS2-transfected HepG2 cells, which is mediated via NFκB. After the binding site of the *CXCL8* promoter for κB is abolished by mutagenesis, increased CXCL8 transcription is no longer observable in NS2-transfected cells (280).

Interestingly, in chronic infection models of HCV, such as the subgenomic replicon cell system (**1.1.5**), upregulation of CXCL8 protein levels correlates with HCV replication and HCV replication stops when CXCL8 is removed, while in an acute infection model of HCV CXCL8 production is inhibitory for HCV replication of low replicative capacity-exhibiting viruses. This data demonstrates both pro- and antiviral effects of CXCL8 depending on different parameters, such as acute or chronic infection or the replication rate of the virus (281).

Besides *CXCL8*, also the mRNA expression of the chemokine *CCL2* is altered during HCV infection. Consequently, hepatic CCL2 is upregulated in response to HCV infection (274). The susceptibility of HCV infection was shown to be associated with a specific single nucleotide

polymorphism (SNP) in the *CCR2* gene. Additionally, it was demonstrated that successful HCV clearance is associated with a SNP in the C allele of *CCL2* and in the T allele of *CCL5* (282). HCV_{cc} particles co-cultured with macrophages upregulated the *CCL2* mRNA expression, as well as the CCL2 protein levels in the macrophages, resulting in enhanced release of CCL2 and subsequently enhanced recruitment of monocytes. Additionally, *IL-1β*, *TNFα* and *IL-6* mRNA expression was upregulated in macrophages co-cultured with HCV_{cc} particles (283).

1.6 Aim of the work

It is well known that HCV interferes in several intra-and intercellular signalling pathways and modulates them. HCV has established several mechanisms to circumvent the immune system and to modulate cell signalling pathways. The liver is composed of different cell types, mainly hepatocytes, which are, among others, capable of releasing different cytokines and chemokines to guide immune cells to the liver after inflammation, as a stress response or after injury. In previous studies it could be demonstrated that the HCV protease NS3/4A not only cleaves viral proteins, but also several host proteins such as TCPTP (36). TCPTP is one of the endogenous negative regulators of EGFR. EGFR is known to play a crucial role during HCV infection, although the mechanism behind it is not precisely elucidated yet. In transgenic mice expressing NS3/4A in the liver, it could be seen that TNFα levels are increased as well as NFκB p65 activation is upregulated. Additionally, these mice are protected from otherwise lethal TNFα and LPS challenges (230, 231). Furthermore, it was shown that the mRNA expression of *CXCL1*, *2*, *3* and *8* as well as the protein levels of those chemokines are upregulated after HCV infection. Recently, our research group demonstrated that this upregulation is further enhanced after EGF stimulation (284).

In this work, it should be investigated whether growth factors, cytokines and/or chemokines are altered in sera of patients chronically infected with HCV.
In addition to that, it should be analysed which EGFR downstream signalling components are involved during EGF-induced mRNA expression of *CXCL1*, *2*, *3* and *8* mRNA enhanced by HCV infection, to identify the underlying molecular mechanisms behind the chemokine expression regulation in context of HCV.
Additionally, it should be determined whether also the cytokines TNFα and IL-1β play a role during HCV-dependent mRNA expression upregulation of the chemokines *CXCL1*, *2*, *3* and *8* and so, the underlying molecular mechanisms should be uncovered.
Furthermore, the effect of HCV infection on the expression regulation of those analytes should be analysed.
The mechanisms behind the upregulation of *CXCL1*, *2*, *3* and *8* mRNA expression in response to HCV infection should be elucidated as well.
Additionally, the role of TCPTP and AKT in the context of HCV should be analysed. Therefore, knockout cell lines should be generated using clustered regularly interspaced short palindromic repeats (CRISPR)/Cas9-mediated genome editing.

2 Materials

2.1 Materials for cell culture

Tab. 3- List of plastic goods used in this study.

Item	Company	Item number
75 cm² tissue culture flask	Greiner (Solingen, Germany)	#658 170
6 cm tissue culture dish	Falcon (Heidelberg, Germany)	#353004
10 cm tissue culture dish	Falcon (Heidelberg, Germany)	#353003
6-well tissue culture plate	Greiner (Solingen, Germany)	#665180
12-well tissue culture plate	Greiner (Solingen, Germany)	#657160
96-well tissue culture plate	Eppendorf (Hamburg, Germany)	#0030730119
Filtropur S 0.2 µm filter	Sarstedt (Nümbrecht, Germany)	#83.1826.001
Filtropur 0.45 µm filter	Sarstedt (Nümbrecht, Germany)	#83.1826
Hybond P 0.45 PVDF blotting membrane	GE Healthcare (Chicago, Illinois, USA)	#10600023

2.2 Cell culture media

Tab. 4- List of cell culture media used in this study.

Item	Company	Item number
DMEM 4.5 g/L glucose	Merck (Darmstadt, Germany)	#FG-0445
DMEM 4.5 g/L glucose	PAN BIOTECH (Aidenbach, Germany)	#P04-03600
DMEM/HAM's F-12	Merck (Darmstadt, Germany)	#FG-4815
DMSO	Sigma Aldrich (St. Louis, Missouri, USA)	#D2650-5X5ML
FBS	Thermo Fisher (Waltham, Massachusetts, USA)	#10270-106
G418 Geneticin	Thermo Fisher (Waltham, Massachusetts, USA)	#10131-027
L-Glutamine (200mM)	Thermo Fisher (Waltham, Massachusetts, USA)	#25040081
MEM Non-essential-amino-acids (NEAA)	Thermo Fisher (Waltham, Massachusetts, USA)	#11140-035

OptiMEM	Thermo Fisher (Waltham, Massachusetts, USA)	#51985-06
PBS	PAN BIOTECH (Aidenbach, Germany)	#P04-36500
Penicillin/Streptomycin	Thermo Fisher (Waltham, Massachusetts, USA)	#15140-122
Trypsin/EDTA	Cytogen (Sinn-Fleisbach, Germany)	#10-023

2.3 Chemicals

Tab. 5- List of chemicals used in this study.

Item	Company	Item number
5x siRNA Buffer	Dharmacon (Colorado, USA)	#B-002000-WB-100
6-aminocaproic acid	AppliChem (Darmstadt, Germany)	#A2266
8-Bromo adenosine 3', 5'-cyclic monophosphate	Sigma Aldrich (St. Louis, Missouri, USA)	#B5386
Acrylamide	AppliChem (Darmstadt, Germany)	#A0951
Agar	Biozym (Oldendorf, Germany)	#840004
Ammonium persulfate	Serva (Heidelberg, Germany)	#13375.05
Ampicillin	Sigma Aldrich (St. Louis, Missouri, USA)	#A1593
Antarctic phosphatase	New England Biolabs (Frankfurt am Main, Germany)	#M02895
Aprotinin	Sigma Aldrich (St. Louis, Missouri, USA)	#A4529-10MG
ATP	Sigma Aldrich (St. Louis, Missouri, USA)	#A1852
Benzamidine	Sigma Aldrich (St. Louis, Missouri, USA)	#12072
β-Glycerophosphate	Sigma Aldrich (St. Louis, Missouri, USA)	#50020
Bradford protein assay	BioRad (Hercules, California, USA)	#500-0006
Bromocresol green sodium salt	Sigma Aldrich (St. Louis, Missouri, USA)	#B1256
BSA	Thermo Fisher (Waltham, Massachusetts, USA)	#15561020
DharmaFECT 4	Dharmacon (Colorado, USA)	#T-2004-03

DNase	Qiagen (Hilden, Germany)	#79254
Dodecyl sulfate/1 l ddH2O	Serva (Heidelberg, Germany)	#20763
DTT	Sigma Aldrich (St. Louis, Missouri, USA)	#DTT-RO
EDTA	Carl Roth (Karlsruhe, Germany)	#CN06
Ethidium bromide	Carl Roth (Karlsruhe, Germany)	#HP47.1
Glucose	Merck (Darmstadt, Germany)	#346351
Glycine	Merck (Darmstadt, Germany)	#104169
GoTaq qPCR and RT-qPCR	Promega (Madison, Wisconsin, USA)	#A6001
HCL	Merck (Darmstadt, Germany)	#4625.2
Kanamycin	Sigma Aldrich (St. Louis, Missouri, USA)	#60615
KCL	Merck (Darmstadt, Germany)	#104936
L-Glutathione, reduced	Sigma Aldrich (St. Louis, Missouri, USA)	#Y0000517
Loading Dye	New England Biolabs (Frankfurt am Main, Germany)	#B70245
Leupeptin	Sigma Aldrich (St. Louis, Missouri, USA)	# L9783-25MG
Lipofectamine 2000™	Thermo Fisher (Waltham, Massachusetts, USA)	#11668027
Methanol	VWR (Radnor, Pennsylvania, USA)	#20847.320
Mg_2Cl	Merck (Darmstadt, Germany)	#1058330250
Na_3VO_4	Sigma Aldrich (St. Louis, Missouri, USA)	#56508
NaCl	Carl Roth (Karlsruhe, Germany)	#3957.1
NaOH	Merck (Darmstadt, Germany)	#1.06498.500
Pefabloc	Sigma Aldrich (St. Louis, Missouri, USA)	# 76307-100MG
ReBlot Plus Strong Antibody Stripping Solution	Merck Millipore (Darmstadt, Germany)	#2504
Recombinant human EGF	Roche (Basel, Switzerland)	#11376454001
Recombinant human IL-1β	Roche (Basel, Switzerland)	#11457756001

Recombinant human TNFα	Roche (Basel, Switzerland)	#11088939001
SDS	Sigma Aldrich (St. Louis, Missouri, USA)	#L3771
siGENOME Non-Targeting-siRNA #1	Dharmacon (Colorado, USA)	#D-001210-01-05
siGENOME Non-Targeting-siRNA #3	Dharmacon (Colorado, USA)	#D-001210-03-05
siGENOME Non-Targeting-siRNA #5	Dharmacon (Colorado, USA)	#D-001210-05-05
siGENOME SMARTpool Human AKT1 siRNA	Dharmacon (Colorado, USA)	#M-003000-03-0005
siGENOME SMARTpool Human ATF2 siRNA	Dharmacon (Colorado, USA)	#M-009871-00-0005
siGENOME SMARTpool Human CREB1 siRNA	Dharmacon (Colorado, USA)	#M-003619-01-0005
siGENOME SMARTpool Human C/EBPβ siRNA	Dharmacon (Colorado, USA)	#M-006423-03-0005
siGENOME SMARTpool Human EGF siRNA	Dharmacon (Colorado, USA)	#M-011650-01-0005
siGENOME SMARTpool Human MEK1 siRNA	Dharmacon (Colorado, USA)	#M-003571-01-0005
siGENOME SMARTpool Human MAP3K7 siRNA	Dharmacon (Colorado, USA)	#M-003790-06-0005
siGENOME SMARTpool Human MAPK8 siRNA	Dharmacon (Colorado, USA)	#M-003514-04-0005
siGENOME SMARTpool Human MAPK9 siRNA	Dharmacon (Colorado, USA)	#M-003505-02-0005
siGENOME SMARTpool Human RELA siRNA	Dharmacon (Colorado, USA)	#M-003533-02-0005
siGENOME SMARTpool Human SP1 siRNA	Dharmacon (Colorado, USA)	#M-026959-00-0005
Spermidine	Sigma Aldrich (St. Louis, Missouri, USA)	#56766
TEMED	Sigma Aldrich (St. Louis, Missouri, USA)	#9281
Tetrasodium pyrophosphate	Sigma Aldrich (St. Louis, Missouri, USA)	#SLBW3580
Tris	VWR (Radnor, Pennsylvania, USA)	#103156X
Triton X-100	Merck (Darmstadt, Germany)	#CC-1025
Tryptone/Peptone	Merck (Darmstadt, Germany)	#1022390500
Tween 20	Merck (Darmstadt, Germany)	#8221840050

Western Lightning Plus-ECL	Perkin Elmer (Waltham, Massachusetts, USA)	# NEL104001EA
Yeast extract	Sigma Aldrich (St. Louis, Missouri, USA)	#70161

2.4 Kits

Tab. 6- List of kits used in this study.

Item	Company	Item number
Human Custom ProcartaPlex 8-plex	Thermo Fisher (Waltham, Massachusetts, USA)	#PPX-08-MXGZFPT
Human IL-8 ELISA Ready-SET GO! (S Generation)	Thermo Fisher (Waltham, Massachusetts, USA)	#88-8086-22
NucleoBond Xtra Midi	Macherey Nagel (Düren, Germany)	#740410
NucleoSpin	Macherey Nagel (Düren, Germany)	#740588
NucleoSpin Gel and PCR clean-up	Macherey Nagel (Düren, Germany)	#740609
QIAGEN Plasmid Giga Kit	Qiagen (Hilden, Germany)	#12191
QIAshredder	Qiagen (Hilden, Germany)	#79656
QuantiTect Reverse Transcription Kit	Qiagen (Hilden, Germany)	#205314
RNeasy Mini Kit	Qiagen (Hilden, Germany)	#74106
Simple ChIP Enzymatic Chromatin IP Kit Magnetic Beads	Cell Signaling (Cambridge, UK)	#9003
VenorGEM Mycoplasma Detection Kit	Minerva Biolabs (Berlin, Germany)	#11-1050

2.5 PCR and molecular cloning

Tab. 7- List of components for PCR and molecular cloning.

Item	Company	Item number
dNTP mix	eBioscience (San Diego, USA)	#15521197
GoTaq qRT-PCR Master Mix	Promega (Madison, Wisconsin, USA)	#A6002
High-Fidelity DNA Polymerase	Qiagen (Hilden, Germany)	#74104
IPTG	Qiagen (Hilden, Germany)	#205314
Oligonucleotides	Eurogentec (Lüttich, Belgium); Eurofins (Luxemburg)	
Restriction enzymes	Macherey Nagel (Düren, Germany)	#740609
RNasin Ribonuclease inhibitor	Macherey Nagel (Düren, Germany)	#740588
rNTP mix	Merck (Darmstadt, Germany)	#79656
Sequencing	Eurofins (Luxemburg)	
Smart Ladder/MassRuler DNA Ladder Mix	Fermentas (Waltham, Massachusetts, USA)	#SM0408
Smart Ladder Low Range/MassRuler	Thermo Fisher (Waltham, Massachusetts, USA)	#SM0383
T4-DNA Ligase	New England Biolabs (Ipswich, Massachusetts, USA)	#M0202
T7-RNA Polymerase	Promega (Madison, Wisconsin, USA)	#P207E
Taq-Polymerase Hot Start 5U/µL 250Units	Minerva Biolabs (Berlin, Germany)	#53-0250

2.6 Antibodies

Tab. 8- List of antibodies used in this study.

Item	Company	Item number
AKT	Cell Signaling (Cambridge, UK)	#9272
AKT (pan) (40D4)	Cell Signaling (Cambridge, UK)	#2920
AKT pS473	Cell Signaling (Cambridge, UK)	#3787
β-actin	Abcam (Cambridge, UK)	#ab6276
EGFR	Cell Signaling (Cambridge, UK)	#2232
EGFR pY1068	Cell Signaling (Cambridge, UK)	#2234
EGFR pY1173	Cell Signaling (Cambridge, UK)	#4407
ERK 1/2	Cell Signaling (Cambridge, UK)	#4695
ERK 1/2 pT202/pY204	Cell Signaling (Cambridge, UK)	#9106
Goat anti-Mouse Alexa Flour 488	Abcam (Cambridge, UK)	#ab150117
Goat anti-Rabbit Alexa Flour 647	Abcam (Cambridge, UK)	#ab150083
HCV NS3 [8-G-2]	Abcam (Cambridge, UK)	#ab65407
HCV NS3 [H23]	Abcam (Cambridge, UK)	#ab13830
HRP-coupled goat anti-rabbit	Agilent Technologies (Glostrup, Denmark)	#P0448
HRP-coupled rabbit anti-mouse	Agilent Technologies (Glostrup, Denmark)	#P0260
JNK	Cell Signaling (Cambridge, UK)	#9252
JNK pT183/pY185	Cell Signaling (Cambridge, UK)	#9251
MEK1/2	Cell Signaling (Cambridge, UK)	#9122
MEK1/2 pS217/pS221	Cell Signaling (Cambridge, UK)	#9121
NFκB p65	Cell Signaling (Cambridge, UK)	#6956
NFκB p65 (D14E12)	Cell Signaling (Cambridge, UK)	#8242
NFκB p65 pS536	Cell Signaling (Cambridge, UK)	#3033

p38^{MAPK}	Cell Signaling (Cambridge, UK)	#9212
p38^{MAPK} pT180/pY182	Cell Signaling (Cambridge, UK)	#9211
TCPTP	Cell Signaling (Cambridge, UK)	#58935

2.7 Inhibitors

Tab. 9- List of inhibitors used in this study.

Item	Company	Item number
AG1478	Sigma Aldrich (St. Louis, Missouri, USA)	#658552
IKK-2 Inhibitor	Sigma Aldrich (St. Louis, Missouri, USA)	#401479
JNK I Inhibitor	Merck (Darmstadt, Germany)	#420116
SB203580 HCl	Promega (Madison, Wisconsin, USA)	#A6001
Triciribine	Merck (Darmstadt, Germany)	#79656
U0126	Qiagen (Hilden, Germany)	#205314

2.8 Bacterial strains

Tab. 10- Bacterial strains used in this study.

Item	Company	Item number
E. coli *JM109*	Promega (Madison, USA)	#L2005

3 Methods

3.1 Cell biological methods

3.1.1 Cell culture

The human hepatoma cell line Huh7 and the Huh9.13 cell line harbouring the subgenomic HCV GT 1b-derived replicon were cultured in Dulbecco's modified Eagle's medium/nutrient mix F-12 (DMEM/F12) supplemented with 10 % (vol/vol) heat-inactivated fetal bovine serum (FBS) at 37 °C in a humidified atmosphere with 5 % CO_2. In the case of Huh9.13 cells, 2 % Geneticin was added to the medium to guarantee integration of the replicon due to Geneticin resistance. The human hepatoma cell line Huh7.5 was cultured in DMEM 4.5 g/L glucose supplemented with 9 % (vol/vol) heat-inactivated FBS, 2 mM glutamine, 100 U/mL penicillin, 100 µg/mL streptomycin, 1 % nonessential amino acids (modified Eagle medium nonessential amino acids solution). Medium was changed 16 h before experiments were performed. The use of the different Huh cell lines is covered by a material transfer agreement with Apath, L.L.C. (New York City, New York, USA). All cell lines were tested regularly for mycoplasma contamination using the Venor GeM Mycoplasma PCR Detection Kit according to the manufacturer's instructions. To freeze cells, they were seeded for 3-4 days in 75 cm^2 cell culture flasks. Once the cells were about 90 % confluent they were washed once with PBS, 1 mL Trypsin was added, and cells were incubated for 4 min at 37 °C and 5 % CO_2 in the incubator. Subsequently 9 mL medium was added for resuspension followed by a centrifugation step at 4 °C at 90 g for 10 min. The supernatant was discarded, and the pellet was resuspended in the medium used for the specific cell type, as depicted in Tab. 11 containing 10 % dimethyl sulfoxide (DMSO) and 20 % FBS. In general, growth medium was changed every 2 days and cells were passaged every 3 to 4 days.

Tab. 11- List of cell lines used in this study. Cell lines, description, cell culture media and supplements to the cell culture media used are listed below.

Cell line	Description	Culture media	Supplements
Huh7	Human hepatoma cell line	DMEM/HAM's F-12	10 % FCS

Huh9.13*	Human hepatoma cell line Huh7 with integrated subgenomic replicon (NS3-NS5B) of HCV (GT1b)	DMEM/HAM's F-12	10 % FCS 1 mg/mL Geneticin
Huh7.5**	Human hepatoma cell line, which carries a *RIG-I* mutation	DMEM (4.5 g/L Glucose)	10 % FCS 2 mM Glutamine 100 U/mL Penicillin 100 µg/mL Streptomycin 1x NEAA
Huh7.5 AKT1 1.1 KO***	Human hepatoma cell line Huh7.5, which carries a *RIG-I* mutation and *AKT1* is stably knocked out	DMEM (4.5 g/L Glucose)	10 % FCS 2 mM Glutamine 100 U/ml Penicillin 100 µg/mL Streptomycin 1x NEAA
Huh7.5 AKT1 2.3.5 KO***	Human hepatoma cell line Huh7.5, which carries a *RIG-I* mutation and *AKT1* is stably knocked out	DMEM (4.5 g/L Glucose)	10 % FCS 2 mM Glutamine 100 U/mL Penicillin 100 µg/mL Streptomycin 1x NEAA
Huh7.5 TCPTP 4.6 KO***	Human hepatoma cell line Huh7.5, which carries a *RIG-I* mutation and *TCPTP* is stably knocked out	DMEM (4.5 g/L Glucose)	10 % FCS 2 mM Glutamine 100 U/mL Penicillin 100 µg/mL Streptomycin 1x NEAA
Huh7.5 TCPTP 2.3 KO***	Human hepatoma cell line Huh7.5, which carries a *RIG-I* mutation and *TCPTP* is stably knocked out	DMEM (4.5 g/L Glucose)	10 % FCS 2 mM Glutamine 100 U/mL Penicillin 100 µg/mL Streptomycin 1x NEAA

Huh7.5 TCPTP 3.4 KO***	Human hepatoma cell line Huh7.5, which carries a *RIG-I* mutation and *TCPTP* is stably knocked out	DMEM (4.5 g/L Glucose)	10 % FCS 2mM Glutamine 100 U/mL Penicillin 100 µg/mL Streptomycin 1x NEAA

*provided by Ralf Bartenschlager, Heidelberg, Germany

**provided by the company Apath, New York, USA

***Generated from Huh7.5 cells using CRISPR/Cas9 **(3.2.8)**

3.1.2 Transfection procedure with small interfering RNA

For lipofection of small interfering RNAs (siRNAs), cells were seeded one day before transfection. Afterwards cells were counted using a Neubauer chamber, 1.5 * 10^5 Huh9.13 cells or 1 * 10^5 Huh7 cells were seeded in 6-well plates or 0.7 * 10^5 Huh7.5 cells were seeded in 12-well plates. On the following day, specific siRNAs were diluted in 1x siRNA buffer to obtain a final concentration of 5 µM. The siRNA or the non-targeting siRNAs were mixed with DharmaFect4 reagent according to the manufacturer´s instructions. Shortly, to obtain a 5 nM concentration of the siRNA in a 6-well with a total volume of 2000 µL, 5 µl Dharmafect4 were added to 195 µL OptiMEM and in parallel 180 µL OptiMEM was mixed with 20 µL of a 5 µM targeting or non-targeting siRNA. After 5 min incubation at room temperature (RT), Dharmafect4 and siRNA dilution were combined and after additional 20 min, 400 µL for 6-well plates or 200 µL for 12-well plates were added to the cells where the media was changed in the meanwhile to 1600 µL for 6-well plates or 800 µL for 12-well plates of the respective culture medium without antibiotics. After 6-8 h transfection medium was changed and the cells were incubated for additional 72 h.

3.1.3 Transfection Procedure with plasmids containing Cas9, gRNA and GFP

Cells were seeded one day before transfection. After counting, 5 * 10^5 cells were seeded in 6-well plates. After 24 h, 2.5 µg of the specific plasmid were added to OptiMEM to receive a total volume of 150 µL. Additionally, 10 µL Lipofectamin2000 were added to 140 µL OptiMEM and incubated for 5 min at RT. The two solutions were combined by pipetting the Lipofectamine2000 solution up and down into the plasmid solution and were incubated for another 20 min at RT. 250 µL of the Lipofectamin2000/plasmid suspension were added dropwise to the cells after adding the respective culture medium (containing antibiotics) to the cells. The plasmid amount was 2 µg. Cells were incubated for 72 h without medium change.

3.2 Molecular biological methods

3.2.1 RNA isolation and cDNA synthesis

For mRNA isolation, cells were lysed in 100-150 µL of RLT buffer containing 0.1 % fresh β-mercaptoethanol. The lysates where homogenized using the QIAshredder and isolated using the RNeasy Mini Kit according to manufacturer's instructions. Afterwards, RNA concentrations were measured at 260 nm using the spectrophotometer Nanodrop1000 (Thermo Scientific). The calculations are based on the Beer-Lambert-law (285). 1 µg of total RNA was reverse transcribed via the QuantiTect Reverse Transcription Kit. To get rid of genomic DNA (gDNA) contamination, 2 µL of gDNA wipe out was added to the sample and the sample was incubated for 2 min at 42 °C. Directly afterwards, 4 µL of 10x reaction buffer and 1 µL of reverse RNA-dependent DNA polymerase reverse transcriptase (rT) and 1 µL primer mix were added to the sample. Reverse transcription was carried out at 42 °C for 25 min and terminated by inactivating the rT via incubation of the sample at 95 °C for 5 min. Finally, the sample was diluted 1/8 with RNase-free water.

3.2.2 Quantitative real time PCR

The quantitative real time PCR (qRT-PCR) is a method to measure the fluorescence increase in real time. In this study the dye cyanine (SYBR Green) was used. SYBR Green intercalates into double-stranded DNA, which leads to a fluorescent signal. The intensity of the fluorescence can be measured in real time. Hence, the amount of a target sequence can be quantified. The quantification is done in the exponential phase of the PCR when the fluorescent signal is higher than the background signal. As SYBR Green can also bind to primer dimers, it is of highest importance to perform a melting curve at every PCR run to check for unspecific binding such as primer dimer formation which results in peaks at a melting temperature different from that of the desired PCR product. Primers were designed using Primer3Plus (http://www.bioinformatics.nl/cgi-bin/primer3plus/primer3plus.cgi/) and checked for specificity in the PubMed database using primer blast (https://www.ncbi.nlm.nih.gov/tools/primer-blast/). 1.6 µL of the diluted cDNA was added as template to a final volume of 20 µL including 1x SYBR Green PCR master mix. The primers used are listed in Tab. 12. The final concentration of the primers was 400 nM. No template and no reverse transcriptase controls were used to control specificity of qRT-PCR. During qRT-PCR, the cDNA was heated for denaturation at 95 °C for 10 min. Amplification was performed for 40 cycles with 2 steps: the cDNA was heated for another 15 s at 95 °C for denaturation and then cooled to 60 °C for 1 min for the elongation process. All samples were measured in duplicates and mean values calculated.

Semiquantitative PCR results were obtained using the $\Delta\Delta C_T$ method (286). The C_T (cycle threshold) value represents the point where the fluorescence of the product overreaches the background fluorescence the first time. Apart from Fig. 11, *SDHA* was used as reference gene for calculation of the qRT-PCR data presented in this thesis. Quantification cycles were normalized to *SDHA* and in Fig. 11 also to the reference genes *HPRT-1*, *HBMS*, *GAPDH* or *TBP*. Data from at least three independent experiments are presented as mean + standard error of means (SEM). For data analysis, the software of ViiA^{TM}7 RUO (Applied Biosystems) (2010) was used.

Tab. 12- Primer pairs used for qRT-PCR. Sequences are given 5´-> 3´.

Name	**NS5A Replicon**
Sense	AAT-TAT-TCT-AGG-GCG-CTG-TGG
Antisense	GAG-CTG-TGA-CCC-AAC-CAG-GT
Name	**CXCL8**
Sense	AGA-AGT-TTT-TGA-AGA-GGG-CTG-AGA
Antisense	CAG-ACC-CAC-ACA-ATA-CAT-GAA-GTG
Name	**NS5A JC1**
Sense	GTT-GCT-GGA-GGG-CTT-CTG-AT
Antisense	CCG-TTG-CTG-GTT-GTG-CTC-T
Name	**SDHA**
Sense	AGA-TGT-GGT-GTC-TCG-GTC-GAT
Antisense	CGT-GAT-CTT-TCT-CAG-GGC-CA
Name	**YWHAZ**
Sense	GTG-AGC-AGC-GAG-ATC-CAG-GG
Antisense	CGA-CAA-TCC-CTT-TCT-TGT-C
Name	**B2M**
Sense	CTC-CGT-GGC-CTT-AGC-TGT-G
Antisense	TTT-GGA-GTA-CGC-TGG-ATA-GCC-T
Name	**GAPDH**
Sense	TGC-ACC-ACC-AAC-TGC-TTA-GC
Antisense	GGC-ATG-GAC-TGT-GGT-CAT-GAG
Name	**HMBS**
Sense	TGC-AAC-GGC-GGA-AGA-AAA
Antisense	ACG-AGG-CTT-TCA-ATG-TTG-CC
Name	**HPRT-1**

Sense	TGA-CAC-TGG-CAA-AAC-AAT-GCA
Antisense	GGT-CCT-TTT-CAC-CAG-CAA-GCT
Name	**UBC**
Sense	CGG-TGA-ACG-CCG-ATG-ATT-AT
Antisense	ATC-TGC-ATT-GTC-AAG-TGA-CGA
Name	**TBP**
Sense	TTC-GGA-GAG-TTC-TGG-GAT-TGT-A
Antisense	TGG-ACT-GTT-CTT-CAC-TCT-TGG-C
Name	**CXCL2**
Sense	GCA-GGG-AAT-TCA-CCT-CAA-GA
Antisense	GAC-AAG-CTT-TCT-GCC-CAT-TC
Name	**PUMA**
Sense	GAC-GAC-CTC-AAC-GCA-CAG-TA
Antisense	GGT-AAG-GGC-AGG-AGT-CCC-AT
Name	**PPARγ**
Sense	GGG-CGA-TCT-TGA-CAG-GAA-AG
Antisense	GGG-GTG-ATG-TGT-TTG-AAC-TTG-AT
Name	**EGF**
Sense	CCA-GCT-CTG-CGT-TCC-TCT-TA
Antisense	GCA-AAC-AGC-AAA-AAT-GGT-TGT-GG
Name	**CXCL1**
Sense	CTG-GCG-GAT-CCA-AGC-AAA-T
Antisense	CAT-TCC-CCT-GCC-TTC-ACA-AT
Name	**CXCL3**
Sense	TGC-TTG-TAG-GGC-ATA-ATG-CCT
Antisense	AGA-GAA-ACG-CTG-CAG-AAT-GGA
Name	**NfκB p65**
Sense	CCT-GTC-CTT-TCT-CAT-CCC-ATC-TTT
Antisense	ATC-TCA-TCC-CCA-CCG-AGG-CA
Name	**NfκB p65**
Sense	CAG-TGT-GTG-AAG-AAG-CGG-GA
Antisense	TCC-CCA-CGC-TGC-TCT-TCT-AT
Name	**NS3 JC1**
Sense	CTA-CGG-TGT-GCG-CCA-GAG
Antisense	CCC-AAA-CGG-TAC-AGG-AGA-GG

Name	**TCPTP or PTPN2**
Sense	CAC-AGG-GTC-CAC-TTC-CTA-ACA
Antisense	TTC-AGC-ATG-ACA-ACT-GCT-TTG
Name	**SLC19A1**
Sense	ACC-TTT-GCT-TCT-ACG-GCT-TC
Antisense	CCG-GCG-TGA-TCT-CGT-TC
Name	**SHMT**
Sense	ACT-ATG-GCG-GGA-CTG-AGT-TT
Antisense	CTG-AGT-AGG-GCT-GGA-CGT-TG
Name	**PHGDH**
Sense	AAA-GAG-GAG-CTG-ATA-GCG-GAG
Antisense	TTT-CTC-AGC-TGC-GTT-GAT-GAC
Name	**PRPS1**
Sense	CAG-AAA-ATT-GCT-GAC-CGC-CTG
Antisense	TCC-TCT-CCA-CGT-ACA-CTT-TCA-C
Name	**UCK2**
Sense	GCC-AGT-TCA-ACT-TTG-ACC-ACC
Antisense	TAC-ACG-GGG-ATC-TGG-ACT-GT
Name	**CXCL8IN1EX2**
Sense	TTA-ACA-ACA-TCG-TAA-GTC-AAA-CTC-A
Antisense	GGA-AAT-TAG-TCC-CAG-CTC-AAC-A
Name	**TAK1 FWD REV1**
Sense	AAC-GGA-CAGC-CAA-GAC-GTA-G
Antisense	TCA-GGG-GTC-CAT-GGA-TGA-CT
Name	**JNK1 FWD REV1**
Sense	AGA-AGC-AAG-CGT-GAC-AAC-AA
Antisense	CGG-CTT-AGC-TTC-TTG-ATT-GC

3.2.3 Restriction and ligation of DNA fragments

To check for correct sizes of cloning reactions, restriction digests were performed. Class II restriction enzymes were used. These restriction enzymes recognize palindromic sequences and cleave them (287). All restriction enzymes were purchased from New England Biolabs with the indicated reaction buffers ensuring highest activity and specificity.
50-200 ng DNA were mixed with 10-20 Units of restriction enzyme, filled to a total volume of 10 µL with water and incubated for 1 h at 37 °C. After heat inactivation for 20 min, at 65 to 80 °C depending on the enzyme, samples were loaded on 1 % agarose gels and gel electrophoresis was performed at 120 V. Linearized plasmid backbones were dephosphorylated by addition of 1/10 volumes Antarctic Phosphatase 10 x reaction buffer and 5 µL Antarctic Phosphatase.
Reaction was applied on an agarose gel and the band was either cut out of the gel or directly purified if only 1 band appeared. The DNA was extracted from the gel piece or PCR product using the NucleoSpin Gel and PCR clean up kit according to the manufacturer`s instructions.
For the ligation of DNA fragments, molar insert to vector ratio was 2: 1. Ligation was carried out by adding 0.5 µL T4 DNA ligase (400 000 U/mL) for a total of 10 µL and 1x ligation buffer (50 M Tris-HCL, 10 mM $MgCl_2$, 1 mM ATP, 10 mM DTT, pH 7.5) were added and incubated for 10 min at RT.

3.2.4 Transformation of competent *E. coli* bacteria

Competent *E. coli* strain JM109 were thawed on ice for 5 min. 5 µL of the ligation mix were added to 50 µL competent *E. coli* and incubated for 10 min on ice. Bacteria were heat shock transformed at 42 °C for 45 s to generate pores in the membrane of *E. coli* and thus introduce the DNA. Cells were then incubated for 2 min on ice and afterwards recovered by addition of 900 µL LB medium (5 g/L yeast extract, 10 g/L tryptone, 5 g/L natrium chloride) and incubation in a shaker at 150-300 rpm for 1 h at 37 °C. 100-200 µL were streaked on an agar plate containing the respective antibiotics (ampicillin [50 mg/L] or kanamycin [25 mg/L]) to allow for selection of successfully transformed cells, and incubated overnight at 37 °C.
For cryoconservation, an overnight culture of 800 µL LB media plus 200 µL glycerol was prepared and stored at -80 °C.

3.2.5 Preparation of plasmid DNA from bacterial cells

The isolation of bacterial DNA was performed according to the manufacturer`s instruction via NucleoBond Xtra Midi or the QIAprep Spin Miniprep or Gigaprep Kit. Afterwards, DNA concentration was measured at 260 nm using the spectrophotometer Nanodrop1000 (Thermo Scientific).

3.2.6 Polymerase chain reaction

For each reaction, 12.8 µL DNase free water, 2 µL 10x RctBuffer, 0.3 µL $MgCl_2$ [100 mM], 0.4 µL dNTPs [10 mM each], 5 µL Taq Polymerase Hot Start, 2 µL Primermix (1: 2 each primer) and 2 µL sample, or water for the negative control, were mixed and added to the polymerase chain reaction (PCR) cycler at the following conditions according to the annealing temperature of the primer pair: 95 °C for 5 min for denaturation, followed by 35 cycles of 95 °C for 30 s (annealing), 62 (RLP30) or 54 °C (*CXCL8* NFκB binding site) for 30 s (dependent on the melting temperature (Tm) of the primer pair) and 72 °C for 30 s (extension). A final elongation step at 72 °C for 5 min was included before samples were cooled to 4 °C. For Tm calculation the New England Biolabs Tm calculator was used which uses the method of Santa Lucia and the alternate salt correction to allow compatibility (288, 289). The PCR reactions were performed in 0.2 mL tubes using the thermocycler PTC-200 (MJ-Research).

Tab. 13- Primer pairs for PCR. Sequences are given 5´-> 3´.

Name	**CXCL8 NFκB binding site**
Sense	AAG-AAA-ACT-TTC-GTC-ATA-CTC-CG
Antisense	TGG-CTT-TTT-ATA-TCA-TCA-CCC-TAC

3.2.7 Agarose gel electrophoresis

To check whether the product of interest was amplified during PCR, the size of the amplified DNA fragment was controlled. Therefore, an agarose gel electrophoresis was performed. 1 % (v/w) agarose gels were cast by dissolving agarose in buffer TAE 1x (242 g/L Tris, 100 mL/L EDTA 0,5 M pH 8.0, 1 mL/L acetic acid) in the microwave at 900 W for 2 min. After cooling down, 6 drops of ethidium bromide [250 µg/mL] were added, and the agarose solution filled into a chamber for polymerization. After polymerization, 6x Gel Loading Dye was added to the samples and the samples loaded. MassRuler or MassRuler Low Range DNA ladder was used as size marker (Thermo Fisher Scientific). Imaging of the gel was performed using a Doc-Print-

Gel documentation system (Peqlab).

3.2.8 Generation of knockout cell lines using the CRISPR/Cas9 method

To protect itself from invading viruses and plasmids, bacteria and archea have developed a system termed clustered regularly-interspaced short palindromic repeats ((CRISPR)/CRISPR-associated endonuclease (Cas)) (290). Gene editing tools perform double strand breaks (DSBs) and therefore switch on the cellular repair machinery, which uses nucleotides in the environment to refill the breaks. This refilling is error-prone and can lead to deletions or insertions causing translation of unfunctional proteins or complete absence of translation of a specific protein. A DSB can be repaired by two different pathways, either the homology-directed repair or the non-homologous end joining (NHEJ) (291) (Fig. 9). To generate knockout (KO) cell lines, the plasmid px458-mCherry expressing Cas9 and fluorescent protein mCherry via a post-translationally cleaved 2A tag (292, 293) was linearized via *BpiI*-HF as described in **3.2.3**. The gene-specific sgRNAs were designed containing 4 nucleotide overhangs for ligation into the plasmid backbone (Tab. 14). The ssDNA sgRNAs were hybridized, phosphorylated, and ligated into dephosphorylated linearized plasmid backbone. To this end, 1 µL sgRNA forward [100 mM], 1 µL sgRNA reverse [100 mM], 1 µL T4 ligation buffer, 1 µL T4 polynucleotidkinase and 6 µL water were mixed per reaction and incubated at 37 °C for 30 min, followed by incubation at 72 °C for 20 min and 5 min at 95 °C, followed by 14 cycles whereby after each cycle the temperature was reduced by 5 °C. The samples were stored at 4 °C. The plasmid additionally contains an ampicillin resistance allowing for positive selection of transformed bacteria. Competent *E. coli* JM109 were transformed as described in **3.2.4** and grown on agar plates containing 1 mg/mL ampicillin.
The day after, DNA was extracted via a mini preparation kit as described in **3.2.5**. The plasmid DNA was sequenced by Sanger sequencing (Eurofins). Huh7.5 cells were transfected with the plasmid according to **3.1.3**. Afterwards, single cells were sorted into 96-well plates containing 100 µL DMEM (DMEM containing 10 % FCS, 1 % Penicillin/Streptomycin, 1 % Glutamine and 1 % non-essential-amino-acids (NEAA)) using the FACS Aria III (BD Bioscience). After sorting, the cells were grown for about 4-5 weeks. Afterwards, genotyping touchdown PCR (**3.2.9**) followed by Sanger sequencing and immunoblot (**3.3.3**) were performed for KO verification. To check the efficacy of the sgRNAs the remaining fluorescence positive cells were sorted into a 6-well plate. The genomic DNA was extracted from fluorescence-positive sorted bulk cells via the GenElute kit according to the manufacturer`s instruction. Elution was performed using 100 µL of the elution buffer. DNA concentration was determined via spectrophotometer NanoDrop1000 (Thermo Scientific) at 260 nm. The efficacy of each gRNA was determined comparing the potential KO to wild type sequence by tracking of indels via decomposition (294) (Tab. 15).

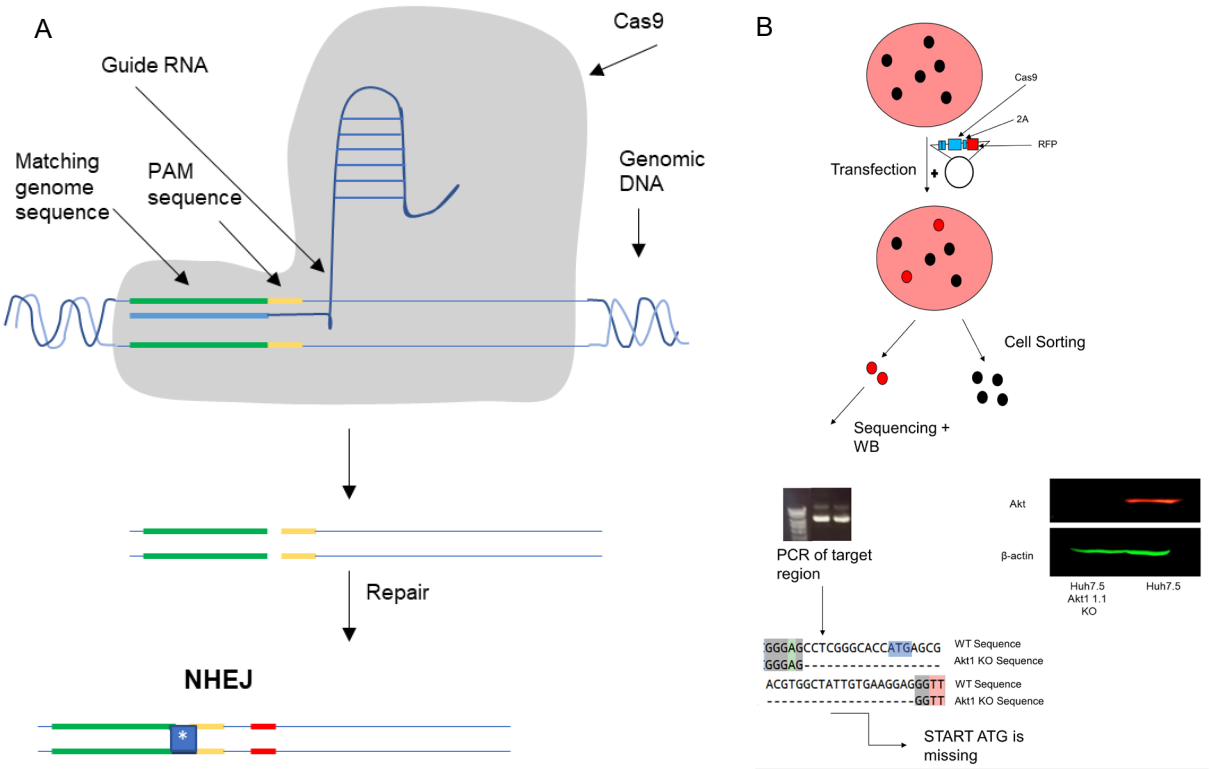

Fig. 9- Schematic depiction of the CRISPR/Cas9 system. A) The Cas9 endonuclease is guided via a specific guide RNA (gRNA) to the target sequence in the genome where it cleaves the DNA double strand. The repair mechanism of the cell refills the strand with nucleotides via non-homologous end joining. This error-prone process often leads to small insertions or deletions (indel mutations) of nucleotides which causes the loss of correct protein translation subsequently. B) The plasmid containing the Cas9 and the gRNA contains also the fluorescent protein RFP/mCherry. The cells were, in the case of this work, transfected via lipofection. Fluorescence-positive cells were then single-sorted via fluorescence-activated cell sorting (FACS) and verified via sequencing and immunoblotting. Modified to: https://www.computescotland.com/crisprcas9-genome-editing-8111.php.

Tab. 14- Sequence of sgRNAs used in this study. Sequences are given 5´-> 3´.

Name	**TCPTP-sgRNA1**
Sense	CAC-CCC-ACT-CTA-TGA-GGA-TAG-TCA
Antisense	AAA-CTG-ACT-ATC-CTC-ATA-GAG-TGG
Name	**TCPTP-sgRNA2**
Sense	CAC-CAA-ACC-CAC-AAG-TAC-TTA-CAT
Antisense	AAA-CAT-GTA-AGT-ACT-TGT-GGG-TTT
Name	**AKT1-sgRNA1**
Sense	CAC-CGA-GCG-ACG-TGG-CTA-TTG-TGA
Antisense	AAA-CTC-ACA-ATA-GCC-ACG-TCG-CTC
Name	**AKT1-sgRNA2**
Sense	CAC-CGA-GGG-TTG-GCT-GCA-CAA-ACG
Antisense	AAA-CCG-TTT-GTG-CAG-CCA-ACC-CTC

Tab. 15- Efficacy of sgRNAs used in this study.

sgRNA	Efficacy (percentage of non-wildtype sequence)
AKT1 sgRNA1	40,2%
AKT1 sgRNA2	43,1%
TCPTP sgRNA1	1%
TCPTP sgRNA2	35,2%

3.2.9 Touchdown PCR

To make sure PCR is working best, different conditions for each primer pair were tested. To this end, different approaches were used: with or without DMSO and with different primer concentrations [500 or 1000 nM]. 5 µL RctBuffer 10x, 2 µL $MgSO_4$ [1 mM final concentration], 0.25 µL VentPolymerase, with or without 2.5 µL DMSO, 1 µL dNTP mix (10 mM each) and 500 nM or 1000 nM of each primer (forward and reverse) were prepared as mastermix and filled with DNAse-free water to a final volume of 50 µL per reaction. The DNA was denaturated at 95 °C for 5 min. Afterwards, 11 cycles of 95 °C for 1 min (annealing), 70 or 65 °C for 1 min (dependent on Tm of the primer pair), and 72 °C for 1 min (extension) followed by 25 cycles of 95 °C for 1 min, 60 °C or 56 °C for 1 min (dependent on Tm of the primer pair), 72 °C for 1 min were performed. A final elongation step at 72 °C for 5 min was included before samples were cooled to 4 °C. For Tm calculation the New England Biolabs Tm calculator was used as described in **3.2.6**. The PCR reactions were performed in 0.2 mL tubes using the thermocycler PTC-200 (MJ-Research). Primer pairs used for touchdown PCR are listed in Tab. 16.

Tab. 16- Primer pairs for touchdown PCR. Sequences are given 5´-> 3´.

Name	**TCPTP**
Sense	AGC-CTT-TCA-TCC-CTC-ACA-GA
Antisense	CCA-AGC-CCT-CCT-TTT-CAC-TA
Name	**AKT**
Sense	TGG-GGG-TCA-GAG-AGC-TTA-GA
Antisense	CAC-AGA-CCC-TGG-GGC-TAC-TA

3.2.10 Chromatin Immunoprecipitation

Chromatin immunoprecipitation (ChIP) is a method for studying DNA-protein interactions (295).

ChIP was performed according to the manufacturer`s instruction. Precisely, 2 * 10^6 Huh9.13 cells and 1.1 * 10^6 Huh7 cells were prepared in 15 cm plates and grown for 72 h. For each condition, 2 15-cm plates of Huh7 cells and 4 15 cm plates of Huh9.13 cells were seeded. Proteins were crosslinked to DNA by addition of 1250 µL 16 % formaldehyde to every 15 cm plate. In addition to that, 2 mL of 10x glycine were added to the cells and cells were incubated for 5 min. Afterwards, cells were washed twice with 20 mL ice-cold PBS and 2 mL pre-prepared PBS and protease inhibitor cocktail (PIC) was added to each 15 cm plate. After harvesting the cells, the plates of each condition were pooled into 15 mL falcons and centrifuged for 5 min at 4 °C at 2000 g. The supernatant was discarded, and the pellet was either frozen in liquid nitrogen or directly processed by resuspending the pellet in 1 mL Buffer A mixture (250 µL 4x buffer A, 750 µL water, 0.5 µL 1M DTT, 5 µL 200x PIC per IP prep) and incubated on ice for 10 min mixing the suspension every 3 min. For nuclei preparation and chromatin digestion, the double amount of buffer was used for Huh9.13 cells. Nuclei were pelleted by centrifugation for 5 min at 4 °C at 2000 g, supernatant removed, and cells resuspended in 1 mL ice-cold 1x Buffer B mixture (275 µL 4x Buffer B, 825 µL water, 0.55 µL 1M dithiothreitol (DTT) per immunoprecipitation (IP) prep). Centrifugation was repeated, the pellet resuspended in 100 µL 1x Buffer B mixture and transferred into a 1.5 mL tube. From here, both cell types were treated equally, meaning the same buffer amount was used for Huh7 and Huh9.13 cells. 0.5 µL Micrococcal Nuclease per IP was added, cells were incubated for 20 min at 37 °C to digest DNA to fragments of approximately 150-900 bp length. Every 3 min the tubes were inverted for mixing. The digestion was stopped by addition of 10 µL 0.5 M EDTA per IP and incubation on ice for 2 min. For nuclei preparation and chromatin digestion, the double amount of buffer was used for Huh9.13 cells. Nuclei were pelleted by centrifugation at 16000 g for 1 min at 4 °C and resuspended in 100 µL of 1x ChIP buffer mixture (10 µL 10x ChIP Buffer, 90 µL water, 0.5 µL 200x PIC per IP prep). The suspension of every sample was divided in two different 1.5 mL tubes and sonicated using the ultrasonic processor UP50H (Hielscher) at an amplitude of 40 %, 1 cycle, needle MS1 in 3 sets of 20 sec pulses with 20 sec pauses after every set. Lysates were clarified by centrifugation at 9400 g for 10 min at 4 °C. Supernatants from the same sample were reunited in a new 1.5 mL tube, 50 µL of each sample was removed for the analysis of chromatin digestion and the rest was frozen at -80 °C. To control whether chromatin digestion occurred correctly, 100 µL water was added to the 50 µL chromatin sample plus 6 µL 5 M NaCl and 2 µL RNAse A, vortexed and incubated at 37 °C for 30 min. Afterwards, additional 2 µL of Proteinase K were added, the samples vortexed and incubated for another

2 h at 65 °C. DNA was purified according to the manufacturer's instructions. 10 µL were applied on a 1 % agarose gel to check chromatin digestion and DNA concentration was determined by spectrophotometry using the spectrophotometer Nanodrop1000 (Thermo Scientific); the expected concentration is about 50-200 ng/µL. To perform chromatin immunoprecipitation, a mastermix containing 400 µL 1x ChIP Buffer and 2 µL 200x PIC per IP sample, including Histone H3 positive control and negative control IgG for each sample was prepared. For each reaction, 10 µg of sample was used and the amount was calculated based on the concentration amount of the sample determined by spectrophotometry. 10 µL were removed for 2 % input sample, which was used as the reference for densitometric analysis, and stored at -20 °C. To perform immunoprecipitation, the specific antibodies were added to the diluted chromatin and incubated overnight at 4 °C with rotation.

Magnetic beads were vortexed and 30 µL were immediately added to each IP sample and incubated for 2 h at 4 °C. Afterwards, the tubes were placed in a magnetic separation rack, supernatant was discarded and the beads washed once with 1 mL low salt wash buffer (300 µL 10x ChIP buffer, 2.7 mL water) and twice with 1 mL high salt wash buffer (100 µL 10x ChIP buffer, 70 µL 5 M NaCl) before 150 µL of 1x ChIP Elution buffer was added to the 2 % input sample and to the IP sample. Chromatin was eluted from the antibody by placing the tubes for 30 min at 65 °C with gentle vortexing (1200 rpm) and additional separation by the magnetic separation rack by transfer eluted chromatin supernatant in a new tube. Reverse cross-linking was performed using 6 µL of 5 M NaCl and 2 µL Proteinase K to all samples (including 2 % input control) and incubation at 65 °C. DNA was purified using spin columns according to the manufacturer's instruction. Primers were designed by determination of the binding site of the transcription factor of interest to the promoter region of interest from a data base (https://epd.epfl.ch//index.php) and primer binding sites were visualized using Snap Gene Viewer 5.0.6. Primers were designed using Primer3Plus. PCR was performed according to **3.2.6**. Densitometric calculations were performed using the Image Lab Software 6.0 (BioRad).

3.3 Biochemical methods

3.3.1 Preparation of total cell lysates, immunoblotting and immunodetection

For protein analysis of whole cell lysate samples, cells were washed once with PBS and resuspended in Triton lysis buffer (1 %Triton, 20 mM Tris/HCl pH 7.4, 13.6 mM NaCl, 2 mM EDTA, 50 mM β-glycerophosphate, 20 mM sodium pyrophosphate, 1 mM Na_3VO_4, 4 mM benzamidine, 0.2 mM Pefabloc, 5 µg/mL aprotinin, 5 µg/mL leupeptin, 10 % glycerol, and 0.2 % SDS) on ice. 100-150 µL Triton lysis buffer was used for one 6- or two 12-wells and 150 µL Triton lysis buffer was used for 6 cm plates. Protein-containing samples were vortexed and kept on ice for 10 min. They were then cleared, centrifuged for 15 min at 14000 rpm and 4 °C, and protein-containing supernatants transferred to fresh reaction tubes.

3.3.2 Protein concentration determination according to Bradford

The Bradford test is a photometric method to determine the protein concentration in a suspension. The triphenylmethane dye Coomassie-brilliant-blue G-250 forms complexes with nonpolar cationic side chains of proteins in an acidic solution resulting in a colour change from originally red to its blue anionic sulfonate mode. The absorption maximum is changing from 470 nm to 595 nm accordingly. Enhancement of the absorption in comparison with the free colour reagent can be measured spectrophotometrically and the protein concentration determined by Ultrospec 2100 *pro* (Amersham Biosciences).

3.3.3 SDS-PAGE and immunoblot

The sodium dodecyl phosphate polyacrylamide gel electrophoresis (SDS-PAGE) is a method to separate proteins according to their mass in an electric field. 30 µg of protein were mixed with 4x Lämmli-buffer (250 mM Tris/HCL pH 6.8, 40 % glycerol, 5 % SDS, 0.002 % bromophenol blue, 8 % 2-mercaptoethanol) and the mixture was boiled at 95 °C for 5 min to denature the proteins. Afterwards, samples were loaded onto a polyacrylamide gel between 10 and 15 % acrylamide content depending on the molecular mass of the proteins of interest. Precision Plus Protein Dual Color Standard (BioRAD) was used as a protein size marker. Separation of proteins during gel electrophoresis was performed at a constant voltage of 120 V. The electrophoretically separated proteins were transferred onto polyvinylidene difluoride (PVDF) membranes with 0.45 µm pore size by semidry western blotting at 1 mA/cm^2 gel constant current. For this, 5 *whatman* papers were dipped into anode buffer 1 (0.3 M Tris, 20

% methanol), 3 *whatman* papers were dipped into anode buffer 2 (0.025 M Tris, 20 % methanol) and placed above the *whatman* papers dipped in anode buffer 1 on the blotting chamber. Then, the preactivated (incubated in methanol for 30 s) PVDF membrane was placed above the *whatman* papers dipped in anode buffer 2, and the SDS gel was placed above the PVDF membrane. Finally, 5 *whatman* papers were dipped into the cathode buffer (0.04 M aminocaproic acid, 20 % methanol) and placed above the gel. The gel was blotted for 1-2 h depending on the molecular mass of the protein of interest. Nonspecific binding was blocked via 5 % bovine serum albumin (BSA) in Tris-buffered saline with Tween-20 (TBS-T) (20 mM Tris/HCl, pH 7.4, 137 mM NaCl, and 0.1 % Tween-20) for 1 h. After extensive washing with TBS-T (3 times 20 min), membranes were incubated with appropriate secondary antibodies (Tab. 7). After further extensive washing with TBS-T, the immunoblots were detected either by chemiluminescence or fluorescence depending on the secondary antibody coupled either to horse radish peroxidase (HRP) or fluorescence protein. Detection was carried out using the ChemiDOC MP system (BioRAD).

3.3.4 Enzyme-linked immunosorbent assay

The enzyme-linked immunosorbent assay (ELISA) is a method to quantify the content of a protein of interest in a given sample. Therefore, a microtiter plate is coated with a primary antibody and incubated with a sample containing the protein of interest which is binding to the primary antibody via antigen-antibody-binding. After this binding, it is immobilized. The secondary antibody is linked to an enzyme. The enzyme´s substrate is then added to the solution, resulting in a colour switch if the secondary antibody has bound to the antigen-antibody-complex. The plate must be washed carefully after every step. The colour switch can be measured photometrically. The manufacturer´s standard containing the protein of interest in known amount is used to create a standard curve to determine the protein concentration of the analysed samples.
To perform the ELISA, serum samples from patients chronically infected with HCV and, as a control, non-infected patients were collected, centrifuged at 1400 g and stored at -80 °C. ELISA was performed according to the manufacturer`s instructions.

3.3.5 ProcartaPlex Immunoassay

The ProcartaPlex Immunoassay allows the measurement of multiple protein targets in one single sample at the same time. Magnetic microsphere technology licensed by Luminex Corporation is used to simultaneously detect up to 100 protein targets. To perform the

ProcartaPlex Immunoassay, sera samples from patients chronically infected with HCV, patients without infection or healthy people were collected, centrifuged at 1400 g and stored at -80 °C until they were used. ProcartaPlex Immunoassay was performed according to the manufacturer`s instructions.

3.4 HCV-derived cell culture system

3.4.1 In vitro transcription

Because HCV is a ssRNA$^+$ virus, viral DNA first needs to be transcribed into RNA. 10 µg of viral DNA were digested using *MluI* and purified via the QIAquick PCR purification kit. The DNA was eluted in 60 µL RNAse free water. 20 µL 5x RRL-buffer (400 mM Hepes pH 7.5, 60 mM $MgCl_2$, 10mM spermidine, 200mM DTT), 12.5 µL rNTPs [25 mM], 2.5 µL RNasin [40 U/µL] and 4 µL T7/RNA polymerase [20 U/µL] were added to the eluate. After 3 h of incubation at 37 °C, another 2 µL of T7/RNA polymerase were added to the solution. The mixture was incubated overnight at 37 °C. On the next day, 2.5 µL [3 U/mL] DNAse were added for 30 min at 37 °C to the mixture to eliminate remaining DNA. The RNA was then purified using the RNeasy Mini Kit. The concentration of RNA was determined photometrically via NanoDrop1000 (Thermo Scientific) at 260 nm.

3.4.2 Electroporation

Huh7.5 cells were used for electroporation at 80-90 % confluency. After washing the cells once with PBS, they were detached using 1 mL trypsin, incubated for 4 min at 37 °C and 5 % CO_2, and resuspended in 9 mL cell culture medium. 1.5 * 10^7 cells were transferred to a 50 mL collection tube and centrifuged at 90 g for 10 min at 4 °C. The pellet was washed once with PBS and after another centrifugation step resuspended in 1 mL cytomix (120 mM KCl, 0.15 mM $CaCl_2$, 10 mM kaliumphosphate buffer pH 7.6, 25 mM Hepes pH 7.6, 2 mM EGTA, 5 mM $MgCl_2$) containing ATP (2mM, pH 7.6) and GSH [5mM]. For the electroporation, 400 µL cell suspension were mixed with 10 µg viral RNA while pipetting the RNA three times up and down in an electroporation tube. The tube was placed inside the electroporation chamber and cells were electroporated with 975 µF and 270 V using the Gene Pulser Xcell Electroporation System (BioRad). The time constant was at 20 ms. One and a half electroporation approaches were pooled in 18 mL Huh7.5 medium and plated on a 15 cm plate.

Tab. 17- Strain used for HCV-derived cell culture system.

Name	Description
JC1	pFK_JH1/J6/C-846_dg

3.4.3 Virus harvest and PEG precipitation

The supernatant of the electroporated cells was collected after 24 h, 48 h and 72 h. At every time point, the supernatant was centrifuged at 1000 rpm for 5 min at RT, transferred into a new falcon and stored at 4 °C. Immediately after collection of the last time point, 4.8 mL PEG-8000/PBS was added to 20 mL of collected supernatant for virus precipitation. The supernatants were then incubated for 72 h at 4 °C. Afterwards, they were centrifuged at 8000 g for 90 min at 4°C. The pellet was resuspended in 250 µL DMEM per plate and all samples pooled, aliquoted and stored at -80 °C.

3.4.4 TCID50

The tissue culture infection dose 50 (TCID50) determines the viral amount which can infect 50 % of the plated cells. 0.01 * 10^6 Huh7.5 cells per well were seeded in a 96-well plate. 24 h later, they were infected with the virus in dilutions from 1: 30 to 1: 50. The dilution was prepared in Huh7.5 cell culture medium for six wells to a total volume of 240 µL. Six wells in a row were infected with either 1: 30, or 1: 40 or 1: 50 dilutions. 200 µL cell culture medium without virus was pipetted to each remaining well. 40 µL of the wells in the first row were transferred to the next row of wells, mixed and 40 µL were transferred to the next row of wells and so on. Therefore, the dilution ratio was every time 1: 6. The cells were then incubated for 72 h at 37 °C and 5 % CO_2 in the incubator. After incubation, they were washed twice with PBS and fixed with ice cold methanol for 15 min at -20 °C. The methanol was discarded, and cells air-dried for 5 min at RT. Then, they were washed once with PBS and permeabilized with 50 µL/well TritonX-100/PBS for 5 min at RT. They were washed three times with PBS. The fixed cells were incubated for 45 min at RT with primary antibody for NS3 [1:1000] diluted in PBS under gentle shaking in the dark. Afterwards, they were washed three times with PBS and incubated with the secondary antibody anti-mouse HRP pre-diluted in PBS [1: 200] for 1 h. They were washed three times with PBS and incubated with carbazole substrate solution (5ml NaOAc (0.5 M sodium acetate, 0.5 M acidic acid, filled at 1050 mL with water), 1.5 mL carbazole (0.16 g 3-amino-ethyl-carbazole, 49.5 mL N-N-N-dimethylformamide for a total of 50ml (stable for 3 months)), 20µl 30 % H_2O_2). The carbazole-substrate-solution must be mixed immediately before usage and filtered using a 0.45 µm pore filter. The reaction must be stopped after 30 min by discarding the solution and adding 50 µL water to the cells. The NS3-positive cells were analysed by light microscopy and the positive wells were counted. A well was counted positive when it had at least one positive cell in it. The TCID50 was calculated by the Spearman and Kaerber algorithm (296).

3.5 Statistical evaluation

Statistics were calculated using the SPSS Statistics software from IBM (Ehningen, Germany). The significance was calculated using the Mann-Whitney-U Test. In Fig. 10 the calculations were performed using the Kruskal-Wallis Test. The Pearson correlation coefficient was used to calculate correlations between the different analytes in Tab. 19. Data are expressed as fractions of the normalized value of the control, which was set to 1. Data are presented as mean + SEM ($n \geq 3$). P values smaller than 0.05 were considered significant. Data were marked with * for $p \leq 0.05$, ** for $p \leq 0.01$, or *** for $p \leq 0.001$.

3.6 Serum sample collection

Serum samples were taken from patients with chronic hepatitis C infection or HCV-negative controls after informed consent and approved by the Ethics Committee of the University of Düsseldorf, Germany (Studiennummer: 5552 “Interferenz des Hepatitis C Virus mit Produktion und Signalwirkung von Wachstumsfaktoren – molekulare Mechanismen und funktionelle Konsequenzen.”), and in consent of the Declaration of Helsinki. Serum samples from patients with other liver diseases excluding HCV were taken after informed consent and approved by the Ethics Committee of the University of Düsseldorf, Germany (Studiennummer: 5350 “Aufklärung von molekularen Mechanismen bei Leberschädigung, Leberregeneration oder Covid-19 Erkrankung“). Information regarding age, sex, viral load, liver status and HBV infection of the group Patients w/o HCV can be found in Tab. 18.

4 Results

4.1 VEGFA, EGF, TNFα and CXCL8 protein levels are elevated in sera of patients chronically infected with HCV when compared to sera of healthy patients

To determine whether chronic HCV infection influences the protein levels of the growth factors, chemokines and cytokines investigated in this study, sera of patients suffering from chronic HCV infection, of patients suffering from liver diseases except HCV and of healthy people were collected with the approval of the Ethics Committee of the University of Düsseldorf.
It was also investigated whether HCV affects the protein levels of the growth factor VEGFA, which was shown to be upregulated in peripheral blood mononuclear macrophages in patients chronically infected with HCV (154). Additionally, the protein levels of the two chemokines CCL2 and CCL7, which are known to be mainly responsible for the recruitment of macrophages, and CXCL8, which is mainly responsible for the recruitment of neutrophil granulocytes (255, 264), were analysed in sera of patients.
Specific information on age, sex, liver fibrosis status, HBV infection and the viral HCV load of the patients is listed in Tab. 18.

Tab. 18- Baseline characteristics of analysed patients.

	Healthy people (n = 10)	**Patients w/o HCV (n = 17)**	**Patients HCV (n = 43)**
Age, year (Mean ± SEM)	34.3 ± 2.9	51.3 ± 3.4	54.8 ± 2.1
Sex - no. (%)			
Female	5 (50 %)	9 (52.9 %)	21 (48.8 %)
Male	5 (50 %)	8 (47.1 %)	22 (51.2 %)
Liver fibrosis	0	3 (17.6 %)	8 (18.6 %)
Steatosis hepatis	0	2 (11.8 %)	11 (25.6 %)
Liver cirrhosis	0	1 (5.9 %)	9 (20.9 %)
HBV (n)	0	2 (11.8 %)	4 (9.3 %)
Viral Load (HCV) [U/mL]	-	-	$2.28 * 10^6 \pm 3.44 * 10^5$

Protein levels of the chemokines CXCL8, CCL2 and CCL7, the cytokines TNFα and IL-1β and the growth factors VEGFA and EGF in sera of patients were analysed by LUMINEX or, in case of CXCL8, by ELISA. Both VEGFA and EGF protein levels were significantly higher in the serum samples of the group of patients chronically infected with HCV when compared to healthy control serum samples (Fig. 10A/B). In case of EGF, these results are in line with published data of our working group (284). The group of patients chronically infected with HCV

displayed nearly the same amount of VEGFA as well as EGF protein levels in their sera compared to the group of patients suffering from liver diseases other than HCV (Fig. 10A/B). In case of EGF, patients w/o HCV exhibited significantly higher serum protein levels compared to healthy people (Fig. 10B), suggesting an upregulation of EGF and VEGFA in the sera of both HCV-infected patients but also patients suffering from other liver diseases.

Neither CCL2 nor CCL7 protein levels in the serum were significantly affected by chronic HCV infection or by other liver diseases (Fig. 10C/D).

The protein levels of CXCL8 were significantly elevated in sera of patients chronically infected with HCV compared to the healthy control sera, but were slightly upregulated in sera of patients w/o HCV infection as well (Fig. 10E).

Patients infected chronically with HCV displayed significantly higher protein levels of TNFα in the serum compared to the healthy control group (Fig. 10F).

Taken together, these results demonstrated elevated CXCL8 protein levels in sera of patients chronically infected with HCV, while protein levels of CCL2 and CCL7 were not affected.

In addition to that, the protein levels of both growth factors VEGFA and EGF and of the cytokine TNFα were elevated in the sera of patients chronically infected with HCV as well as in sera of patients suffering from other liver diseases than HCV.

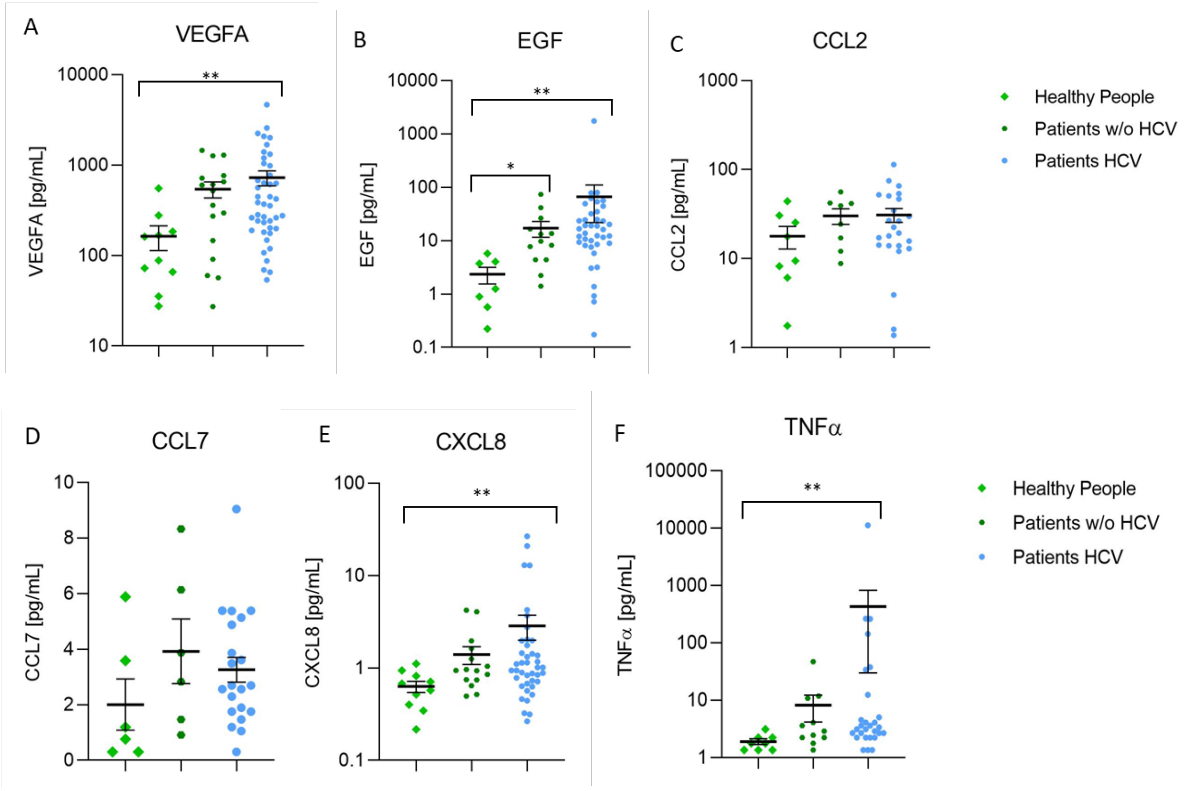

Fig. 10- VEGFA, EGF, CCL2, CCL7, CXCL8 and TNFα protein levels in sera of analysed patients. Serum samples were collected, and protein levels were measured using LUMINEX multiplex or ELISA (for CXCL8 only). **(A)** VEGFA (n = 10, 11, 43), **(B)** EGF (n = 10, 17, 41), **(C)** CCL2 (n = 8, 8, 24), **(D)** CCL7 (n = 4, 5, 21) and **(E)** CXCL8 (n = 10, 15, 41) and **(F)** TNFα (n = 8, 11, 28) levels of healthy people, patients w/o HCV or of patients

chronically infected with HCV were determined. n for each condition is given in this order. Data are presented as individual data points and mean ± SEM. Asterisks mark significant protein level changes in sera of patients or healthy people versus the different cohorts of patients or healthy people calculated by the Kruskal-Wallis-Test: p<0.05 = *, p<0.01 = **, p<0.001 = ***.

Next, correlation analysis was performed to identify proteins with potentially related patterns. Tab. 19 shows the pairwise analysis of correlation coefficients (Pearson) for every analysed group. TNFα protein levels correlated significantly positive with both EGF (r = 0.655; p < 0.001**) or VEGFA (r = 0.904; p < 0.001**) protein levels in sera of patients chronically infected with HCV, while there was no correlation between these proteins in sera of healthy people or of patients w/o HCV.

In healthy people, CCL2 (r = 0.770; p < 0.05*) and CCL7 (r = 0.840; p < 0.05*) protein levels positively correlated with the TNFα protein levels and CCL7 protein levels correlated strongly positive with the VEGFA protein levels (r = 0.993; p < 0.001**).

The EGF protein levels of patients w/o HCV positively correlated with the CXCL8 (r = 0.800; p < 0.001**) and the VEGFA protein levels (r = 0.613; p < 0.05*).

TNFα, EGF and VEGFA protein levels significantly correlated in the serum of patients chronically infected with HCV, suggesting that these three proteins may somehow be interrelated.

Tab. 19- Pearson correlation analysis for CCL2, CCL7, CXCL8, EGF, VEGFA and TNFα protein levels in sera of the analysed patients' groups and the group of healthy people. Analytes correlating significantly with each other are marked in light green for p<0.05 = * and dark green for p<0.01 = **.

	Healthy People		Patients w/o HCV		Patients HCV	
Analytes	*R*	*p*	*r*	*p*	*r*	*p*
CCL2/CCL7	0.274	0.599	-0.770	0.073	0.197	0.392
CCL2/CXCL8	-0.193	0.648	0.679	0.064	0.055	0.804
CCL2/EGF	0.098	0.853	0.668	0.070	0.404	0.050
CCL2/VEGFA	0.447	0.267	0.410	0.314	-0.080	0.711
CCL2/TNFα	0.770	0.025*	-0.340	0.410	-0.038	0.859
CCL7/CXCL8	-0.052	0.922	-0.120	0.820	-0.061	0.799
CCL7/EGF	-0.433	0.467	0.016	0.976	0.146	0.529
CCL7/VEGFA	0.993	0.000**	0.260	0.619	0.261	0.254
CCL7/TNFα	0.840	0.037*	0.725	0.103	0.241	0.294
CXCL8/EGF	0.532	0.214	0.800	0.001**	0.090	0.596
CXCL8/VEGFA	-0.165	0.649	0.437	0.080	-0.112	0.484
CXCL8/TNFα	-0.181	0.667	0.073	0.843	-0.037	0.857
EGF/VEGFA	-0.441	0.381	0.613	0.026*	0.197	0.230
EGF/TNFα	-0.276	0.597	0.096	0.799	0.655	0.000**
VEGFA/TNFα	0.699	0.054	0.420	0.227	0.904	0.000**

4.2 HCV interference with EGF signalling pathways

4.2.1 HCV upregulates the basal and EGF-induced mRNA expression of CXCR2 ligands

The EGFR is essential for HCV cell entry, which was shown in 2011 by Lupberger *et al.* (77). The exact mechanism how HCV influences downstream signalling pathways of EGFR is not yet established. In general, the immunological composition of the liver is dependent on several small signalling molecules, such as chemokines, which guide different immune cells to the inflamed organ. Previous work from our group, using a proteome profiler chemokine array and qRT-PCR, showed that the mRNA expression of several chemokines was upregulated in Huh9.13 cells harbouring the subgenomic replicon of HCV compared to Huh7 control cells. Among them, the strongest mRNA expression upregulation was seen for *CXCL1, 2, 3* and *8*. Additionally, upregulation of CXCL8 protein levels in cells harbouring the subgenomic replicon of HCV was shown in previous work of our working group (284). Therefore, *CXCL1*, *2*, *3* and especially *8* were of interest for further studies.

To test whether these HCV effects are also observable in a model of acute infection, Huh7.5 cells were infected with HCV, mRNA was collected, and qRT-PCR was performed. In line with the previously obtained results, it could be demonstrated that *CXCL1, 2, 3* and *8* mRNA expression levels were induced by HCV in the HCV_{cc} model of acute infection as well (284).

To rule out the influence of HCV on the housekeeping gene used (*SDHA*), *CXCL8* mRNA expression was additionally normalized to other housekeeping genes: *hypoxanthin-phosphoribosyl-transferase 1 (HPRT-1), glycerinaldehyd-3-phosphat-dehydrogenase (GAPDH), hydroxymethylbilan-synthase (HMBS), TATA-box binding protein (TPB) and beta-2 microglobulin (B2M)* levels were measured by qRT-PCR and induction of gene expression calculated via the ΔΔCT method (286).

The results clearly show that HCV upregulated the *CXCL8* mRNA expression levels independent of the reference gene used for normalization (Fig. 11A/B), indicating that HCV infection enhances basal as well as EGF-induced expression of *CXCL8* mRNA.

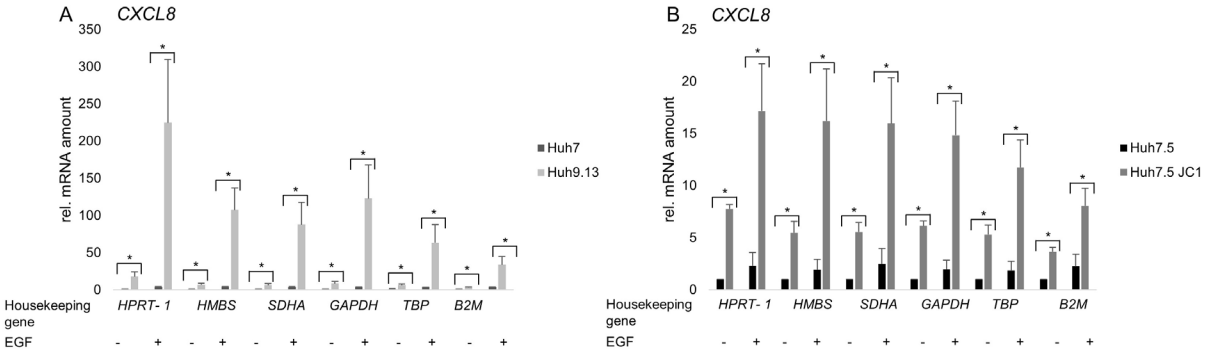

Fig. 11- *CXCL8* mRNA expression normalized to different housekeeping genes in two HCV cell culture systems with and without EGF administration. Expression of *CXCL8* mRNA was analysed by qRT-PCR **(A)** in Huh9.13 replicon or **(B)** Huh7.5 cells infected with the HCV_{cc} strain JC1 (MOI = 1) and compared to respective control cells. Cells were stimulated with 40 ng/mL EGF [40 ng/mL] for 160 min or left unstimulated. Results are expressed as fractions of the normalized value of the control, which was set to 1, and data are presented as means + SEM of at least three independent experiments. Asterisks mark significant differences versus the infected and control cell lines described as follows: $p<0.05$ = *, $p<0.01$ = **, $p<0.001$ = ***.

4.2.2 HCV enhances basal expression of *CXCL8* mRNA and results in a substantial enhancement of *CXCL8* mRNA expression even in response to low EGF concentrations

To examine down to which concentration of EGF the enhancing effect of HCV on EGF-inducible *CXCL8* mRNA expression is still detectable, cells were stimulated with different concentrations of EGF, and *CXCL8* mRNA expression was determined via qRT-PCR.
It could be demonstrated that already a EGF concentration of 1.25 ng/mL leads to a 7-fold upregulation of *CXCL8* mRNA expression in cells infected with HCV compared to unstimulated cells infected with HCV. With increasing EGF concentrations, also the mRNA expression of *CXCL8* increased in cells harbouring the subgenomic replicon of HCV (Fig. 12, light grey bars). Although also in Huh7 cells EGF stimulation resulted in a 3-fold induction of the *CXCL8* mRNA expression, the enhancement was not as high as seen in Huh9.13 cells (Fig. 12, dark grey bars), once again pointing at HCV to substantially enhance EGF-induced expression of *CXCL8* mRNA.

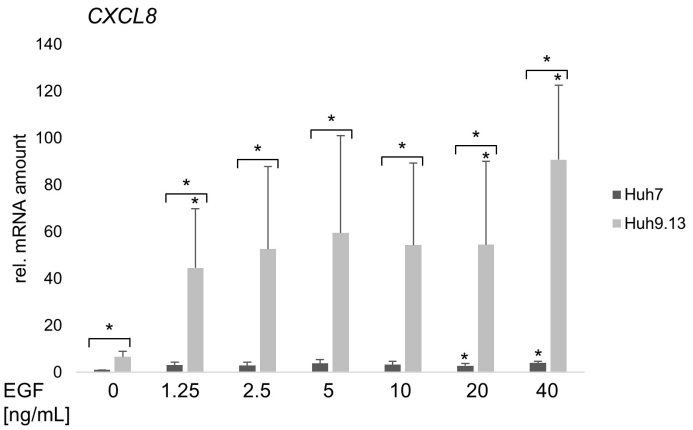

Fig. 12- *CXCL8* mRNA expression after administration of EGF in concentrations up to 40 ng/mL in both Huh9.13 and Huh7 control cells. Expression of *CXCL8* mRNA was analysed by qRT-PCR in Huh9.13 replicon cells and compared to respective control cells. Cells were stimulated with the indicated concentrations of EGF for 160 min. *SDHA* was used as reference gene. Results are expressed as fractions of the normalized value of the control, which was set to 1, and data are presented as means + SEM of at least three independent experiments. Asterisks mark significant differences versus the infected and control cell lines described as follows: $p<0.05$ = *, $p<0.01$ = **, $p<0.001$ = ***.

4.2.3 EGF-induced activation of EGFR downstream signalling is enhanced after HCV infection

EGF protein levels were found to be upregulated in sera of patients chronically infected with HCV (**4.1**). Additionally, prior work from our group demonstrated that TCPTP, an endogenous negative regulator of the EGFR, is degraded by HCV, leading to an upregulation of relative EGFR phosphorylation levels (36). Furthermore, it could be demonstrated that EGFR protein levels are enhanced on the cell surface, while ErbB3 protein levels are decreased, demonstrating cross-regulation between the different ErbB receptors (150). Therefore, the question arose, whether the activation of the downstream signalling pathways of EGFR is also influenced by HCV. To address this question, cells harbouring the subgenomic replicon of HCV (Huh9.13) and cells infected with HCV (HCV_{cc}) as well as Huh7 and Huh7.5 control cells were stimulated with EGF [40 ng/mL] for 20 or 40 min, proteins were extracted, and immunoblotting was performed.

Relative EGFR phosphorylation levels at Y1068 tended to be higher in Huh9.13 cells than in Huh7 cells. However, these differences did not reach the level of significance (Fig. 13A/B), whereas TCPTP was downregulated significantly (Fig. 13A/C).

Phosphorylation of PLCγ at Y783 was neither affected by HCV alone nor by HCV after EGF stimulation compared to control cells (Fig. 13A/D).

EGF-induced AKT phosphorylation at S473 was found to be significantly enhanced in cells harbouring the subgenomic replicon of HCV after 20 min of EGF stimulation, whereas basal

as well as EGF-induced AKT phosphorylation levels were slightly upregulated after 40 min EGF stimulation (Fig. 13A/E). Phosphorylation of the MAPKs MEK1/2 at S217/T221 and p38 at T180/Y182 was upregulated after EGF stimulation in Huh7 as well as Huh9.13 cells (Fig. 13A/F/G/H) but did not differ between Huh7 and Huh9.13 cells, while phosphorylation of ERK1/2 on T202/Y204 appeared to be stronger in Huh9.13 cells than in Huh7 cells, but these differences also did not reach the level of significance.

Taken together, the obtained results are, at least with respect to the impact of HCV on TCPTP protein levels and on AKT activation, in line with results published from our group in 2009 (36). HCV infection resulted in reduced TCPTP protein levels. AKT phosphorylation levels were increased in cells harbouring the subgenomic replicon of HCV and EGF-induced AKT phosphorylation levels were significantly enhanced by HCV after 20 min, indicating that AKT was activated after HCV infection and that EGF-induced AKT activation was enhanced by HCV infection. These results suggest that AKT may be also a candidate that could play a role in mediating the impact of HCV on *CXCL8* mRNA expression.

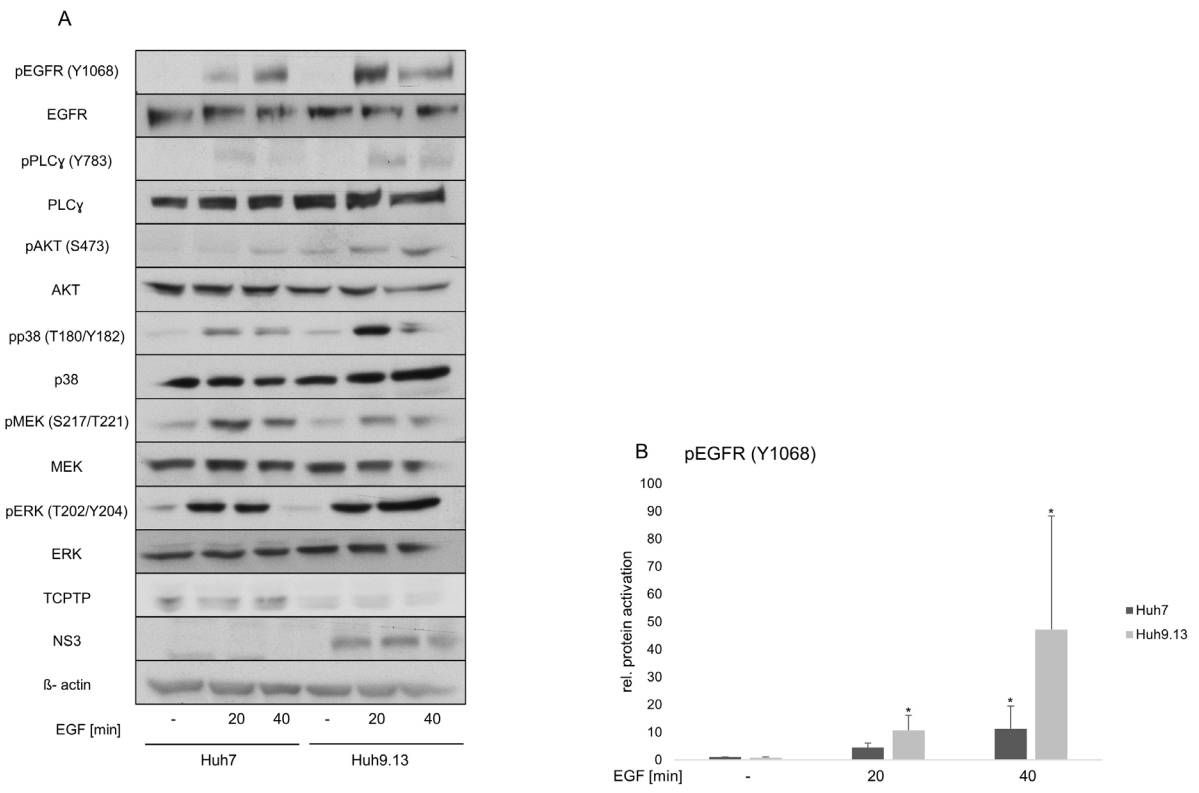

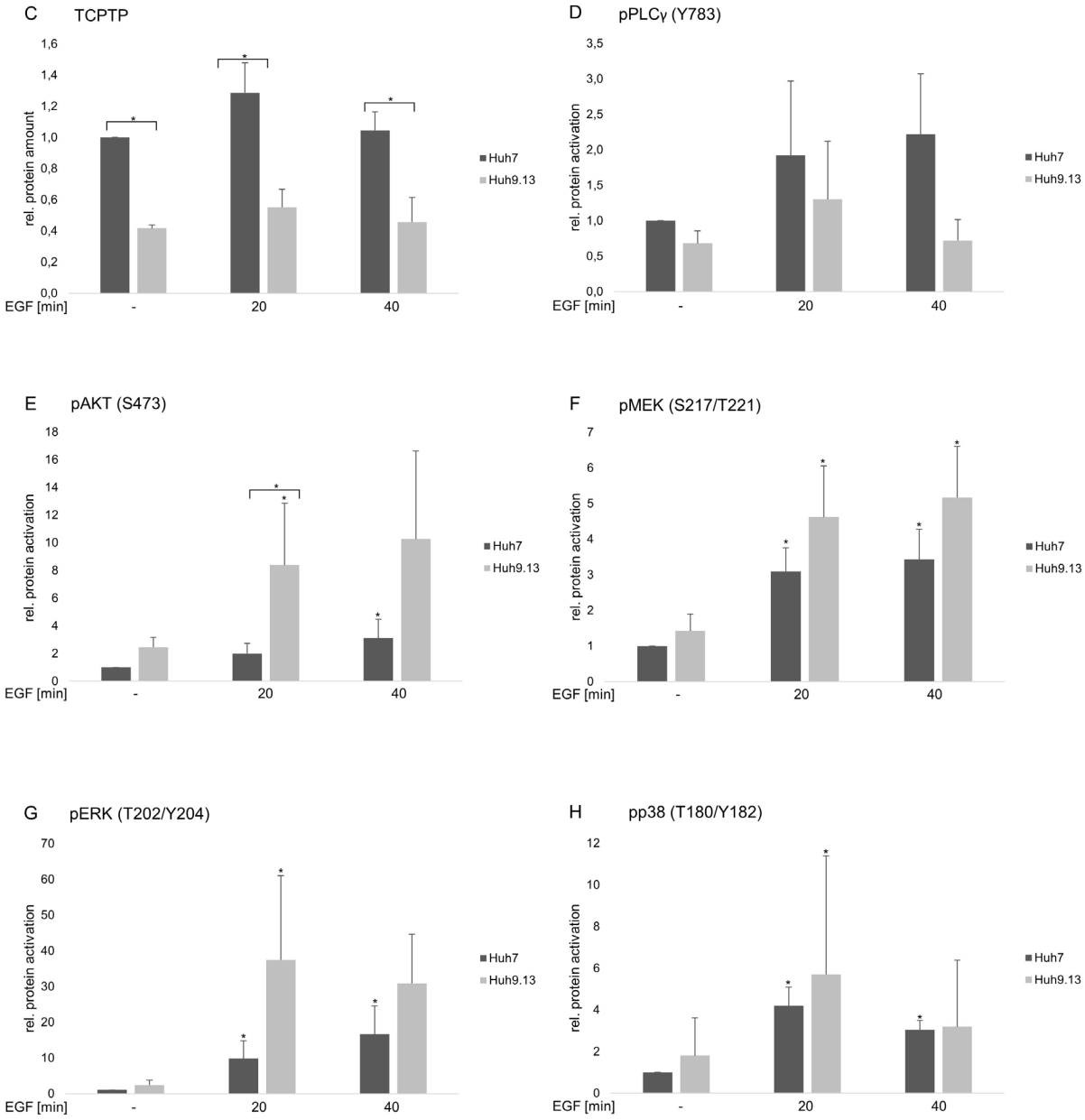

Fig. 13- Protein activation of key proteins in the downstream signalling pathways of the EGFR and total protein levels of TCPTP in Huh9.13 and Huh7 control cells. Abundance and activation of key proteins of the PI3K/AKT and the MAPK signalling pathway were analysed by immunoblotting in Huh9.13 replicon cells and compared to respective controls. Cells were stimulated with 40 ng/mL of EGF for the indicated time periods or left untreated. **(A)** Representative immunoblots for the analysed proteins are depicted. Densitometric analyses were performed for the protein amounts or activation of **(B)** pEGFR (Y1068), **(C)** TCPTP, **(D)** pPLCγ (Y783), **(E)** pAKT (S473), **(F)** pMEK (S217/T221), **(G)** pERK (T202/Y204) and **(H)** pp38 (T180/Y182) and calculated to the respective total protein levels, which were normalized to the reference protein β-actin. Results are expressed as fractions of the normalized value of the control, which was set to 1, and data are presented as means + SEM of at least three independent experiments. Asterisks without lines mark differences between stimulated cells compared to the respective unstimulated control cells. Asterisks mark significant differences versus the infected and control cell lines described as follows: $p<0.05$ = *, $p<0.01$ = **, $p<0.001$ = ***.

In case of the HCV_{cc} system, relative phosphorylation of EGFR was significantly upregulated at Y1068 after HCV infection, while the EGF-induced EGFR phosphorylation was not significantly affected by HCV infection (Fig. 14A/B).

As in the subgenomic replicon system, also in the HCV_{cc} system TCPTP was downregulated significantly in the infected cells compared to control cells (Fig. 14A/C), while PLCγ phosphorylation at Y783 was not affected by HCV (Fig. 14A/D).

Additionally, relative AKT phosphorylation levels at S473 were slightly upregulated in cells infected with HCV and EGF-induced AKT phosphorylation was significantly enhanced after HCV infection after 20 min of EGF stimulation (Fig. 14A/E).

MEK1/2 phosphorylation at S217/T221 was not affected by HCV, but as seen before in the subgenomic replicon system, upregulated in both HCV-infected as well as in Huh7.5 control cells in response to EGF (Fig. 14A/F).

In contrast, EGF-induced ERK1/2 phosphorylation at T202/Y204 was enhanced significantly in the presence of HCV (Fig. 14A/G).

Additionally, contrary to the results obtained for the replicon system, the basal p38 phosphorylation as well as the EGF-induced p38 phosphorylation at T180/Y182 was likewise significantly upregulated after HCV infection (Fig. 14A/H).

Hence, the data presented herein provide evidence that the effects previously described in the replicon system could be also observed in a system that is based on infectious cell culture- adapted HCV.

Interestingly, in the acute infection system the EGF-induced phosphorylation of the two MAPKs p38 and ERK as well as the phosphorylation of AKT was significantly enhanced after HCV infection, rendering them potential candidates for transducing signals being responsible for *CXCL8* mRNA expression enhancement after HCV infection in response to EGF.

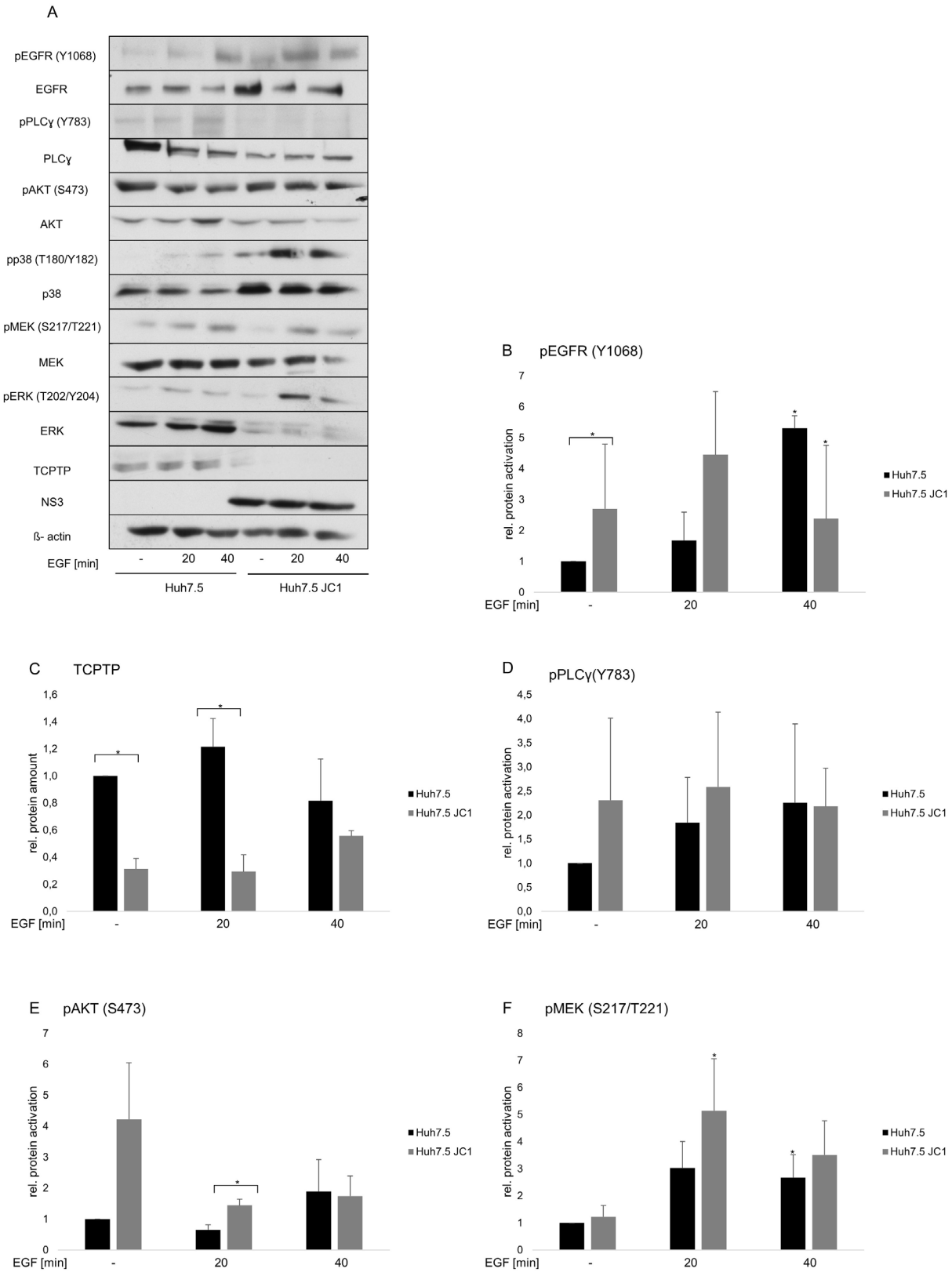
A
pEGFR (Y1068)
EGFR
pPLCγ (Y783)
PLCγ
pAKT (S473)
AKT
pp38 (T180/Y182)
p38
pMEK (S217/T221)
MEK
pERK (T202/Y204)
ERK
TCPTP
NS3
ß- actin
EGF [min] - 20 40 - 20 40
Huh7.5
Huh7.5 JC1
B pEGFR (Y1068)
rel. protein activation
EGF [min] - 20 40
Huh7.5
Huh7.5 JC1
C TCPTP
rel. protein amount
EGF [min] - 20 40
Huh7.5
Huh7.5 JC1
D pPLCγ(Y783)
rel. protein activation
EGF [min] - 20 40
Huh7.5
Huh7.5 JC1
E pAKT (S473)
rel. protein activation
EGF [min] - 20 40
Huh7.5
Huh7.5 JC1
F pMEK (S217/T221)
rel. protein activation
EGF [min] - 20 40
Huh7.5
Huh7.5 JC1

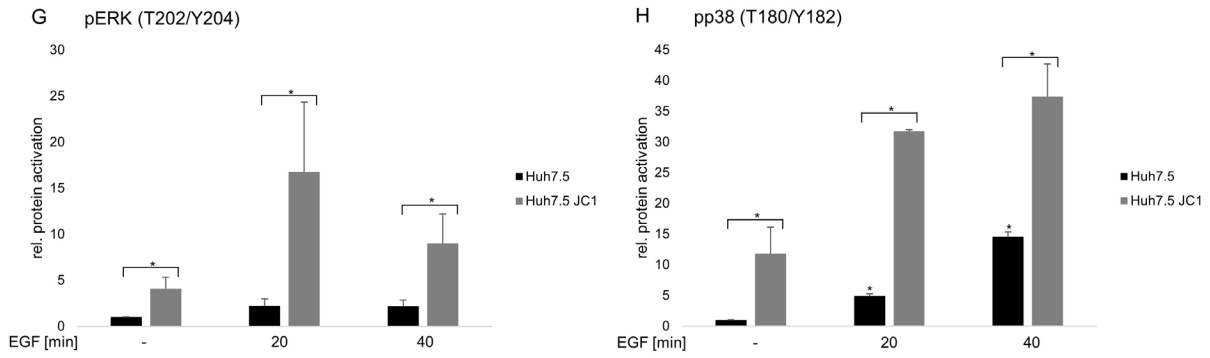

Fig. 14- Protein activation of key proteins in the downstream signalling pathways of the EGFR and total protein levels of TCPTP in HCV-infected Huh7.5 and Huh7.5 control cells. Abundance and activation of key proteins of the PI3K/AKT and the MAPK signalling pathway were analysed by immunoblotting in Huh7.5 cells infected with the HCV_{cc} strain JC1 (MOI = 1) and compared to respective controls. Cells were stimulated with 40 ng/mL of EGF for the indicated time periods or left untreated. **(A)** Representative immunoblots for the analysed proteins are depicted. Densitometric calculations were performed for the protein amounts or activation of **(B)** pEGFR (Y1068), **(C)** TCPTP, **(D)** pPLCγ (Y783), **(E)** pAKT (S473), **(F)** pMEK 1/2 (S217/T221), **(G)** pERK 1/2 (T202/Y204) and **(H)** pp38 (T180/Y182) and calculated to the respective total protein levels, which were normalized to the reference protein β-actin. Results are expressed as fractions of the normalized value of the control, which was set to 1, and data are presented as means + SEM of at least three independent experiments. Asterisks without lines mark differences between stimulated cells compared to the respective unstimulated control cells. Asterisks mark significant differences versus the infected and control cell lines described as follows: $p<0.05$ = *, $p<0.01$ = **, $p<0.001$ = ***.

4.2.4 EGF-induced expression of *CXCL1, 2, 3* and *8* mRNA enhanced by HCV infection is regulated via different signalling pathways

As described (**4.2.1**), earlier studies from our group could demonstrate that HCV enhances the mRNA expression of CXCR2 chemokine ligands *CXCL1*, *2*, *3* and especially *8*. Additionally, EGF-induced mRNA expression of those chemokines was enhanced after HCV infection of the cells (284).

EGF-induced expression of *CXCL1*, *2*, *3* and *8* mRNA enhanced by HCV infection was next investigated via inhibition or knockdown of several key proteins downstream of EGFR. In previous work, it could be shown that MEK1, p38, AKT and EGF positively influence the upregulation of *CXCL8* mRNA expression in Huh9.13 cells (284).

To examine whether these proteins are also involved in the upregulation of the different CXCR2 chemokine ligands in the HCV_{cc} system of acute infection, they were either knocked down by siRNA or inhibited by use of chemical inhibitors. Afterwards, the mRNA expression of the different CXCR2 ligands was analysed by qRT-PCR.

The EGF-induced expression of *CXCL8* mRNA enhanced by HCV infection was slightly reduced after MEK1 inhibition (U0126) as well as significantly in response to EGFR inhibition

(AG1478) (Fig. 15A/B), while AKT inhibition (Triciribine) did not prevent the enhancement of *CXCL8* mRNA expression in response to HCV infection (Fig. 15C). Additionally, *NFκB p65* knockdown resulted in an impaired HCV-specific *CXCL8* mRNA expression enhancement as well as in a reduction of EGF-induced expression of *CXCL8* mRNA enhanced by HCV infection (Fig. 15F).

Additionally, *NFκB p65* knockdown resulted in a slight reduction of *CXCL8* mRNA expression in Huh7 control cells as well, indicating that *CXCL8* mRNA expression regulation is, at least partly, mediated by NFκB p65 (Fig. 15F).

Contrary to the assumption that AKT plays a major role in the EGF-induced expression of *CXCL8* mRNA enhanced by HCV infection, MEK and EGFR seem to be the major regulators of this, while AKT does not seem to have any impact.

Additionally, these results indicate that MEK induces NFκB p65 signalling leading to an EGF-induced expression of *CXCL8* mRNA enhanced by HCV infection.

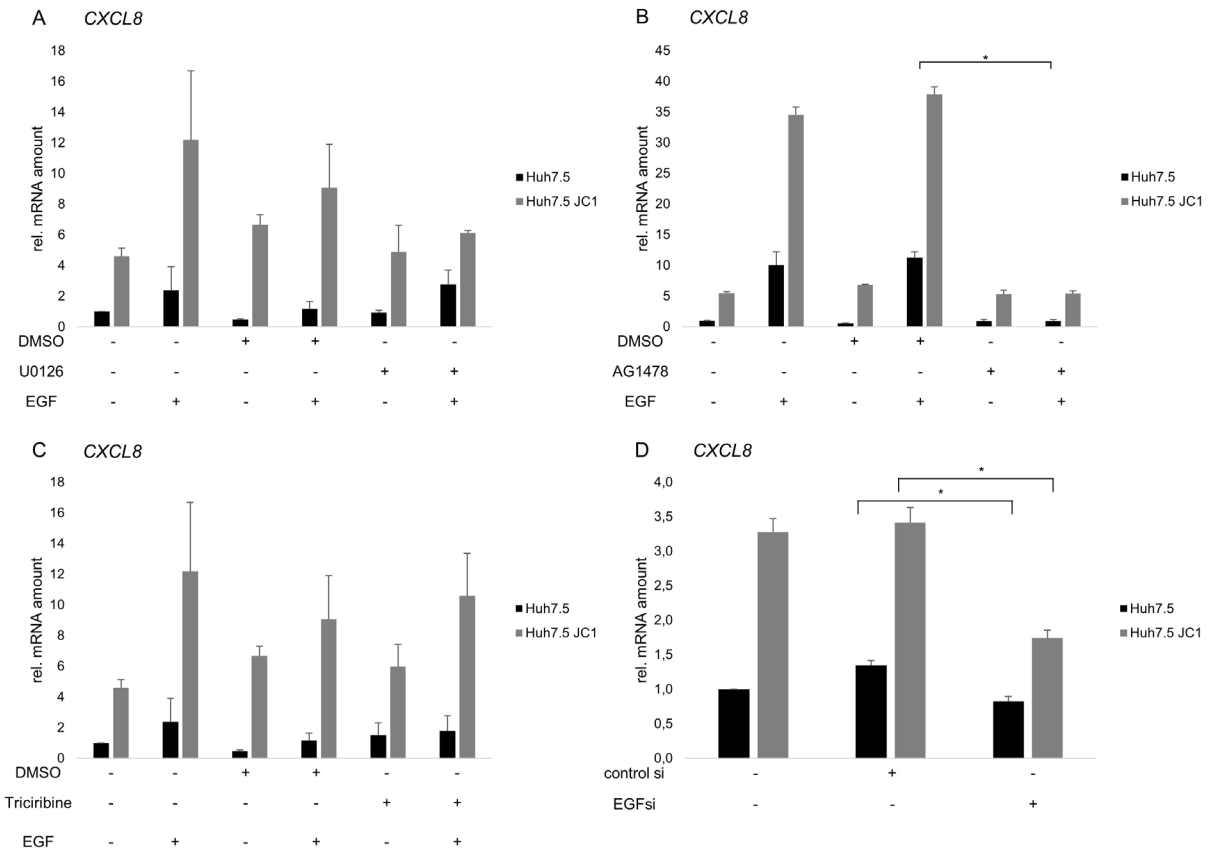

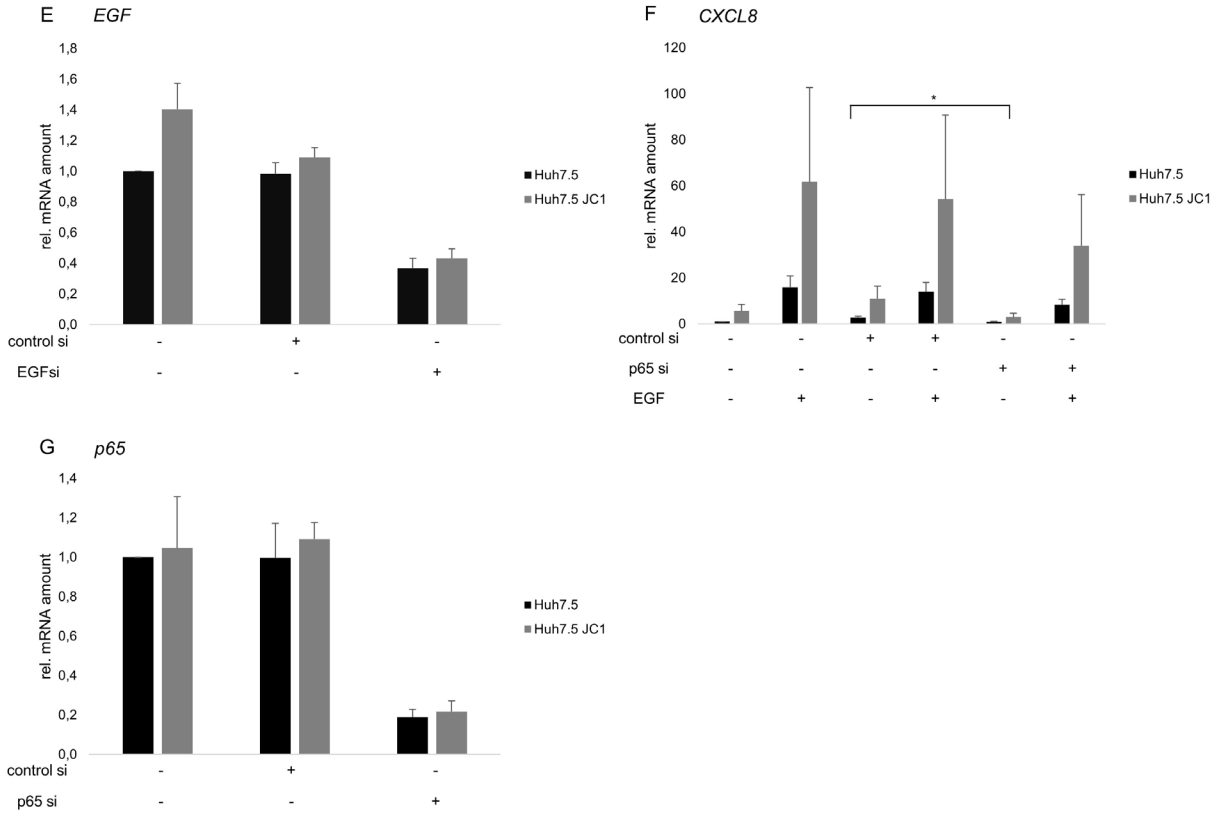

Fig. 15- *CXCL8* mRNA expression in both HCV-infected Huh7.5 and Huh7.5 control cells after inhibition or knockdown of different EGFR downstream signalling components with or without EGF administration. Expression of *CXCL8, EGF* and *p65* mRNA was analysed by qRT-PCR in Huh7.5 cells infected with the HCV_{cc} strain JC1 (MOI = 1) and compared to respective control cells. Cells were treated with **(A)** MEK1 inhibitor U0126 [10 µM], **(B)** EGFR inhibitor AG1788 [10 µM] or **(C)** AKT inhibitor Triciribine [10 µM]. Inhibitors or DMSO, as a control for all inhibitors, were added to the cells 1 h prior to a 160 min EGF [40 ng/mL] stimulation. Cells were treated with **(D)+(E)** EGF siRNA or **(F)+(G)** p65 siRNA and stimulated with EGF [40 ng/mL] for 160 min 72 h after transfection. **(F)** *EGF* and **(G)** *p65* knockdown were verified by qRT-PCR. Control siRNA was added as a control for all siRNA experiments. *SDHA* was used as reference gene. Results are expressed as fractions of the normalized value of the control, which was set to 1, and data are presented as means + SEM of at least three independent experiments. Asterisks without lines mark differences between stimulated cells compared to the respective unstimulated control cells. Asterisks mark significant differences versus the infected and control cell lines described as follows: $p<0.05$ = *, $p<0.01$ = **, $p<0.001$ = ***.

CXCL1 mRNA expression was significantly upregulated in HCV-infected cells compared to control cells. EGF-induced expression of *CXCL1* mRNA was enhanced by HCV infection. Knockdown of *EGF* resulted in a slightly reduced *CXCL1* mRNA expression in cells infected with HCV (Fig. 16A). The enhancement of EGF-induced *CXCL1* mRNA expression by HCV was downregulated by inhibition of AKT using the inhibitor Triciribine (Fig. 16B). This suggests that activation of AKT may be involved in the regulation of *CXCL1* mRNA expression by HCV. Of note, in particular in the absence of addition of EGF stimulation, inhibition of AKT completely abolished the enhancing effect of HCV on induction of *CXCL1* mRNA expression by HCV. This

indicates that upregulation of *CXCL1* mRNA by HCV alone requires activation of AKT. MEK1 inhibition (U0126) did not influence the *CXCL1* mRNA expression (Fig. 16C).
While the EGF-induced expression of *CXCL8* mRNA enhanced by HCV is thus suggested to be mediated by MEK1 (Fig. 15A), the EGF-induced expression of *CXCL1* mRNA enhanced by HCV infection seems to be mediated by AKT (Fig. 16B).

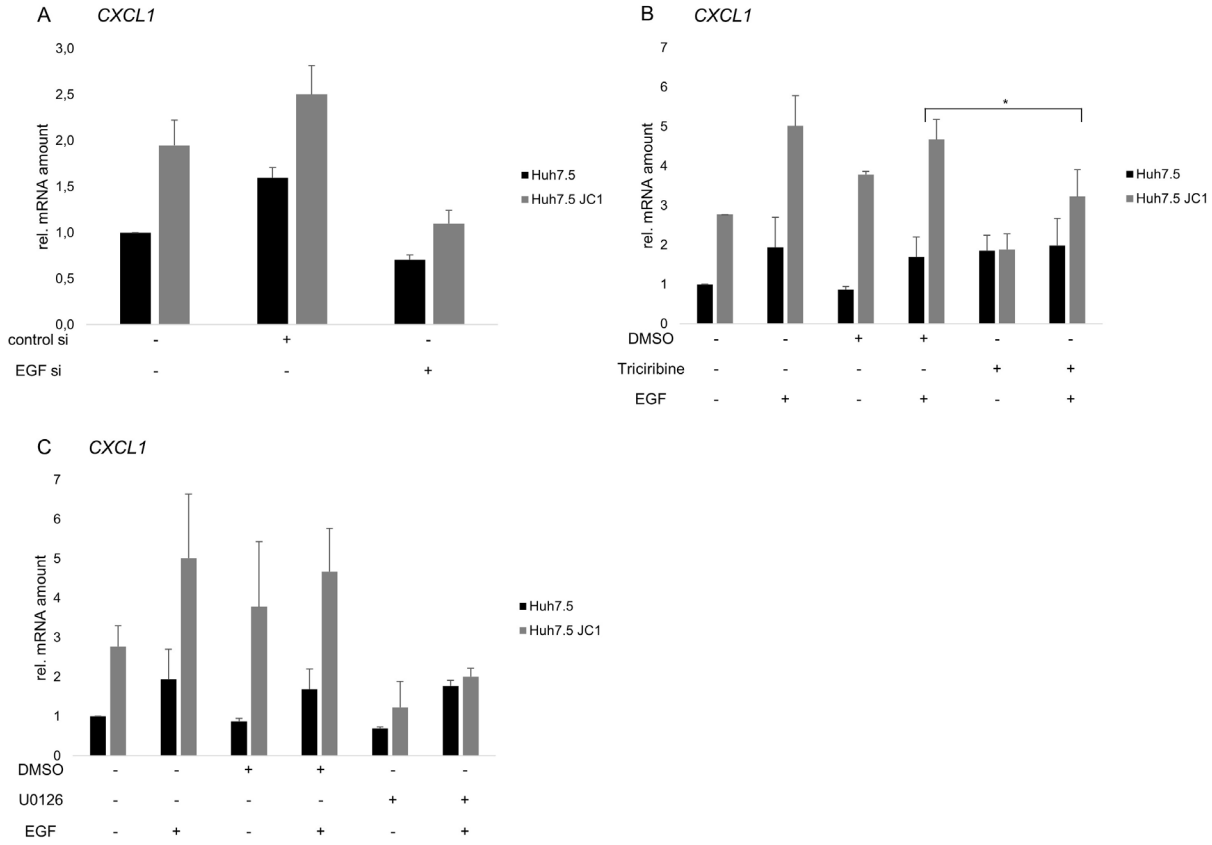

Fig. 16- *CXCL1* mRNA expression in both HCV-infected Huh7.5 and Huh7.5 control cells after inhibition of AKT or MEK1 or knockdown of EGF with or without EGF administration. Expression of *CXCL1* mRNA was analysed by qRT-PCR in Huh7.5 cells infected with the HCV_{cc} strain JC1 (MOI = 1) and compared to respective control cells. Cells were treated with **(A)** EGF siRNA, **(B)** AKT inhibitor Triciribine [10 µM] or **(C)** MEK1 inhibitor U0126 [10 µM]. In case of inhibitor experiments inhibitors were added to the cells 1 h prior to a 160 min EGF [40 ng/mL] stimulation of the cells. In case of siRNA cells were stimulated with EGF [40 ng/mL] for 160 min 72 h after transfection. DMSO was added as a control for all inhibitors. Control siRNA was added as a control for the siRNA experiment. *SDHA* was used as reference gene. Results are expressed as fractions of the normalized value of the control, which was set to 1 and data are presented as means + SEM of at least three independent experiments. Asterisks without lines mark differences between stimulated cells compared to the respective unstimulated control cells. Asterisks mark significant differences versus the infected and control cell lines described as follows: $p<0.05$ = *, $p<0.01$ = **, $p<0.001$ = ***.

The basal upregulation of *CXCL2* and *3* mRNA expression in response to HCV infection was slightly reduced after *EGF* knockdown (Fig. 17A/D). Neither inhibition of AKT nor of MEK1 significantly affected the induction of *CXCL2* and *3* expression after EGF treatment and/or after

HCV infection, suggesting that upregulation of *CXCL2* and *3* expression in this context occurs independent of AKT or MEK1 (Fig. 17B/C). The signalling pathways leading to enhancement of *CXCL2* and *3* mRNA expression and EGF-induced expression of *CXCL2* and *3* enhancement by HCV need to be elucidated in future studies.

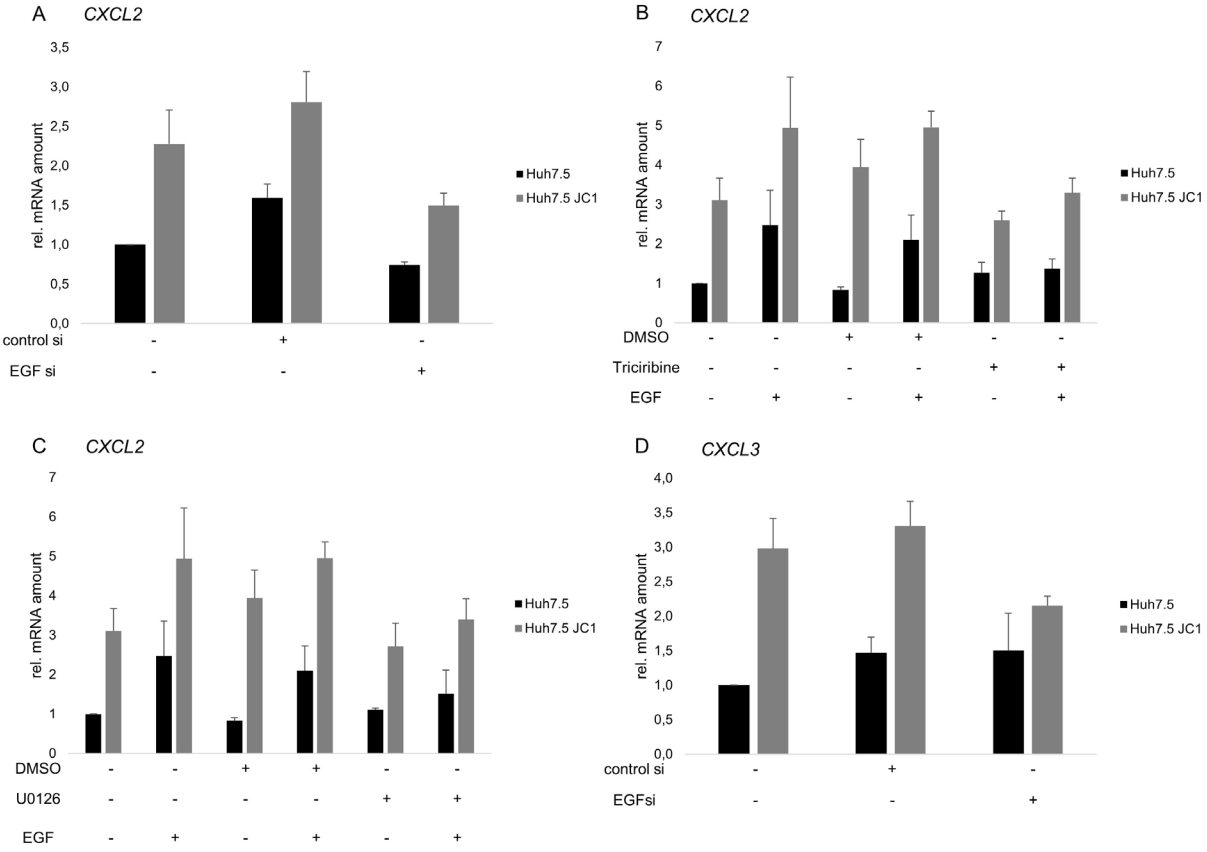

Fig. 17- *CXCL2* mRNA expression after inhibition of AKT or MEK with and without EGF administration and *CXCL2* and *3* mRNA expression after EGF knockdown in both HCV-infected Huh7.5 and Huh7.5 control cells. Expression of *CXCL2* and *3* mRNA was analysed by qRT-PCR in Huh7.5 cells infected with the HCV_{cc} strain JC1 (MOI = 1) and compared to respective control cells. Cells were treated with **(A)+(D)** EGF siRNA, **(B)** AKT inhibitor Triciribine [10 µM] or **(C)** MEK1 inhibitor U0126 [10 µM]. In case of inhibitor experiments inhibitors were added to the cells 1 h prior to a 160 min EGF [40 ng/mL] stimulation of the cells. In case of siRNA, cells were stimulated with EGF [40 ng/mL] for 160 min 72 h after transfection. DMSO was added as a control for all inhibitors. Control siRNA was added as a control for all siRNA experiments. *SDHA* was used as reference gene. Results are expressed as fractions of the normalized value of the control, which was set to 1, and data are presented as means + SEM of at least three independent experiments. Asterisks without lines mark differences between stimulated cells compared to the respective unstimulated control cells. Asterisks mark significant differences versus the infected and control cell lines described as follows: $p<0.05$ = *, $p<0.01$ = **, $p<0.001$ = ***.

4.3 Interference of HCV with IL-1β signalling pathways

4.3.1 IL-1β-induced expression of CXCR2 ligands is enhanced by HCV infection in a time and concentration dependent manner

As described, it could be shown that HCV upregulates the mRNA expression and protein levels of CXCR2 chemokine ligands and EGF-induced mRNA expression of CXCR2 chemokine ligands was enhanced after HCV infection ((284) and (**4.2.1**)).
Moreover, additionally to increased protein levels of EGF, it has been reported that patients infected with HCV display higher protein levels of IL-1β in the serum (198, 199).
Therefore, the question whether also IL-1β influences the expression of these chemokines during HCV infection arose. Hence, concentration and time course experiments with IL-1β stimulation were performed.
To elucidate whether IL-1β-induced expression of CXCR2 chemokine ligand mRNA is affected by HCV infection, Huh9.13 subgenomic replicon cells and cells infected with the HCV_{cc} strain JC1 (MOI = 1), as well as Huh7 and Huh7.5 control cells, were stimulated with different concentrations of IL-1β for 8 h. To perform time course experiments, Huh7.5 cells infected with HCV and control cells were stimulated with 5 U/mL IL-1β for up to 32 h and compared to control cells.
IL-1β-induced expression of *CXCL8* mRNA was time- and concentration dependently enhanced by HCV infection (Fig. 18A/B). In Huh9.13 cells, the HCV-dependent enhancement of *CXCL8* mRNA expression was observable when the cells were stimulated with IL-1β concentrations as low as 0.1 U/mL (Fig. 18C), which are near to the pathophysiological levels measured in human serum samples of patients [0.1 U/mL = 2 pg/mL] (199). The expression of *CXCL1, 2* and *3* mRNA was also shown to be upregulated after HCV infection, and IL-1β-induced expression of *CXCL1, 2* and *3* mRNA was enhanced by HCV (Fig. 18D/E). As shown in Fig. 18A/C, the fold induction of *CXCL8* mRNA expression in Huh9.13 cells after stimulation with 0.1 U/mL was as high as in Huh7.5 infected cells after stimulation with 5 U/mL of IL-1β. Therefore, these two concentrations were used in further experiments.
The results allow to conclude that besides EGF- also IL-1β-induced expression of *CXCL1, 2, 3* and *8* mRNA is enhanced by HCV infection of the cells.

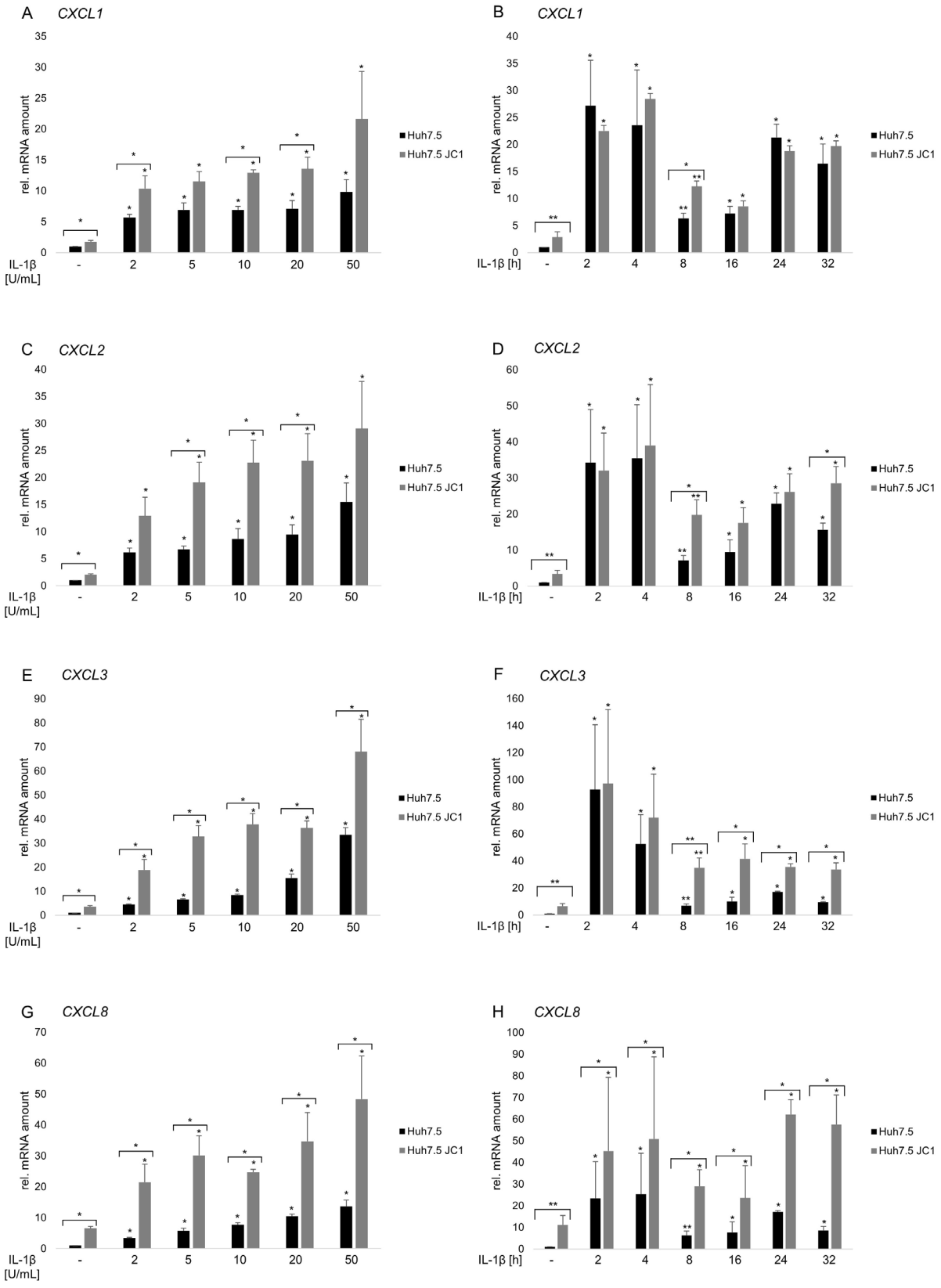
A CXCL1
B CXCL1
C CXCL2
D CXCL2
E CXCL3
F CXCL3
G CXCL8
H CXCL8
rel. mRNA amount
IL-1β [U/mL]
IL-1β [h]
Huh7.5
Huh7.5 JC1

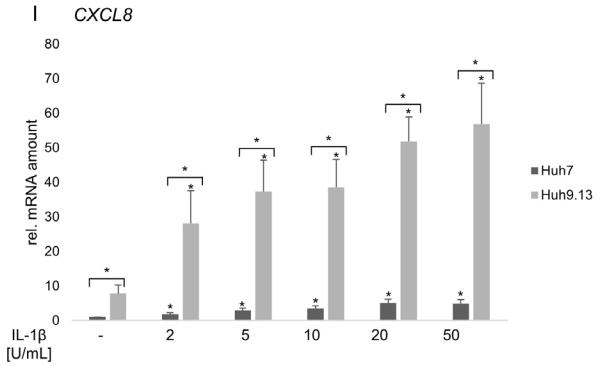

Fig. 18- *CXCL1*, *2*, *3* and *8* mRNA expression after administration of IL-1β in concentrations up to 50 U/mL or for different time periods in both HCV-infected Huh7.5 and Huh7.5 control cells as well as in Huh9.13 and Huh7 cells for *CXCL8* mRNA expression. Expression of *CXCL1, 2, 3* and *8* mRNA was analysed by qRT-PCR in Huh9.13 or in Huh7.5 cells infected with the HCV_{cc} strain JC1 (MOI = 1) and compared to respective control cells. Cells were treated with **(A)+(C)+(E)+(G)** different concentrations of IL-1β for 8 h or **(B)+(D)+(F)+(H)** 5 U/mL IL-1β for the indicated time periods. *SDHA* was used as reference gene. Results are expressed as fractions of the normalized value of the control, which was set to 1, and data are presented as means + SEM of at least three independent experiments. Asterisks without lines mark differences between stimulated cells compared to the respective unstimulated control cells. Asterisks mark significant differences versus the infected and control cell lines described as follows: $p<0.05$ = *, $p<0.01$ = **, $p<0.001$ = ***.

4.3.2 IL-1β-induced expression of *CXCL8* mRNA enhanced by HCV infection occurs before splicing

As described in **4.3.1**, HCV infection results in upregulation of *CXCL8* mRNA expression and enhances IL-1β-induced expression of *CXCL8* mRNA expression. To check whether also *CXCL8* pre-mRNA is upregulated after HCV infection, intron-exon spanning primers were designed, and pre-mRNA was measured via qRT-PCR. Consistent with *CXCL8* mRNA expression, *CXCL8* pre-mRNA expression was upregulated in cells infected with HCV and IL-1β-induced *CXCL8* pre-mRNA expression was enhanced in response to HCV infection (Fig. 19), suggesting that both the IL-1β-induced as well as HCV-enhanced IL-1β-induced expression of *CXCL8* mRNA occurs before splicing.

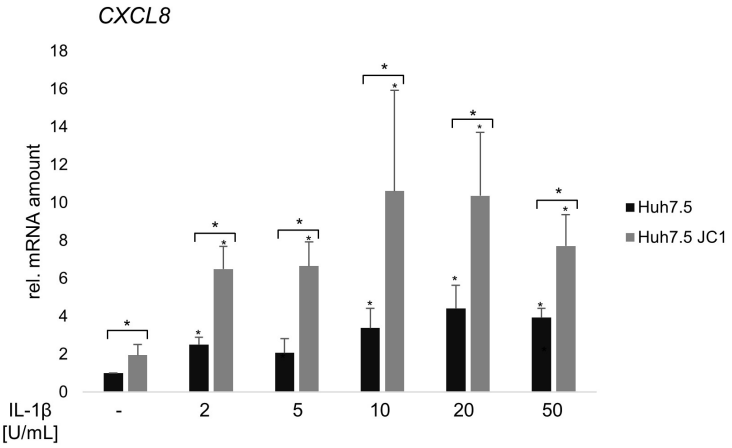

Fig. 19- *CXCL8* pre-mRNA expression after administration of IL-1β in concentrations up to 50 U/mL in both HCV-infected Huh7.5 and Huh7.5 control cells. Expression of *CXCL8* pre-mRNA was analysed by qRT-PCR in Huh7.5 cells infected with the HCV_{cc} strain JC1 (MOI = 1) and compared to respective control cells. Cells were stimulated with different concentrations of IL-1β for 8 h or left unstimulated. *SDHA* was used as reference gene. Results are expressed as fractions of the normalized value of the control, which was set to 1, and data are presented as means + SEM of at least three independent experiments. Asterisks without lines mark differences between stimulated cells compared to the respective unstimulated control cells. Asterisks mark significant differences versus the infected and control cell lines described as follows: $p<0.05$ = *, $p<0.01$ = **, $p<0.001$ = ***.

4.3.3 Promoter analysis to identify transcription factors regulating *CXCL8* expression

To investigate which transcription factors are mainly responsible for the upregulation of *CXCL8* mRNA expression in response to HCV infection as well as the enhancement of IL-1β-induced *CXCL8* mRNA expression upon infection with HCV, the promoter region of *CXCL8* gene was analysed and potential candidate transcription factors identified. As NFκB p65 was found to be important in upregulation of *CXCL8* mRNA expression after HCV infection, transcription factors known to act as co-transcription factors of NFκB p65 were analysed. Thus, besides NFκB p65, also SP1, C/EBPβ and CREB1 were chosen for further investigation (Fig. 20).

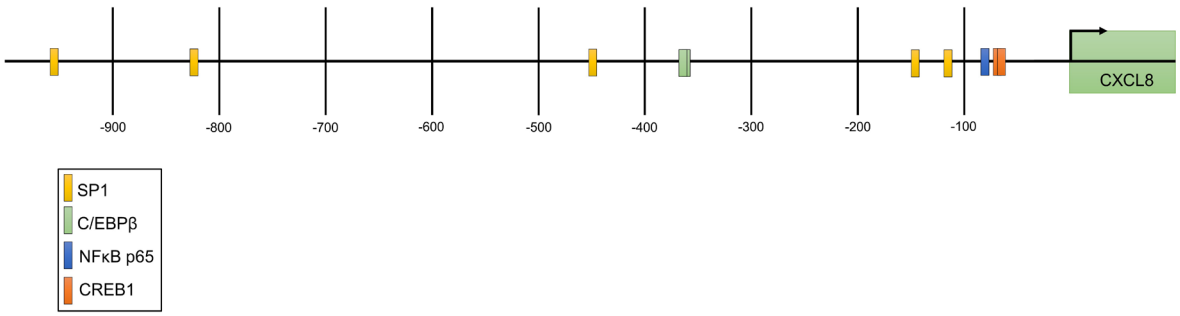

Fig. 20- Promoter region of *CXCL8* with binding sites of different transcription factors. Binding sites of several transcription factors are highlighted in different colours and the bases where the transcription factors bind to from -1000 to 100 bp relative to the transcription start site (TSS) of CXCL8 and a p-value of 0.001 are indicated in

brackets: yellow: SP1 (-959, -828; -446; -145; -114); orange: CREB1 (-77; -76); green: C/EBPβ (-371; -370) and blue: NFκB p65 (-87). The TSS of the *CXCL8* gene is marked by an arrow and a green square. The analysis was performed using the Eukaryotic promoter database. Modified to Dreos *et al.* 2017, The eukaryotic promoter database in its 30th year: focus on non-vertebrate organisms, Nucleic Acids Res. 2017 Jan 4;45(D1):D51-D55 (297).

4.3.4 IL-1β-induced expression of *CXCL1*, *2*, *3* and *8* mRNA enhanced by HCV is mediated by different signalling pathways

To check which signalling pathways are involved in the enhancing effect of HCV on the IL-1β-induced expression of *CXCL1, 2, 3* and *8* mRNA, several signalling pathways and transcription factors were analysed using either siRNA mediated gene knockdown or inhibition of the respective signalling intermediates. Transcription factors were selected according to the *CXCL8* promoter analysis (**4.3.3**).

It is noteworthy to mention that siRNA treatment of the subgenomic replicon cells resulted in some experiments in an enhancement of CXCR2 ligand mRNA expression per se. To calculate statistical significance of differences, siRNA transfected cells were therefore compared with corresponding control cells transfected with control siRNA.

As demonstrated, IL-1β-induced expression of *CXCL8* mRNA was increased in HCV-infected cells (Fig. 18G-I). Because of *NFκB p65* knockdown, upregulation of *CXCL8* mRNA expression by HCV infection was significantly reduced in both the replicon (Fig. 21A) and the HCV_{cc} cell culture system (Fig. 21C). Additionally, the enhancement of IL-1β-induced *CXCL8* mRNA expression by HCV infection was also significantly diminished (Fig. 21A/C). Both results indicate that the NFκB subunit p65 plays an important role in the HCV mediated upregulation of *CXCL8* mRNA expression but is also induced in regulation of *CXCL8* mRNA expression by IL-1β. Besides *NFκB p65*, also *TAK1* knockdown resulted in a significant reduction of *CXCL8* mRNA expression enhancement by HCV infection and IL-1β-induced expression of *CXCL8* mRNA enhanced by HCV infection, although the reduction was lower compared to the reduction after *NFκB p65* knockdown.

The data thus suggest an influence of TAK1 on IL-1β-induced expression of *CXCL8* mRNA enhanced in response to HCV infection. The exact mechanism by which NFκB p65 promotes IL-1β-induced *CXCL8* mRNA expression enhanced by HCV infection remains to be elucidated, but TAK1 may play a (subordinate) role.

Additionally, *NFκB p65* and *TAK1* knockdown resulted in a slight reduction of *CXCL8* mRNA expression in Huh7 cells as well (Fig. 21C/E), suggesting an involvement of both proteins in the basal regulation of *CXCL8* mRNA expression.

Interestingly, EGFR inhibition using AG1478 [10 µM] resulted in a slightly reduced IL-1β-induced expression of *CXCL8* mRNA enhanced by HCV infection (Fig. 21G), indicating involvement of EGFR transactivation by IL-1β under these conditions.

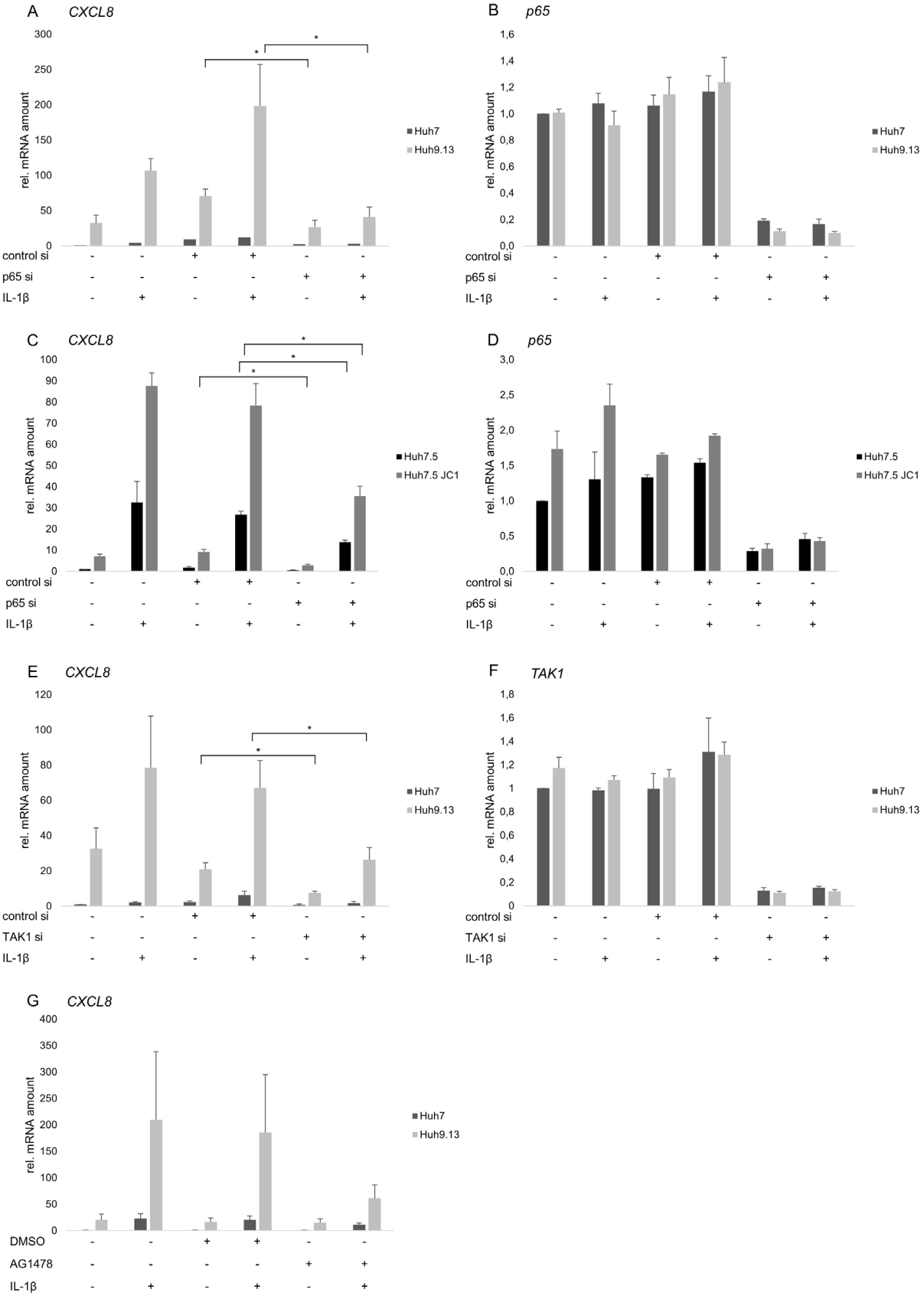

Fig. 21- *CXCL8* mRNA expression after knockdown of *NFκB p65* or *TAK1* or inhibition of the EGFR in both Huh9.13 and Huh7 cells as well as after *NFκB p65* knockdown in HCV-infected Huh7.5 and Huh7.5 control cells with and without IL-1β administration. Expression of *CXCL8, p65* and *TAK1* mRNA was analysed by qRT-PCR in Huh9.13 or in Huh7.5 cells infected with the HCV_{cc} strain JC1 (MOI = 1) and compared to respective control cells. Cells were treated with **(A)+(B)+(C)+(D)** p65 siRNA **(E)+(F)** TAK1 siRNA or **(G)** EGFR inhibitor AG1478 [10 µM]. The inhibitor was added to the cells 1 h prior to a 8 h IL-1β (0.1 U/mL; in case of AG1478 with 5 U/mL) stimulation of the cells. siRNA experiments were performed after stimulation with 0.1 U/mL IL-1β for Huh9.13 cells and respective control cells or 5 U/mL IL-1β for Huh7.5 cells infected with the HCV_{cc} strain JC1 (MOI = 1) and respective control cells for 8 h and 72 h after transfection. **(F)** *TAK1*, and **(B)+(D)** *p65* knockdown was verified by qRT-PCR. DMSO was added as a control for the inhibitor. Control siRNA was added as a control for siRNA experiments. *SDHA* was used as reference gene. Results are expressed as fractions of the normalized value of the control, which was set to 1, and data are presented as means + SEM of at least three independent experiments. Asterisks without lines mark differences between stimulated cells compared to the respective unstimulated control cells. Asterisks mark significant differences versus the infected and control cell lines described as follows: $p<0.05$ = *, $p<0.01$ = **, $p<0.001$ = ***.

Neither p38 inhibitor (SB203580), nor IKKα/β inhibitor (IKK Inhibitor II), nor AKT inhibitor (Triciribine), nor MEK1 inhibitor (U0126), nor JNK1 inhibitor (JNK Inhibitor I), nor siRNA targeting *C/EBPβ*, *SP1*, *CREB1* and *ATF2* resulted in any obvious effects on the HCV and IL-1β-induced expression of *CXCL8* mRNA enhanced by HCV infection (Fig. 22A-F/H/J/L), indicating that none of these factors is involved in the regulation of this chemokines under the analysed conditions.

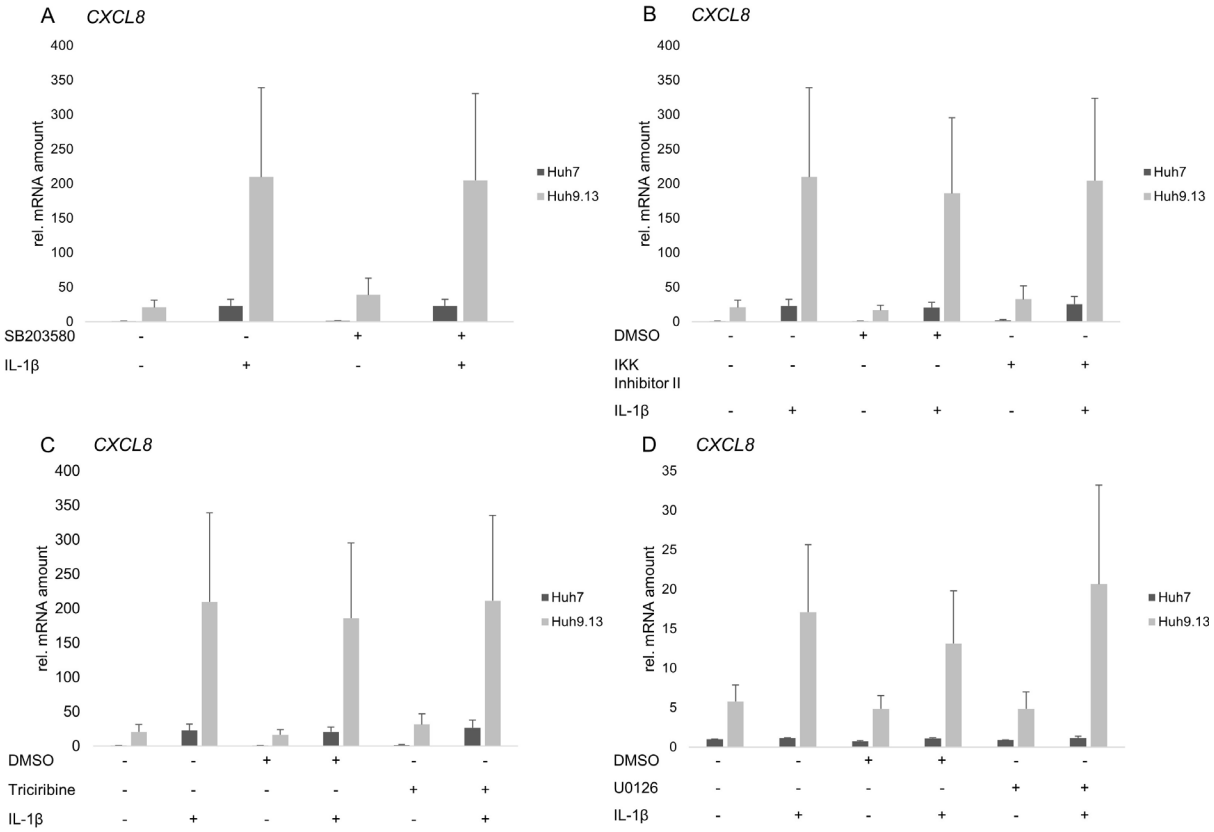

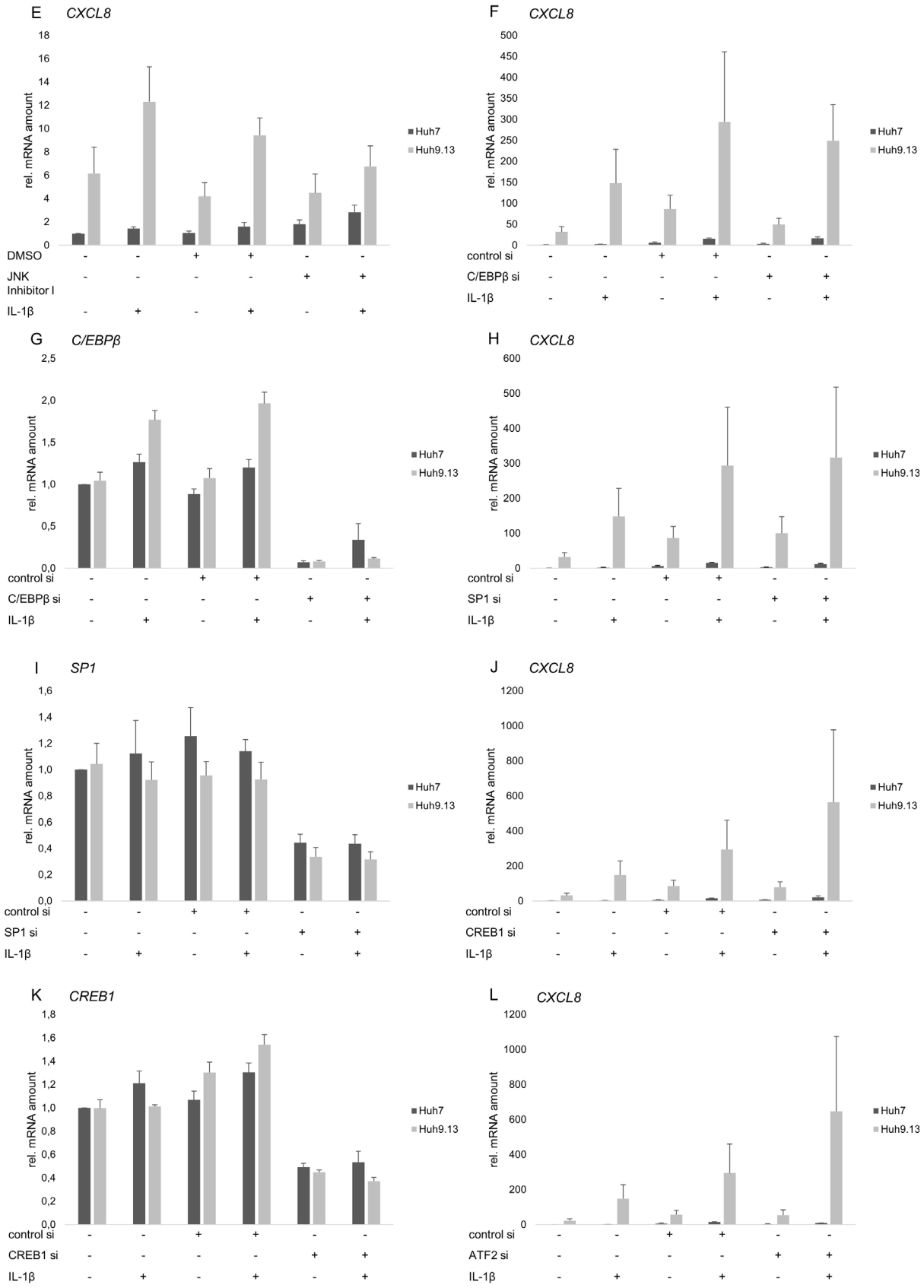
E CXCL8
rel. mRNA amount
Huh7
Huh9.13
DMSO
JNK Inhibitor I
IL-1β
F CXCL8
rel. mRNA amount
Huh7
Huh9.13
control si
C/EBPβ si
IL-1β
G C/EBPβ
rel. mRNA amount
Huh7
Huh9.13
control si
C/EBPβ si
IL-1β
H CXCL8
rel. mRNA amount
Huh7
Huh9.13
control si
SP1 si
IL-1β
I SP1
rel. mRNA amount
Huh7
Huh9.13
control si
SP1 si
IL-1β
J CXCL8
rel. mRNA amount
Huh7
Huh9.13
control si
CREB1 si
IL-1β
K CREB1
rel. mRNA amount
Huh7
Huh9.13
control si
CREB1 si
IL-1β
L CXCL8
rel. mRNA amount
Huh7
Huh9.13
control si
ATF2 si
IL-1β

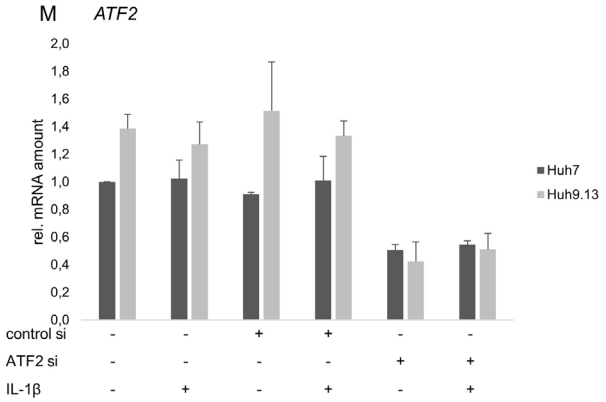

Fig. 22- *CXCL8* mRNA expression after inhibition of key components of the PI3K/AKT or MAPK signalling pathway or after knockdown of different *NFκB p65* co-transcription factors in both Huh9.13 and Huh7 cells with and without IL-1β administration. Expression of *CXCL8, C/EBPβ, SP1, CREB1 and ATF2* mRNA was analysed by qRT-PCR in Huh9.13 and compared to respective control cells. Cells were treated with **(A)** p38 inhibitor SB203580 [10 µM] **(B)** IKKα and β inhibitor IKK Inhibitor II [10 µM] **(C)** AKT inhibitor Triciribine [10 µM] **(D)** MEK1 inhibitor U0126 [10 µM] **(E)** JNK1 Inhibitor JNK Inhibitor I [10 µM] **(F)+(G)** C/EBPβ siRNA **(H)+(I)** SP1 siRNA **(J)+(K)** CREB1 siRNA and **(L)+(M)** ATF2 siRNA**.** In case of inhibitor experiments inhibitors were added to the cells 1 h prior to 8 h IL-1β (0.1 U/mL; in case of SB203580, IKK Inhibitor II and Triciribine experiments 5 U/mL) stimulation of the cells. siRNA experiments were performed 72 h after transfection. Cells were stimulated with 0.1 U/mL IL-1β for Huh9.13 and respective control cells or 5 U/mL IL-1β for Huh7.5 infected with the HCV_{cc} strain JC1 (MOI = 1) and respective control cells for 8 h. DMSO was added as a control for all inhibitors. Control siRNA was added as a control for all siRNA experiments. *SDHA* was used as reference gene. Results are expressed as fractions of the normalized value of the control, which was set to 1. Data are presented as means + SEM of at least three independent experiments. Asterisks without lines mark differences between stimulated cells compared to the respective unstimulated control cells. Asterisks mark significant differences versus the infected and control cell lines described as follows: $p<0.05$ = *, $p<0.01$ = **, $p<0.001$ = ***.

As described before, *CXCL1* mRNA expression was upregulated by HCV (Fig. 18A/B). IL-1β-induced expression of *CXCL1* mRNA was found to be enhanced after HCV infection of the cells, as demonstrated in Fig. 18. Knockdown of *NFκB p65* resulted in diminished upregulation of *CXCL1* mRNA expression in HCV-infected cells as well as in diminished IL-1β-induced expression of *CXCL1* mRNA enhanced in response to HCV infection (Fig. 23A/B). *TAK1* downregulation resulted in a slight reduction of the IL-1β-induced expression of *CXCL1* mRNA enhanced by HCV infection (Fig. 23C). These data indicate that *CXCL1* mRNA expression regulation seems to be mediated by NFκB p65 and to a lesser extent by TAK1 (Fig. 23A-C).
Both *NFκB p65* and *TAK1* knockdown resulted in a significant reduction of *CXCL1* mRNA expression in Huh7 cells as well, suggesting that *CXCL1* mRNA expression regulation is mediated by NFκB p65 and TAK1, while IL-1β-induced expression of *CXCL1* mRNA was not affected (Fig. 23A-C).

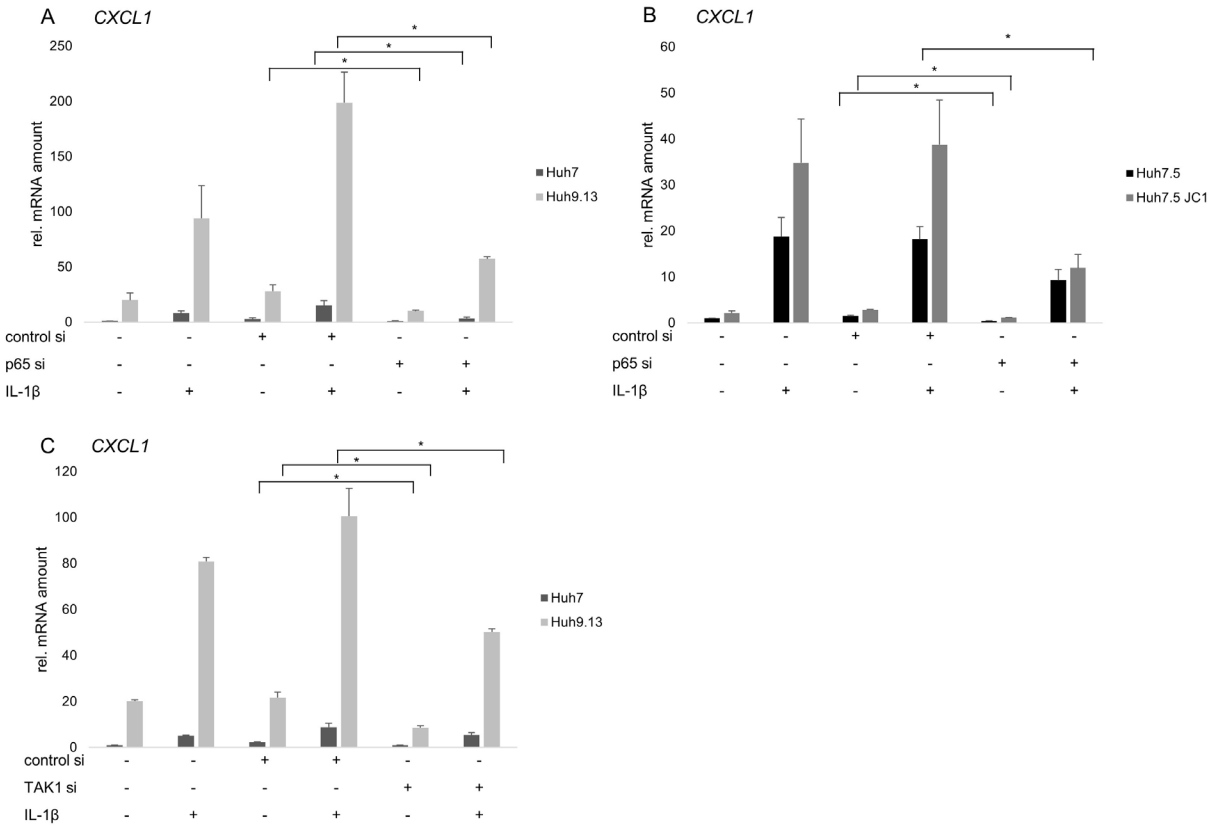

Fig. 23- *CXCL1* mRNA expression after knockdown of *NFκB p65* or *TAK1* in both Huh9.13 and Huh7 cells as well as after *NFκB p65* knockdown in HCV-infected Huh7.5 and Huh7.5 control cells with and without IL-1β administration. Expression of *CXCL1* mRNA was analysed by qRT-PCR in Huh9.13 or in Huh7.5 cells infected with the HCV_{cc} strain JC1 (MOI = 1) and compared to respective control cells. Cells were treated with **(A)+(B)** p65 siRNA and **(C)** TAK1 siRNA. siRNA experiments were performed after stimulation with 0.1 U/mL IL-1β for Huh9.13 and respective control cells or 5 U/mL IL-1β for Huh7.5 infected with the HCV_{cc} strain JC1 (MOI = 1) and respective control cells for 8 h, 72 h after transfection. DMSO was added as a control for all inhibitors. Control siRNA was added as a control for all siRNA experiments. *SDHA* was used as reference gene. Results are expressed as fractions of the normalized value of the control, which was set to 1 and data are presented as means + SEM of at least three independent experiments. Asterisks without lines mark differences between stimulated cells compared to the respective unstimulated control cells. Asterisks mark significant differences versus the infected and control cell lines described as follows: $p<0.05$ = *, $p<0.01$ = **, $p<0.001$ = ***.

Neither use of EGFR inhibitor (AG1478), nor p38 inhibitor (SB203580), nor IKKα/β inhibitor (IKK Inhibitor II), nor AKT inhibitor (Triciribine), nor JNK1 inhibitor (JNK Inhibitor I) showed any effect on *CXCL1* mRNA expression regulation (Fig. 24A-E).

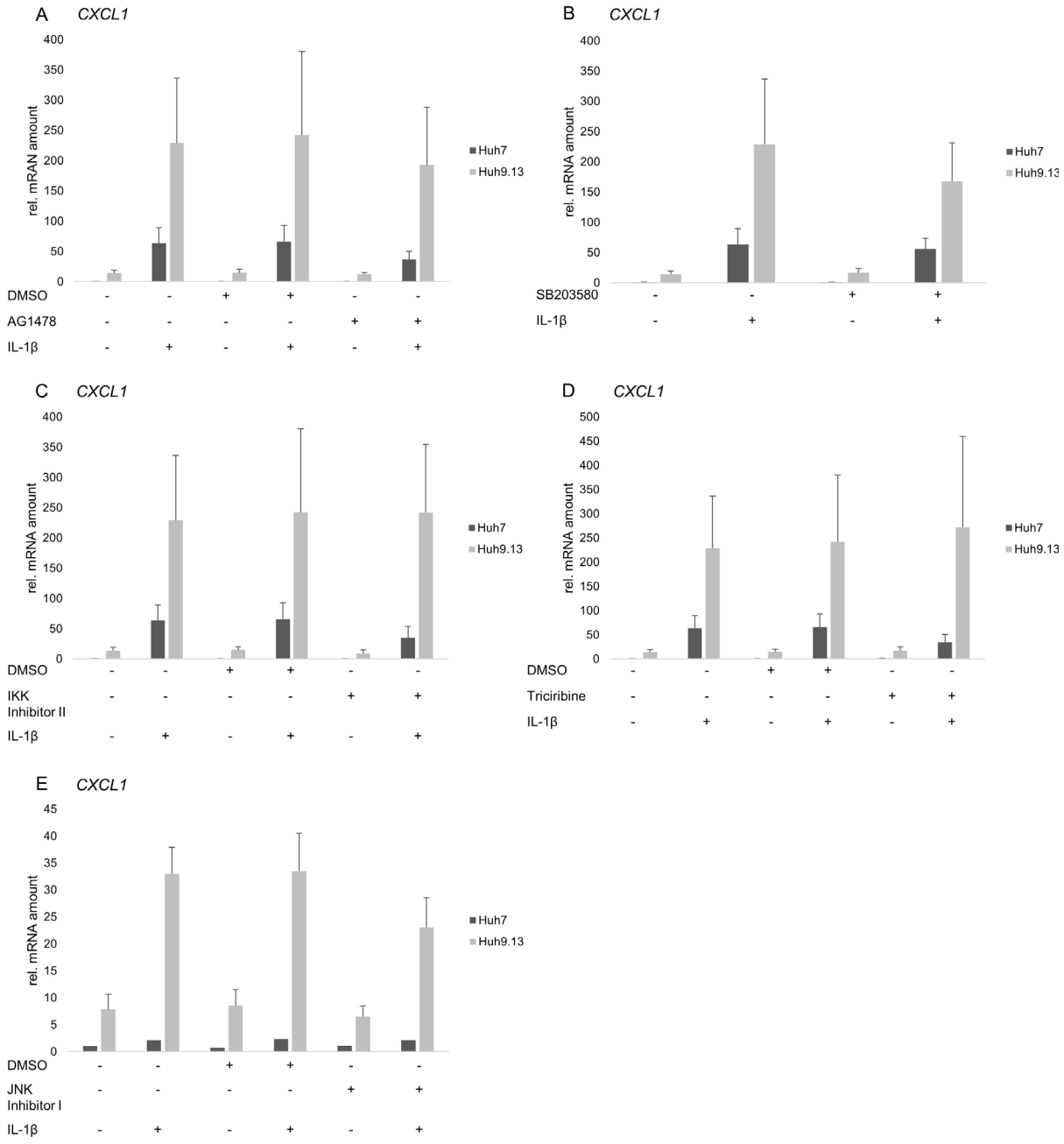

Fig. 24- *CXCL1* mRNA expression after inhibition of different key components of the PI3K/AKT or MAPK signalling pathway in both Huh9.13 and Huh7 cells with and without IL-1β administration. Expression of *CXCL1* mRNA was analysed by qRT-PCR in Huh9.13 and compared to respective control cells. Cells were treated with **(A)** EGFR inhibitor AG1478 [10 μM], **(B)** p38 inhibitor SB203580 [10 μM] **(C)** IKKα and β inhibitor IKK Inhibitor II [10 μM] **(D)** AKT inhibitor Triciribine [10 μM] **(E)** JNK1 Inhibitor JNK Inhibitor I [10 μM]. Inhibitors were added to the cells 1 h prior to a 8 h IL-1β (5 U/mL; in case of JNK Inhibitor I experiments 0.1 U/mL) stimulation of the cells. DMSO was added as a control for all inhibitors. *SDHA* was used as reference gene. Results are expressed as fractions of the normalized value of the control, which was set to 1, and data are presented as means + SEM of at least three independent experiments. Asterisks without lines mark differences between stimulated cells compared to the respective unstimulated control cells. Asterisks mark significant differences versus the infected and control cell lines described as follows: $p<0.05$ = *, $p<0.01$ = **, $p<0.001$ = ***.

Additionally, IL-1β-induced expression of *CXCL2* mRNA was enhanced in HCV-infected cells. *NFκB p65* or *TAK1* knockdown resulted in reduced upregulation of *CXCL2* mRNA expression by IL-1β (Fig. 25A-C), while JNK1 inhibition slightly reduced the IL-1β-induced expression of *CXCL2* mRNA enhanced by HCV (Fig. 25D).

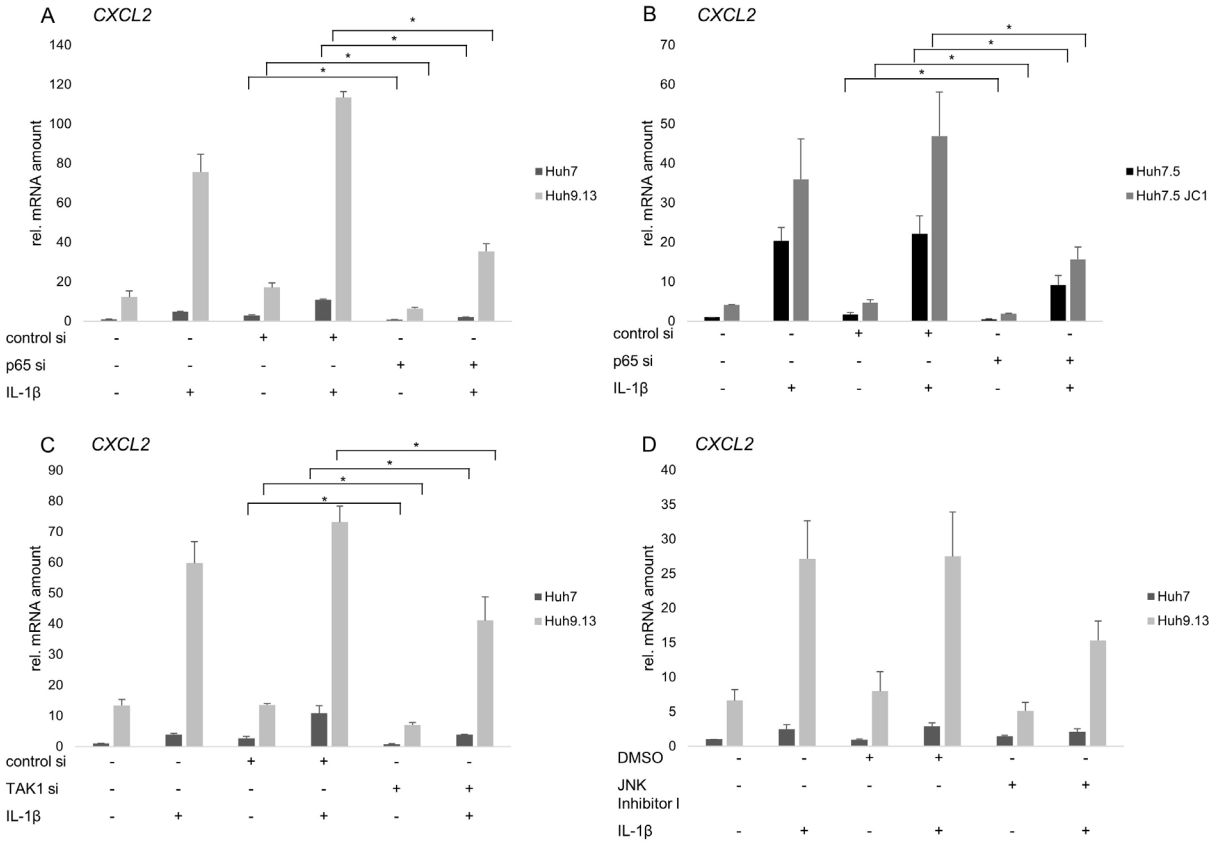

Fig. 25- *CXCL2* mRNA expression after knockdown of *NFκB p65* or *TAK1* or inhibition of JNK1 in both Huh9.13 and Huh7 cells as well as after *NFκB p65* knockdown in HCV-infected Huh7.5 and Huh7.5 control cells with and without IL-1β administration. Expression of *CXCL2* mRNA was analysed by qRT-PCR in Huh9.13 or in Huh7.5 cells infected with the HCV_{cc} strain JC1 (MOI = 1) and compared to respective control cells. Cells were treated with **(A)+(B)** p65 siRNA, **(C)** TAK1 siRNA or **(D)** JNK inhibitor (JNK Inhibitor I). The inhibitor was added to the cells 1 h prior to 8 h IL-1β [0.1 U/mL] stimulation of the cells. In case of siRNA, Huh9.13 and respective control cells were stimulated with 0.1 U/mL IL-1β, Huh7.5 cells infected with the HCV_{cc} strain JC1 and respective control cells with 5 U/mL IL-1β for 8 h, 72 h after transfection. DMSO was added as a control for the inhibitor. Control siRNA was added as a control for all siRNA experiments. *SDHA* was used as reference gene. Results are expressed as fractions of the normalized value of the control, which was set to 1. Data are presented as means + SEM of at least three independent experiments. Asterisks without lines mark differences between stimulated cells compared to the respective unstimulated control cells. Asterisks mark significant differences versus the infected and control cell lines described as follows: $p<0.05$ = *, $p<0.01$ = **, $p<0.001$ = ***.

Neither EGFR inhibitor (AG1478), nor p38 inhibitor (SB203580), nor IKKα/β inhibitor (IKK Inhibitor II), nor AKT inhibitor (Triciribine) showed any effect on *CXCL2* mRNA expression regulation (Fig. 26A-D). This data indicates that induction of *CXCL2* mRNA expression by IL-

1β in hepatic cell lines requires activation of p65, whereas it appears not to play a major role in the enhancement of *CXCL2* mRNA expression by HCV.

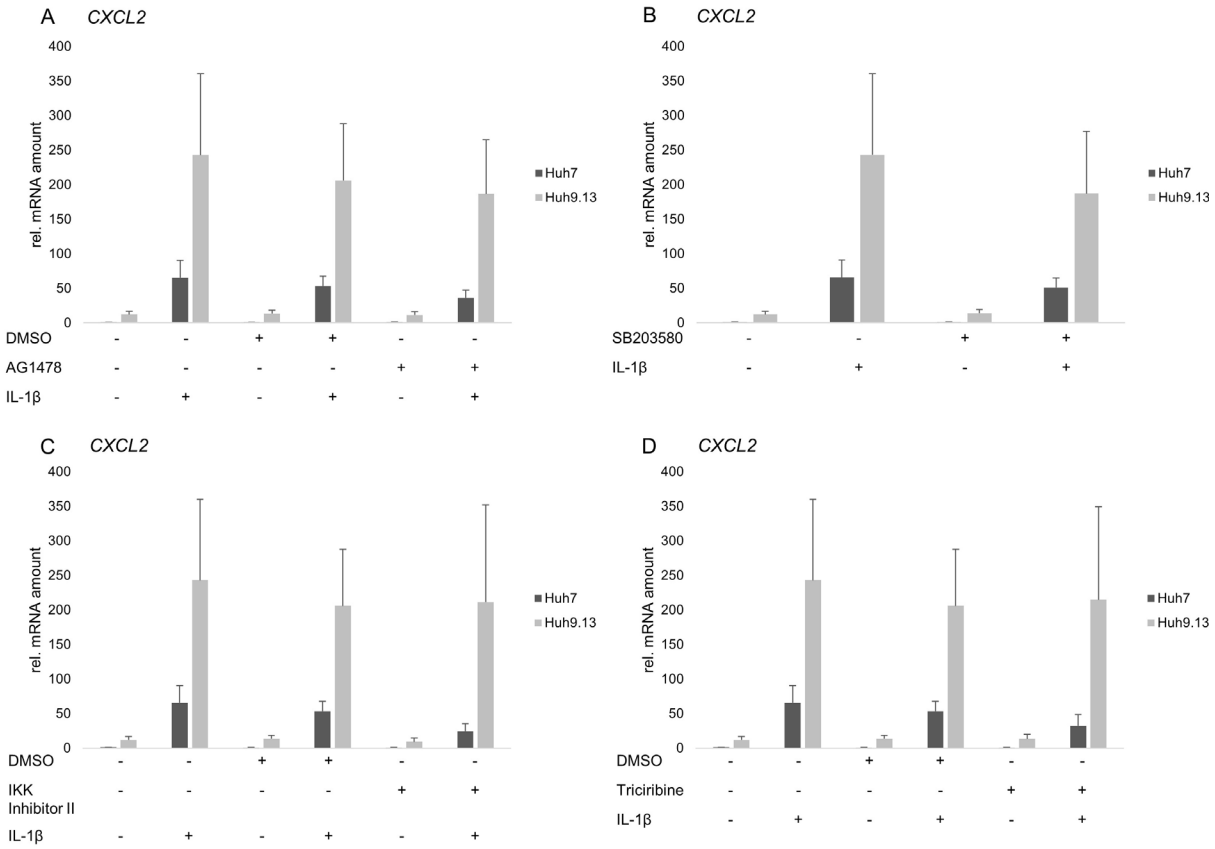

Fig. 26- *CXCL2* mRNA expression after inhibition of different key components of the PI3K/AKT or MAPK signalling pathway in both Huh9.13 and Huh7 cells with and without IL-1β administration. Expression of *CXCL2* mRNA was analysed by qRT-PCR in Huh9.13 and compared to respective control cells. Cells were treated with **(A)** EGFR inhibitor AG1478 [10 µM], **(B)** p38 inhibitor SB203580 [10 µM] **(C)** IKKα and β inhibitor IKK Inhibitor II [10 µM] **(D)** AKT inhibitor Triciribine [10 µM]. Inhibitors were added to the cells 1 h prior to 8 h IL-1β [5 U/mL] stimulation of the cells. DMSO was added as a control for all inhibitors, except for SB203580, which was diluted in water. *SDHA* was used as reference gene. Results are expressed as fractions of the normalized value of the control, which was set to 1. Data are presented as means + SEM of at least three independent experiments. Asterisks without lines mark differences between stimulated cells compared to the respective unstimulated control cells. Asterisks mark significant differences versus the infected and control cell lines described as follows: $p<0.05$ = *, $p<0.01$ = **, $p<0.001$ = ***.

CXCL3 mRNA expression was upregulated in response to HCV infection. Additionally, IL-1β-induced expression of *CXCL3* mRNA was enhanced after HCV infection (Fig. 19). Knockdown of either *NFκB p65* or *TAK1* resulted in a diminished upregulation of *CXCL3* mRNA expression in both Huh9.13 replicon as well as Huh7 control cells (Fig. 27A-C), suggesting NFκB p65 and TAK1 being mediators of *CXCL3* mRNA expression regulation.

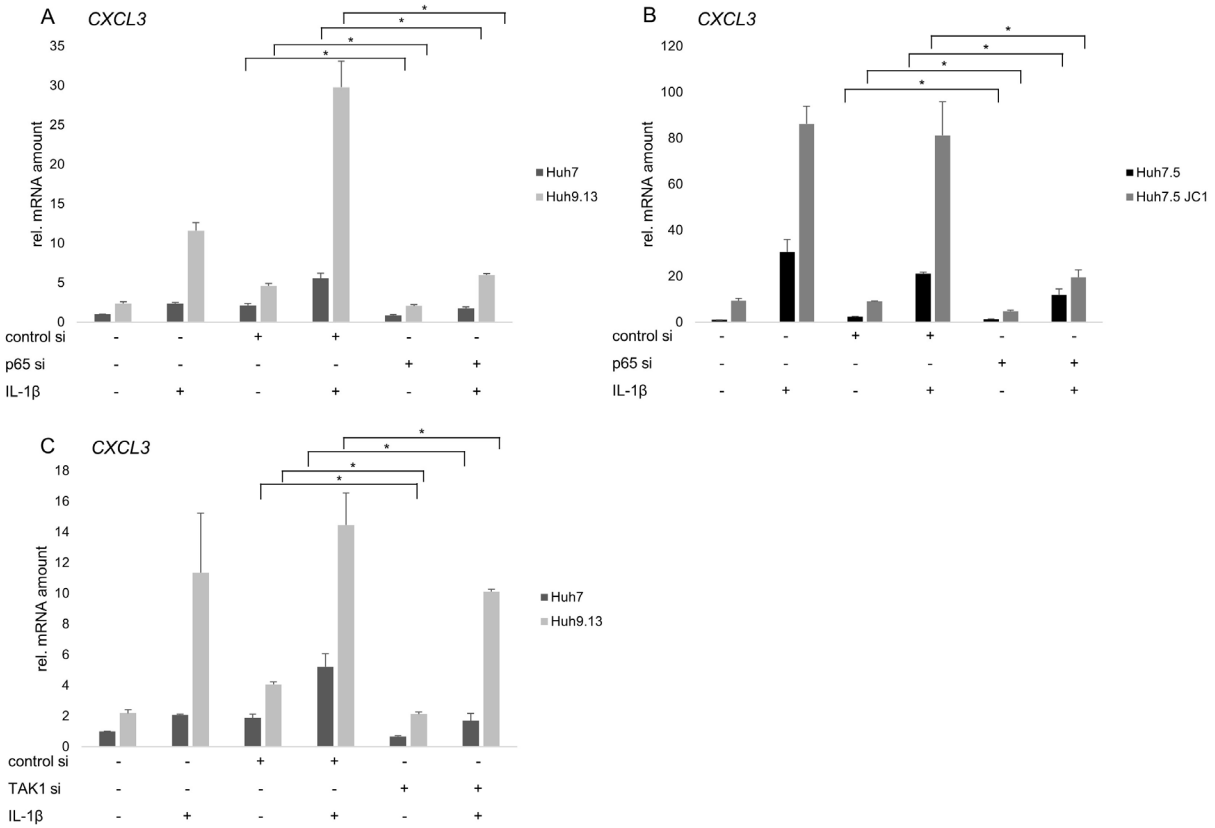

Fig. 27- *CXCL3* mRNA expression after knockdown of *NFκB p65* or *TAK1* in both Huh9.13 and Huh7 cells as well as after *NFκB p65* knockdown in HCV-infected Huh7.5 and Huh7.5 control cells with and without IL-1β administration. Expression of *CXCL3* mRNA was analysed by qRT-PCR in Huh9.13 or in Huh7.5 cells infected with the HCV_{cc} strain JC1 (MOI = 1) and compared to respective control cells. Cells were treated with **(A)+(B)** p65 siRNA or **(C)** TAK1 siRNA. Huh9.13 and respective control cells were stimulated with 0.1, Huh7.5 cells infected with the HCV_{cc} strain JC1 and respective control cells with 5 U/mL IL-1β for 8 h, 72 h after transfection. Control siRNA was added as a control for all siRNA experiments. *SDHA* was used as reference gene. Results are expressed as fractions of the normalized value of the control, which was set to 1. Data are presented as means + SEM of at least three independent experiments. Asterisks without lines mark differences between stimulated cells compared to the respective unstimulated control cells. Asterisks mark significant differences versus the infected and control cell lines described as follows: $p<0.05$ = *, $p<0.01$ = **, $p<0.001$ = ***.

Neither EGFR inhibitor (AG1478), nor p38 inhibitor (SB203580), nor IKKα/β inhibitor (IKK Inhibitor II), nor AKT inhibitor (Triciribine), nor JNK1 inhibitor (JNK Inhibitor I) showed any effect on *CXCL3* mRNA expression regulation (Fig. 28A-E). This data indicates that IL-1β induction of *CXCL3* mRNA expression in hepatic cell lines requires activation of p65, whereas it appears not to play a major role for enhancement of CXCL3 expression by HCV.

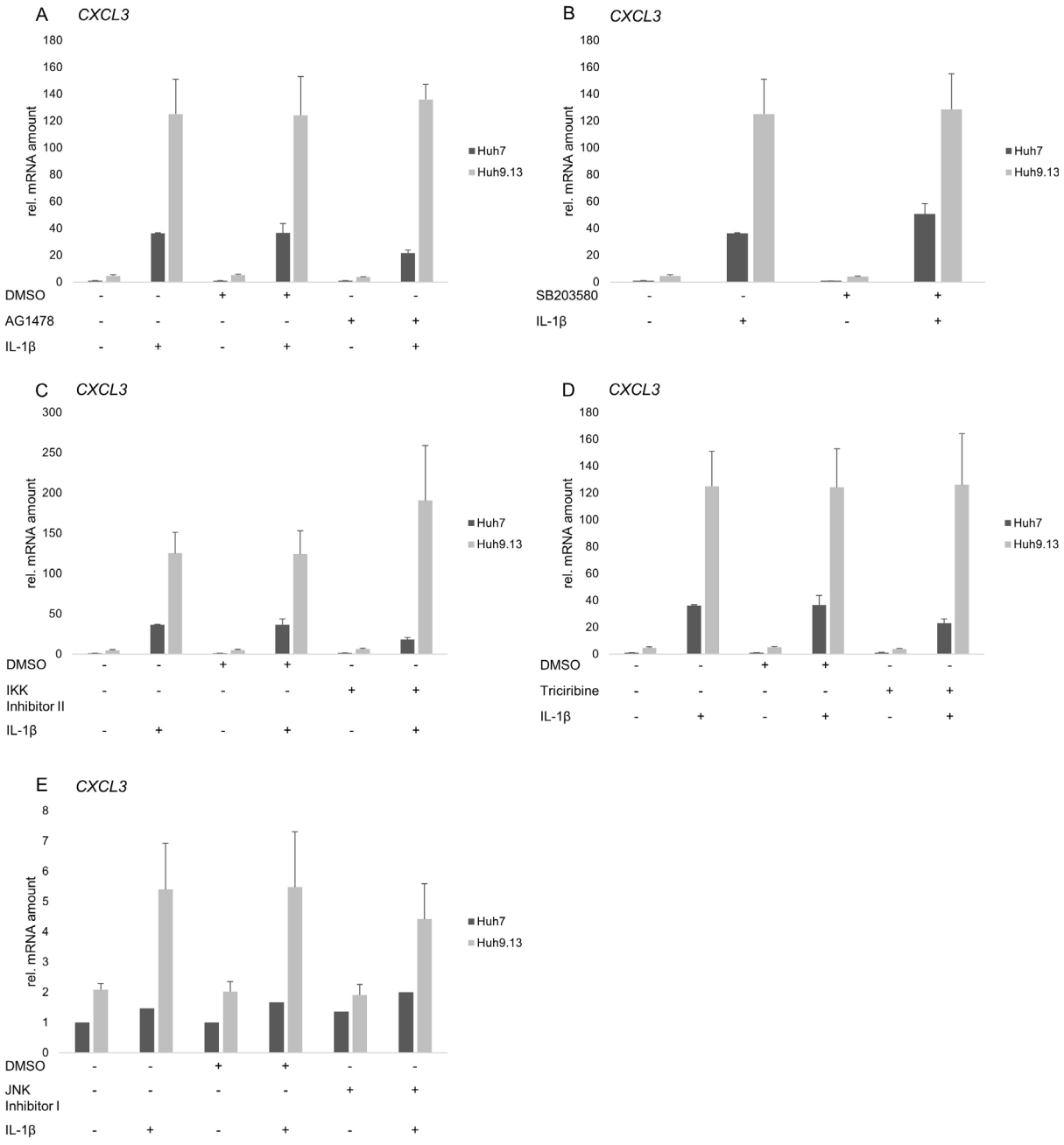

Fig. 28- *CXCL3* mRNA expression after inhibition of different key components of the PI3K/AKT or MAPK signalling pathway in both Huh9.13 and Huh7 cells with and without IL-1β administration. Expression of *CXCL3* mRNA was analysed by qRT-PCR in Huh9.13 and compared to respective control cells. Cells were treated with **(A)** EGFR inhibitor AG1478 [10 µM], **(B)** p38 inhibitor SB203580 [10 µM] **(C)** IKKα and β inhibitor IKK Inhibitor II [10 µM] **(D)** AKT inhibitor Triciribine [10 µM] or **(E)** JNK inhibitor JNK inhibitor I [10 µM]. Inhibitors were added to the cells 1 h prior to 8 h IL-1β (5 U/mL; in case of JNK inhibitor I experiments 0.1 U/mL) stimulation of the cells. DMSO was added as a control for all inhibitors, except for SB203580, which was diluted in water. *SDHA* was used as reference gene. Results are expressed as fractions of the normalized value of the control, which was set to 1. Data are presented as means + SEM of at least three independent experiments. Asterisks without lines mark differences between stimulated cells compared to the respective unstimulated control cells. Asterisks mark significant differences versus the infected and control cell lines described as follows: $p<0.05$ = *, $p<0.01$ = **, $p<0.001$ = ***.

4.3.5 HCV infection causes enhanced binding of NFκB p65 to the *CXCL8* transcription factor binding site in response to IL-1β

The observation that *NFκB p65* knockdown diminished the IL-1β-induced expression of *CXCL8* mRNA enhanced by HCV infection and that HCV infection enhances the IL-1β-induced pre-mRNA expression of *CXCL8* was decisive to perform a chromatin immunoprecipitation (ChIP) assay. Therefore, Huh7 and Huh9.13 cells were stimulated with IL-1β for 30 min or left untreated. Afterwards, proteins were chemically crosslinked to DNA and binding to the *CXCL8* promoter region was analysed by PCR. After IL-1β stimulation, binding of NFκB p65 to the NFκB p65 transcription factor binding site of *CXCL8* was strongly and significantly increased in cells harbouring the HCV replicon compared to Huh7 control cells, strongly suggesting that p65 plays a key regulatory role during IL-1β-mediated chemokine transcription in HCV-infected cells (Fig. 29).

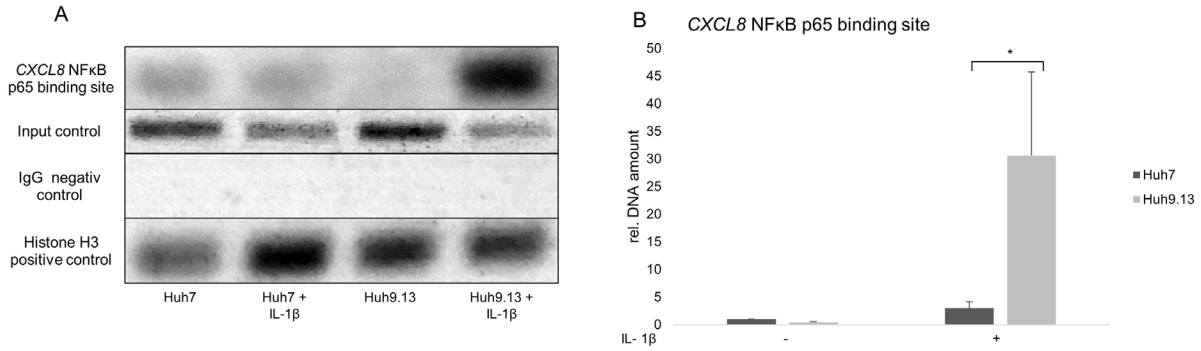

Fig. 29- DNA levels of the chromatin-immunoprecipitated NFκB p65 bound *CXCL8* promoter region in both Huh9.13 and Huh7 control cells with or without IL-1β administration. (A) Relative amount of chromatin-immunoprecipitated NFκB p65 bound *CXCL8* DNA were analysed by PCR in Huh9.13 and Huh7 cells with and without IL-1β stimulation for 30 min at a concentration of 5 U/mL. **(B)** PCR products were size separated via agarose gel electrophoresis and densitometric analysis was performed. Results are expressed as fractions of the normalized value of the control, which was set to 1, and data are presented as means + SEM of at least three independent experiments. Input was used as reference for normalization. Asterisks mark significant differences versus the infected and control cell lines described as follows: $p<0.05$ = *, $p<0.01$ = **, $p<0.001$ = ***.

4.3.6 IL-1β-induced phosphorylation of p38 and NFκB p65 is upregulated after HCV infection

To determine whether HCV influences the upregulation of NFκB p65 or MAPK p38 phosphorylation in response to IL-1β, cells harbouring the HCV subgenomic replicon or cells infected with HCV were stimulated with IL-1β [5 U/mL] for different time periods or left untreated for control. Afterwards, total NFκB p65 protein as well as relative phosphorylation of p38 and NFκB p65 were analysed by immunoblotting.

Interestingly, total protein levels of p65 were slightly enhanced in cells harbouring the subgenomic replicon of HCV, whereas this effect disappeared after IL-1β stimulation (Fig. 30D).

In Huh9.13 cells the relative phosphorylation of p38 at T180/Y182 was significantly upregulated in response to IL-1β stimulation of the cells for 240 min (Fig. 30A/B). Additionally, the relative phosphorylation of NFκB p65 at S536 was significantly upregulated in Huh9.13 cells after 10, 30, and 60 min IL-1β stimulation of the cells when compared to Huh7 control cells (Fig. 30A/C).

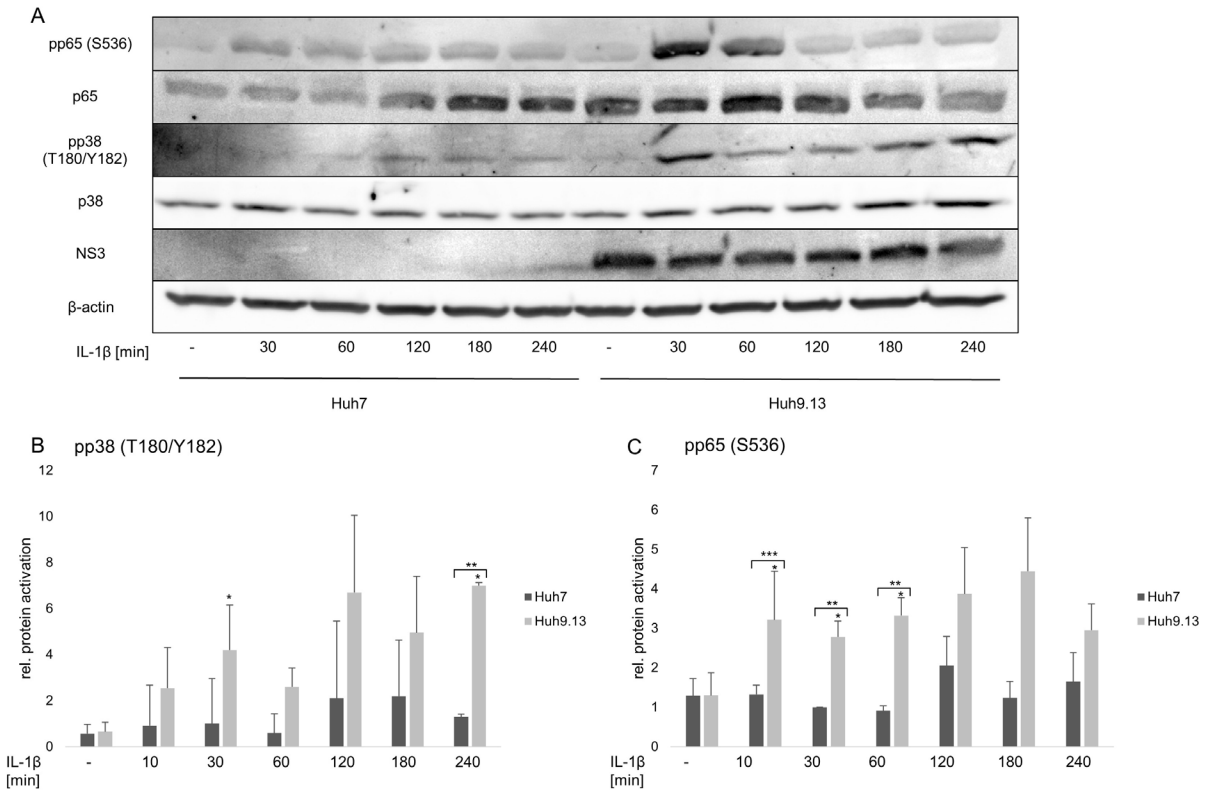

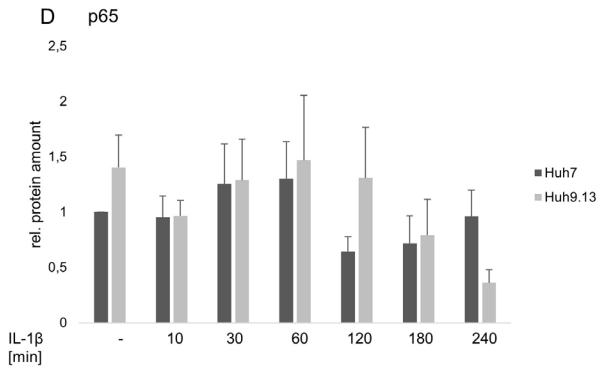

Fig. 30- Protein activation NFκB p65 or p38 and of total NFκB p65 protein levels in Huh9.13 and Huh7 control cells with or without IL-1β stimulation for the indicated time periods. Protein levels of p38 and NFκB p65 were analysed by immunoblotting in Huh9.13 replicon and compared to respective controls. Cells were stimulated with 5 U/mL of IL-1β for the indicated time periods or left untreated. **(A)** Representative immunoblots of at least three independent experiments are shown. Densitometric calculations were performed for the total protein levels of **(B)** pp38 (T180/Y182), **(C)** pp65 (Ser536) and **(D)** p65. Total protein levels were calculated relative to the reference β-actin. Relative phosphorylation levels of proteins were calculated to total protein levels. Results are expressed as fractions of the normalized value of the control, which was set to 1. Data are presented as means + SEM of at least three independent experiments. Asterisks without lines mark differences between stimulated cells compared to the respective unstimulated control cells. Asterisks mark significant differences versus the infected and control cell lines described as follows: $p<0.05$ = *, $p<0.01$ = **, $p<0.001$ = ***.

In contrast to Huh9.13 replicon cells, Huh7.5 cells infected with HCV displayed higher basal phosphorylation levels of p38 at T180/Y182. IL-1β stimulation of these cells resulted in significant upregulation of p38 phosphorylation at T180/Y182 after 10 or 30 min of IL-1β stimulation in Huh7.5 cells infected with HCV compared to uninfected control cells (Fig. 31A/B). Total protein amount of NFκB p65 was not influenced by HCV infection compared to uninfected control cells (Fig. 31A).

NFκB p65 phosphorylation at S536 was significantly higher in HCV-infected cells after stimulation with IL-1β for 30 min compared to uninfected control cells (Fig. 31A/C).

Since phosphorylated NFκB p65 at S536 has a lower affinity to IκBα, it can act as a transcription factor even when IκBα is not degraded (298), pointing at HCV to activate NFκB p65 activity independent of IκBα.

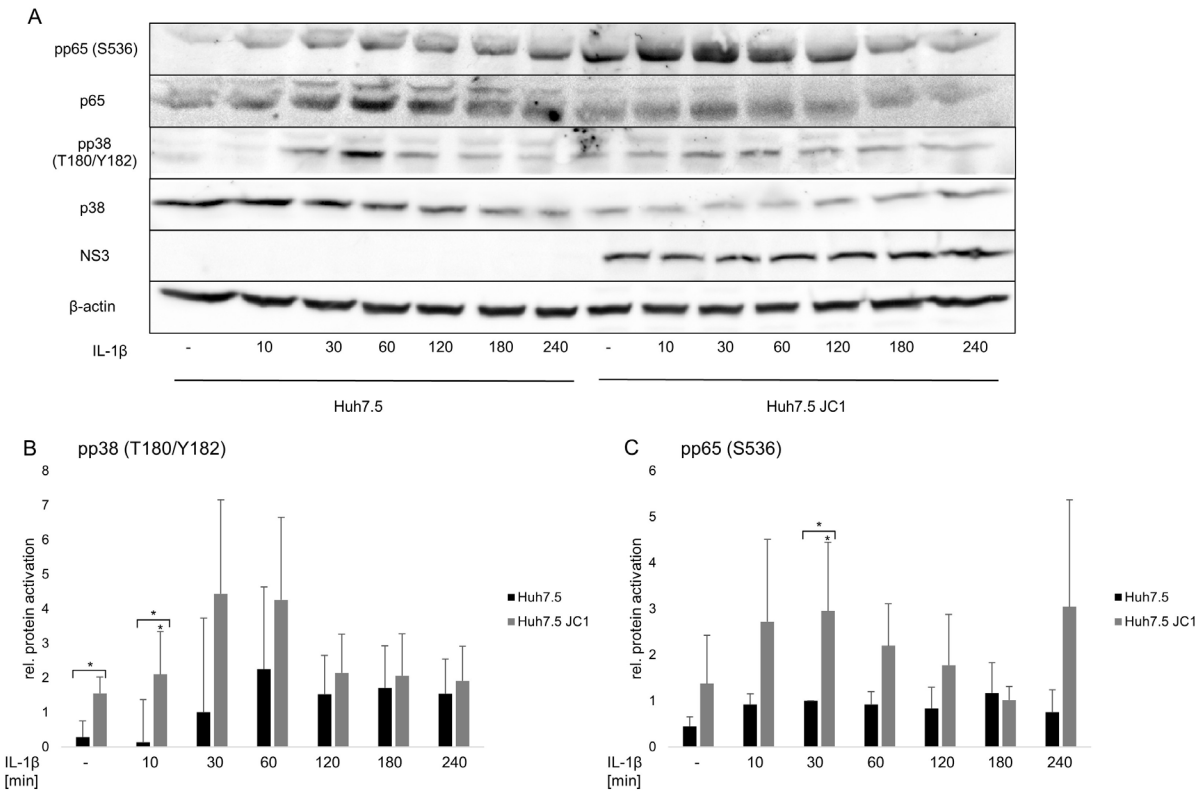

Fig. 31- Protein activation of NFκB p65 or p38 in HCV-infected Huh7.5 and Huh7.5 control cells with or without IL-1β stimulation for the indicated time periods. Protein levels of p38 and NFκB p65 were analysed by immunoblotting in Huh7.5 cells infected with the HCV_{cc} strain JC1 (MOI = 1) and compared to respective controls. Cells were stimulated with 5 U/mL of IL-1β for the indicated time periods or left untreated. **(A)** Representative immunoblots for the analysed proteins. Densitometric calculations were performed for the protein levels of **(B)** pp38 (T180/Y182) and **(C)** pp65 (Ser536). Total protein levels were calculated to the reference β-actin. Relative phosphorylation levels of proteins were calculated to total protein levels. Results are expressed as fractions of the normalized value of the control, which was set to 1. Data are presented as means + SEM of at least three independent experiments. Asterisks without lines mark differences between stimulated cells compared to the respective unstimulated control cells. Asterisks mark significant differences versus the infected and control cell lines described as follows: $p<0.05$ = *, $p<0.01$ = **, $p<0.001$ = ***.

4.3.7 IL-1β-induced expression of *CXCL8* mRNA enhanced by HCV infection is mediated by degradation of IκBα and activation of NFκB p65

To check whether IL-1β *de novo synthesis* is responsible for the long-term observed activation of *CXCL8* mRNA expression (Fig. 18), 1 ng/mL cycloheximide (CHX), a protein *de novo synthesis* inhibitor, was added to the cells for 8 or 24 h. After 1 h, cells were stimulated with IL-1β [5 U/mL]. As shown in Fig. 32A+D, IL-1β-induced upregulation of *CXCL8* mRNA expression was further enhanced in HCV-infected cells. After CHX treatment for 8 and 24 h, *CXCL8* mRNA expression was further increased (Fig. 32A+D). The *NS5A* and *NS3* mRNA expression was downregulated significantly after CHX treatment for 24 h, while after 8 h it was

not significantly affected compared to absence of treatment (Fig. 32B/C+D/E), indicating a reduction of viral replication after inhibition of protein *de novo synthesis* for 24 h.

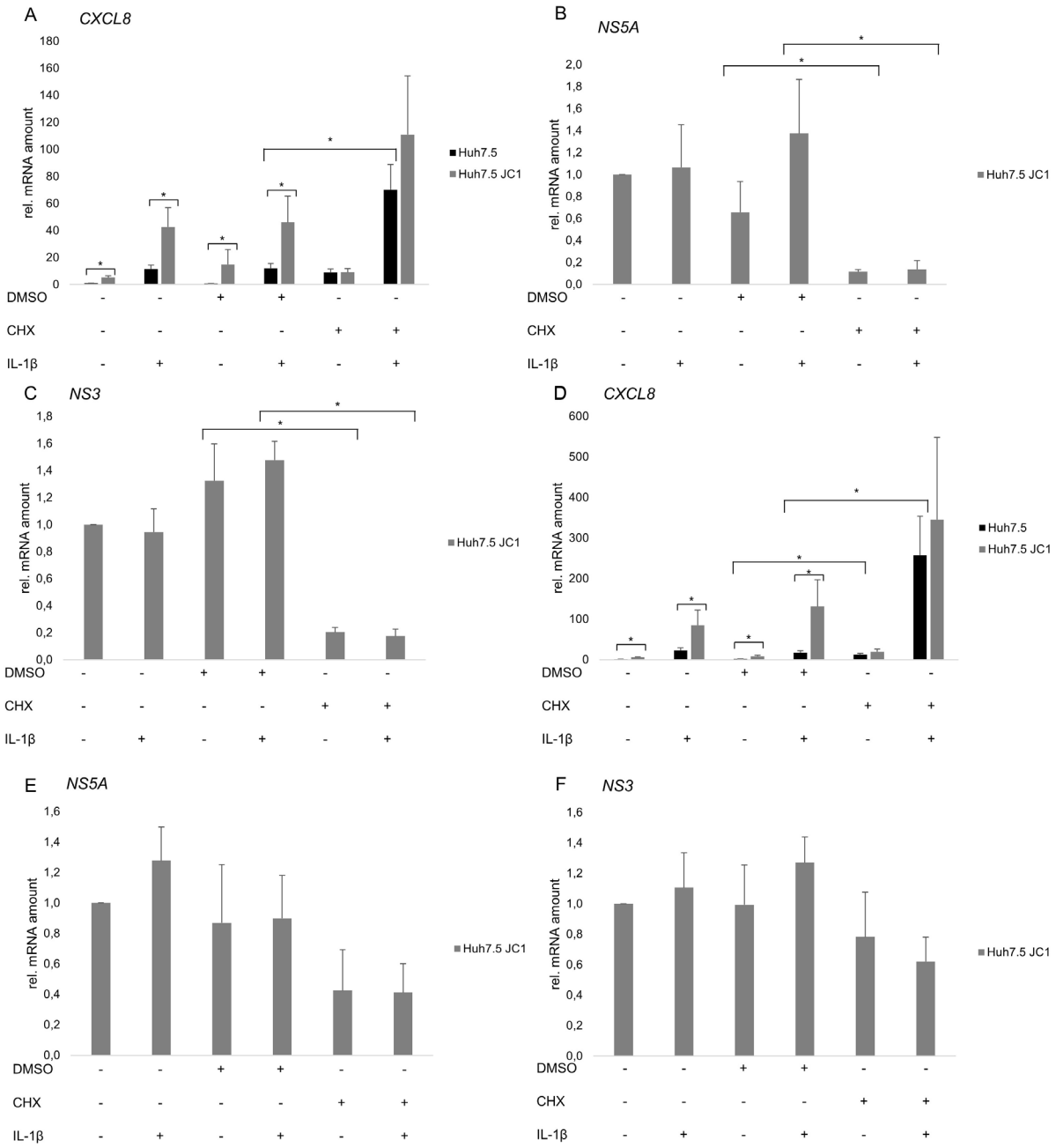

Fig. 32- *NS3*, *NS5A* and *CXCL8* mRNA expression before and after protein *de novo synthesis* inhibition with or without IL-1β administration in Huh9.13 or Huh7 control cells. Expression of *CXCL8, NS5A* and *NS3* mRNA was analysed by qRT-PCR in Huh7.5 cells infected with the HCV_{cc} strain JC1 (MOI = 1) and compared to respective control cells. Cells were treated with the protein *de novo synthesis* inhibitor Cycloheximide [1 ng/mL] for 8h or 24h and mRNA expression of **(A)+(D)** *CXCL8,* **(B)+(E)** *NS5A* or **(C)** *NS3* was analysed by qRT-PCR. The inhibitor was added to the cells 1 h prior to **(A)+(B)+(C)** 23 or **(D)+(E)+(F)** 7 h of IL-1β [5 U/mL] stimulation of the cells. DMSO was added as a control. *SDHA* was used as reference gene. Results are expressed as fractions of the normalized value of the control, which was set to 1, and data are presented as means + SEM of at least three independent experiments. Asterisks without lines mark differences between stimulated cells compared to the respective

unstimulated control cells. Asterisks mark significant differences versus the infected and control cell lines described as follows: p<0.05 = *, p<0.01 = **, p<0.001 = ***.

Furthermore, the protein levels of NS3 were significantly downregulated after CHX treatment for 24 h, whereas already after 1 h 40 min of CHX treatment the NS3 protein amount was decreasing (Fig. 33A/B+D/E). IκBα, which traps NFκB p65 in the cytoplasm and therefore inactivates it, was downregulated significantly after HCV infection and IL-1β-induced downregulation of IκBα was further reduced in HCV-infected cells (Fig. 33C+F). After treatment of cells with CHX for 24 h, IκBα protein levels were strongly decreased, suggesting an enhanced release of NFκB p65 and, in turn, an enhanced activation of *CXCL8* transcription (Fig. 32A/D+ 33A/C). Taken together, these results additionally indicate an IκBα-dependent activation of NFκB p65 by HCV in addition to the prior noted IκBα-independent activation of NFκB p65 by HCV.

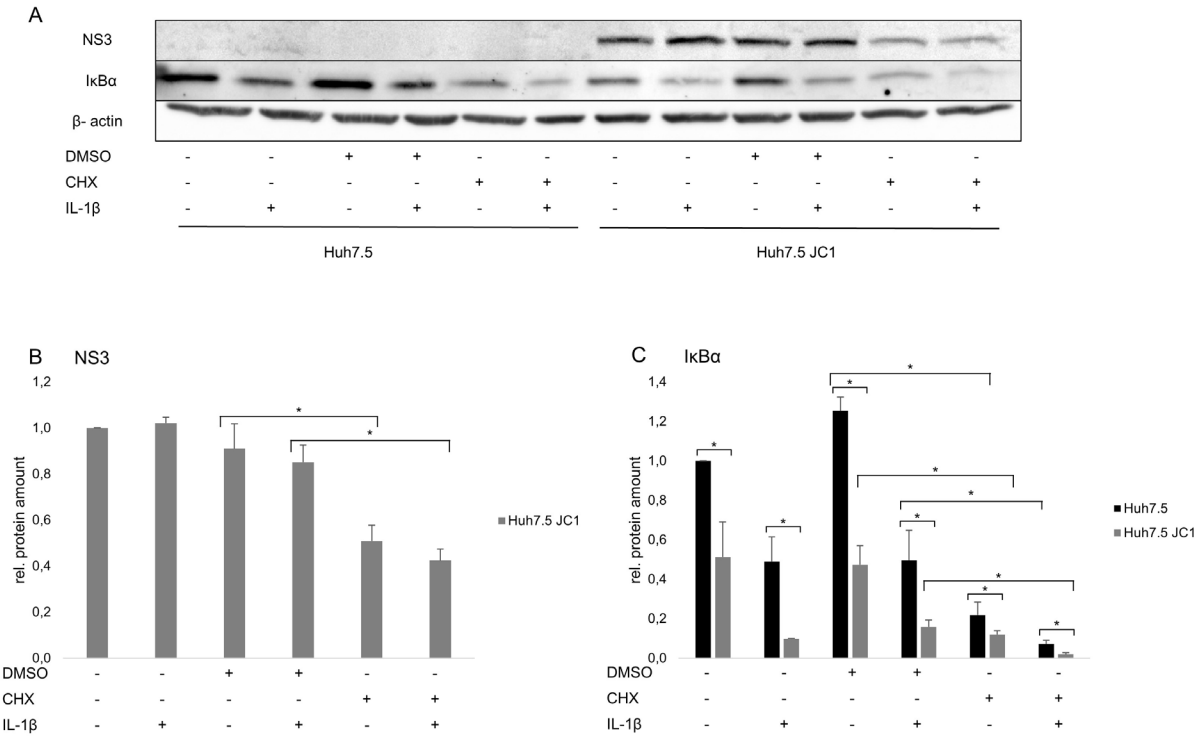

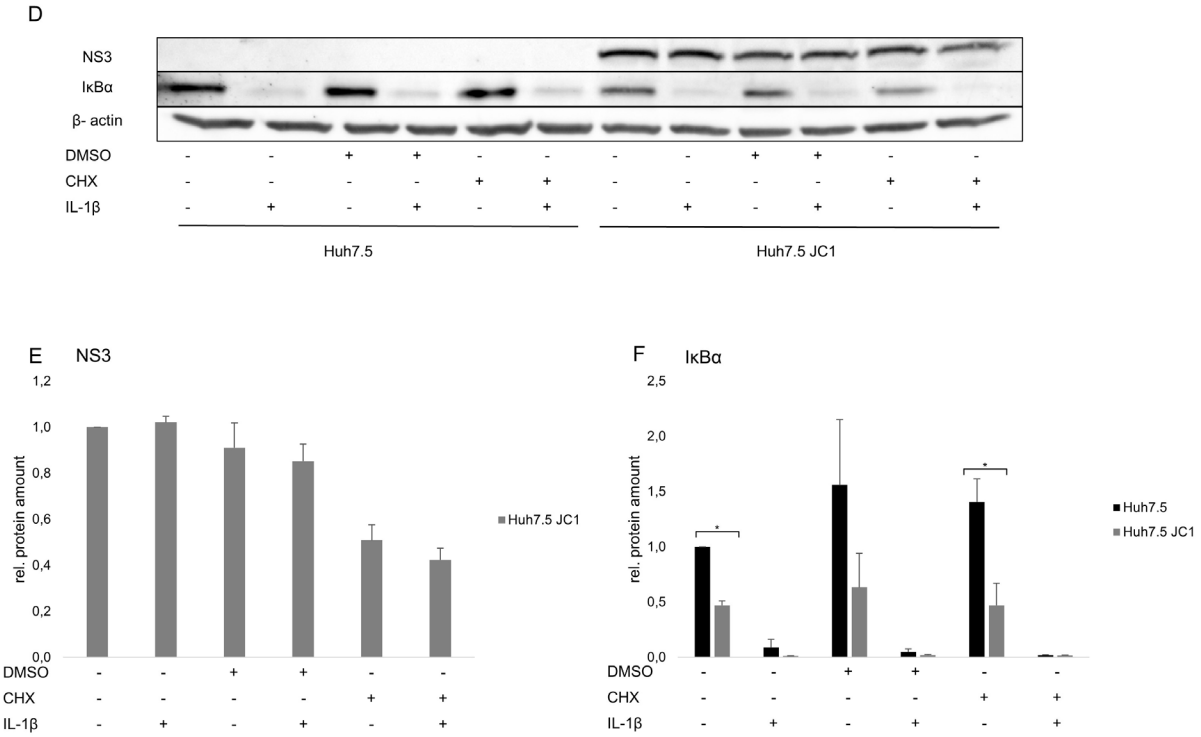

Fig. 33- Protein levels of NS3 and IκBα in HCV-infected Huh7.5 and Huh7.5 control cells after and before inhibition of protein *de novo synthesis* for different time periods and with or without IL-1β stimulation for the indicated time periods. Protein levels of IκBα and NS3 were analysed by immunoblotting in Huh7.5 cells infected with the HCV_{cc} strain JC1 (MOI = 1) and compared to respective controls. Cells were stimulated with 5 U/mL of IL-1β 1 h after inhibitor addition for the indicated time periods or left untreated. **(A)+(D)** Representative immunoblots for the analysed proteins. Densitometric calculations were performed for the protein levels of **(B)+(E)** NS3 and **(C)+(F)** IκBα. Total protein levels were calculated to the reference β-actin. The inhibitor was added to the cells 1 h prior to a **(A)+(B)+(C)** 23 or **(D)+(E)+(F)** 7 h IL-1β [5 U/mL] stimulation of the cells. DMSO was added as a control. Results are expressed as fractions of the normalized value of the control, which was set to 1. Data are presented as means + SEM of at least three independent experiments. Asterisks without lines mark differences between stimulated cells compared to the respective unstimulated control cells. Asterisks mark significant differences versus the infected and control cell lines described as follows: $p<0.05$ = *, $p<0.01$ = **, $p<0.001$ = ***.

4.4 Interference of HCV with TNFα signalling pathways

4.4.1 TNFα-induced expression of *CXCL3* and *8* mRNA is enhanced by HCV

As described in **4.2.1** and **4.3.1**, the mRNA expression of *CXCL1*, *2*, *3* and *8* is increased by HCV and EGF- and IL-1β-induced expression of those chemokines is enhanced by HCV infection of the cells.

TNFα levels were shown to be enhanced in transgenic mice expressing NS3/4A in the liver and thus leading to the protection of the mice upon TNFα/D-galactosamine (D-galN)- and LPS/D-galN-induced liver damage (231).

In addition, it was demonstrated previously in the literature and in our own cohorts that TNFα protein levels are significantly elevated in the sera of HCV-infected patients (199, 226, 227) and **4.1**).

Therefore, it was investigated whether HCV also interferes with TNFα-mediated upregulation of the CXCR2 ligands CXCL1, 2, 3 and 8. Therefore, cells infected with HCV were stimulated for different time periods with 1 or 5 ng/mL TNFα or with different concentrations of TNFα for 8 h. Fig. 34A-F shows that TNFα-induced concentration-dependent expression of *CXCL3* and *8* mRNA was enhanced by HCV infection. After 2 and 4 h, the TNFα-induced expression of *CXCL3* mRNA was not enhanced by HCV infection, while after 8 h HCV enhancement of the TNFα-induced *CXCL3* mRNA expression by HCV could be observed (Fig. 34B/C).

Interestingly, when cells were stimulated with 1 ng/mL TNFα for 16 h, TNFα-induced expression of *CXCL3* mRNA was enhanced by HCV infection, while this was not the case when cells were stimulated with 5 ng/mL TNFα (Fig. 34B/C).

In case of *CXCL8* mRNA expression, HCV enhanced TNFα-induced expression of *CXCL8* mRNA after 8 h, while after 2, 4 and 16 h HCV infection did not result in an enhancement of the TNFα-induced expression of *CXCL8* mRNA (Fig. 34F/E).

The data presented in this thesis thus show that, besides EGF- and IL-1β-, also TNFα-induced expression of *CXCL3* and *8* mRNA is enhanced by HCV infection.

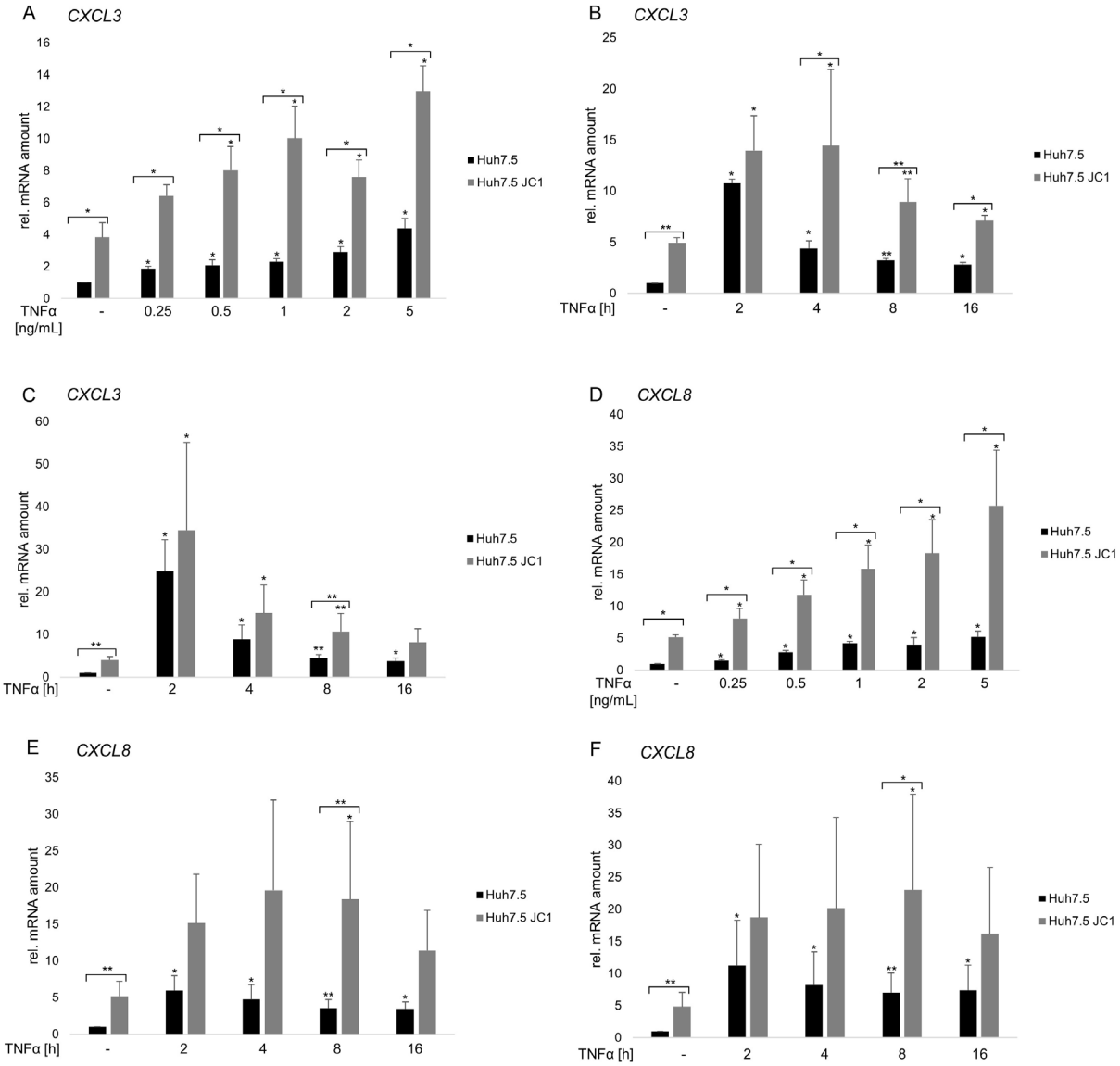

Fig. 34- *CXCL3* and *8* mRNA expression after administration of TNFα in concentrations up to 5 ng/mL for the indicated time periods in both HCV-infected Huh7.5 and Huh7.5 control cells. Expression of *CXCL3* and *8* mRNA was analysed by qRT-PCR in Huh7.5 cells infected with the HCV_{cc} strain JC1 (MOI = 1) and compared to respective control cells. Cells were treated with **(A)+(D)** different concentrations of TNFα for 8 h, **(B)+(E)** 1 ng/mL TNFα for different time periods, **(C)+(F)** 5 ng/mL TNFα for different time periods. *SDHA* was used as reference gene. Results are expressed as fractions of the normalized value of the control, which was set to 1. Data are presented as means + SEM of at least three independent experiments. Asterisks without lines mark differences between stimulated cells compared to the respective unstimulated control cells. Asterisks mark significant differences versus the infected and control cell lines described as follows: $p<0.05$ = *, $p<0.01$ = **, $p<0.001$ = ***.

In contrast to *CXCL3* and *8* mRNA expression, TNFα-induced expression of *CXCL1* and *2* mRNA was not enhanced by HCV infection (Fig. 35A-F), indicating that in contrast to EGF- and IL-1β-, TNFα-induced expression of *CXCL1* and *2* mRNA is not affected by HCV.

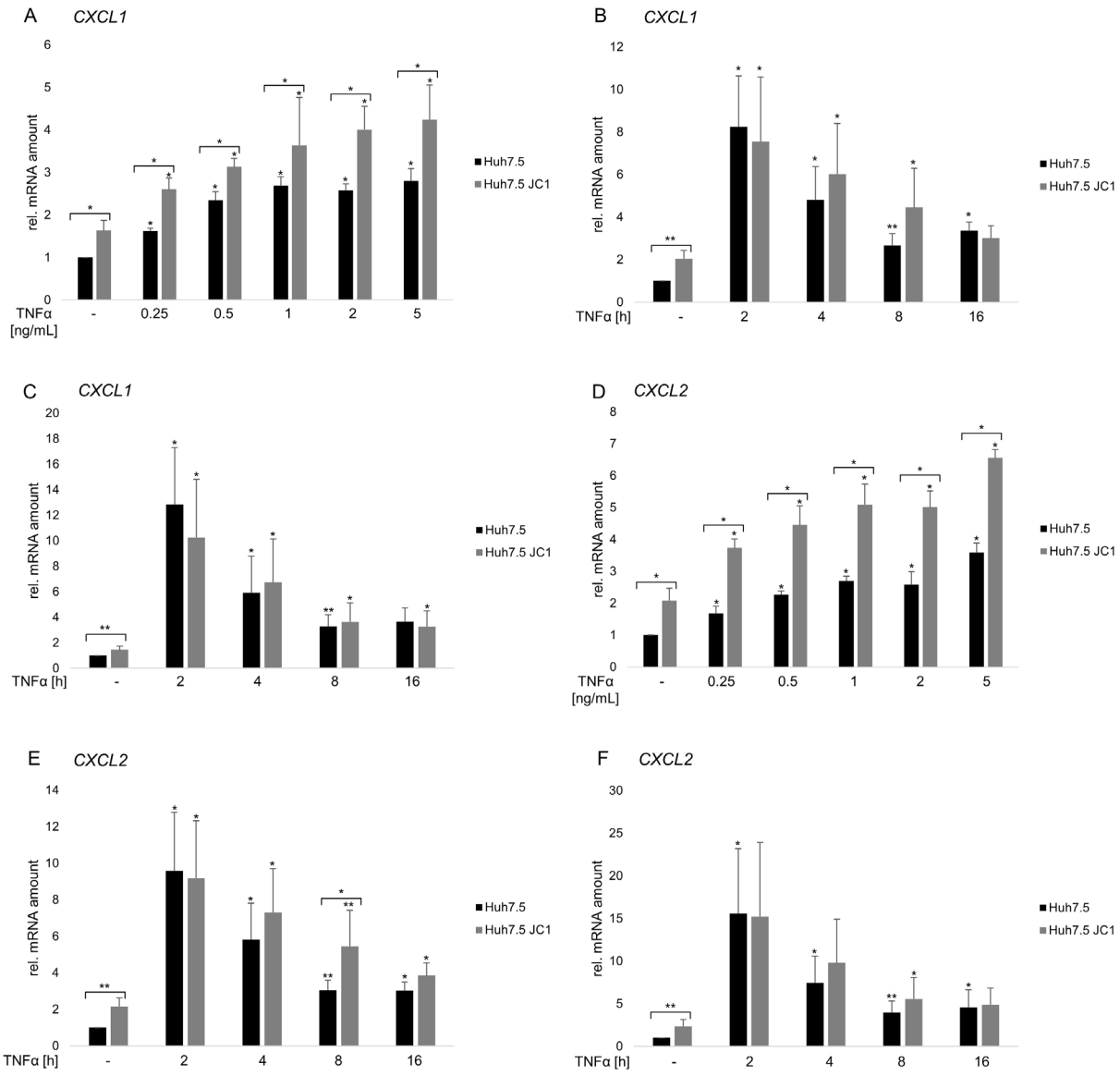

Fig. 35- *CXCL1* and *2* mRNA expression after administration of TNFα in concentrations up to 5 ng/mL for the indicated time periods in both HCV-infected Huh7.5 and Huh7.5 control cells. Expression of *CXCL1* and *2* mRNA was analysed by qRT-PCR in Huh7.5 cells infected with the HCV_{cc} strain JC1 (MOI = 1) and compared to respective control cells. Cells were treated with **(A)+(D)** different concentrations of TNFα for 8 h, **(B)+(E)** 1 ng/mL TNFα for different time periods, or **(C)+(F)** 5 ng/mL TNFα for different time periods. *SDHA* was used as reference gene. Results are expressed as fractions of the normalized value of the control, which was set to 1. Data are presented as means + SEM of at least three independent experiments. Asterisks without lines mark differences between stimulated cells compared to the respective unstimulated control cells. Asterisks mark significant differences versus the infected and control cell lines described as follows: $p<0.05$ = *, $p<0.01$ = **, $p<0.001$ = ***.

4.4.2 TNFα-induced expression of *CXCL8* pre-mRNA is enhanced by HCV infection

As described in **4.4.1**, HCV enhanced TNFα-induced expression of *CXCL8* mRNA. To check whether *CXCL8* pre-mRNA is upregulated by TNFα and whether HCV infection affects the *CXCL8* expression at pre-mRNA level, intron-exon spanning primers (**4.3.2**) were used to quantify pre-mRNA via qRT-PCR. Here, it could be demonstrated that administration of a concentration of 1 ng/mL or higher concentrations of TNFα-induced *CXCL8* pre-mRNA expression (Fig. 36). Additionally, HCV enhanced *CXCL8* pre-mRNA expression significantly. The TNFα-induced expression of pre-mRNA was significantly enhanced in response to HCV infection after administration of 2 ng/mL TNFα. In summary, the data presented in Fig. 36 suggest that TNFα- as well as HCV-dependent enhancement of *CXCL8* mRNA expression occurs, at least partly, before splicing. How exactly this specific significant enhancement of TNFα-induced expression of *CXCL8* pre-mRNA by HCV is mediated has to be further investigated.

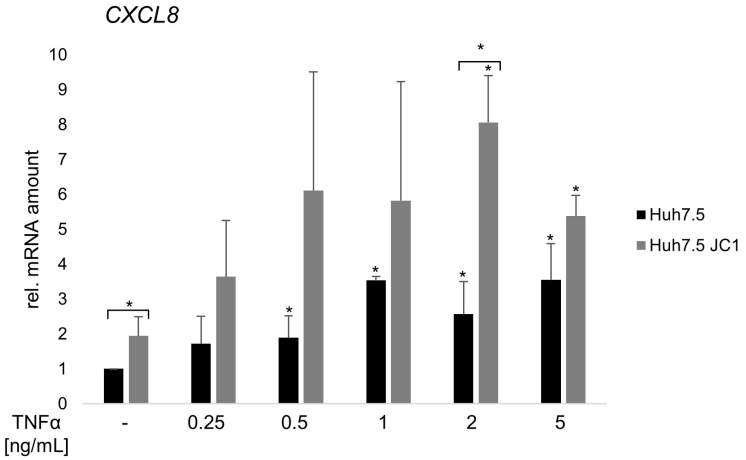

Fig. 36- *CXCL8* pre-mRNA expression after administration of TNFα in concentrations up to 5 ng/mL in both HCV-infected Huh7.5 and Huh7.5 control cells. Expression of *CXCL8* pre-mRNA was analysed by qRT-PCR in Huh7.5 cells infected with the HCV_{cc} strain JC1 (MOI = 1) and compared to respective control cells. *CXCL8* pre-mRNA expression was measured after treatment of the cells with different concentrations of TNFα for 8 h. *SDHA* was used as reference gene. Results are expressed as fractions of the normalized value of the control, which was set to 1. Data are presented as means + SEM of at least three independent experiments. Asterisks without lines mark differences between stimulated cells compared to the respective unstimulated control cells. Asterisks mark significant differences versus the infected and control cell lines described as follows: $p<0.05$ = *, $p<0.01$ = **, $p<0.001$ = ***.

4.4.3 IL-1β and TNFα do not act synergistically to enhance *CXCL8* mRNA expression in response to HCV infection

To analyse whether IL-1β can further enhance the TNFα-induced expression of *CXCL8* mRNA enhanced by HCV infection, cells were stimulated with varying concentrations of TNFα and with or without IL-1β [0.1 U/mL] for 8 h. The TNFα-induced expression of *CXCL8* mRNA enhanced after HCV infection was not further enhanced by addition of IL-1β (Fig. 37). Thus, a synergistic effect of the two cytokines is not suggested by these experiments. Fig. 37 shows that the relative *CXCL8* mRNA levels were nearly the same in Huh9.13 cells after stimulation with IL-1β at a concentration of 0.1 U/mL as they were after stimulation with TNFα at a concentration of 100 pg/mL. Considering that 0.1 U/mL IL-1 β reflect a concentration of 2 pg/mL, a 50-fold higher concentration of TNFα is necessary to reach the same effect on *CXCL8* mRNA expression levels.

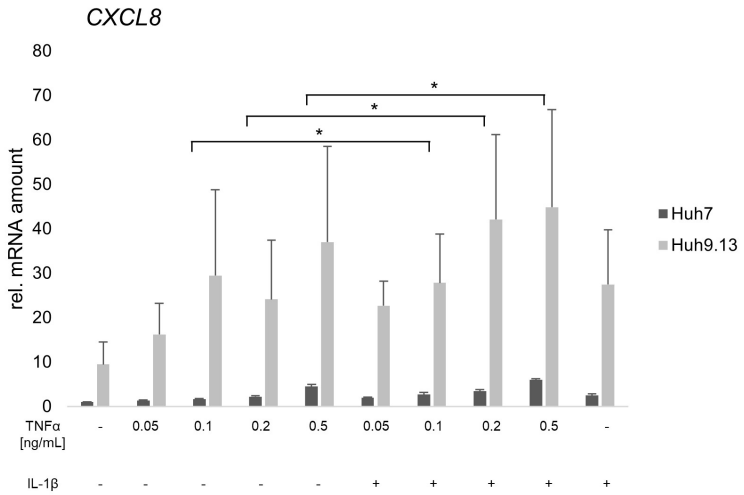

Fig. 37- *CXCL8* mRNA expression after administration of TNFα in concentrations up to 0.5 ng/mL in both Huh9.13 and Huh7 control cells with and without IL-1β administration. Expression of *CXCL8* mRNA was analysed by qRT-PCR in Huh9.13 cells compared to respective control cells. Cells were treated with the indicated concentrations of TNFα for 8 h with or without the addition of 0.1 U/mL IL-1β for 8 h or left untreated. *SDHA* was used as reference gene. Results are expressed as fractions of the normalized value of the control, which was set to 1. Data are presented as means + SEM of at least three independent experiments. Asterisks mark significant differences versus the infected and control cell lines described as follows: $p<0.05$ = *, $p<0.01$ = **, $p<0.001$ = ***.

4.4.4 TNFα-induced *CXCL8* mRNA expression is mediated by NFκB p65

To investigate the involved signalling pathways in the TNFα-induced expression of *CXCL1*, *2*, *3* and *8* mRNA as well as the TNFα-induced expression of *CXCL3* and *8* mRNA enhanced by HCV infection, siRNA and inhibitor experiments were performed.

Overall, the herein used inhibitors (MEK, JNK, EGFR, p38, IKKα and β and AKT) showed no effects on the regulation of *CXCL8* mRNA expression (Fig. 38A-F).

In contrast, TNFα-induced expression of *CXCL8* mRNA enhanced by HCV infection was diminished significantly after siRNA-mediated *NFκB p65* knockdown when compared to control siRNA-treated Huh9.13 cells, while *TAK1* knockdown only slightly reduced the TNFα-induced expression of *CXCL8* mRNA in Huh9.13 cells (Fig. 38G/I), suggesting that NFκB p65 signalling has to be, at least partially, activated via other mechanisms in this context.

TNFα- induced *CXCL8* mRNA expression was also reduced, although not significantly, in Huh7 cells after *NFκB p65* knockdown (Fig. 38G/I), while *TAK1* knockdown did not influence TNFα- induced expression of *CXCL8* mRNA in Huh7 cells, suggesting that NFκB p65 may be activated via other signalling pathways in this context.

In addition, *CXCL8* mRNA expression was, although not significantly, reduced in Huh7 and Huh9.13 cells after both *NFκB p65* and *TAK1* knockdown (Fig. 38G).

Taken together, these experiments suggest that the NFκB subunit p65 is the leading mediator in TNFα-induced expression of *CXCL8* mRNA enhanced by HCV infection, and partly mediates the TNFα-induced expression of *CXCL8* mRNA in Huh7 cells as well, TAK1 on the other hand is suggested to partly mediate TNFα-induced expression of *CXCL8* mRNA only if it is enhanced after HCV infection.

In contrast, *CXCL8* mRNA expression is slightly reduced in Huh9.13 and in Huh7 cells in response to both *NFκB p65* and *TAK1* knockdown, indicating that both factors mediate *CXCL8* mRNA expression regulation in both cell lines.

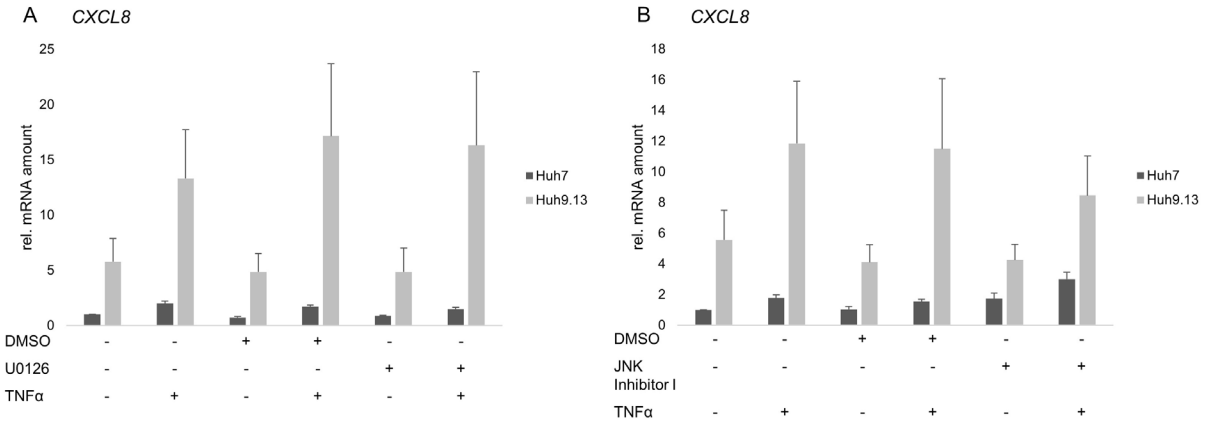

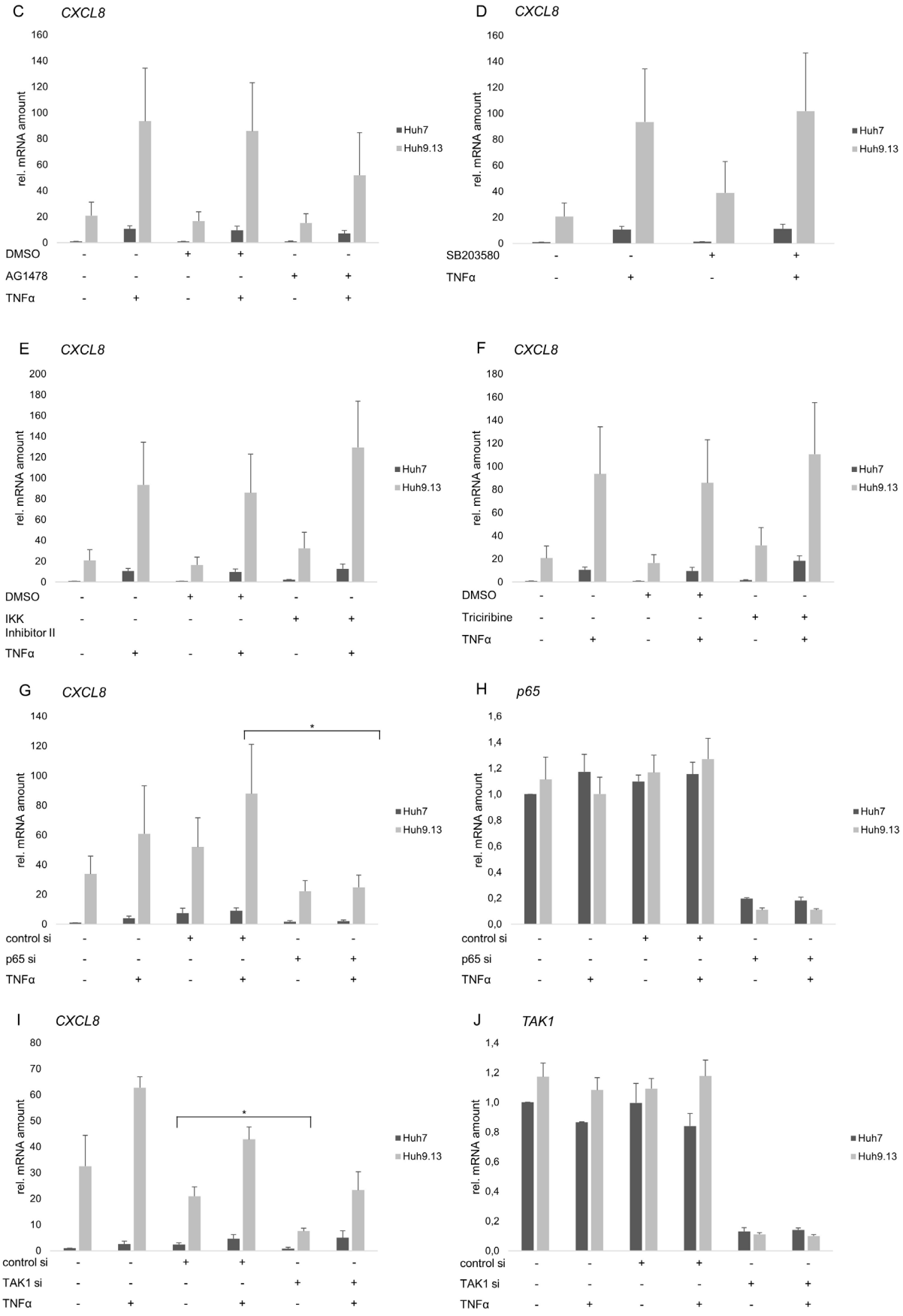

Fig. 38- *CXCL8* mRNA expression after knockdown of *NFκB p65* or *TAK1* or inhibition of the EGFR, IKK as well as key components of the PI3K/AKT or MAPK signalling pathway in Huh9.13 and Huh7 cells with and without TNFα administration. Expression of *CXCL8, p65* and *TAK1* mRNA was analysed by qRT-PCR in Huh9.13

and compared to respective control cells. Cells were treated with **(A)** MEK 1 inhibitor U0126 [10 µM], **(B)** JNK inhibitor JNK inhibitor I [10 µM], **(C)** EGFR inhibitor AG1478 [10 µM], **(D)** p38 inhibitor SB203580 [10 µM], **(E)** IKKα/β inhibitor IKK Inhibitor II [10 µM] or **(F)** AKT inhibitor Triciribine [10 µM]. DMSO was added as a control for all inhibitors, except for SB203580 which was diluted in water. Inhibitors were added to the cells 1 h prior to 8 h TNFα (1 ng/mL; 0.1 ng/mL in case of p65 and TAK1 siRNA as well as JNK inhibitor I experiments) stimulation of the cells. Furthermore, cells were treated with **(G)+(H)** p65 siRNA or **(I)+(J)** TAK1 siRNA and stimulated with TNFα [1 ng/mL] for 8 h without or 72 h after transfection. Control siRNA was added as a control for all siRNA experiments. *SDHA* was used as reference gene. Results are expressed as fractions of the normalized value of the control, which was set to 1. Data are presented as means + SEM of at least three independent experiments. Asterisks without lines mark differences between stimulated cells compared to the respective unstimulated control cells. Asterisks mark significant differences versus the infected and control cell lines described as follows: $p<0.05$ = *, $p<0.01$ = **, $p<0.001$ = ***.

Inhibition of MEK, JNK, EGFR, p38, IKKα and β and AKT did not show any effects on the *CXCL1* mRNA expression regulation (Fig. 39A-D).

TNFα-induced *CXCL1* mRNA expression was not enhanced by HCV infection (**4.4.1**). Knockdown of *NFκB p65* resulted in reduced *CXCL1* mRNA expression (Fig. 39E). *TAK1* knockdown significantly reduced the *CXCL1* mRNA expression in Huh7 as well as in Huh9.13 cells (Fig. 39F). This suggests that TAK1 as well as NFκB p65 mediate *CXCL1* mRNA expression regulation in these cells.

Interestingly, *TAK1* knockdown did not affect TNFα-induced *CXCL1* mRNA expression in Huh7 cells, whereas NFκB p65 did, suggesting that NFκB p65 needs to be activated via other upstream mediators in this context.

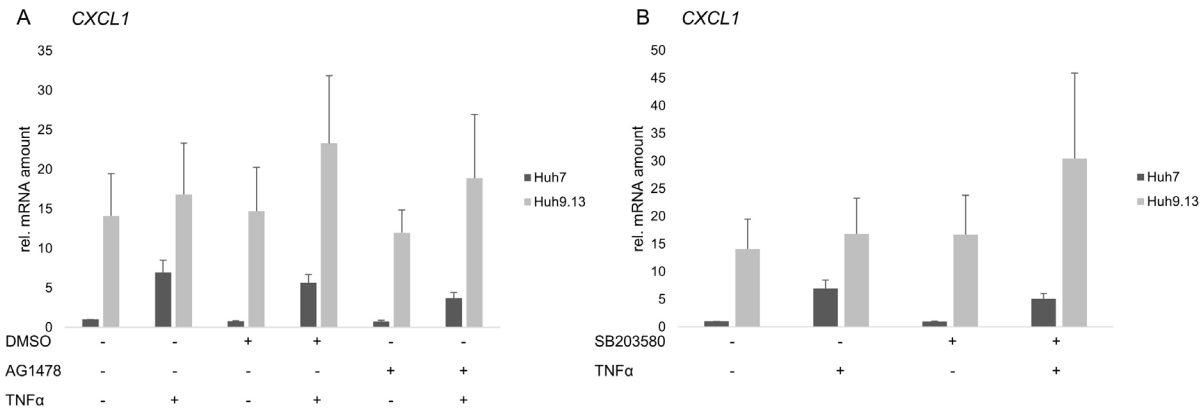

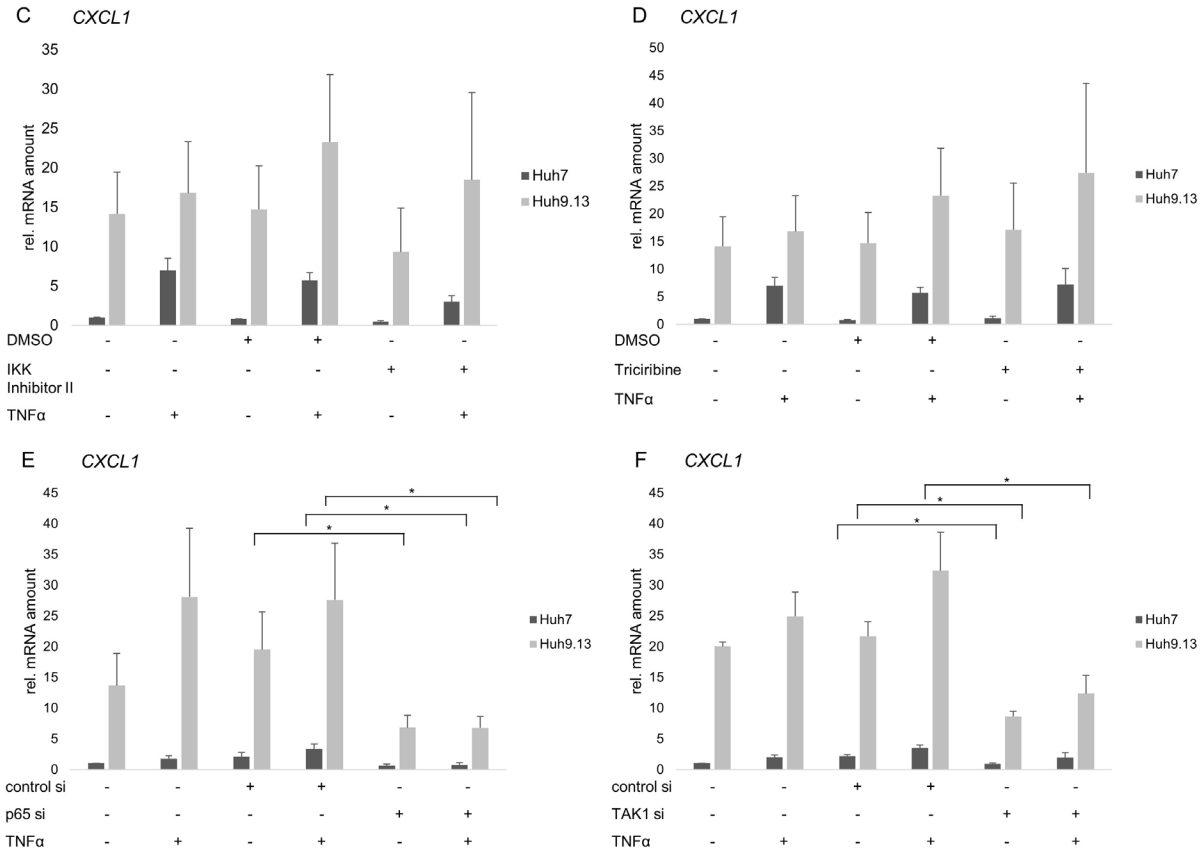

Fig. 39- *CXCL1* mRNA expression after knockdown of *NFκB p65* or *TAK1* or inhibition of the EGFR, IKKα/β, AKT and p38 in Huh9.13 and Huh7 cells with and without TNFα administration. Expression of *CXCL1* mRNA was analysed by qRT-PCR in Huh9.13 and compared to respective control cells. Cells were treated with **(A)** EGFR inhibitor AG1478 [10 µM], **(B)** p38 inhibitor SB203580 [10 µM], **(C)** IKKα/β inhibitor IKK Inhibitor II [10 µM] or **(D)** AKT inhibitor Triciribine [10 µM]. Inhibitors were added to the cells 1 h prior to a 8 h TNFα (1 ng/mL; 0.1 ng/mL in case of siRNA experiments) stimulation. DMSO was added as a control for all inhibitors, except for SB203580, which was diluted in water. Cells were treated with **(E)** p65 siRNA or **(F)** TAK1 siRNA and were stimulated with TNFα [1 ng/mL] for 8 h, 72 h after transfection. Control siRNA was added as a control for all siRNA experiments. *SDHA* was used as reference gene. Results are expressed as fractions of the normalized value of the control, which was set to 1. Data are presented as means + SEM of at least three independent experiments. Asterisks mark significant differences versus the infected and control cell lines described as follows: $p<0.05$ = *, $p<0.01$ = **, $p<0.001$ = ***.

Consistently, HCV infection also resulted in enhancement of *CXCL2* and *3* mRNA expression levels. TNFα-induced *CXCL3* mRNA expression was enhanced by HCV, while TNFα-induced *CXCL2* mRNA expression was not affected by HCV infection.

Neither inhibition of MEK, nor JNK, nor EGFR, nor p38, nor IKKα/β, nor AKT showed any effects on the regulation of *CXCL2* or *3* mRNA expression levels (Fig. 40A-D/G-J).

CXCL2 mRNA expression was reduced upon *NFκB p65* or *TAK1* knockdown, suggesting that *CXCL2* mRNA expression regulation is mediated by both NFκB p65 and TAK1 (Fig. 40E/F).

CXCL3 mRNA expression was already upregulated by control siRNA in cells harbouring the subgenomic replicon of HCV, indicating that siRNA treatment per se influences *CXCL3* mRNA

expression in Huh9.13 cells. Therefore, experiments performed with siRNA must be compared to control siRNA experiments. When compared to control siRNA, *CXCL3* mRNA expression was reduced after *NFκB p65* or *TAK1* knockdown, suggesting that *CXCL3* mRNA expression might be regulated by NFκB p65 as well as TAK1 (Fig. 40K/L).

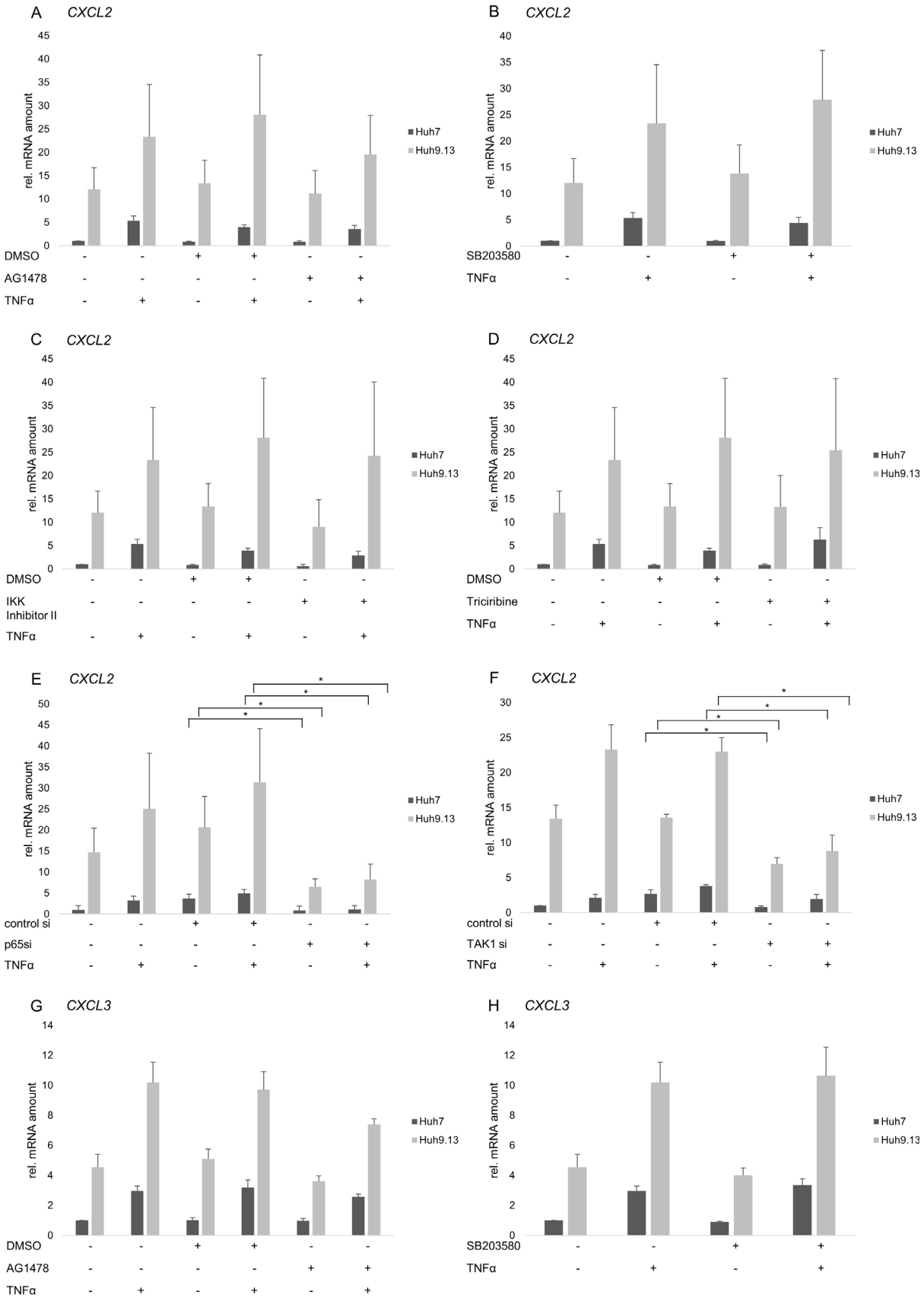
A CXCL2
rel. mRNA amount
Huh7
Huh9.13
DMSO
AG1478
TNFα
B CXCL2
rel. mRNA amount
Huh7
Huh9.13
SB203580
TNFα
C CXCL2
rel. mRNA amount
Huh7
Huh9.13
DMSO
IKK Inhibitor II
TNFα
D CXCL2
rel. mRNA amount
Huh7
Huh9.13
DMSO
Triciribine
TNFα
E CXCL2
rel. mRNA amount
Huh7
Huh9.13
control si
p65si
TNFα
F CXCL2
rel. mRNA amount
Huh7
Huh9.13
control si
TAK1 si
TNFα
G CXCL3
rel. mRNA amount
Huh7
Huh9.13
DMSO
AG1478
TNFα
H CXCL3
rel. mRNA amount
Huh7
Huh9.13
SB203580
TNFα

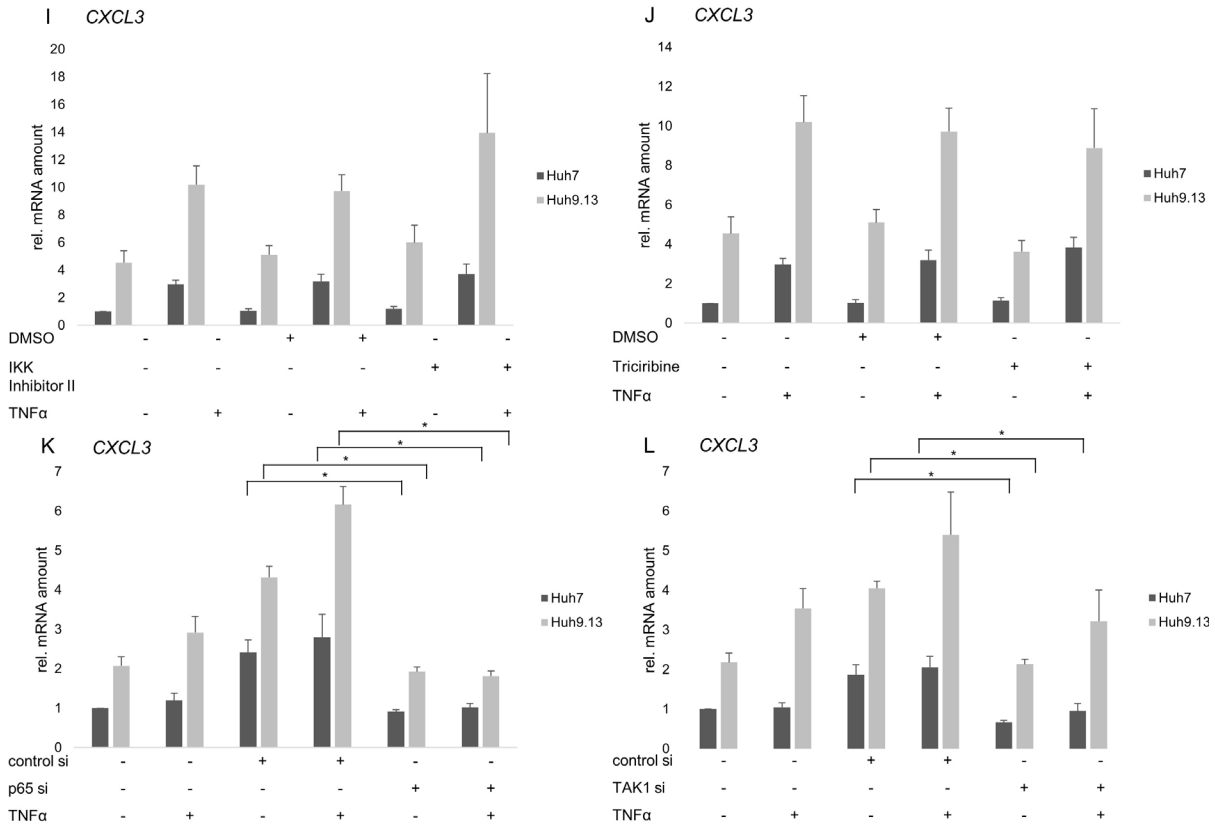

Fig. 40- *CXCL2* and *3* mRNA expression after knockdown of *NFκB p65* or *TAK1* or inhibition of the EGFR, IKKα/β, AKT or p38 in Huh9.13 and Huh7 cells with and without TNFα. Expression of *CXCL2* and *3* mRNA was analysed by qRT-PCR in Huh9.13 and compared to respective control cells. Cells were treated with **(A)+(G)** EGFR inhibitor AG1478 [10 µM], **(B)+(H)** p38 inhibitor SB203580 [10 µM], **(C)+(I)** IKKα/β inhibitor IKK Inhibitor II [10 µM] or **(D)+(J)** AKT inhibitor Triciribine [10 µM]. Inhibitors were added to the cells 1 h prior to a 8 h TNFα (1 ng/mL; 0.01 ng/mL in case of siRNA experiments) stimulation of the cells. DMSO was added as a control for all inhibitors, except for SB203580, which was diluted in water. Furthermore, cells were treated with **(E)+(K)** p65 siRNA or **(F)+(L)** TAK1 siRNA, stimulated with TNFα [1 ng/mL] for 8 h, 72 h after transfection. Control siRNA was added as a control for all siRNA experiments. *SDHA* was used as reference gene. Results are expressed as fractions of the normalized value of the control, which was set to 1. Data are presented as means + SEM of at least three independent experiments. Asterisks mark significant differences versus the infected and control cell lines described as follows: $p<0.05$ = *, $p<0.01$ = **, $p<0.001$ = ***.

4.4.5 Total p65 protein levels are elevated in response to HCV infection after TNFα stimulation

To determine whether TNFα stimulation of the HCV-infected cells results, as observed for IL-1β (**4.3.6**), in enhanced phosphorylation of p38 at T180/Y182 or NFκB p65 at S536, cells were stimulated with TNFα, the proteins extracted and phosphorylation status as well as total protein levels of both p38 and NFκB p65 determined via immunoblot.

TNFα-induced phosphorylation of NFκB p65 at S536 was not further enhanced after HCV infection. The phosphorylation of p38 at T180/Y182 was neither affected by TNFα stimulation nor by HCV infection of the cells.

Interestingly, as shown in Fig. 41, cells harbouring the subgenomic replicon of HCV displayed higher total protein levels of NFκB p65.

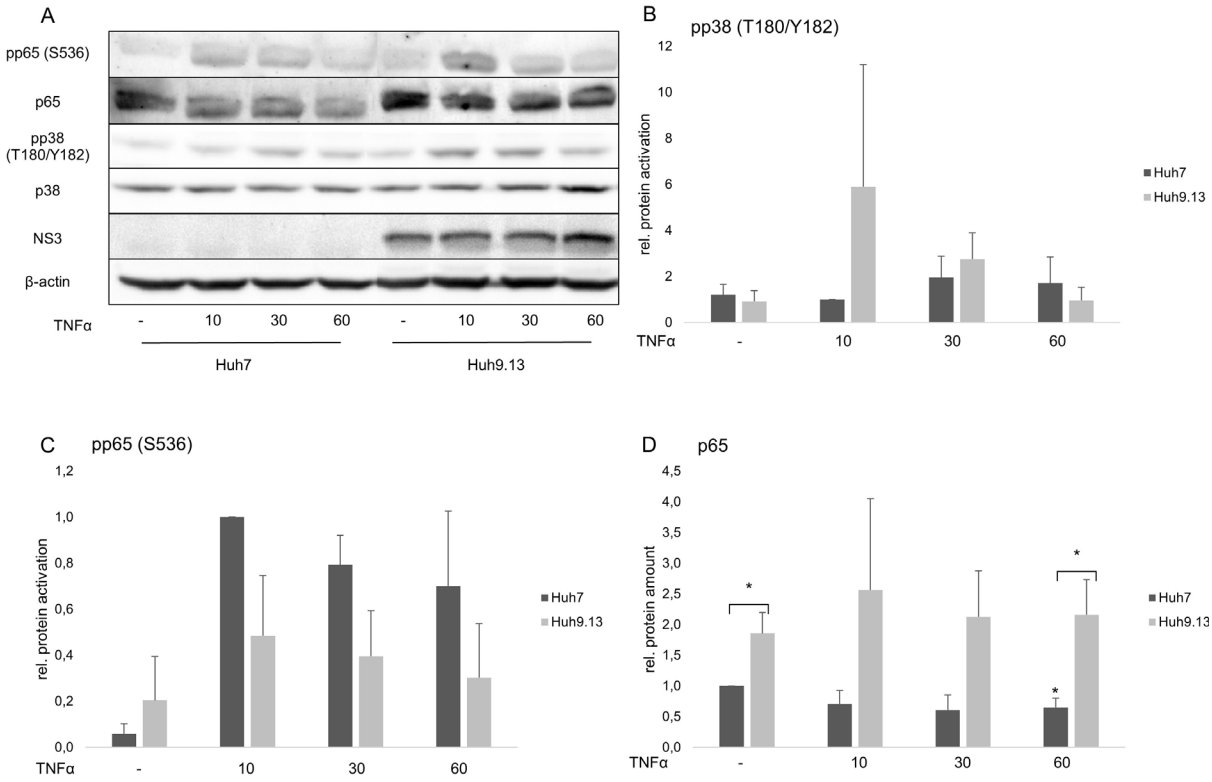

Fig. 41- Protein activation of NFκB p65 or p38 and total protein levels of NFκB p65 in both Huh9.13 and Huh7 control cells with or without TNFα stimulation for the indicated time periods. Protein levels of p38 and NFκB p65 were analysed by immunoblotting in Huh9.13 cells and compared to respective controls. Cells were stimulated with 1 ng/mL of TNFα for the stated time periods or left untreated. **(A)** Representative immunoblots for the analysed proteins are shown. Densitometric calculations were performed for the protein levels of **(B)** pp38 (T180/Y182), **(C)** pp65 (Ser536) and **(D)** p65. Total protein levels were calculated to the reference β-actin. Relative phosphorylation levels of proteins were calculated to total protein levels. Results are expressed as fractions of the normalized value of the control, which was set to 1. Data are presented as means + SEM of at least three independent experiments. Asterisks without lines mark differences between stimulated cells compared to the respective unstimulated control cells. Asterisks mark significant differences versus the infected and control cell lines described as follows: $p<0.05$ = *, $p<0.01$ = **, $p<0.001$ = ***.

4.5 The role of AKT1 and TCPTP during acute HCV infection

4.5.1 AKT1 knockout results in decreased HCV infection in Huh7.5 cells

In previous experiments, it could be shown that HCV infection results in upregulation of relative phosphorylation levels of AKT at S473 (Figs. 13+14). To further investigate the role of AKT1 during HCV infection AKT1 knockout (KO) cell lines were generated using CRISPR/Cas9. Mutants were confirmed via sanger sequencing and immunoblotting (Fig. 42A/B).

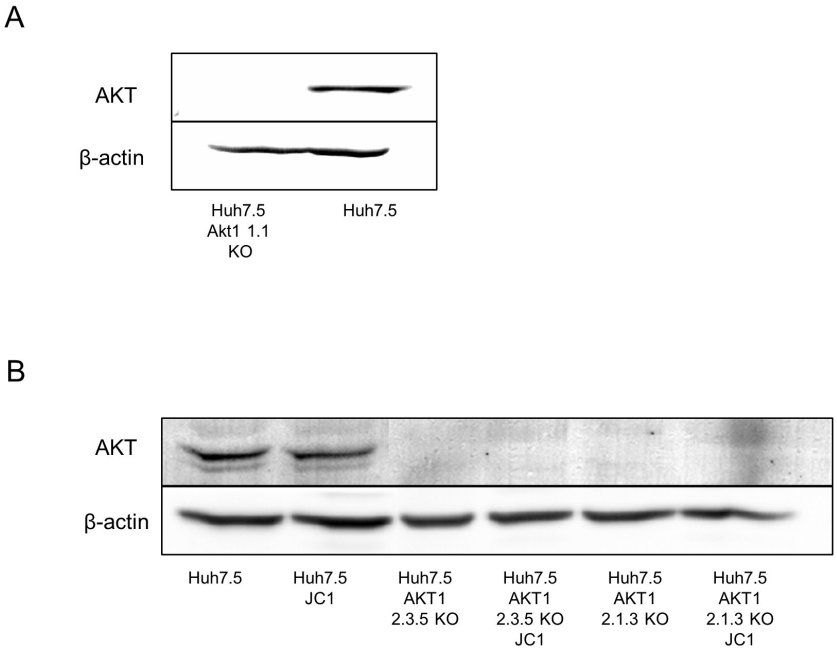

Fig. 42- AKT1 knockout verification by immunoblotting. Protein levels of AKT1 and β-actin were analysed by immunoblotting in **(A)** Huh7.5 AKT1 1.1 KO and control cells, **(B)** Huh7.5 AKT1 2.3.5 KO, Huh7.5 AKT1 2.1.3 KO and in Huh7.5 cells either infected with the HCV_{cc} strain JC1 (MOI = 1) or left uninfected.

Two different clones were used to study the influences of AKT1 on HCV infection. The clonal lines termed Huh7.5 AKT1 2.3.5 KO and Huh7.5 AKT1 1.1 KO, and Huh7.5 control cells were infected with HCV. Subsequently, NS3 protein levels were determined via immunoblotting. All AKT1 KO cell lines showed decreased viral protein levels (Fig. 43A-D), suggesting an important role of AKT1 for viral replication or infection.

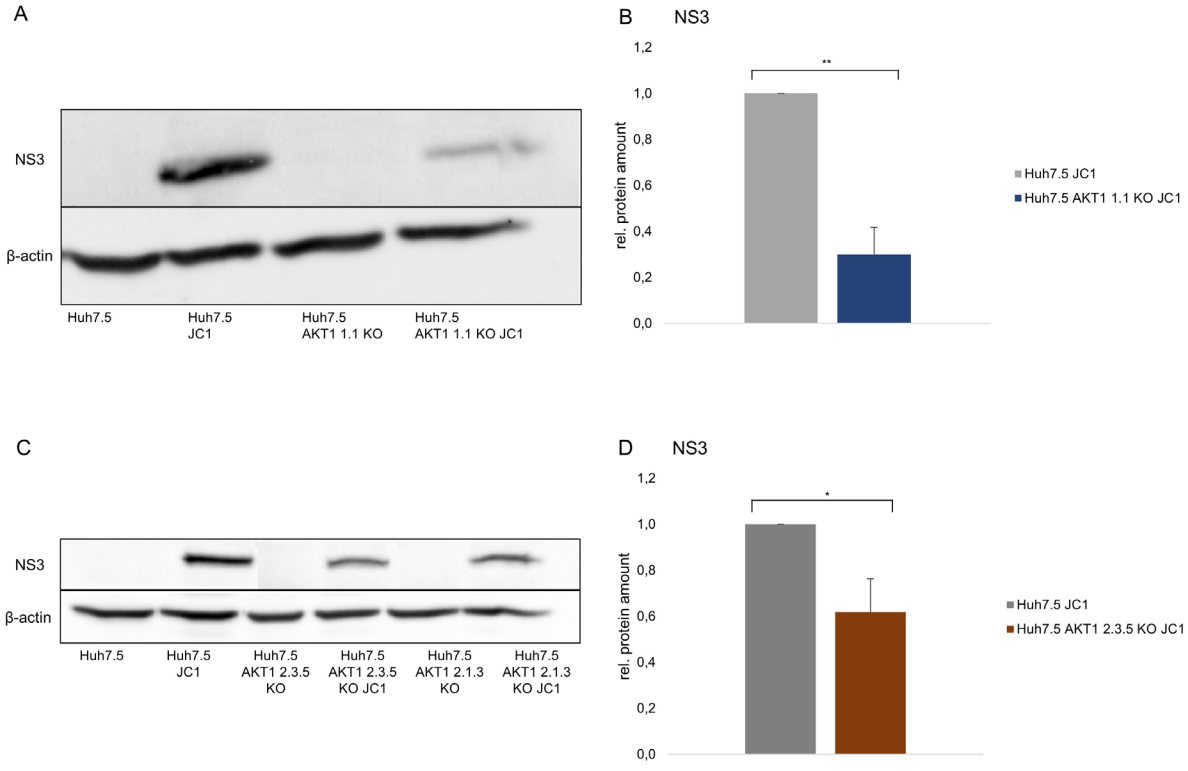

Fig. 43- Protein levels of NS3 in HCV-infected Huh7.5 AKT1 1.1 KO, Huh7.5 AKT1 2.3.5 KO and Huh7.5 control cells. Protein levels of NS3 and β-actin were analysed by immunoblotting in **(A)** Huh7.5 and Huh7.5 AKT1 1.1 KO cells either infected with the HCV_{cc} strain JC1 (MOI = 1) or left uninfected. **(B)** Densitometric calculation was performed for NS3. Protein levels of NS3 and β-actin were analysed by immunoblotting in **(C)** Huh7.5 AKT1 2.3.5 KO cells with or without HCV infection (MOI=1). **(D)** Densitometric calculation was performed for NS3. Total protein level was normalized to the reference β-actin. Results are expressed as fractions of the normalized value of the control, which was set to 1. Data are presented as means + SEM of at least three independent experiments. Asterisks mark significant differences versus the infected and control cell lines described as follows: $p<0.05$ = *, $p<0.01$ = **, $p<0.001$ = ***.

Additionally, *NS5A* mRNA expression was determined using qRT-PCR. Consistently, *NS5A* mRNA expression was significantly downregulated in both AKT1 1.1 KO and AKT1 2.3.5 KO cells compared to control cells (Fig. 44A-C).

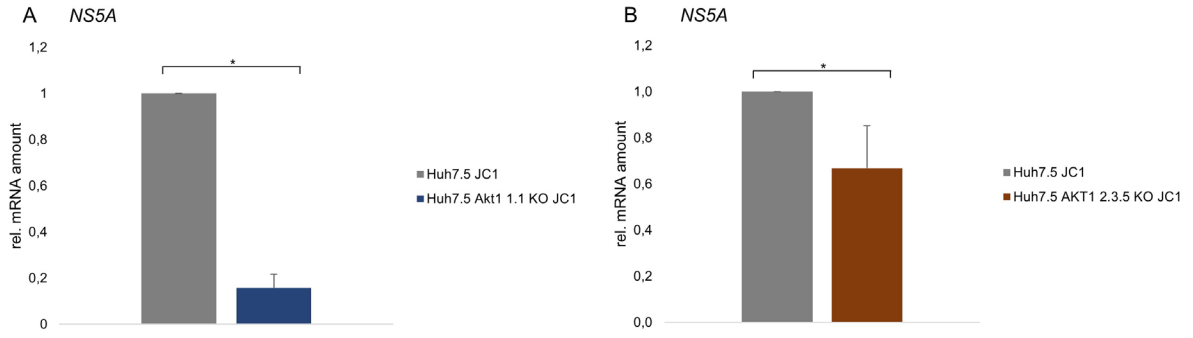

Fig. 44- *NS5A* mRNA expression in HCV-infected Huh7.5 AKT1 1.1 KO, Huh7.5 AKT1 2.3.5 KO and Huh7.5 control cells. Expression of *NS5A* mRNA was analysed by qRT-PCR in **(A)** Huh7.5 AKT1 1.1 KO, **(B)** Huh7.5 AKT1 2.3.5 KO cells infected with the HCV_{cc} strain JC1 (MOI = 1) and compared to control cells. *sDHA* was used

as reference gene. Results are expressed as fractions of the normalized value of the control, which was set to 1. Data are presented as means + SEM of at least three independent experiments. Asterisks mark significant differences versus the infected and control cell lines described as follows: p<0.05 = *, p<0.01 = **, p<0.001 = ***.

4.5.2 Enhancement of chemokine expression by HCV is abolished in Huh7.5 AKT1 1.1 KO cells

To elucidate the effect of AKT1 on the chemokine expression after HCV infection, Huh7.5 cells were infected with HCV, mRNA was extracted, and qRT-PCR analyses were performed. The individual clones showed different results regarding the amplitude of the influence of AKT1 on the mRNA expression of *CXCL1*, *2*, *3* and *8*.

Huh7.5 AKT1 1.1 KO cells displayed significantly lower *CXCL1* and *2* mRNA expression when compared to control cells (Fig. 45A/B+E/F/H+I/J), and the upregulating effect of HCV on *CXCL1*, *2*, *3* and *8* mRNA expression was completely abolished (Fig. 45A-D).

To analyse whether the EGF- , IL-1β- or TNFα-induced expression of CXCR2 ligand mRNA enhanced by HCV infection is affected by AKT1 KO, the cells were infected with HCV or left uninfected and stimulated with EGF, IL-1β or TNFα.

EGF-induced expression of *CXCL1* and *2* mRNA enhanced by HCV infection was unaffected by AKT1 KO in Huh7.5 AKT1 1.1 KO cells compared to control cells, whereas EGF-induced expression of *CXCL3* and *8* mRNA enhanced by HCV infection was reduced significantly in the Huh7.5 AKT1 1.1 KO cells (Fig. 45A-D).

TNFα-induced expression of *CXCL1* and *2* mRNA as well as TFNα-induced expression of *CXCL3* mRNA enhancement by HCV infection was unaffected by AKT1 KO in Huh7.5 AKT1 1.1 KO cells compared to control cells (Fig. 45E-G). In contrast, TNFα-induced expression of *CXCL8* mRNA enhanced by HCV infection was reduced, although not significantly, in Huh7.5 AKT1 1.1 KO cells when compared to Huh7.5 control cells (Fig. 45H).

IL-1β-induced expression of *CXCL1* and *2* mRNA enhanced by HCV infection was reduced, although not significantly, in AKT1 KO cells (Fig. 45I/J). Interestingly, IL-1β-induced expression of *CXCL3* and *8* mRNA enhanced by HCV was significantly reduced in Huh7.5 AKT1 1.1 KO cells (Fig. 45J-L).

Taken together, these results indicate that AKT1 plays a pivotal role in the HCV-dependent upregulation of *CXCL1*, *2*, *3* and *8* mRNA expression as well as in the EGF- and IL-1β-induced expression of *CXCL3* and *8* mRNA enhanced by HCV infection.

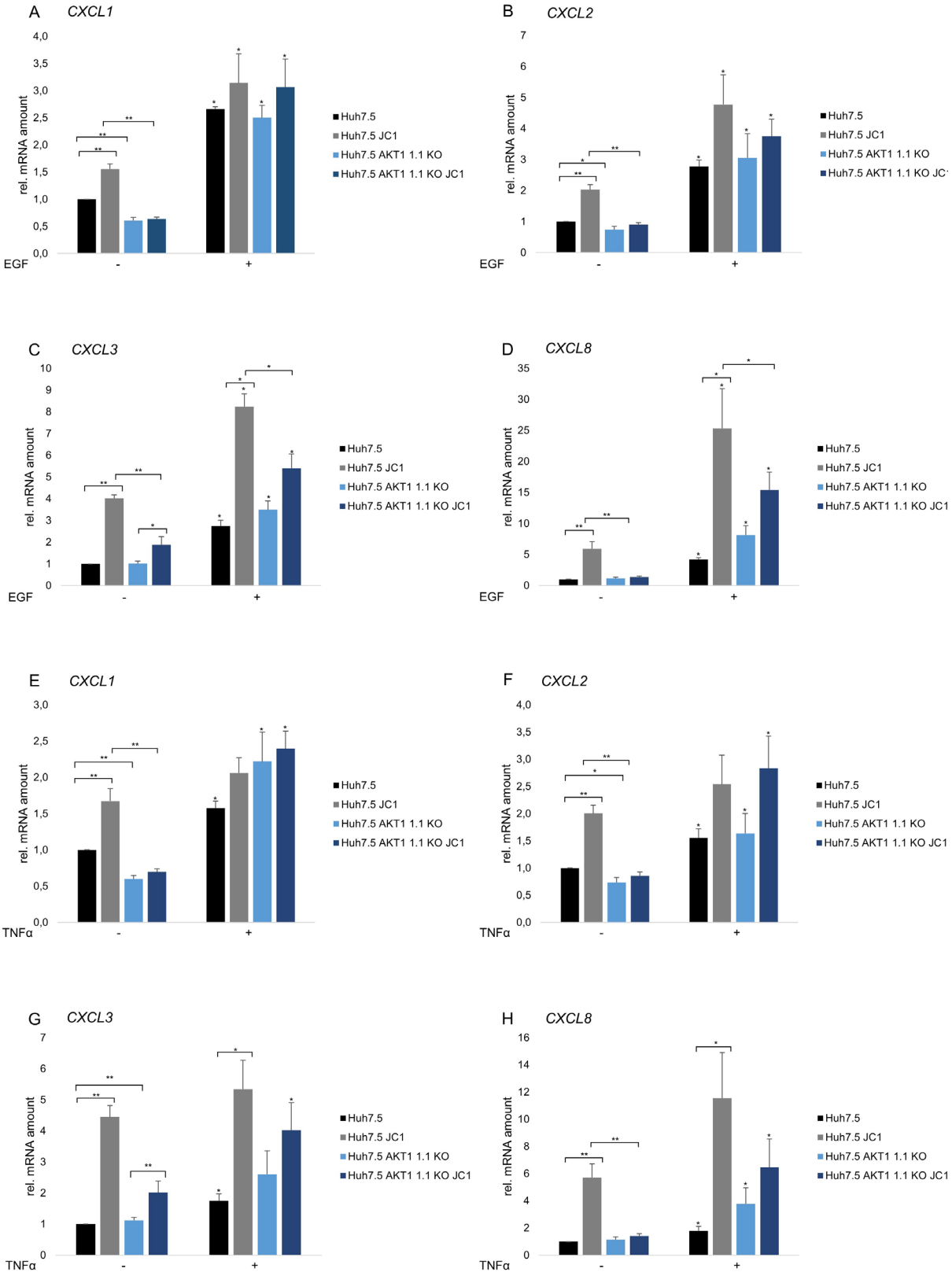
A
CXCL1
rel. mRNA amount
EGF
Huh7.5
Huh7.5 JC1
Huh7.5 AKT1 1.1 KO
Huh7.5 AKT1 1.1 KO JC1
B
CXCL2
C
CXCL3
D
CXCL8
E
CXCL1
TNFα
F
CXCL2
G
CXCL3
H
CXCL8

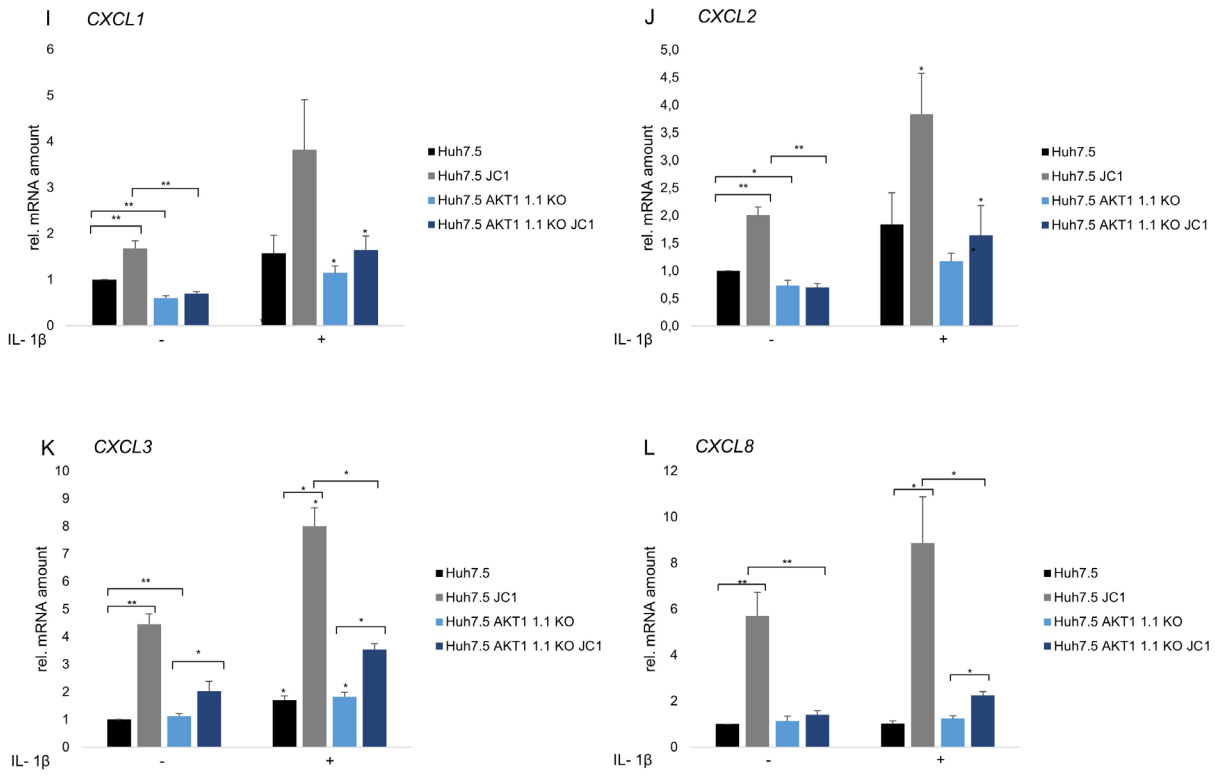

Fig. 45- *CXCL1*, *2*, *3* and *8* mRNA expression in Huh7.5 AKT1 1.1, Huh7.5 control cells as well as in HCV-infected Huh7.5 AKT1 1.1 KO and Huh7.5 control cells with and without EGF, TNFα or IL-1β administration. Expression of *CXCL1, 2, 3* and *8* mRNA was analysed by qRT-PCR in Huh7.5 AKT1 1.1 KO and Huh7.5 cells infected with the HCV_{cc} strain JC1 (MOI = 1) and compared to respective controls. Cells were treated with EGF [40 ng/mL] for 160 min or TNFα [1 ng/mL] or IL-1β [5U/mL] for 8 h and the mRNA expression levels of **(A)+(E)+(I)** *CXCL1*, **(B)+(F)+(J)** *CXCL2*, **(C)+(G)+(K)** *CXCL3* and **(D)+(H)+(L)** *CXCL8* were analysed by qRT-PCR. *sDHA* was used as reference gene. Results are expressed as fractions of the normalized value of the control, which was set to 1. Data are presented as means + SEM of at least three independent experiments. Asterisks mark significant differences versus the infected and control cell lines described as follows: $p<0.05$ = *, $p<0.01$ = **, $p<0.001$ = ***.

In contrast to the Huh7.5 AKT1 1.1 KO cells, *CXCL2* and *8* mRNA expression enhancement after HCV infection was only weakly reduced in Huh7.5 AKT1 2.3.5 KO cells when compared to control cells and no effect was observable for *CXCL1* and *3* mRNA expression.

Interestingly, *CXCL1, 2, 3* and *8* expression was downregulated significantly in Huh7.5 AKT1 2.3.5 KO cells when compared to Huh7.5 cells (Fig. 46A-D).

In case of AKT1 2.3.5 KO cells, AKT1 KO resulted in impaired HCV replication as determined by total protein levels of the viral non-structural protein NS3 (Fig. 43), while in contrast to the Huh7.5 AKT1 1.1 KO cells, the upregulation of *CXCL1*, *2*, *3* and *8* mRNA expression after HCV infection was nearly unaltered compared to Huh7.5 control cells (Fig. 45/46).

In Huh7.5 AKT1 2.3.5 KO cells as well as in Huh7.5 AKT1 1.1 KO cells, *CXCL1* and *2* mRNA expression was reduced when compared to Huh7.5 cells, suggesting that AKT1 is important for *CXCL1* and *2* mRNA expression regulation (Fig. 45/46).

Interestingly, in Huh7.5 AKT1 2.3.5 KO cells, *CXCL3* and *8* mRNA expression was also significantly reduced when compared to Huh7.5 cells, which was not the case for Huh7.5 AKT1 1.1 KO cells. The different clones need to be studied more closely to find out how these different effects can be explained.

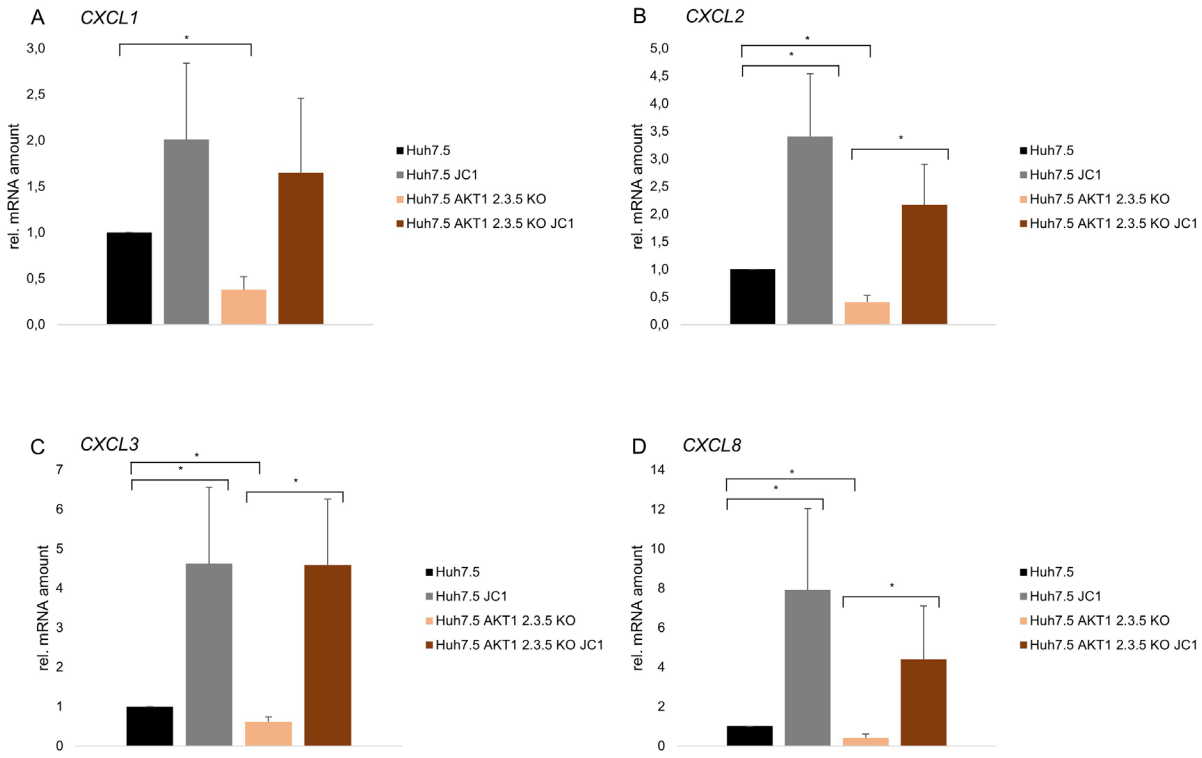

Fig. 46- *CXCL1*, *2*, *3* and *8* mRNA expression in Huh7.5 AKT1 2.3.5, Huh7.5 control cells as well as in HCV-infected Huh7.5 AKT1 2.3.5 KO and Huh7.5 control cells. Expression of *CXCL1* **(A)**, *2* **(B)**, *3* **(C)** and *8* **(D)** mRNA was analysed in Huh7.5 AKT1 2.3.5 KO and Huh7.5 cells infected with the HCV_{cc} strain JC1 (MOI = 1) and compared to respective controls. *sDHA* was used as reference gene. Results are expressed as fractions of the normalized value of the control, which was set to 1. Data are presented as means + SEM of at least three independent experiments. Asterisks mark significant differences versus the infected and control cell lines described as follows: $p<0.05$ = *, $p<0.01$ = **, $p<0.001$ = ***.

4.5.3 TCPTP knockout results in decreased HCV infection in Huh7.5 cells

Previous studies demonstrated that HCV influences the phosphorylation levels of the EGFR by cleavage and thereby degradation of TCPTP (36). TCPTP is a tyrosine phosphatase and act as an endogenous negative regulator of EGFR. EGFR is necessary for a successful HCV infection (77). It was therefore hypothesized that TCPTP plays a crucial role during HCV infection. TCPTP KO cells were generated as AKT1 KO cells using the CRISPR/Cas9 method and verified via immunoblotting and sanger sequencing (Fig. 47A/B). Contrary to the

hypothesis, all three TCPTP KO cell lines (2.3, 3.4 and 4.6) displayed reduced HCV infection as measured by NS3 protein levels compared to Huh7.5 control cells (Fig. 47A-D).

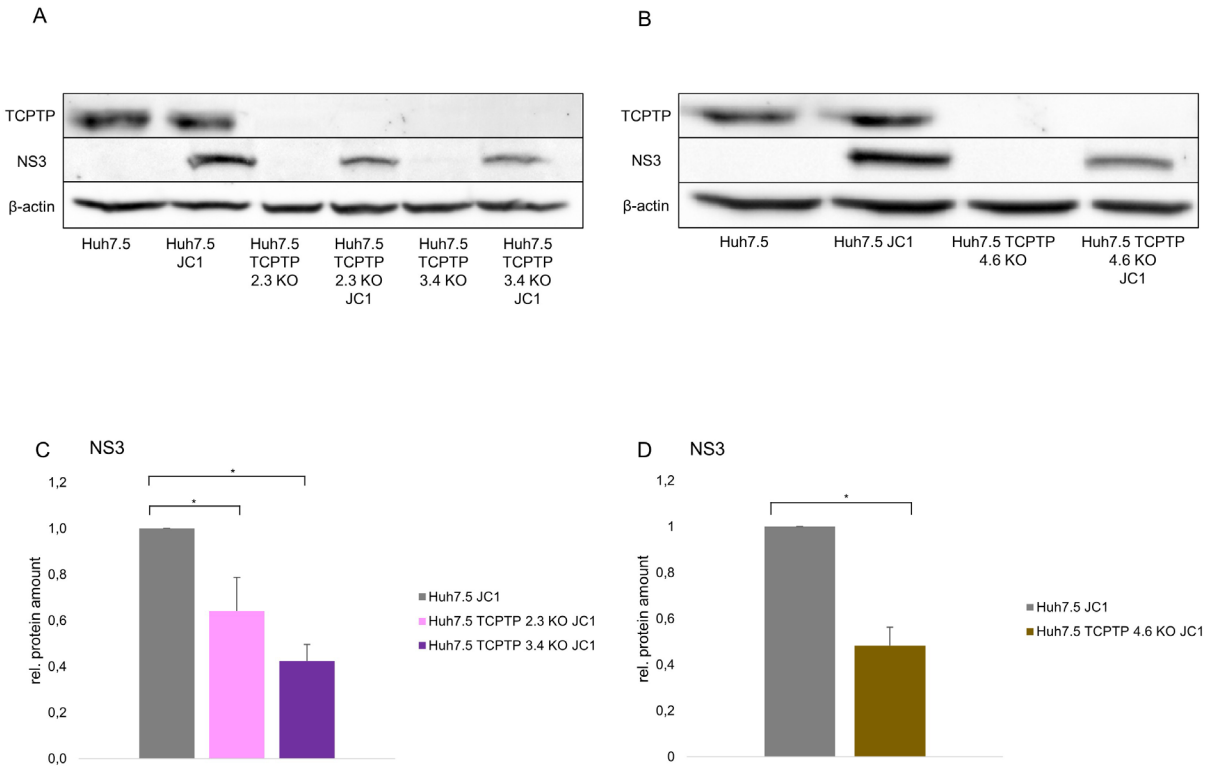

Fig. 47- Protein levels of NS3 in HCV-infected Huh7.5 TCPTP 2.3 KO, Huh7.5 TCPTP 3.4 KO and Huh7.5 control cells. Protein levels of TCPTP, NS3 and β-actin were analysed by immunoblotting in **(A)** Huh7.5, Huh7.5 TCPTP 2.3 and Huh7.5 TCPTP 3.4 KO cells or in **(B)** Huh7.5, Huh7.5 TCPTP 4.6 KO cells infected with the HCV_{cc} strain JC1 (MOI = 1) and compared to the respective controls. **(C)** Densitometric calculations were performed for NS3. Total protein level was calculated to the reference β-actin. Results are expressed as fractions of the normalized value of the control, which was set to 1. Data are presented as means + SEM of at least three independent experiments. Asterisks mark significant differences versus the infected and control cell lines described as follows: $p<0.05$ = *, $p<0.01$ = **, $p<0.001$ = ***.

5 Discussion

Today, 71 million people are chronically infected with HCV. HCV can persist in patients over decades without being cleared by the immune system, even though the immune system is activated vigorously. Decades after initial infection, patients can develop irreversible liver damage, like liver cirrhosis, which can lead to the development of liver cancer. HCV is thought to escape the immune system by interfering with host cell processes without affecting the viability of the cell. Communication signals, such as chemokines which are released from the cells, are important for immune cell recruitment. HCV is suggested to have the capability to modify this process. The aim of this PhD project was thus to elucidate how HCV interferes with the expression of different chemokines in response to EGF or the cytokines TNFα and IL-1β. To that end, two different cell culture systems where used: the replicon system, which stably expresses the NS proteins NS3-NS5B and thus is a model for chronic infection, and the HCV_{cc}-modelling an acute stage of HCV infection with cells being infected for 72 h with the virus.

5.1 Protein levels of EGF, VEGFA and TNFα positively correlate in serum samples of patients chronically infected with HCV

Protein levels of the growth factors VEGFA and EGF were significantly upregulated in the serum samples of patients infected chronically with HCV when compared to the serum samples of healthy people (Tab. 18; Fig. 10A/B). Besides, also patients with other liver diseases than HCV displayed higher VEGFA and EGF protein levels in their serum samples when compared to serum samples of healthy people (Tab. 18; Fig. 10A/B). Taken together, these results suggest that both VEGFA and EGF protein level upregulation may be due to liver damage in general, but to a higher extent after chronic HCV infection. In line with the results shown in this thesis, recently published work from Salum *et al.* demonstrates that both mRNA expression and protein levels of VEGFA are highly upregulated in peripheral blood mononuclear cells isolated from HCV-infected patients (154). Additionally, it could be shown in a previous study from our group that both *EGF* mRNA expression as well as protein levels are upregulated in cells infected with HCV and in cells harbouring the subgenomic replicon of HCV (284), suggesting both growth factors to be important in the context of HCV infection. To further investigate the influences of HCV on EGF and VEGFA signalling was thus of great interest.
Neither the protein levels of CCL2 nor of CCL7 were found to be affected in patients with chronic HCV infection (Fig. 10C/D), while CXCL8 protein levels were significantly upregulated in patients infected chronically with HCV when compared to protein levels in the serum of healthy people (Fig. 10E). Upregulation of CXCL8 protein levels in serum samples of patients

infected chronically with HCV is in line with several publications (227, 279, 299). CXCL8 is known to mainly recruit neutrophil granulocytes, while CCR2 chemokine ligands such as CCL2 and CCL7, are known to mainly recruit monocytes and macrophages to the site of infection or to the damaged tissue (266, 267, 300), suggesting that macrophage and monocyte recruitment when compared to neutrophil granulocyte recruitment, might be lower in response to chronic HCV infection. Results obtained in previous studies from our group could demonstrate that neutrophil granulocyte but not monocyte recruitment is indeed enhanced after chronic HCV infection (284).

Additionally, TNFα protein levels were significantly increased in serum samples of patients infected chronically with HCV when compared to serum samples of healthy people (Fig. 10F). These results are in line with the literature, because TNFα protein levels are known to be enhanced in plasma as well as in liver tissue of HCV-infected patients (301). In addition to that, HCV was found to interact directly with the TNF type I receptor via the HCV specific core protein and to thereby influence the activity of the TNF receptor (302). It was further shown that TNFα levels as well as NFκB activation are enhanced in the liver of mice expressing the non-structural proteins NS3/4A of HCV (231).

Notably, in the herein presented PhD work it was shown that TNFα protein levels were strongly and significantly positively correlated with both EGF and VEGFA protein levels in the serum of patients chronically infected with HCV, whereas they were neither correlated in the serum samples of healthy people nor of patients with other liver diseases than HCV (Tab. 19), suggesting these three protein patterns to be somehow interrelated during chronic HCV infection.

Furthermore, these results support the assumption that HCV modulates the protein levels of TNFα, EGF, CXCL8 and VEGFA.

5.2 Enhancement of EGF-induced expression of CXCR2 ligands by HCV infection is mediated by different signalling pathways

In 2011, Lupberger *et al.* identified the EGFR as an essential co-factor for HCV cell entry (77). Protein phosphorylation of the EGFR at Y1068 as well as EGF-induced protein phosphorylation of the EGFR downstream effector proteins of the PI3K/AKT and MAPK signalling pathways (Fig. 14), and mRNA expression of *CXCL1*, *2*, *3* and *8* were upregulated in response to HCV infection in the HCV_{cc} model of acute infection (Fig. 12), suggesting an activation of those signalling pathways and in turn enhancement of chemokine mRNA expression by HCV.

Enhancement of EGF-induced expression of *CXCL1, 2, 3* and *8* mRNA (Fig. 11 and (284)) and protein phosphorylation enhancement of AKT (Fig. 13/14) in response to HCV infection were observed in both the subgenomic replicon as well as the HCV_{cc} cell culture model. In contrast to the HCV_{cc} system, the phosphorylation of the MAPKs MEK and ERK was not affected in cells harbouring the subgenomic replicon of HCV (Fig. 13). The increase in activating phosphorylation of AKT in response to EGF strongly suggests an EGF-dependent activation of the AKT signalling pathway resulting in enhancement of chemokine expression regulation in cells harbouring the subgenomic replicon of HCV (Fig. 13/14 and (284)).

Protein levels of TCPTP, which is an endogenous negative regulator of EGFR (148), were observed to be downregulated in cells harbouring the subgenomic replicon of HCV (Fig. 13A/C). This is in line with previously obtained results of our group and caused by cleavage of TCPTP by the viral NS3/4A protease (36). Additionally, TCPTP protein levels were also strongly reduced in HCV-infected cells (Fig. 14A/C).

Interestingly, in replicon cells, which express only the NS proteins NS3-NS5B of HCV and thus partly mimic a chronic infection, the basal relative EGFR phosphorylation was not enhanced when compared to control cells (Fig. 13A/B). On the other hand, in the acute system, where cells are infected with the whole genome of HCV, EGFR phosphorylation was significantly enhanced by HCV infection (Fig. 14A/B). The enhanced phosphorylation and therefore activation of the EGFR in response to HCV infection may be induced by the virus via various signalling pathways to facilitate viral entry which is in line with assumed necessity of phosphorylation-induced EGFR internalization being critical for HCV cell entry (125, 147).

It is conceivable that cells acutely infected with HCV behave differently than cells stably expressing only the viral NS proteins. An obvious explanation may be the interference of structural proteins with different host cell signalling pathways. This idea is supported by the fact that activation of MAPK signalling (MAPKs ERK and p38) was influenced by HCV only in acutely infected cells (Fig. 14G/H) but not in the replicon system (Fig. 13G/H). This is in line with the results of another study showing that soluble E2 protein of HCV, which is not

expressed in cells harbouring the subgenomic replicon of HCV, causes upregulation of the phosphorylation of the MAPKs ERK and p38 in NIH3T3 as well as HEK293T cells expressing the HCV binding receptor dendritic cell-specific intracellular adhesion molecule-3-grabbing nonintegrin (303).

In contrast to this, He *et al.* demonstrated in 2001 that the HCV NS5A protein causes downregulation of the EGF-induced phosphorylation of p38 MAPK in cultured cells (304). However, these experiments were performed in HeLa cells stably expressing the HCV NS protein NS5A, and different results may thus reflect cell type-specific cell signalling responses.

Regarding the PI3K signalling pathway, AKT signalling was enhanced, although not significantly, in both cell culture systems already at basal levels (Fig. 13/14E). This is in line with the literature and previous results from our group (150). Furthermore, it is known that NS5A binds to the SH3 domain of the PI3K p58 regulatory subunit and causes its activation (305). As a result, AKT is constitutively activated and promotes cell survival which the authors hypothesized to potentially lead to HCC formation (305). Additionally, activation of PI3K/AKT signalling by HCV was demonstrated to occur due to induction of oxidative stress by HCV (306). Previous studies from our group demonstrate that TCPTP is cleaved by the viral protease NS3/4A and that EGF and PI3K/AKT signalling is constitutively active in cells harbouring the subgenomic replicon of HCV as well as in transgenic mice expressing NS3/4A stably in the liver (36). These results highly suggest that the cleavage of TCPTP by NS3/4A constitutively activates the PI3K/AKT signalling in the context of HCV.

EGF-induced expression of *CXCL8* mRNA enhanced by HCV infection in a concentration dependent manner is in line with previous experiments of our working group which have shown that HCV upregulates *CXCL1*, *2*, *3* and *8* mRNA as well as chemokine protein levels in replicon cells (284).

To identify the involved factors and chronology of events, key proteins of EGFR and downstream signalling pathways were then inhibited chemically or by siRNA knockdown.

Knockdown of *EGF* resulted in a significant reduction of the prior noted upregulation of *CXCL8* mRNA expression via HCV and in a partial downregulation of the prior noted upregulation of *CXCL1*, *2* and *3* mRNA expression, suggesting that HCV influences EGF signalling to induce *CXCL8* mRNA expression enhancement and, at least partially, to induce *CXCL1*, *2* and *3* mRNA expression enhancement (Fig. 15D/16-17A/17D).

The EGF-induced further enhancement of *CXCL1*, *2*, *3* and *8* mRNA expression in response to HCV is suggested to be regulated via different signalling pathways by the data presented herein. While *CXCL8* expression is mainly regulated via the MEK/ERK signalling pathway (Fig. 15A), *CXCL1* mRNA expression is mainly regulated via the AKT signalling pathway (Fig. 16B and (284)). The results further suggest that both *CXCL2* and *3* mRNA expression levels are neither regulated by MAPK nor by AKT signalling pathways (Fig. 17B/C). The signalling

pathways underlying the observed enhancement in response to HCV need to be investigated in future studies.

In addition, enhancement of *CXCL8* mRNA expression in HCV-infected cells as well as EGF-induced expression of *CXCL8* mRNA enhanced by HCV infection was impaired after *NFκB p65* knockdown (Fig. 15F), pointing at NFκB p65 to be involved in the regulation of *CXCL8* mRNA expression. Considering that replicon cells at least in part reflect the situation of chronic infection (87), NFκB p65 appears to play a role in upregulation of *CXCL8* mRNA expression, particularly in the context of chronic infection, but also in the situation of acute infection.

Data on the interference of HCV with the regulation of the NFκB p65 signalling in the literature are conflicting. While several publications suggest that HCV triggers release and nuclear translocation of the p65 subunit of the NFκB complex (205, 307), others show the exact opposite (235, 308). These conflicting data may be attributed to the expression of isolated viral proteins in different cell types (205, 235, 307, 308). Hence, the exact mechanism between HCV infection and regulation of the transcription factor NFκB p65, and the genes activated by it, must be further delineated in future studies.

In summary, the present PhD work shows that EGFR downstream signalling pathways are affected after HCV infection. In prior studies from our group, it could be shown that HCV infection enhances the mRNA expression of the chemokines *CXCL1*, *2*, *3* and *8* as well as the EGF-induced upregulation of those chemokines (284). In the herein presented thesis, evidence is provided that EGF stimulation results in activation of the MAPKs ERK and p38 in the HCV_{cc} system, mimicking acute HCV infection, whereas this was not seen in cells stably expressing the NS3-NS5B viral proteins, mimicking chronic HCV infection. This suggests that either the different results are attributed to structural proteins missing in the subgenomic replicon system or MAPKs signalling is affected only during the acute status of HCV infection. This may reflect the acute or chronic status of the disease. Additionally, activation of AKT phosphorylation was shown to be enhanced in both cell culture systems, pointing at AKT as being important during acute as well as chronic HCV infection. *CXCL8* mRNA expression enhancement was significantly impaired after *EGF* knockdown, suggesting EGF to be one of the factors that plays an overall role in HCV-mediated regulation of *CXCL8* mRNA expression. EGF-induced further enhancement of *CXCL8* mRNA expression by HCV infection was impaired after *NFκB p65* knockdown and after inhibition of MEK1, while *CXCL1* mRNA expression was impaired after inhibition of AKT, suggesting that *CXCL1* and *CXCL8* mRNA expression regulation in response to EGF during HCV infection is regulated via two different EGFR downstream signalling pathways.

5.3 Enhancement of IL-1β-induced expression of *CXCL1*, *2*, *3* and *8* mRNA after HCV infection is mediated by different signalling components

IL-1 family members induce mRNA expression of hundreds of genes, including CXCR2 ligands, as well as of IL1 family members themselves via activation of different transcription factors such as NFκB, CREB1, C/EBPβ and SP1 (161). Considering this and based on the effects of HCV on EGF-induced regulation of cellular chemokine expression levels discussed in **5.2**, the influence of HCV on IL1β-induced cellular chemokine expression levels was investigated.

The IL-1β-induced expression of *CXCL1, 2, 3* and *8* mRNA was concentration- and time-dependently enhanced after HCV infection (Fig. 18).

The data presented herein demonstrate that IL-1β-induced expression of chemokines enhanced by HCV is much higher compared to EGF-induced expression of chemokines enhanced by HCV infection, indicating that IL-1β is strongly activating downstream signalling pathways resulting in transcriptional regulation of chemokine expression during HCV infection. In line with this, serum levels of IL-1β are increased in individuals chronically infected with HCV (199), which, at least in part, might cause the observed upregulation of *CXCL8* mRNA expression (Fig. 18). It has been reported that HCV proteins enhance IL-1β secretion from THP-1 cells, primary macrophages and Kupffer cells via NFκB-induced upregulation of *IL-1β* (168), potentially resulting in an additional upregulation of IL-1β in HCV-infected patient sera (199). Since the IL-1β-induced expression of *CXCL8* mRNA was enhanced in HCV-infected cells even after 32 h stimulation, the data points at IL-1β to induce its own expression by a positive feedback loop.

In addition to that, knockdown experiments using specific siRNAs showed that IL-1β-induced expression of *CXCL8* mRNA enhanced by HCV infection was TAK1-dependent (Fig. 21E). TAK1 is a member of the MAPKKK family, which is activated after IL-1β binding to the IL-1 receptor (174), indicating that HCV directly influences IL-1β signalling at the receptor level. Further, HCV-dependent upregulation of *CXCL1* mRNA expression was found to be mediated by TAK1 (Fig. 23C). Whether TAK1 is activated by HCV infection directly or indirectly should be analysed in future studies. Chronic HCV infection can, in a subset of patients, lead to the development of fibrosis, steatosis and HCC (3). In line with this notion, it was demonstrated that high-fat diet-fed mice overexpressing tumour-necrosis factor receptor-associated factor 3 (TRAF3) displayed enhanced hepatic steatosis formation, while high fat diet fed mice lacking TRAF3 displayed ameliorated liver function (309). Since TRAF3 directly activates TAK1 and subsequently NFκB and JNK signalling, thus causing increased hepatic steatosis (310), a link between TAK1 during HCV infection and liver injury is suggested.

However, knockdown of *NFκB p65*, which is activated downstream of TAK1 (174), almost

abolished HCV-induced *CXCL8* mRNA expression and resulted in a strong reduction of IL-1β-induced expression of *CXCL8* mRNA enhanced by HCV infection (Fig. 21A/C). Taken together, these results suggest that TAK1 and NFκB are involved in regulation of *CXCL8* mRNA expression in response to IL-1β as also reported by others (108, 309, 311) and may be involved in the enhancement of basal and inducible expression of *CXCL8* mRNA expression by HCV. *CXCL8* mRNA expression was reported to be also induced by viral infection dependent on RIG-I signalling and downstream activation of NFκB p65 which then binds to the promoter region of *CXCL8* (312, 313). In line with this, HCV has been previously reported by our group and in this thesis to mediate *CXCL8* mRNA expression via EGF signalling in a NFκB p65-dependent manner (284). Additionally, p65 NFκB has been reported by prior studies of our group to mediate the protective effects of NS3/4A in this context (231).

Additionally, *NFκB p65* and *TAK1* knockdown resulted in a slight reduction of *CXCL8* mRNA expression in Huh7 cells as well (Fig. 21A/C/E), suggesting an involvement of both proteins in the regulation of basal *CXCL8* mRNA expression without infection which has been described already in other studies in different cell types (108, 174, 314) and further highlights the essential role for these proteins to regulate chemokine expression.

Interestingly, EGFR inhibition also led to a slightly diminished IL-1β-induced expression of *CXCL8* mRNA enhanced by HCV infection (Fig. 21G). As IL-1β was described to transactivate the EGFR (196), this may be also the case for HCV-dependent *CXCL8* mRNA expression induction. The exact mechanism is not yet known and further studies are needed to elucidate the underlying molecular mechanisms behind this potential EGFR transactivation by IL-1β in the context of HCV infection.

Additionally, *NFκB p65* knockdown resulted in diminished upregulation of the *CXCL1* mRNA expression after HCV infection, both at basal levels as well as for IL-1β-induced expression of *CXCL1* mRNA enhanced by HCV infection (Fig. 23A/B), while *TAK1* downregulation resulted in a slight reduction of the IL-1β-induced expression of *CXCL1* mRNA enhancement after HCV infection (Fig. 23C). These data indicate that HCV mediates upregulation of *CXCL1* mRNA expression involving NFκB and in part also TAK1. Additionally, both *NFκB p65* and *TAK1* knockdown resulted in a significant reduction of *CXCL1* mRNA expression in Huh7 cells as well, indicating that basal *CXCL1* mRNA expression regulation is mediated by NFκB p65 and TAK1, while IL-1β-induced expression of *CXCL1* mRNA was not affected (Fig. 23A-C). In the serum of primary liver cancer patients, CXCL1 as well as IL-1β protein levels were found to be increased (315). Additionally, it was demonstrated in another study that the CXCL1 rs4074 polymorphism represents a genetic risk factor for cirrhosis development during chronic HCV infection (316). In sum, this leads to the assumption that *CXCL1* mRNA expression is enhanced by HCV, mediated by NFκB and TAK1, and this enhancement could thus result in an increased risk of HCC development.

In case of *CXCL2* and *3* mRNA expression, *NFκB p65* or *TAK1* knockdown resulted in reduced upregulation of *CXCL2* and *3* mRNA expression (Fig. 25A-C), while JNK1 inhibition slightly reduced the enhancing effect of HCV on IL-1β-induced expression of *CXCL2* mRNA (Fig. 25D).

These data suggest that both *NFκB p65* and *TAK1* mediate the mRNA expression regulation of *CXCL2* and *3*, while JNK1 activates, at least partially, IL-1β-induced *CXCL2* mRNA expression enhanced after HCV infection. NFκB p65 and TAK1 are known to induce expression of *CXCL2* and *3* mRNA in different cell types (144, 190, 191). In bone marrow macrophages, it was demonstrated that upon LPS challenge, *CXCL2* mRNA expression was upregulated via JNK1, p38 and NFκB signalling (317). IL-1β might induce *CXCL2* mRNA expression and HCV might in parallel enhance the expression via JNK1 activation in response to IL-1β.

As already described in the results (**4.3.4** and **4.4.4**), it has to be kept in mind that siRNA treatment of the subgenomic replicon cells resulted in some experiments in an enhancement of CXCR2 ligand mRNA expression, especially of *CXCL3* mRNA expression, per se. It might therefore be the best way for data analysis to calculate statistical significance of differences between siRNA-transfected cells and corresponding control cells transfected with control siRNA.

Neither p38, nor IKKα/β, nor AKT inhibition showed any effect on *CXCL1*, *2*, *3* or *8* mRNA expression enhancement (Fig. 22/24/26/28).

In contrast to this, IL-1β was shown to activate p38, which in turn activates MK2 in hepatocytes (318), which is known to play an important role during chemokine regulation in different cell types (319). Additionally, a study published in 2001 reported upregulation of *CXCL8* and *CXCL1* mRNA expression in human retinal pigment epithelial cells after IL-1β and TNFα stimulation and this upregulation was diminished after MEK1 or p38 inhibition (320). However, in line with the results described herein, the study additionally showed that IL-1β and TNFα stimulation of the cells results in IκBα degradation followed by NFκB p65 translocation into the nucleus independent from p38 or MEK1 (320). The involvement of different pathways to induce chemokine expression after cytokine treatment most likely is cell type-dependent and might thus explain the discrepancies between the observations reported herein and those of the aforementioned study.

IL-1β is known to trigger its own synthesis in a positive feedback loop in multiple different cell types, such as e. g. macrophages and monocytes, chondrocytes and fibroblasts (161). In principle, this could explain the observed long-lasting IL-1β-induced expression of *CXCL1*, *2*, *3* and *8* mRNA enhanced by HCV infection (Fig. 18). However, inhibition of de novo protein synthesis resulted in an enhancement of the effects of IL-1β and/or HCV on *CXCL8* mRNA expression and not in an inhibition. As NFκB p65 induces its own inhibition via upregulation of

IκBα production, this effect most likely is due to a block of de novo IκB synthesis (Fig. 32A/D). Therefore, the effect may not be attributable to a positive feedback loop of IL-1β. Additionally, IL-1β is known to strongly induce NFκB signalling by degradation of IκBα via IKKs and subsequent release and nuclear translocation of NFκB (186, 187). The protein levels of IκBα were decreased by HCV and IL-1β in a synergistic manner (Fig. 33), strongly suggesting that upregulation of chemokine expression by HCV is mediated by enhanced degradation of IκBα and subsequent increase of NFκB levels. Taken together, these results suggest that the upregulation of *CXCL8* mRNA expression is independent of de novo synthesis of regulatory factors and strongly corroborate the described influence of NFκB p65 during HCV and IL-1β-dependent *CXCL8* mRNA expression enhancement.

ChIP analysis (Fig. 29) confirmed p65 as one of the major transcription factors binding to the promoter region of the *CXCL8* gene in the presence of both IL-1β, as an inflammatory stimulus, and HCV.

Phosphorylation of p65 at S536, which is known to occur independent from IκBα action (321) and modulates the transcriptional activity of p65 (322), was enhanced in both the chronic and acute HCV infection model after IL-1β stimulation (Fig. 30/31), indicating that HCV activates and/or modulates NFκB p65 signalling both via enhanced cleavage of IκBα and via increased phosphorylation IκBα of NFκB p65.

Phosphorylation of p65 S536 can be regulated by at least five different proteins: IKKα, IKKβ, IKKε, TBK1 and Ribosomal subunit S6 kinase 1 (323-326). Buss *et al.* demonstrated that NFκB p65 phosphorylation is independent of p38 or AKT activation (323). In contrast to this, Madrid *et al*. showed an involvement of p38 in p65 phosphorylation at S536 (225). Both studies are in line with the results obtained in this thesis, because phosphorylation of both proteins p38 and p65 was enhanced in HCV-infected cells in response to IL-1β stimulation (Fig. 30/31), while IL-1β-induced expression of *CXCL8* mRNA enhanced by HCV infection was reduced after *NFκB p65* knockdown, whereas neither p38, nor MEK1, nor AKT inhibition showed any effect regarding *CXCL8* mRNA expression upregulation (Fig. 18).

Surprisingly, none of the NFκB p65 co-transcription factors C/EBPβ, CREB1 and SP1 (193-195) showed any considerable effect on *CXCL8* mRNA expression regulation in this context (Fig. 22).

The herein presented results comprehensively illustrate that HCV modulates IL-1β-induced signalling by enhancing the binding of p65 to the *CXCL8* promoter region where it acts as a transcription factor for *CXCL8* gene expression. Knockdown of *NFκB p65* consequently nearly resulted in abolishment of the IL-1β-induced expression of *CXCL8* mRNA enhanced by HCV infection in the HCV_{cc} as well as in the subgenomic replicon system.

5.4 Enhancement of TNFα-induced expression of *CXCL3* and *8* mRNA by HCV is mediated by NFκB p65 signalling

VEGFA, TNFα, IL-1β and CXCL8 protein levels have been described to be upregulated in the serum of HCV-infected patients (**4.1** and (154, 199, 279, 299)). Additionally, TNFα levels were observed to be upregulated in transgenic mice expressing the HCV proteins NS3/4A in the liver, resulting in protection of these mice against TNFα/D-galactosamine (D-galN) or LPS/D-galN-induced liver damage (231).

Hence, potential interference of HCV with TNFα-induced upregulation of chemokine expression was investigated.

TNFα-induced expression of *CXCL3* and *CXCL8* mRNA was enhanced after HCV infection (Fig. 34), indicating that HCV, besides the EGF- and IL-1β-induced also interferes with TNFα-induced expression of *CXCL3* and *CXCL8* mRNA.

In contrast to *CXCL3* and *8*, *CXCL1* and *2* mRNA expression levels were found to be upregulated by TNFα, but not further affected by HCV infection (Fig. 35). Compared to the IL-1β-induced expression of chemokines enhanced by HCV infection, TNFα-induced expression of chemokines enhanced by HCV infection was much weaker in terms of fold-induction, because as concentration of 2 pg/mL IL-1β resulted in an equal upregulation of chemokine expression in HCV-infected cells compared to 500 pg/mL TNFα (Fig. 37).

In human hepatoma cell lines, it was demonstrated that HCV infection results in activation of TLR3 and subsequent regulation of NFκB-mediated expression of different chemokines, including CCL3, CXCL10, CCL4 and IL-6 (111), suggesting that also other chemokine mRNA expression apart from *CXCL3* and *8*, is mediated by HCV infection. Additionally, liver-specific NS3/4A expression in mice was shown to result in enhanced intrahepatic *CCL2* and *TNFα* expression levels as well as in an enhanced number of macrophages in these livers (230). In addition to that also TNFα-induced *CXCL8* expression is known to activate recruitment of immune cells to the liver (108). Since CXCL8 is a chemoattractant for neutrophil granulocytes (327), its secretion can result in recruitment of these immune cells to the liver and therefore alter the hepatic immunological environment.

The knockdown experiments performed during this thesis revealed that TNFα-induced upregulation of *CXCL1* mRNA expression was mediated by both TAK1 and NFκB p65 (Fig. 39E/F). Interestingly, *TAK1* knockdown did not affect the upregulation of *CXCL1* mRNA expression by TNFα in Huh7 cells, whereas NFκB p65 did, suggesting that NFκB p65 needs to be activated via other upstream mediators in this context. Since TNFα can activate NFκB p65 via a non-canonical pathway via activation of the NFκB-inducing kinase (NIK) or the canonical pathway via activation of TAK1 (328), it is suggested that the TNFα-induced *CXCL1* mRNA expression in Huh7 might be activated via the non-canonical NFκB pathway activated

by NIK.

CXCL2 and *3* mRNA expression was reduced upon *NFκB p65* or *TAK1* knockdown, suggesting that both *CXCL2* and *3* mRNA expression regulation is mediated by NFκB p65 and TAK1 (Fig. 40E/F+K/L) and therefore via the canonical NFκB pathway, which is activated by TAK1 (328).

Furthermore, TAK1 inhibition diminished the *CXCL8* mRNA expression upregulation after HCV infection, while it had no influence on the TNFα-induced expression of *CXCL8* mRNA in Huh7 cells which was shown to be mediated by NFκB p65 only (Fig. 38G/I). The data suggest that TNFα-induced mRNA expression of *CXCL1* as well as of *CXCL8* is regulated via the non-canonical NFκB p65 pathway (328). To strengthen this suggestion, the non-canonical NFκB p65 pathway should be investigated in future studies. Knockdown studies performed in this thesis further suggest NFκB p65 to have a decisive influence on the TNFα-induced expression of *CXCL8* mRNA (Fig. 38G). Therefore, in addition to the prior described IL-1β and EGF-induced (**5.2** and **5.3**) expression of *CXCL8* mRNA, NFκB also mediates TNFα-induced expression of *CXCL8* mRNA (Fig. 21A/C/15F).

Furthermore, NFκB p65 can be phosphorylated at several different phosphorylation residues, of which today 11 different ones are known. Among them, the best studied is the phosphorylation residue at S536. When phosphorylated, e. g. by IKKα, IKKβ or IKKε, p65 undergoes conformational changes and the affinity to IκBα decreases (329). Because IκBα degradation occurs upon phosphorylation by IKK and this is known to be partly mediated by TAK1 (330), and TNFα-induced expression of *CXCL8* mRNA enhanced by HCV was observed to be NFκB p65- but not TAK1-mediated, it is conceivable that NFκB p65 mediates *CXCL8* mRNA expression independent of IκBα degradation. Therefore, relative phosphorylation of p65 was analysed, but was not found to be enhanced after TNFα stimulation of the cells. Whether HCV alters the subcellular localization of p65, thereby resulting in enrichment of nuclear p65, will thus be an interesting point to investigate in the future.

5.5 AKT1 as well as TCPTP knockout results in reduced HCV infection rate and altered signal transduction

As it was described in previous studies from our group, TCPTP is degraded by the viral protease NS3/4A (36). Therefore, the effects of downregulation of TCPTP on viral replication were investigated.

In case of AKT, it was demonstrated in previous studies that the ErbB family member ErbB3 is downregulated via SP1-dependent upregulation of NRG1 and AKT activation in HCV-infected cells and that this downregulation enhances the upregulation of EGFR and ErbB2 on the cell surface, demonstrating cross-regulation between the different ErbB receptors (150). Furthermore, it was demonstrated that the basal activating phosphorylation of AKT was enhanced in HCV replicon cells. Additionally, EGF-induced phosphorylation of AKT was enhanced in HCV replicon cells when compared to Huh7 control cells (36).

To investigate the role of both proteins during HCV infection, AKT and TCPTP KO cell lines were generated using the CRISPR/Cas9 system of genome editing (Fig. 42/47).

Both TCPTP and AKT1 KO led to reduced HCV infection compared to control cells as determined by immunoblot of viral proteins (Fig. 43/47). In case of AKT1 KO, mRNA expression levels of transcription coding for viral proteins were reduced as determined by qRT-PCR (Fig. 44). The findings regarding AKT1 are in line with the literature, demonstrating that *AKT* gene knockdown or inhibition of the protein abolished HCV entry in the HCV_{pp} system (331).

Surprisingly, the absence of TCPTP also resulted in downregulation of HCV infection. This is in contrast to the expected increase in infection due to the fact that TCPTP is cleaved by the viral protease NS3/4A (36). Since this finding was confirmed in three different TCPTP KO cell lines (Fig. 47), clonal effects can be nearly ruled out. Mechanistically, this might suggest that HCV downregulates TCPTP to a level that is beneficial for the virus and a complete KO is conversely detrimental for the virus. Alternatively, absence of TCPTP might affect cell viability, but further analysis will be necessary to clarify this. The EGFR is known to be internalized via endocytosis after activation. When EGF binds to EGFR at low concentrations, EGFR is mainly recycled to the plasma membrane, while high concentrations of EGF enhance degradation of EGFR (86). It thus may be assumed that TCPTP KO results in prolonged activation of the EGFR, thereby resulting in enhanced EGFR degradation and reduction of cell surface levels. Following that line of thought, HCV cell entry could be reduced as a result of absence of TCPTP.

Alternatively, HCV might be degraded alongside the EGFR within the lysosomal lumen and thus infection levels might also be lowered.

Although the occurrence of off-target effects caused by unspecific Cas9 targeting to undesired genomic loci can be reduced by sophisticated computational guide design (332), they cannot

be fully excluded without sequencing the whole genome of the respective KO cell line. Re-insertion of the correct coding sequence mediated by CRISPR/Cas9-mediated HDR (333) could be performed to test whether the phenotype can be rescued.

Huh7.5 AKT1 1.1 KO cells showed an abolishment of the upregulation of *CXCL1, 2, 3* and *8* mRNA expression levels after HCV infection compared to control cells (Fig. 45), while Huh7.5 AKT 2.3.5 KO cells showed nearly no effect on chemokine expression enhancement after HCV infection when compared to Huh7.5 control cells (Fig. 46).

Besides, basal *CXCL1* and *2* mRNA expression was reduced in both analysed AKT1 KO cell lines (Fig. 45/46), strongly suggesting an important role of AKT1 in the regulation of these chemokines in general and especially in the context of HCV infection.

IL-1β as well as EGF stimulation could not restore the abrogated HCV effect on basal chemokine expression of *CXCL3* and *8* in Huh7.5 AKT1 1.1 KO cells, indicating that AKT1 mediates the IL-1β- and EGF-induced expression of *CXCL3* and *8* mRNA enhanced by HCV infection (Fig. 45C/D+K/L).

That AKT1 KO results in impaired HCV infection of the cells is in line with previous studies from our and from other groups (36, 150, 331, 334). In AKT1 1.1 KO cells, the enhanced *CXCL1*, *2*, *3* and *8* mRNA expression after HCV infection was nearly abolished, suggesting that AKT1 activation is responsible for the enhancement of CXCR2 ligand expression in response to HCV infection. However, clonal effects must be excluded since AKT1 2.3.5 KO cells showed nearly no reduction in HCV-induced CXCR2 ligand chemokine mRNA expression enhancement (Fig. 46).

Further analysis of the complex interplay between TCPTP, AKT1, EGFR and HCV will be of high importance in the future to further understand the molecular mechanisms underlying HCV infection and chronic persistence.

6 Summary

The hepatitis C virus (HCV) persists in patients for decades without causing recognisable symptoms. Such chronic infection leads to the development of chronic hepatitis, progression to liver cirrhosis and its consequences in a subset of patients. This long-lasting and slowly progressive course, despite sustained viral replication presupposes that HCV must possess mechanisms that enable it to undermine antiviral immunity, to influence the inflammatory response of the host, and ultimately to use the infrastructure of the host cell without impairing its viability too much.

It is therefore obvious that HCV must have developed mechanisms in the course of co-evolution that enable the virus to influence the intercellular communication of the host cell and, via this, the local immunological milieu. In addition, preliminary findings, in which our research group was involved, suggest that a sustained, limited increase in serum concentrations of inflammatory cytokines such as TNFα activates latency mechanisms that can ultimately also mediate protective effects.

Preliminary findings of the research group, predominantly collected at the replicon system, further demonstrate that HCV modifies epidermal growth factor (EGF)-dependent signal transmission of the host cell and influences the regulation of chemokine expression in response to EGF. Based on these findings, the molecular mechanisms were to be further investigated in the present thesis using cell culture models based on infectious HCV particles. In addition, it should be investigated to what extent HCV also influences the expression of chemokines in the host cell induced by inflammatory cytokines such as IL-1β and TNFα and to clarify the underlying molecular mechanisms.

In agreement with the results of previous studies of the research group, the present work could demonstrate that HCV infection leads to an increased mRNA expression of the chemokines *CXCL1*, *2*, *3* and *8*, which belong to the group of CXCR2 ligands, and that this is based on an EGF-mediated feedback mechanism. Furthermore, it could be demonstrated that EGF-induced expression of transcripts encoding the analysed CXCR2 ligands is enhanced by HCV and that this occurs at the level of NFκB-dependent regulation and, in part, via MEK1-mediated signalling. In addition, HCV was also shown to induce IL-1β- and to a limited extent TNFα-induced expression of the aforementioned CXCR2 ligands, although in the case of TNFα this was limited to chemokines *CXCL3* and *8*. Knockdown experiments using siRNA as well as chromatin immunoprecipitation experiments and experiments with inhibition of *de novo* protein synthesis suggest that, in the case of IL-1β, the amplification occurs at the level of degradation of IκBα and activation of NFκB.

In addition, knockout cell lines of T-cell protein tyrosine phosphatase (TCPTP), an important negative regulator of the EGFR, and of AKT1, an important signalling molecule in EGF

signalling, were generated using the CRISPR/Cas9 technology. Initial studies on these cells suggest that AKT1 may play a role in the regulation of expression of *CXCL1* and *2* in Huh7.5 cells.

In summary, the findings described in this work demonstrate that HCV influences host cell-derived intercellular communication in response to concurrent signals such as growth factors or inflammatory mediators. It thus can be assumed that HCV is able to influence the local composition of immune cell populations and thereby the inflammatory reaction as well as the immune response of the host.

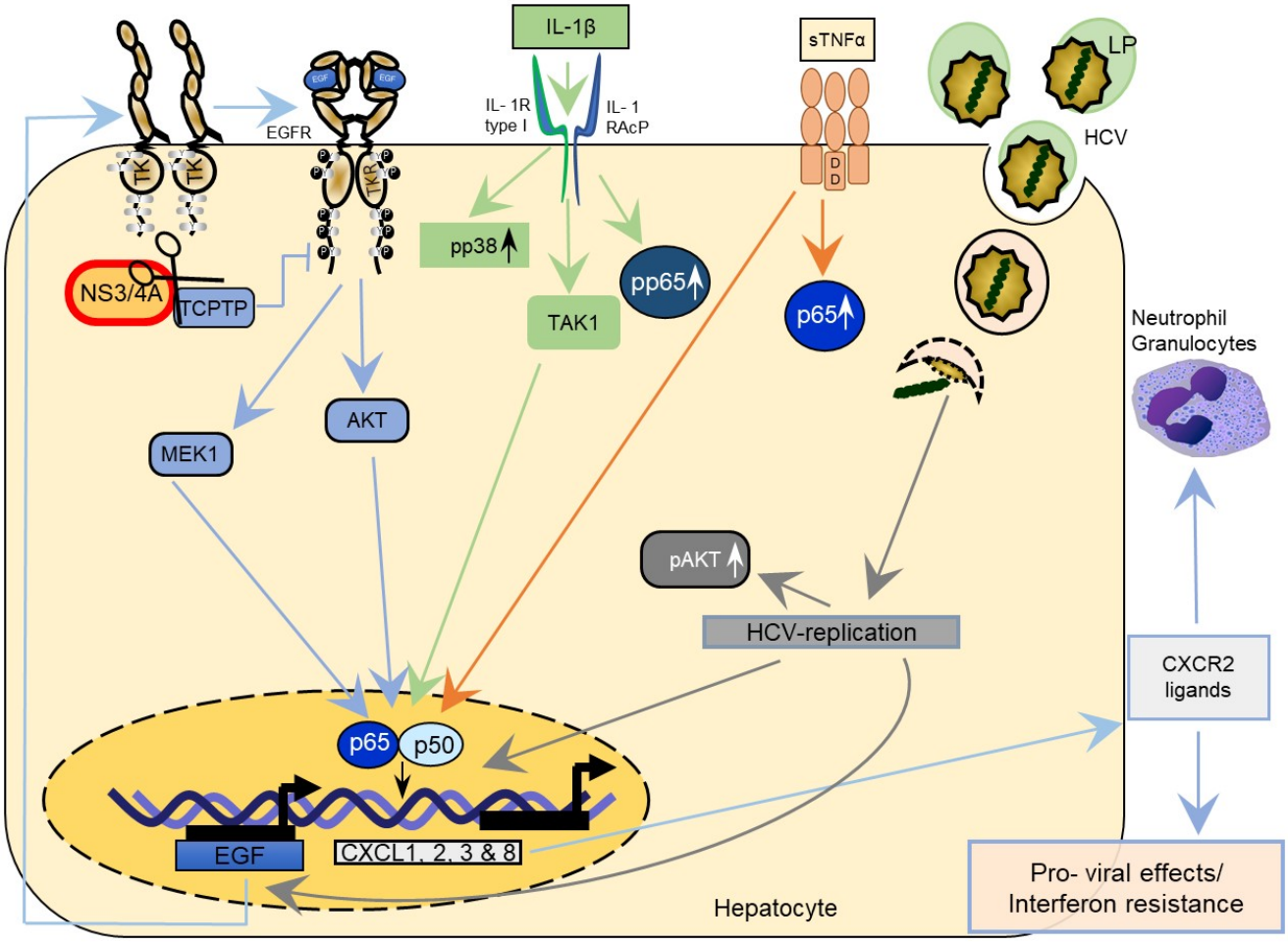

Fig. 48- Schematic depiction of the summary. HCV infection of the cell enhances the mRNA expression of EGF and *CXCL1, 2, 3* and *8*. EGF binds to the EGFR, which results in homo-or heterodimerization of the receptor and enhanced phosphorylation of EGFR. EGFR activation results in a further upregulation of *CXCL1, 2, 3* and *8* mRNA expression mediated by MEK1, AKT and NFκB p65. IL-1β further upregulates the *CXCL1, 2, 3* and *8* mRNA expression in HCV-infected cells via enhanced translocation of NFκB p65 into the nucleus mediated by TAK1 where it functions as transcription factor for CXCL8. Additionally, phosphorylation of both p38 and p65 is enhanced in infected cells after IL-1β stimulation. Additionally, TNFα further enhances the upregulation of *CXCL3* and *8* mRNA expression in HCV-infected cells mediated by NFκB p65 and upregulates p65 protein levels in total cell lysates. In previous studies from our group, it was demonstrated that TCPTP is degraded by HCV leading to enhanced EGFR phosphorylation (36) and that recruitment of neutrophil granulocytes but not monocytes is enhanced in HCV-infected cells (284).

7 Zusammenfassung

Das Hepatitis C Virus (HCV) persistiert in Patienten über Jahrzehnte, ohne erkennbare Symptome zu verursachen und führt nur bei einem Teil der Patienten zur Ausbildung einer chronischen Hepatitis und ihrer Progression zu Leberzirrhose und deren Folgen. Dieser, trotz anhaltender viraler Replikation, vieljährige und nur langsam progrediente Verlauf setzt voraus, dass HCV über Mechanismen verfügen muss, die es ihm ermöglichen die antivirale Immunität zu unterlaufen, die Entzündungsantwort des Wirtes zu beeinflussen und letztlich die Infrastruktur der Wirtszelle zu nutzen, ohne ihre Lebensfähigkeit zu sehr zu beeinträchtigen.
Es ist daher naheliegend, dass HCV im Verlauf der Coevolution Mechanismen entwickelt haben muss, die es dem Virus ermöglichen die interzelluläre Kommunikation der Wirtszelle zu beeinflussen und hierüber das lokale immunologische Milieu zu verändern. Darüber hinaus legen Vorbefunde, an denen unsere Arbeitsgruppe beteiligt war, nahe, dass über eine anhaltende, begrenzte Erhöhung der Serumkonzentrationen inflammatorischer Zytokine, wie zum Beispiel TNFα, Latenzmechanismen aktiviert werden, die letztlich auch protektive Effekte vermitteln können.
Überwiegend am Replikonsystem erhobene Vorbefunde der Arbeitsgruppe belegen, dass HCV die EGF-abhängige Signalübertragung der Wirtszelle modifiziert und die Regulation der Chemokin-Expression in Reaktion auf EGF beeinflusst. Ausgehend von diesen Befunden sollten im Rahmen der vorliegenden Dissertation unter Hinzuziehung von auf infektiösen HCV Partikeln basierenden Zellkulturmodellen die molekularen Mechanismen weitergehend untersucht werden. Darüber hinaus sollte untersucht werden inwieweit HCV auch die durch inflammatorische Zytokine wie IL-1β und TNFα induzierte Expression von Chemokinen in der Wirtszelle beeinflusst, sowie die zugrundeliegenden molekularen Mechanismen aufgeklärt werden.
In Übereinstimmung mit den Ergebnissen vorangehender Untersuchungen der Arbeitsgruppe konnte in der vorliegenden Arbeit belegt werden, dass eine HCV-Infektion zu einer erhöhten mRNA-Expression der zur Gruppe der CXCR2-Liganden gehörenden Chemokine *CXCL1*, *2*, *3* und *8* führt und dass diesem ein EGF-vermittelter Rückkopplungsmechanismus zugrunde liegt. Darüber hinaus wurde nachgewiesen, dass die EGF-induzierte Expression von Transkripten, die für die oben genannten CXCR2-Liganden kodieren, durch HCV verstärkt wird und dass dies auf der Ebene der NFκB-abhängigen Regulation erfolgt und zum Teil über eine durch MEK1 vermittelte Signalübertragung. Darüber hinaus konnte belegt werden, dass HCV auch die durch IL-1β- und in begrenztem Umfang auch die TNFα induzierte Expression oben genannter CXCR2 Liganden induziert, wobei sich dies im Falle von TNFα auf die Chemokine *CXCL3* und *8* begrenzt. Sowohl knockdown Experimente mittels siRNA als auch Chromatin-Immunopräzipitationsexperimente und Untersuchungen unter Hemmung der *de novo*

Proteinsynthese legen hierbei nahe, dass im Falle von IL-1β die Verstärkung auf Ebene der Degradation von IκBα und der Aktivierung von NFκB erfolgt.

Im Rahmen der hier vorgelegten Doktorarbeit wurden zusätzlich mittels der CRISPR/Cas9 Technologie Knockout (KO)-Zelllinien der T-Zell Protein Tyrosin Phosphatase (TCPTP), einem wichtigen Negativ-Regulator des EGF-Rezeptors, generiert. Ferner wurden KO-Zellen für AKT1, einem wichtigen Signalmolekül in der EGF Signalübertragung, hergestellt, wobei erste Untersuchungen an diesen Zellen nahelegen, dass AKT1 für die Expression von *CXCL1* und *2* in Huh7.5 Zellen eine Rolle spielen könnte.

Zusammenfassend, belegen die in dieser Arbeit erhobenen Befunde, dass HCV die von der Wirtszelle ausgehende interzelluläre Kommunikation in Abhängigkeit von gleichzeitig agierenden Signalen wie Wachstums- oder Entzündungsfaktoren beeinflusst. Es ist deshalb davon auszugehen, dass HCV hierüber die lokale Zusammensetzung der Immunzellpopulationen beeinflussen kann und hierdurch die Entzündungsreaktion wie auch die Immunantwort des Wirtes moduliert.

8 References

1. Organization. WH. Global Hepatitis Report. In: Organization WH, editor.; 2017.
2. Ortega-Prieto AM, Dorner M. Immune Evasion Strategies during Chronic Hepatitis B and C Virus Infection. Vaccines (Basel) 2017;5.
3. Brenner DA. Molecular pathogenesis of liver fibrosis. Trans Am Clin Climatol Assoc 2009;120:361-368.
4. Bartenschlager R, Baumert TF, Bukh J, Houghton M, Lemon SM, Lindenbach BD, Lohmann V, et al. Critical challenges and emerging opportunities in hepatitis C virus research in an era of potent antiviral therapy: Considerations for scientists and funding agencies. Virus Res 2018;248:53-62.
5. Choo QL, Kuo G, Weiner AJ, Overby LR, Bradley DW, Houghton M. Isolation of a cDNA clone derived from a blood-borne non-A, non-B viral hepatitis genome. Science 1989;244:359-362.
6. Choo QL, Richman KH, Han JH, Berger K, Lee C, Dong C, Gallegos C, et al. Genetic organization and diversity of the hepatitis C virus. Proc Natl Acad Sci U S A 1991;88:2451-2455.
7. Stapleton JT, Foung S, Muerhoff AS, Bukh J, Simmonds P. The GB viruses: a review and proposed classification of GBV-A, GBV-C (HGV), and GBV-D in genus Pegivirus within the family Flaviviridae. J Gen Virol 2011;92:233-246.
8. Simmonds P, Holmes EC, Cha TA, Chan SW, McOmish F, Irvine B, Beall E, et al. Classification of hepatitis C virus into six major genotypes and a series of subtypes by phylogenetic analysis of the NS-5 region. J Gen Virol 1993;74 (Pt 11):2391-2399.
9. Simmonds P, Becher P, Bukh J, Gould EA, Meyers G, Monath T, Muerhoff S, et al. ICTV Virus Taxonomy Profile: Flaviviridae. J Gen Virol 2017;98:2-3.
10. de Souza WM, Fumagalli MJ, Sabino-Santos G, Jr., Motta Maia FG, Modha S, Teixeira Nunes MR, Murcia PR, et al. A Novel Hepacivirus in Wild Rodents from South America. Viruses 2019;11.
11. Smith DB, Bukh J, Kuiken C, Muerhoff AS, Rice CM, Stapleton JT, Simmonds P. Expanded classification of hepatitis C virus into 7 genotypes and 67 subtypes: updated criteria and genotype assignment web resource. Hepatology 2014;59:318-327.
12. Simmonds P, Bukh J, Combet C, Deleage G, Enomoto N, Feinstone S, Halfon P, et al. Consensus proposals for a unified system of nomenclature of hepatitis C virus genotypes. Hepatology 2005;42:962-973.
13. Borgia SM, Hedskog C, Parhy B, Hyland RH, Stamm LM, Brainard DM, Subramanian MG, et al. Identification of a Novel Hepatitis C Virus Genotype From Punjab, India: Expanding Classification of Hepatitis C Virus Into 8 Genotypes. J Infect Dis 2018;218:1722-1729.
14. Polaris Observatory HCVC. Global prevalence and genotype distribution of hepatitis C virus infection in 2015: a modelling study. Lancet Gastroenterol Hepatol 2017;2:161-176.
15. Steinmann E, Brohm C, Kallis S, Bartenschlager R, Pietschmann T. Efficient trans-encapsidation of hepatitis C virus RNAs into infectious virus-like particles. J Virol 2008;82:7034-7046.
16. Herod MR, Jones DM, McLauchlan J, McCormick CJ. Increasing rate of cleavage at boundary between non-structural proteins 4B and 5A inhibits replication of hepatitis C virus. J Biol Chem 2012;287:568-580.

17. Pene V, Hernandez C, Vauloup-Fellous C, Garaud-Aunis J, Rosenberg AR. Sequential processing of hepatitis C virus core protein by host cell signal peptidase and signal peptide peptidase: a reassessment. J Viral Hepat 2009;16:705-715.
18. Pene V, Lemasson M, Harper F, Pierron G, Rosenberg AR. Role of cleavage at the core-E1 junction of hepatitis C virus polyprotein in viral morphogenesis. PLoS One 2017;12:e0175810.
19. Dubuisson J. Hepatitis C virus proteins. World J Gastroenterol 2007;13:2406-2415.
20. Tellinghuisen TL, Rice CM. Interaction between hepatitis C virus proteins and host cell factors. Curr Opin Microbiol 2002;5:419-427.
21. McLauchlan J. Properties of the hepatitis C virus core protein: a structural protein that modulates cellular processes. J Viral Hepat 2000;7:2-14.
22. Ray RB, Ray R. Hepatitis C virus core protein: intriguing properties and functional relevance. FEMS Microbiol Lett 2001;202:149-156.
23. Pazienza V, Clement S, Pugnale P, Conzelman S, Foti M, Mangia A, Negro F. The hepatitis C virus core protein of genotypes 3a and 1b downregulates insulin receptor substrate 1 through genotype-specific mechanisms. Hepatology 2007;45:1164-1171.
24. Wu Q, Li Z, Mellor P, Zhou Y, Anderson DH, Liu Q. The role of PTEN - HCV core interaction in hepatitis C virus replication. Sci Rep 2017;7:3695.
25. Ruan ZP, Xu R, Lv Y, Tian T, Wang WJ, Guo H, Nan KJ. PTEN enhances the sensitivity of human hepatocellular carcinoma cells to sorafenib. Oncol Res 2012;20:113-121.
26. Zhang Y, Li RQ, Feng XD, Zhang YH, Wang L. Down-regulation of PTEN by HCV core protein through activating nuclear factor-kappaB. Int J Clin Exp Pathol 2014;7:7351-7359.
27. Douam F, Dao Thi VL, Maurin G, Fresquet J, Mompelat D, Zeisel MB, Baumert TF, et al. Critical interaction between E1 and E2 glycoproteins determines binding and fusion properties of hepatitis C virus during cell entry. Hepatology 2014;59:776-788.
28. Mazumdar B, Banerjee A, Meyer K, Ray R. Hepatitis C virus E1 envelope glycoprotein interacts with apolipoproteins in facilitating entry into hepatocytes. Hepatology 2011;54:1149-1156.
29. Douam F, Fusil F, Enguehard M, Dib L, Nadalin F, Schwaller L, Hrebikova G, et al. A protein coevolution method uncovers critical features of the Hepatitis C Virus fusion mechanism. PLoS Pathog 2018;14:e1006908.
30. Tong Y, Lavillette D, Li Q, Zhong J. Role of Hepatitis C Virus Envelope Glycoprotein E1 in Virus Entry and Assembly. Front Immunol 2018;9:1411.
31. Denolly S, Mialon C, Bourlet T, Amirache F, Penin F, Lindenbach B, Boson B, et al. The amino-terminus of the hepatitis C virus (HCV) p7 viroporin and its cleavage from glycoprotein E2-p7 precursor determine specific infectivity and secretion levels of HCV particle types. PLoS Pathog 2017;13:e1006774.
32. Jirasko V, Montserret R, Lee JY, Gouttenoire J, Moradpour D, Penin F, Bartenschlager R. Structural and functional studies of nonstructural protein 2 of the hepatitis C virus reveal its key role as organizer of virion assembly. PLoS Pathog 2010;6:e1001233.
33. Bartenschlager R, Ahlborn-Laake L, Mous J, Jacobsen H. Nonstructural protein 3 of the hepatitis C virus encodes a serine-type proteinase required for cleavage at the NS3/4 and NS4/5 junctions. J Virol 1993;67:3835-3844.
34. Bartenschlager R, Lohmann V, Wilkinson T, Koch JO. Complex formation between the NS3 serine-type proteinase of the hepatitis C virus and NS4A and its importance for polyprotein maturation. J Virol 1995;69:7519-7528.

35. Tomei L, Failla C, Santolini E, De Francesco R, La Monica N. NS3 is a serine protease required for processing of hepatitis C virus polyprotein. J Virol 1993;67:4017-4026.
36. Brenndorfer ED, Karthe J, Frelin L, Cebula P, Erhardt A, Schulte am Esch J, Hengel H, et al. Nonstructural 3/4A protease of hepatitis C virus activates epithelial growth factor-induced signal transduction by cleavage of the T-cell protein tyrosine phosphatase. Hepatology 2009;49:1810-1820.
37. Bode JG, Brenndorfer ED, Haussinger D. Hepatitis C virus (HCV) employs multiple strategies to subvert the host innate antiviral response. Biol Chem 2008;389:1283-1298.
38. Egger D, Wolk B, Gosert R, Bianchi L, Blum HE, Moradpour D, Bienz K. Expression of hepatitis C virus proteins induces distinct membrane alterations including a candidate viral replication complex. J Virol 2002;76:5974-5984.
39. David N, Yaffe Y, Hagoel L, Elazar M, Glenn JS, Hirschberg K, Sklan EH. The interaction between the hepatitis C proteins NS4B and NS5A is involved in viral replication. Virology 2015;475:139-149.
40. Ross-Thriepland D, Harris M. Hepatitis C virus NS5A: enigmatic but still promiscuous 10 years on! J Gen Virol 2015;96:727-738.
41. Asabe SI, Tanji Y, Satoh S, Kaneko T, Kimura K, Shimotohno K. The N-terminal region of hepatitis C virus-encoded NS5A is important for NS4A-dependent phosphorylation. J Virol 1997;71:790-796.
42. Koch JO, Bartenschlager R. Modulation of hepatitis C virus NS5A hyperphosphorylation by nonstructural proteins NS3, NS4A, and NS4B. J Virol 1999;73:7138-7146.
43. Popescu CI, Callens N, Trinel D, Roingeard P, Moradpour D, Descamps V, Duverlie G, et al. NS2 protein of hepatitis C virus interacts with structural and non-structural proteins towards virus assembly. PLoS Pathog 2011;7:e1001278.
44. Penin F, Brass V, Appel N, Ramboarina S, Montserret R, Ficheux D, Blum HE, et al. Structure and function of the membrane anchor domain of hepatitis C virus nonstructural protein 5A. J Biol Chem 2004;279:40835-40843.
45. Brass V, Bieck E, Montserret R, Wolk B, Hellings JA, Blum HE, Penin F, et al. An amino-terminal amphipathic alpha-helix mediates membrane association of the hepatitis C virus nonstructural protein 5A. J Biol Chem 2002;277:8130-8139.
46. Tellinghuisen TL, Marcotrigiano J, Rice CM. Structure of the zinc-binding domain of an essential component of the hepatitis C virus replicase. Nature 2005;435:374-379.
47. Tellinghuisen TL, Marcotrigiano J, Gorbalenya AE, Rice CM. The NS5A protein of hepatitis C virus is a zinc metalloprotein. J Biol Chem 2004;279:48576-48587.
48. Poch O, Sauvaget I, Delarue M, Tordo N. Identification of four conserved motifs among the RNA-dependent polymerase encoding elements. EMBO J 1989;8:3867-3874.
49. Behrens SE, Tomei L, De Francesco R. Identification and properties of the RNA-dependent RNA polymerase of hepatitis C virus. EMBO J 1996;15:12-22.
50. Lohmann V, Korner F, Herian U, Bartenschlager R. Biochemical properties of hepatitis C virus NS5B RNA-dependent RNA polymerase and identification of amino acid sequence motifs essential for enzymatic activity. J Virol 1997;71:8416-8428.
51. Nikonov A, Juronen E, Ustav M. Functional characterization of fingers subdomain-specific monoclonal antibodies inhibiting the hepatitis C virus RNA-dependent RNA polymerase. J Biol Chem 2008;283:24089-24102.

52. Ago H, Adachi T, Yoshida A, Yamamoto M, Habuka N, Yatsunami K, Miyano M. Crystal structure of the RNA-dependent RNA polymerase of hepatitis C virus. Structure 1999;7:1417-1426.
53. Harrus D, Ahmed-El-Sayed N, Simister PC, Miller S, Triconnet M, Hagedorn CH, Mahias K, et al. Further insights into the roles of GTP and the C terminus of the hepatitis C virus polymerase in the initiation of RNA synthesis. J Biol Chem 2010;285:32906-32918.
54. Gosert R, Egger D, Lohmann V, Bartenschlager R, Blum HE, Bienz K, Moradpour D. Identification of the hepatitis C virus RNA replication complex in Huh-7 cells harboring subgenomic replicons. J Virol 2003;77:5487-5492.
55. Ashfaq UA, Javed T, Rehman S, Nawaz Z, Riazuddin S. An overview of HCV molecular biology, replication and immune responses. Virol J 2011;8:161.
56. Burstow NJ, Mohamed Z, Gomaa AI, Sonderup MW, Cook NA, Waked I, Spearman CW, et al. Hepatitis C treatment: where are we now? Int J Gen Med 2017;10:39-52.
57. Calogero A, Sagnelli E, Creta M, Angeletti S, Peluso G, Incollingo P, Candida M, et al. Eradication of HCV Infection with the Direct-Acting Antiviral Therapy in Renal Allograft Recipients. Biomed Res Int 2019;2019:4674560.
58. McHutchison JG, Gordon SC, Schiff ER, Shiffman ML, Lee WM, Rustgi VK, Goodman ZD, et al. Interferon alfa-2b alone or in combination with ribavirin as initial treatment for chronic hepatitis C. Hepatitis Interventional Therapy Group. N Engl J Med 1998;339:1485-1492.
59. European Association for Study of L. EASL Recommendations on Treatment of Hepatitis C 2015. J Hepatol 2015;63:199-236.
60. European Association for the Study of the Liver. Electronic address eee, European Association for the Study of the L. EASL Recommendations on Treatment of Hepatitis C 2018. J Hepatol 2018;69:461-511.
61. de Oliveria Andrade LJ, D'Oliveira A, Melo RC, De Souza EC, Costa Silva CA, Parana R. Association between hepatitis C and hepatocellular carcinoma. J Glob Infect Dis 2009;1:33-37.
62. Sandmann L, Ploss A. Barriers of hepatitis C virus interspecies transmission. Virology 2013;435:70-80.
63. Ding Q, von Schaewen M, Ploss A. The impact of hepatitis C virus entry on viral tropism. Cell Host Microbe 2014;16:562-568.
64. Flint M, von Hahn T, Zhang J, Farquhar M, Jones CT, Balfe P, Rice CM, et al. Diverse CD81 proteins support hepatitis C virus infection. J Virol 2006;80:11331-11342.
65. Ploss A, Evans MJ, Gaysinskaya VA, Panis M, You H, de Jong YP, Rice CM. Human occludin is a hepatitis C virus entry factor required for infection of mouse cells. Nature 2009;457:882-886.
66. Masciopinto F, Freer G, Burgio VL, Levy S, Galli-Stampino L, Bendinelli M, Houghton M, et al. Expression of human CD81 in transgenic mice does not confer susceptibility to hepatitis C virus infection. Virology 2002;304:187-196.
67. Forton DM. Hepatitis C - the brain strain. Liver Int 2016;36:1415-1417.
68. Meredith LW, Wilson GK, Fletcher NF, McKeating JA. Hepatitis C virus entry: beyond receptors. Rev Med Virol 2012;22:182-193.
69. Ploss A, Evans MJ. Hepatitis C virus host cell entry. Curr Opin Virol 2012;2:14-19.
70. Miao Z, Xie Z, Miao J, Ran J, Feng Y, Xia X. Regulated Entry of Hepatitis C Virus into Hepatocytes. Viruses 2017;9.

71. Zhu YZ, Qian XJ, Zhao P, Qi ZT. How hepatitis C virus invades hepatocytes: the mystery of viral entry. World J Gastroenterol 2014;20:3457-3467.
72. Agnello V, Abel G, Elfahal M, Knight GB, Zhang QX. Hepatitis C virus and other flaviviridae viruses enter cells via low density lipoprotein receptor. Proc Natl Acad Sci U S A 1999;96:12766-12771.
73. Scarselli E, Ansuini H, Cerino R, Roccasecca RM, Acali S, Filocamo G, Traboni C, et al. The human scavenger receptor class B type I is a novel candidate receptor for the hepatitis C virus. EMBO J 2002;21:5017-5025.
74. Pileri P, Uematsu Y, Campagnoli S, Galli G, Falugi F, Petracca R, Weiner AJ, et al. Binding of hepatitis C virus to CD81. Science 1998;282:938-941.
75. Evans MJ, von Hahn T, Tscherne DM, Syder AJ, Panis M, Wolk B, Hatziioannou T, et al. Claudin-1 is a hepatitis C virus co-receptor required for a late step in entry. Nature 2007;446:801-805.
76. Liu S, Yang W, Shen L, Turner JR, Coyne CB, Wang T. Tight junction proteins claudin-1 and occludin control hepatitis C virus entry and are downregulated during infection to prevent superinfection. J Virol 2009;83:2011-2014.
77. Lupberger J, Zeisel MB, Xiao F, Thumann C, Fofana I, Zona L, Davis C, et al. EGFR and EphA2 are host factors for hepatitis C virus entry and possible targets for antiviral therapy. Nat Med 2011;17:589-595.
78. Martin DN, Uprichard SL. Identification of transferrin receptor 1 as a hepatitis C virus entry factor. Proc Natl Acad Sci U S A 2013;110:10777-10782.
79. Sainz B, Jr., Barretto N, Martin DN, Hiraga N, Imamura M, Hussain S, Marsh KA, et al. Identification of the Niemann-Pick C1-like 1 cholesterol absorption receptor as a new hepatitis C virus entry factor. Nat Med 2012;18:281-285.
80. Alazard-Dany N, Denolly S, Boson B, Cosset FL. Overview of HCV Life Cycle with a Special Focus on Current and Possible Future Antiviral Targets. Viruses 2019;11.
81. Ogden SC, Tang H. The missing pieces of the HCV entry puzzle. Future Virol 2015;10:415-428.
82. Andre P, Komurian-Pradel F, Deforges S, Perret M, Berland JL, Sodoyer M, Pol S, et al. Characterization of low- and very-low-density hepatitis C virus RNA-containing particles. J Virol 2002;76:6919-6928.
83. Bartenschlager R, Penin F, Lohmann V, Andre P. Assembly of infectious hepatitis C virus particles. Trends Microbiol 2011;19:95-103.
84. Sourisseau M, Michta ML, Zony C, Israelow B, Hopcraft SE, Narbus CM, Parra Martin A, et al. Temporal analysis of hepatitis C virus cell entry with occludin directed blocking antibodies. PLoS Pathog 2013;9:e1003244.
85. Lindenbach BD, Rice CM. The ins and outs of hepatitis C virus entry and assembly. Nat Rev Microbiol 2013;11:688-700.
86. Zeisel MB, Felmlee DJ, Baumert TF. Hepatitis C virus entry. Curr Top Microbiol Immunol 2013;369:87-112.
87. Lohmann V, Korner F, Koch J, Herian U, Theilmann L, Bartenschlager R. Replication of subgenomic hepatitis C virus RNAs in a hepatoma cell line. Science 1999;285:110-113.
88. Lohmann V, Bartenschlager R. On the history of hepatitis C virus cell culture systems. J Med Chem 2014;57:1627-1642.
89. Lohmann V, Hoffmann S, Herian U, Penin F, Bartenschlager R. Viral and cellular determinants of hepatitis C virus RNA replication in cell culture. J Virol 2003;77:3007-3019.
90. Krieger N, Lohmann V, Bartenschlager R. Enhancement of hepatitis C virus RNA replication by cell culture-adaptive mutations. J Virol 2001;75:4614-4624.

91. Reiss S, Rebhan I, Backes P, Romero-Brey I, Erfle H, Matula P, Kaderali L, et al. Recruitment and activation of a lipid kinase by hepatitis C virus NS5A is essential for integrity of the membranous replication compartment. Cell Host Microbe 2011;9:32-45.
92. Harak C, Meyrath M, Romero-Brey I, Schenk C, Gondeau C, Schult P, Esser-Nobis K, et al. Tuning a cellular lipid kinase activity adapts hepatitis C virus to replication in cell culture. Nat Microbiol 2016;2:16247.
93. Lohmann V. Hepatitis C virus cell culture models: an encomium on basic research paving the road to therapy development. Med Microbiol Immunol 2019;208:3-24.
94. Pietschmann T, Lohmann V, Kaul A, Krieger N, Rinck G, Rutter G, Strand D, et al. Persistent and transient replication of full-length hepatitis C virus genomes in cell culture. J Virol 2002;76:4008-4021.
95. Blight KJ, McKeating JA, Rice CM. Highly permissive cell lines for subgenomic and genomic hepatitis C virus RNA replication. J Virol 2002;76:13001-13014.
96. Date T, Morikawa K, Tanaka Y, Tanaka-Kaneko K, Sata T, Mizokami M, Wakita T. Replication and infectivity of a novel genotype 1b hepatitis C virus clone. Microbiol Immunol 2012;56:308-317.
97. Grobler JA, Markel EJ, Fay JF, Graham DJ, Simcoe AL, Ludmerer SW, Murray EM, et al. Identification of a key determinant of hepatitis C virus cell culture adaptation in domain II of NS3 helicase. J Biol Chem 2003;278:16741-16746.
98. Bartosch B, Dubuisson J, Cosset FL. Infectious hepatitis C virus pseudo-particles containing functional E1-E2 envelope protein complexes. J Exp Med 2003;197:633-642.
99. Hsu M, Zhang J, Flint M, Logvinoff C, Cheng-Mayer C, Rice CM, McKeating JA. Hepatitis C virus glycoproteins mediate pH-dependent cell entry of pseudotyped retroviral particles. Proc Natl Acad Sci U S A 2003;100:7271-7276.
100. Steinmann E, Pietschmann T. Cell culture systems for hepatitis C virus. Curr Top Microbiol Immunol 2013;369:17-48.
101. Lindenbach BD, Evans MJ, Syder AJ, Wolk B, Tellinghuisen TL, Liu CC, Maruyama T, et al. Complete replication of hepatitis C virus in cell culture. Science 2005;309:623-626.
102. Wakita T, Pietschmann T, Kato T, Date T, Miyamoto M, Zhao Z, Murthy K, et al. Production of infectious hepatitis C virus in tissue culture from a cloned viral genome. Nat Med 2005;11:791-796.
103. Zhong J, Gastaminza P, Cheng G, Kapadia S, Kato T, Burton DR, Wieland SF, et al. Robust hepatitis C virus infection in vitro. Proc Natl Acad Sci U S A 2005;102:9294-9299.
104. Kato T, Furusaka A, Miyamoto M, Date T, Yasui K, Hiramoto J, Nagayama K, et al. Sequence analysis of hepatitis C virus isolated from a fulminant hepatitis patient. J Med Virol 2001;64:334-339.
105. Pietschmann T, Kaul A, Koutsoudakis G, Shavinskaya A, Kallis S, Steinmann E, Abid K, et al. Construction and characterization of infectious intragenotypic and intergenotypic hepatitis C virus chimeras. Proc Natl Acad Sci U S A 2006;103:7408-7413.
106. Gale M, Jr., Foy EM. Evasion of intracellular host defence by hepatitis C virus. Nature 2005;436:939-945.
107. Sumpter R, Jr., Loo YM, Foy E, Li K, Yoneyama M, Fujita T, Lemon SM, et al. Regulating intracellular antiviral defense and permissiveness to hepatitis C virus RNA replication through a cellular RNA helicase, RIG-I. J Virol 2005;79:2689-2699.

108. Brass A, Brenndorfer ED. The role of chemokines in hepatitis C virus-mediated liver disease. Int J Mol Sci 2014;15:4747-4779.
109. Meylan E, Curran J, Hofmann K, Moradpour D, Binder M, Bartenschlager R, Tschopp J. Cardif is an adaptor protein in the RIG-I antiviral pathway and is targeted by hepatitis C virus. Nature 2005;437:1167-1172.
110. Seki E, Brenner DA. Toll-like receptors and adaptor molecules in liver disease: update. Hepatology 2008;48:322-335.
111. Li K, Li NL, Wei D, Pfeffer SR, Fan M, Pfeffer LM. Activation of chemokine and inflammatory cytokine response in hepatitis C virus-infected hepatocytes depends on Toll-like receptor 3 sensing of hepatitis C virus double-stranded RNA intermediates. Hepatology 2012;55:666-675.
112. Li K, Foy E, Ferreon JC, Nakamura M, Ferreon AC, Ikeda M, Ray SC, et al. Immune evasion by hepatitis C virus NS3/4A protease-mediated cleavage of the Toll-like receptor 3 adaptor protein TRIF. Proc Natl Acad Sci U S A 2005;102:2992-2997.
113. Lucas M, Ulsenheimer A, Pfafferot K, Heeg MH, Gaudieri S, Gruner N, Rauch A, et al. Tracking virus-specific CD4+ T cells during and after acute hepatitis C virus infection. PLoS One 2007;2:e649.
114. Erickson AL, Kimura Y, Igarashi S, Eichelberger J, Houghton M, Sidney J, McKinney D, et al. The outcome of hepatitis C virus infection is predicted by escape mutations in epitopes targeted by cytotoxic T lymphocytes. Immunity 2001;15:883-895.
115. Seshacharyulu P, Ponnusamy MP, Haridas D, Jain M, Ganti AK, Batra SK. Targeting the EGFR signaling pathway in cancer therapy. Expert Opin Ther Targets 2012;16:15-31.
116. Purba ER, Saita EI, Maruyama IN. Activation of the EGF Receptor by Ligand Binding and Oncogenic Mutations: The "Rotation Model". Cells 2017;6.
117. Hynes NE, MacDonald G. ErbB receptors and signaling pathways in cancer. Curr Opin Cell Biol 2009;21:177-184.
118. Schlessinger J. Receptor tyrosine kinases: legacy of the first two decades. Cold Spring Harb Perspect Biol 2014;6.
119. Karunagaran D, Tzahar E, Beerli RR, Chen X, Graus-Porta D, Ratzkin BJ, Seger R, et al. ErbB-2 is a common auxiliary subunit of NDF and EGF receptors: implications for breast cancer. EMBO J 1996;15:254-264.
120. Fuller SJ, Sivarajah K, Sugden PH. ErbB receptors, their ligands, and the consequences of their activation and inhibition in the myocardium. J Mol Cell Cardiol 2008;44:831-854.
121. Shi F, Telesco SE, Liu Y, Radhakrishnan R, Lemmon MA. ErbB3/HER3 intracellular domain is competent to bind ATP and catalyze autophosphorylation. Proc Natl Acad Sci U S A 2010;107:7692-7697.
122. Citri A, Yarden Y. EGF-ERBB signalling: towards the systems level. Nat Rev Mol Cell Biol 2006;7:505-516.
123. Varadi T, Schneider M, Sevcsik E, Kiesenhofer D, Baumgart F, Batta G, Kovacs T, et al. Homo- and Heteroassociations Drive Activation of ErbB3. Biophys J 2019;117:1935-1947.
124. Steinkamp MP, Low-Nam ST, Yang S, Lidke KA, Lidke DS, Wilson BS. erbB3 is an active tyrosine kinase capable of homo- and heterointeractions. Mol Cell Biol 2014;34:965-977.
125. Tanaka T, Zhou Y, Ozawa T, Okizono R, Banba A, Yamamura T, Oga E, et al. Ligand-activated epidermal growth factor receptor (EGFR) signaling governs endocytic trafficking of unliganded receptor monomers by non-canonical phosphorylation. J Biol Chem 2018;293:2288-2301.

126. Yarden Y, Schlessinger J. Epidermal growth factor induces rapid, reversible aggregation of the purified epidermal growth factor receptor. Biochemistry 1987;26:1443-1451.
127. Lowenstein EJ, Daly RJ, Batzer AG, Li W, Margolis B, Lammers R, Ullrich A, et al. The SH2 and SH3 domain-containing protein GRB2 links receptor tyrosine kinases to ras signaling. Cell 1992;70:431-442.
128. Batzer AG, Rotin D, Urena JM, Skolnik EY, Schlessinger J. Hierarchy of binding sites for Grb2 and Shc on the epidermal growth factor receptor. Mol Cell Biol 1994;14:5192-5201.
129. Owens DM, Keyse SM. Differential regulation of MAP kinase signalling by dual-specificity protein phosphatases. Oncogene 2007;26:3203-3213.
130. Cargnello M, Roux PP. Activation and function of the MAPKs and their substrates, the MAPK-activated protein kinases. Microbiol Mol Biol Rev 2011;75:50-83.
131. Peti W, Page R. Molecular basis of MAP kinase regulation. Protein Sci 2013;22:1698-1710.
132. Kondoh K, Nishida E. Regulation of MAP kinases by MAP kinase phosphatases. Biochim Biophys Acta 2007;1773:1227-1237.
133. Hill CS, Treisman R. Transcriptional regulation by extracellular signals: mechanisms and specificity. Cell 1995;80:199-211.
134. Liebmann C. Regulation of MAP kinase activity by peptide receptor signalling pathway: paradigms of multiplicity. Cell Signal 2001;13:777-785.
135. Benasciutti E, Pages G, Kenzior O, Folk W, Blasi F, Crippa MP. MAPK and JNK transduction pathways can phosphorylate Sp1 to activate the uPA minimal promoter element and endogenous gene transcription. Blood 2004;104:256-262.
136. Cuevas BD, Lu Y, Mao M, Zhang J, LaPushin R, Siminovitch K, Mills GB. Tyrosine phosphorylation of p85 relieves its inhibitory activity on phosphatidylinositol 3-kinase. J Biol Chem 2001;276:27455-27461.
137. Mattoon DR, Lamothe B, Lax I, Schlessinger J. The docking protein Gab1 is the primary mediator of EGF-stimulated activation of the PI-3K/Akt cell survival pathway. BMC Biol 2004;2:24.
138. Bellacosa A, Chan TO, Ahmed NN, Datta K, Malstrom S, Stokoe D, McCormick F, et al. Akt activation by growth factors is a multiple-step process: the role of the PH domain. Oncogene 1998;17:313-325.
139. Alessi DR, James SR, Downes CP, Holmes AB, Gaffney PR, Reese CB, Cohen P. Characterization of a 3-phosphoinositide-dependent protein kinase which phosphorylates and activates protein kinase Balpha. Curr Biol 1997;7:261-269.
140. Toker A, Newton AC. Akt/protein kinase B is regulated by autophosphorylation at the hypothetical PDK-2 site. J Biol Chem 2000;275:8271-8274.
141. Zhang X, Jin B, Huang C. The PI3K/Akt pathway and its downstream transcriptional factors as targets for chemoprevention. Curr Cancer Drug Targets 2007;7:305-316.
142. Aggarwal BB. Nuclear factor-kappaB: the enemy within. Cancer Cell 2004;6:203-208.
143. Hisatsune J, Nakayama M, Isomoto H, Kurazono H, Mukaida N, Mukhopadhyay AK, Azuma T, et al. Molecular characterization of Helicobacter pylori VacA induction of IL-8 in U937 cells reveals a prominent role for p38MAPK in activating transcription factor-2, cAMP response element binding protein, and NF-kappaB activation. J Immunol 2008;180:5017-5027.
144. Richmond A. Nf-kappa B, chemokine gene transcription and tumour growth. Nat Rev Immunol 2002;2:664-674.

145. Chen P, Xie H, Sekar MC, Gupta K, Wells A. Epidermal growth factor receptor-mediated cell motility: phospholipase C activity is required, but mitogen-activated protein kinase activity is not sufficient for induced cell movement. J Cell Biol 1994;127:847-857.
146. Scaltriti M, Baselga J. The epidermal growth factor receptor pathway: a model for targeted therapy. Clin Cancer Res 2006;12:5268-5272.
147. Diao J, Pantua H, Ngu H, Komuves L, Diehl L, Schaefer G, Kapadia SB. Hepatitis C virus induces epidermal growth factor receptor activation via CD81 binding for viral internalization and entry. J Virol 2012;86:10935-10949.
148. Tiganis T, Bennett AM, Ravichandran KS, Tonks NK. Epidermal growth factor receptor and the adaptor protein p52Shc are specific substrates of T-cell protein tyrosine phosphatase. Mol Cell Biol 1998;18:1622-1634.
149. Staal SP. Molecular cloning of the akt oncogene and its human homologues AKT1 and AKT2: amplification of AKT1 in a primary human gastric adenocarcinoma. Proc Natl Acad Sci U S A 1987;84:5034-5037.
150. Stindt S, Cebula P, Albrecht U, Keitel V, Schulte am Esch J, Knoefel WT, Bartenschlager R, et al. Hepatitis C Virus Activates a Neuregulin-Driven Circuit to Modify Surface Expression of Growth Factor Receptors of the ErbB Family. PLoS One 2016;11:e0148711.
151. Frank S, Hubner G, Breier G, Longaker MT, Greenhalgh DG, Werner S. Regulation of vascular endothelial growth factor expression in cultured keratinocytes. Implications for normal and impaired wound healing. J Biol Chem 1995;270:12607-12613.
152. Leung DW, Cachianes G, Kuang WJ, Goeddel DV, Ferrara N. Vascular endothelial growth factor is a secreted angiogenic mitogen. Science 1989;246:1306-1309.
153. Mee CJ, Farquhar MJ, Harris HJ, Hu K, Ramma W, Ahmed A, Maurel P, et al. Hepatitis C virus infection reduces hepatocellular polarity in a vascular endothelial growth factor-dependent manner. Gastroenterology 2010;138:1134-1142.
154. Salum GM, Bader El Din NG, Ibrahim MK, Anany MA, Dawood RM, Khairy A, El Awady MK. Vascular Endothelial Growth Factor Expression in Hepatitis C Virus-Induced Liver Fibrosis: A Potential Biomarker. J Interferon Cytokine Res 2017;37:310-316.
155. Zhang JM, An J. Cytokines, inflammation, and pain. Int Anesthesiol Clin 2007;45:27-37.
156. Kany S, Vollrath JT, Relja B. Cytokines in Inflammatory Disease. Int J Mol Sci 2019;20.
157. Dinarello CA. Historical insights into cytokines. Eur J Immunol 2007;37 Suppl 1:S34-45.
158. Cytokines in the balance. Nat Immunol 2019;20:1557.
159. Sillanpaa M, Kaukinen P, Melen K, Julkunen I. Hepatitis C virus proteins interfere with the activation of chemokine gene promoters and downregulate chemokine gene expression. J Gen Virol 2008;89:432-443.
160. Dinarello CA. Proinflammatory cytokines. Chest 2000;118:503-508.
161. Weber A, Wasiliew P, Kracht M. Interleukin-1 (IL-1) pathway. Sci Signal 2010;3:cm1.
162. Dinarello CA, Ikejima T, Warner SJ, Orencole SF, Lonnemann G, Cannon JG, Libby P. Interleukin 1 induces interleukin 1. I. Induction of circulating interleukin 1 in rabbits in vivo and in human mononuclear cells in vitro. J Immunol 1987;139:1902-1910.

163. Werman A, Werman-Venkert R, White R, Lee JK, Werman B, Krelin Y, Voronov E, et al. The precursor form of IL-1alpha is an intracrine proinflammatory activator of transcription. Proc Natl Acad Sci U S A 2004;101:2434-2439.
164. Dinarello CA. Overview of the IL-1 family in innate inflammation and acquired immunity. Immunol Rev 2018;281:8-27.
165. Franchi L, Munoz-Planillo R, Nunez G. Sensing and reacting to microbes through the inflammasomes. Nat Immunol 2012;13:325-332.
166. Franchi L, Eigenbrod T, Munoz-Planillo R, Nunez G. The inflammasome: a caspase-1-activation platform that regulates immune responses and disease pathogenesis. Nat Immunol 2009;10:241-247.
167. Poeck H, Bscheider M, Gross O, Finger K, Roth S, Rebsamen M, Hannesschlager N, et al. Recognition of RNA virus by RIG-I results in activation of CARD9 and inflammasome signaling for interleukin 1 beta production. Nat Immunol 2010;11:63-69.
168. Shrivastava S, Mukherjee A, Ray R, Ray RB. Hepatitis C virus induces interleukin-1beta (IL-1beta)/IL-18 in circulatory and resident liver macrophages. J Virol 2013;87:12284-12290.
169. Dinarello CA, Renfer L, Wolff SM. Human leukocytic pyrogen: purification and development of a radioimmunoassay. Proc Natl Acad Sci U S A 1977;74:4624-4627.
170. Auron PE, Webb AC, Rosenwasser LJ, Mucci SF, Rich A, Wolff SM, Dinarello CA. Nucleotide sequence of human monocyte interleukin 1 precursor cDNA. Proc Natl Acad Sci U S A 1984;81:7907-7911.
171. Greenfeder SA, Nunes P, Kwee L, Labow M, Chizzonite RA, Ju G. Molecular cloning and characterization of a second subunit of the interleukin 1 receptor complex. J Biol Chem 1995;270:13757-13765.
172. Brikos C, Wait R, Begum S, O'Neill LA, Saklatvala J. Mass spectrometric analysis of the endogenous type I interleukin-1 (IL-1) receptor signaling complex formed after IL-1 binding identifies IL-1RAcP, MyD88, and IRAK-4 as the stable components. Mol Cell Proteomics 2007;6:1551-1559.
173. Cao Z, Henzel WJ, Gao X. IRAK: a kinase associated with the interleukin-1 receptor. Science 1996;271:1128-1131.
174. Takaesu G, Ninomiya-Tsuji J, Kishida S, Li X, Stark GR, Matsumoto K. Interleukin-1 (IL-1) receptor-associated kinase leads to activation of TAK1 by inducing TAB2 translocation in the IL-1 signaling pathway. Mol Cell Biol 2001;21:2475-2484.
175. Deng L, Wang C, Spencer E, Yang L, Braun A, You J, Slaughter C, et al. Activation of the IkappaB kinase complex by TRAF6 requires a dimeric ubiquitin-conjugating enzyme complex and a unique polyubiquitin chain. Cell 2000;103:351-361.
176. Newton K, Matsumoto ML, Wertz IE, Kirkpatrick DS, Lill JR, Tan J, Dugger D, et al. Ubiquitin chain editing revealed by polyubiquitin linkage-specific antibodies. Cell 2008;134:668-678.
177. Kanayama A, Seth RB, Sun L, Ea CK, Hong M, Shaito A, Chiu YH, et al. TAB2 and TAB3 activate the NF-kappaB pathway through binding to polyubiquitin chains. Mol Cell 2004;15:535-548.
178. Ninomiya-Tsuji J, Kishimoto K, Hiyama A, Inoue J, Cao Z, Matsumoto K. The kinase TAK1 can activate the NIK-I kappaB as well as the MAP kinase cascade in the IL-1 signalling pathway. Nature 1999;398:252-256.
179. Malinin NL, Boldin MP, Kovalenko AV, Wallach D. MAP3K-related kinase involved in NF-kappaB induction by TNF, CD95 and IL-1. Nature 1997;385:540-544.
180. Huang Q, Yang J, Lin Y, Walker C, Cheng J, Liu ZG, Su B. Differential regulation of interleukin 1 receptor and Toll-like receptor signaling by MEKK3. Nat Immunol 2004;5:98-103.

181. Baud V, Liu ZG, Bennett B, Suzuki N, Xia Y, Karin M. Signaling by proinflammatory cytokines: oligomerization of TRAF2 and TRAF6 is sufficient for JNK and IKK activation and target gene induction via an amino-terminal effector domain. Genes Dev 1999;13:1297-1308.
182. Raingeaud J, Gupta S, Rogers JS, Dickens M, Han J, Ulevitch RJ, Davis RJ. Pro-inflammatory cytokines and environmental stress cause p38 mitogen-activated protein kinase activation by dual phosphorylation on tyrosine and threonine. J Biol Chem 1995;270:7420-7426.
183. Cirillo G, Casalino L, Vallone D, Caracciolo A, De Cesare D, Verde P. Role of distinct mitogen-activated protein kinase pathways and cooperation between Ets-2, ATF-2, and Jun family members in human urokinase-type plasminogen activator gene induction by interleukin-1 and tetradecanoyl phorbol acetate. Mol Cell Biol 1999;19:6240-6252.
184. Liu T, Zhang L, Joo D, Sun SC. NF-kappaB signaling in inflammation. Signal Transduct Target Ther 2017;2.
185. Hiscott J, Kwon H, Genin P. Hostile takeovers: viral appropriation of the NF-kappaB pathway. J Clin Invest 2001;107:143-151.
186. DiDonato JA, Hayakawa M, Rothwarf DM, Zandi E, Karin M. A cytokine-responsive IkappaB kinase that activates the transcription factor NF-kappaB. Nature 1997;388:548-554.
187. Mercurio F, Zhu H, Murray BW, Shevchenko A, Bennett BL, Li J, Young DB, et al. IKK-1 and IKK-2: cytokine-activated IkappaB kinases essential for NF-kappaB activation. Science 1997;278:860-866.
188. Hoffmann E, Dittrich-Breiholz O, Holtmann H, Kracht M. Multiple control of interleukin-8 gene expression. J Leukoc Biol 2002;72:847-855.
189. Amiri KI, Richmond A. Fine tuning the transcriptional regulation of the CXCL1 chemokine. Prog Nucleic Acid Res Mol Biol 2003;74:1-36.
190. Burke SJ, Lu D, Sparer TE, Masi T, Goff MR, Karlstad MD, Collier JJ. NF-kappaB and STAT1 control CXCL1 and CXCL2 gene transcription. Am J Physiol Endocrinol Metab 2014;306:E131-149.
191. Anisowicz A, Messineo M, Lee SW, Sager R. An NF-kappa B-like transcription factor mediates IL-1/TNF-alpha induction of gro in human fibroblasts. J Immunol 1991;147:520-527.
192. Wolter S, Doerrie A, Weber A, Schneider H, Hoffmann E, von der Ohe J, Bakiri L, et al. c-Jun controls histone modifications, NF-kappaB recruitment, and RNA polymerase II function to activate the ccl2 gene. Mol Cell Biol 2008;28:4407-4423.
193. Haack KK, Mitra AK, Zucker IH. NF-kappaB and CREB are required for angiotensin II type 1 receptor upregulation in neurons. PLoS One 2013;8:e78695.
194. Xia C, Cheshire JK, Patel H, Woo P. Cross-talk between transcription factors NF-kappa B and C/EBP in the transcriptional regulation of genes. Int J Biochem Cell Biol 1997;29:1525-1539.
195. Perkins ND, Edwards NL, Duckett CS, Agranoff AB, Schmid RM, Nabel GJ. A cooperative interaction between NF-kappa B and Sp1 is required for HIV-1 enhancer activation. EMBO J 1993;12:3551-3558.
196. Lee CH, Syu SH, Liu KJ, Chu PY, Yang WC, Lin P, Shieh WY. Interleukin-1 beta transactivates epidermal growth factor receptor via the CXCL1-CXCR2 axis in oral cancer. Oncotarget 2015;6:38866-38880.
197. Stienstra R, Tack CJ, Kanneganti TD, Joosten LA, Netea MG. The inflammasome puts obesity in the danger zone. Cell Metab 2012;15:10-18.

198. Lapinski TW. The levels of IL-1beta, IL-4 and IL-6 in the serum and the liver tissue of chronic HCV-infected patients. Arch Immunol Ther Exp (Warsz) 2001;49:311-316.
199. Antonelli A, Ferri C, Ferrari SM, Ghiri E, Goglia F, Pampana A, Bruschi F, et al. Serum levels of proinflammatory cytokines interleukin-1beta, interleukin-6, and tumor necrosis factor alpha in mixed cryoglobulinemia. Arthritis Rheum 2009;60:3841-3847.
200. Sobchak DM, Korochkina OV. [Immune system reactivity in patients with chronic hepatitis c]. Ter Arkh 2008;80:61-66.
201. Baranova A, Jarrar MH, Stepanova M, Johnson A, Rafiq N, Gramlich T, Chandhoke V, et al. Association of serum adipocytokines with hepatic steatosis and fibrosis in patients with chronic hepatitis C. Digestion 2011;83:32-40.
202. Okamoto K, Ishida C, Ikebuchi Y, Mandai M, Mimura K, Murawaki Y, Yuasa I. The genotypes of IL-1 beta and MMP-3 are associated with the prognosis of HCV-related hepatocellular carcinoma. Intern Med 2010;49:887-895.
203. Tanaka Y, Furuta T, Suzuki S, Orito E, Yeo AE, Hirashima N, Sugauchi F, et al. Impact of interleukin-1beta genetic polymorphisms on the development of hepatitis C virus-related hepatocellular carcinoma in Japan. J Infect Dis 2003;187:1822-1825.
204. Minton EJ, Smillie D, Smith P, Shipley S, McKendrick MW, Gleeson DC, Underwood JC, et al. Clearance of hepatitis C virus is not associated with single nucleotide polymorphisms in the IL-1, -6, or -10 genes. Hum Immunol 2005;66:127-132.
205. Tai DI, Tsai SL, Chen YM, Chuang YL, Peng CY, Sheen IS, Yeh CT, et al. Activation of nuclear factor kappaB in hepatitis C virus infection: implications for pathogenesis and hepatocarcinogenesis. Hepatology 2000;31:656-664.
206. Rayet B, Gelinas C. Aberrant rel/nfkb genes and activity in human cancer. Oncogene 1999;18:6938-6947.
207. Altomare DA, Testa JR. Perturbations of the AKT signaling pathway in human cancer. Oncogene 2005;24:7455-7464.
208. Negash AA, Ramos HJ, Crochet N, Lau DT, Doehle B, Papic N, Delker DA, et al. IL-1beta production through the NLRP3 inflammasome by hepatic macrophages links hepatitis C virus infection with liver inflammation and disease. PLoS Pathog 2013;9:e1003330.
209. Burdette D, Haskett A, Presser L, McRae S, Iqbal J, Waris G. Hepatitis C virus activates interleukin-1beta via caspase-1-inflammasome complex. J Gen Virol 2012;93:235-246.
210. Carswell EA, Old LJ, Kassel RL, Green S, Fiore N, Williamson B. An endotoxin-induced serum factor that causes necrosis of tumors. Proc Natl Acad Sci U S A 1975;72:3666-3670.
211. Zelova H, Hosek J. TNF-alpha signalling and inflammation: interactions between old acquaintances. Inflamm Res 2013;62:641-651.
212. Qu Y, Zhao G, Li H. Forward and Reverse Signaling Mediated by Transmembrane Tumor Necrosis Factor-Alpha and TNF Receptor 2: Potential Roles in an Immunosuppressive Tumor Microenvironment. Front Immunol 2017;8:1675.
213. Tartaglia LA, Ayres TM, Wong GH, Goeddel DV. A novel domain within the 55 kd TNF receptor signals cell death. Cell 1993;74:845-853.
214. Schulze-Osthoff K, Ferrari D, Los M, Wesselborg S, Peter ME. Apoptosis signaling by death receptors. Eur J Biochem 1998;254:439-459.
215. Wajant H, Scheurich P. TNFR1-induced activation of the classical NF-kappaB pathway. FEBS J 2011;278:862-876.

216. Devin A, Lin Y, Yamaoka S, Li Z, Karin M, Liu Z. The alpha and beta subunits of IkappaB kinase (IKK) mediate TRAF2-dependent IKK recruitment to tumor necrosis factor (TNF) receptor 1 in response to TNF. Mol Cell Biol 2001;21:3986-3994.
217. Fullsack S, Rosenthal A, Wajant H, Siegmund D. Redundant and receptor-specific activities of TRADD, RIPK1 and FADD in death receptor signaling. Cell Death Dis 2019;10:122.
218. Wajant H, Siegmund D. TNFR1 and TNFR2 in the Control of the Life and Death Balance of Macrophages. Front Cell Dev Biol 2019;7:91.
219. Fan Y, Yu Y, Shi Y, Sun W, Xie M, Ge N, Mao R, et al. Lysine 63-linked polyubiquitination of TAK1 at lysine 158 is required for tumor necrosis factor alpha- and interleukin-1beta-induced IKK/NF-kappaB and JNK/AP-1 activation. J Biol Chem 2010;285:5347-5360.
220. Yoo J, Rodriguez Perez CE, Nie W, Edwards RA, Sinnett-Smith J, Rozengurt E. TNF-alpha induces upregulation of EGFR expression and signaling in human colonic myofibroblasts. Am J Physiol Gastrointest Liver Physiol 2012;302:G805-814.
221. Ramaswamy P, Goswami K, Dalavaikodihalli Nanjaiah N, Srinivas D, Prasad C. TNF-alpha mediated MEK-ERK signaling in invasion with putative network involving NF-kappaB and STAT-6: a new perspective in glioma. Cell Biol Int 2019;43:1257-1266.
222. Baud V, Karin M. Signal transduction by tumor necrosis factor and its relatives. Trends Cell Biol 2001;11:372-377.
223. Reinhard C, Shamoon B, Shyamala V, Williams LT. Tumor necrosis factor alpha-induced activation of c-jun N-terminal kinase is mediated by TRAF2. EMBO J 1997;16:1080-1092.
224. Liu ZG, Hsu H, Goeddel DV, Karin M. Dissection of TNF receptor 1 effector functions: JNK activation is not linked to apoptosis while NF-kappaB activation prevents cell death. Cell 1996;87:565-576.
225. Madrid LV, Mayo MW, Reuther JY, Baldwin AS, Jr. Akt stimulates the transactivation potential of the RelA/p65 Subunit of NF-kappa B through utilization of the Ikappa B kinase and activation of the mitogen-activated protein kinase p38. J Biol Chem 2001;276:18934-18940.
226. Lee J, Tian Y, Chan ST, Kim JY, Cho C, Ou JH. TNF-alpha Induced by Hepatitis C Virus via TLR7 and TLR8 in Hepatocytes Supports Interferon Signaling via an Autocrine Mechanism. PLoS Pathog 2015;11:e1004937.
227. Menezes EG, Coelho-Dos-Reis JG, Cardoso LM, Lopes-Ribeiro A, Jonathan-Goncalves J, Porto Goncalves MT, Cambraia RD, et al. Strategies for serum chemokine/cytokine assessment as biomarkers of therapeutic response in HCV patients as a prototype to monitor immunotherapy of infectious diseases. Antiviral Res 2017;141:19-28.
228. Sypniewski D, Jurzak M, Cholewa K, Gola J, Mazurek U, Wilczok T, Rozek-Kostorkiewicz J, et al. Changes in TNF-alpha mRNA levels in the peripheral blood of patients with chronic hepatitis C virus (HCV) infection during alpha-interferon and ribavirin therapy. Viral Immunol 2004;17:580-587.
229. Larrea E, Garcia N, Qian C, Civeira MP, Prieto J. Tumor necrosis factor alpha gene expression and the response to interferon in chronic hepatitis C. Hepatology 1996;23:210-217.
230. Brenndorfer ED, Weiland M, Frelin L, Derk E, Ahlen G, Jiao J, Bode JG, et al. Anti-tumor necrosis factor alpha treatment promotes apoptosis and prevents liver regeneration in a transgenic mouse model of chronic hepatitis C. Hepatology 2010;52:1553-1563.
231. Frelin L, Brenndorfer ED, Ahlen G, Weiland M, Hultgren C, Alheim M, Glaumann H, et al. The hepatitis C virus and immune evasion: non-structural 3/4A transgenic mice

are resistant to lethal tumour necrosis factor alpha mediated liver disease. Gut 2006;55:1475-1483.
232. Brenndorfer ED, Brass A, Karthe J, Ahlen G, Bode JG, Sallberg M. Cleavage of the T cell protein tyrosine phosphatase by the hepatitis C virus nonstructural 3/4A protease induces a Th1 to Th2 shift reversible by ribavirin therapy. J Immunol 2014;192:1671-1680.
233. Miyasaka Y, Enomoto N, Kurosaki M, Sakamoto N, Kanazawa N, Kohashi T, Ueda E, et al. Hepatitis C virus nonstructural protein 5A inhibits tumor necrosis factor-alpha-mediated apoptosis in Huh7 cells. J Infect Dis 2003;188:1537-1544.
234. You LR, Chen CM, Lee YH. Hepatitis C virus core protein enhances NF-kappaB signal pathway triggering by lymphotoxin-beta receptor ligand and tumor necrosis factor alpha. J Virol 1999;73:1672-1681.
235. Chen Y, He L, Peng Y, Shi X, Chen J, Zhong J, Chen X, et al. The hepatitis C virus protein NS3 suppresses TNF-alpha-stimulated activation of NF-kappaB by targeting LUBAC. Sci Signal 2015;8:ra118.
236. Moser B, Willimann K. Chemokines: role in inflammation and immune surveillance. Ann Rheum Dis 2004;63 Suppl 2:ii84-ii89.
237. Hughes CE, Nibbs RJB. A guide to chemokines and their receptors. FEBS J 2018;285:2944-2971.
238. Zhu Y, Murakami F. Chemokine CXCL12 and its receptors in the developing central nervous system: emerging themes and future perspectives. Dev Neurobiol 2012;72:1349-1362.
239. Flad HD, Brandt E. Platelet-derived chemokines: pathophysiology and therapeutic aspects. Cell Mol Life Sci 2010;67:2363-2386.
240. Zhang M, Zhu ZL, Gao XL, Wu JS, Liang XH, Tang YL. Functions of chemokines in the perineural invasion of tumors (Review). Int J Oncol 2018;52:1369-1379.
241. Miller MC, Mayo KH. Chemokines from a Structural Perspective. Int J Mol Sci 2017;18.
242. Moussouras NA, Getschman AE, Lackner ER, Veldkamp CT, Dwinell MB, Volkman BF. Differences in Sulfotyrosine Binding amongst CXCR1 and CXCR2 Chemokine Ligands. Int J Mol Sci 2017;18.
243. Murphy PM, Baggiolini M, Charo IF, Hebert CA, Horuk R, Matsushima K, Miller LH, et al. International union of pharmacology. XXII. Nomenclature for chemokine receptors. Pharmacol Rev 2000;52:145-176.
244. Lodowski DT, Palczewski K. Chemokine receptors and other G protein-coupled receptors. Curr Opin HIV AIDS 2009;4:88-95.
245. Strieter RM, Polverini PJ, Kunkel SL, Arenberg DA, Burdick MD, Kasper J, Dzuiba J, et al. The functional role of the ELR motif in CXC chemokine-mediated angiogenesis. J Biol Chem 1995;270:27348-27357.
246. Sarmiento J, Shumate C, Suetomi K, Ravindran A, Villegas L, Rajarathnam K, Navarro J. Diverging mechanisms of activation of chemokine receptors revealed by novel chemokine agonists. PLoS One 2011;6:e27967.
247. Cheng Y, Ma XL, Wei YQ, Wei XW. Potential roles and targeted therapy of the CXCLs/CXCR2 axis in cancer and inflammatory diseases. Biochim Biophys Acta Rev Cancer 2019;1871:289-312.
248. Saiman Y, Friedman SL. The role of chemokines in acute liver injury. Front Physiol 2012;3:213.
249. Gerritsma JS, van Kooten C, Gerritsen AF, van Es LA, Daha MR. Transforming growth factor-beta 1 regulates chemokine and complement production by human proximal tubular epithelial cells. Kidney Int 1998;53:609-616.

250. Harvey CE, Post JJ, Palladinetti P, Freeman AJ, Ffrench RA, Kumar RK, Marinos G, et al. Expression of the chemokine IP-10 (CXCL10) by hepatocytes in chronic hepatitis C virus infection correlates with histological severity and lobular inflammation. J Leukoc Biol 2003;74:360-369.
251. Steib CJ, Bilzer M, Hartl JM, Beitinger F, Gulberg V, Goke B, Gerbes AL. Kupffer cell activation by hydrogen peroxide: a new mechanism of portal pressure increase. Shock 2010;33:412-418.
252. Karlmark KR, Wasmuth HE, Trautwein C, Tacke F. Chemokine-directed immune cell infiltration in acute and chronic liver disease. Expert Rev Gastroenterol Hepatol 2008;2:233-242.
253. Chen YX, Sato M, Kawachi K, Abe Y. Neutrophil-mediated liver injury during hepatic ischemia-reperfusion in rats. Hepatobiliary Pancreat Dis Int 2006;5:436-442.
254. Kobayashi Y. The role of chemokines in neutrophil biology. Front Biosci 2008;13:2400-2407.
255. Yoshimura T, Matsushima K, Tanaka S, Robinson EA, Appella E, Oppenheim JJ, Leonard EJ. Purification of a human monocyte-derived neutrophil chemotactic factor that has peptide sequence similarity to other host defense cytokines. Proc Natl Acad Sci U S A 1987;84:9233-9237.
256. Brat DJ, Bellail AC, Van Meir EG. The role of interleukin-8 and its receptors in gliomagenesis and tumoral angiogenesis. Neuro Oncol 2005;7:122-133.
257. Ha H, Debnath B, Neamati N. Role of the CXCL8-CXCR1/2 Axis in Cancer and Inflammatory Diseases. Theranostics 2017;7:1543-1588.
258. Haskill S, Peace A, Morris J, Sporn SA, Anisowicz A, Lee SW, Smith T, et al. Identification of three related human GRO genes encoding cytokine functions. Proc Natl Acad Sci U S A 1990;87:7732-7736.
259. De Filippo K, Dudeck A, Hasenberg M, Nye E, van Rooijen N, Hartmann K, Gunzer M, et al. Mast cell and macrophage chemokines CXCL1/CXCL2 control the early stage of neutrophil recruitment during tissue inflammation. Blood 2013;121:4930-4937.
260. Jin L, Batra S, Douda DN, Palaniyar N, Jeyaseelan S. CXCL1 contributes to host defense in polymicrobial sepsis via modulating T cell and neutrophil functions. J Immunol 2014;193:3549-3558.
261. Sawant KV, Poluri KM, Dutta AK, Sepuru KM, Troshkina A, Garofalo RP, Rajarathnam K. Chemokine CXCL1 mediated neutrophil recruitment: Role of glycosaminoglycan interactions. Sci Rep 2016;6:33123.
262. Sepuru KM, Rajarathnam K. CXCL1/MGSA Is a Novel Glycosaminoglycan (GAG)-binding Chemokine: STRUCTURAL EVIDENCE FOR TWO DISTINCT NON-OVERLAPPING BINDING DOMAINS. J Biol Chem 2016;291:4247-4255.
263. Ahuja SK, Murphy PM. The CXC chemokines growth-regulated oncogene (GRO) alpha, GRObeta, GROgamma, neutrophil-activating peptide-2, and epithelial cell-derived neutrophil-activating peptide-78 are potent agonists for the type B, but not the type A, human interleukin-8 receptor. J Biol Chem 1996;271:20545-20550.
264. Fantuzzi L, Belardelli F, Gessani S. Monocyte/macrophage-derived CC chemokines and their modulation by HIV-1 and cytokines: a complex network of interactions influencing viral replication and AIDS pathogenesis. J Leukoc Biol 2003;74:719-725.
265. Charo IF, Myers SJ, Herman A, Franci C, Connolly AJ, Coughlin SR. Molecular cloning and functional expression of two monocyte chemoattractant protein 1 receptors reveals alternative splicing of the carboxyl-terminal tails. Proc Natl Acad Sci U S A 1994;91:2752-2756.

266. Yamagami S, Tokuda Y, Ishii K, Tanaka H, Endo N. cDNA cloning and functional expression of a human monocyte chemoattractant protein 1 receptor. Biochem Biophys Res Commun 1994;202:1156-1162.
267. Tan JH, Ludeman JP, Wedderburn J, Canals M, Hall P, Butler SJ, Taleski D, et al. Tyrosine sulfation of chemokine receptor CCR2 enhances interactions with both monomeric and dimeric forms of the chemokine monocyte chemoattractant protein-1 (MCP-1). J Biol Chem 2013;288:10024-10034.
268. Jiang Y, Beller DI, Frendl G, Graves DT. Monocyte chemoattractant protein-1 regulates adhesion molecule expression and cytokine production in human monocytes. J Immunol 1992;148:2423-2428.
269. Obstfeld AE, Sugaru E, Thearle M, Francisco AM, Gayet C, Ginsberg HN, Ables EV, et al. C-C chemokine receptor 2 (CCR2) regulates the hepatic recruitment of myeloid cells that promote obesity-induced hepatic steatosis. Diabetes 2010;59:916-925.
270. Mandrekar P, Ambade A, Lim A, Szabo G, Catalano D. An essential role for monocyte chemoattractant protein-1 in alcoholic liver injury: regulation of proinflammatory cytokines and hepatic steatosis in mice. Hepatology 2011;54:2185-2197.
271. Karlmark KR, Weiskirchen R, Zimmermann HW, Gassler N, Ginhoux F, Weber C, Merad M, et al. Hepatic recruitment of the inflammatory Gr1+ monocyte subset upon liver injury promotes hepatic fibrosis. Hepatology 2009;50:261-274.
272. Deshmane SL, Kremlev S, Amini S, Sawaya BE. Monocyte chemoattractant protein-1 (MCP-1): an overview. J Interferon Cytokine Res 2009;29:313-326.
273. Marra F, Tacke F. Roles for chemokines in liver disease. Gastroenterology 2014;147:577-594 e571.
274. Fahey S, Dempsey E, Long A. The role of chemokines in acute and chronic hepatitis C infection. Cell Mol Immunol 2014;11:25-40.
275. Kadoya H, Nagano-Fujii M, Deng L, Nakazono N, Hotta H. Nonstructural proteins 4A and 4B of hepatitis C virus transactivate the interleukin 8 promoter. Microbiol Immunol 2005;49:265-273.
276. Gale MJ, Jr., Korth MJ, Tang NM, Tan SL, Hopkins DA, Dever TE, Polyak SJ, et al. Evidence that hepatitis C virus resistance to interferon is mediated through repression of the PKR protein kinase by the nonstructural 5A protein. Virology 1997;230:217-227.
277. Taylor DR, Shi ST, Romano PR, Barber GN, Lai MM. Inhibition of the interferon-inducible protein kinase PKR by HCV E2 protein. Science 1999;285:107-110.
278. Polyak SJ, Khabar KS, Paschal DM, Ezelle HJ, Duverlie G, Barber GN, Levy DE, et al. Hepatitis C virus nonstructural 5A protein induces interleukin-8, leading to partial inhibition of the interferon-induced antiviral response. J Virol 2001;75:6095-6106.
279. Polyak SJ, Khabar KS, Rezeiq M, Gretch DR. Elevated levels of interleukin-8 in serum are associated with hepatitis C virus infection and resistance to interferon therapy. J Virol 2001;75:6209-6211.
280. Oem JK, Jackel-Cram C, Li YP, Kang HN, Zhou Y, Babiuk LA, Liu Q. Hepatitis C virus non-structural protein-2 activates CXCL-8 transcription through NF-kappaB. Arch Virol 2008;153:293-301.
281. Koo BC, McPoland P, Wagoner JP, Kane OJ, Lohmann V, Polyak SJ. Relationships between hepatitis C virus replication and CXCL-8 production in vitro. J Virol 2006;80:7885-7893.
282. El-Bendary M, Neamatallah M, Elalfy H, Besheer T, El-Setouhy M, Youssef MM, Zein M, et al. Association of genetic polymorphisms of chemokines and their receptors

with clearance or persistence of hepatitis C virus infection. Br J Biomed Sci 2019;76:11-16.
283. Liu Y, Wang W, Zou Z, Fan Q, Hu Z, Feng Z, Zhu B, et al. Monocyte chemoattractant protein 1 released from macrophages induced by hepatitis C virus promotes monocytes migration. Virus Res 2017;240:190-196.
284. Groepper C, Rufinatscha K, Schroder N, Stindt S, Ehlting C, Albrecht U, Bock HH, et al. HCV modifies EGF signalling and upregulates production of CXCR2 ligands: Role in inflammation and antiviral immune response. J Hepatol 2018;69:594-602.
285. Commoner B, Lipkin D. The Application of the Beer-Lambert Law to Optically Anisotropic Systems. Science 1949;110:41-43.
286. Livak KJ, Schmittgen TD. Analysis of relative gene expression data using real-time quantitative PCR and the 2(-Delta Delta C(T)) Method. Methods 2001;25:402-408.
287. Pingoud A, Jeltsch A. Structure and function of type II restriction endonucleases. Nucleic Acids Res 2001;29:3705-3727.
288. SantaLucia J, Jr. A unified view of polymer, dumbbell, and oligonucleotide DNA nearest-neighbor thermodynamics. Proc Natl Acad Sci U S A 1998;95:1460-1465.
289. Owczarzy R, You Y, Moreira BG, Manthey JA, Huang L, Behlke MA, Walder JA. Effects of sodium ions on DNA duplex oligomers: improved predictions of melting temperatures. Biochemistry 2004;43:3537-3554.
290. Jinek M, Chylinski K, Fonfara I, Hauer M, Doudna JA, Charpentier E. A programmable dual-RNA-guided DNA endonuclease in adaptive bacterial immunity. Science 2012;337:816-821.
291. Kotagama OW, Jayasinghe CD, Abeysinghe T. Era of Genomic Medicine: A Narrative Review on CRISPR Technology as a Potential Therapeutic Tool for Human Diseases. Biomed Res Int 2019;2019:1369682.
292. Ebner M, Lucic I, Leonard TA, Yudushkin I. PI(3,4,5)P3 Engagement Restricts Akt Activity to Cellular Membranes. Mol Cell 2017;65:416-431 e416.
293. Dobner J, Simons IM, Rufinatscha K, Hansch S, Schwarten M, Weiergraber OH, Abdollahzadeh I, et al. Deficiency of GABARAP but not its Paralogs Causes Enhanced EGF-induced EGFR Degradation. Cells 2020;9.
294. Brinkman EK, Chen T, Amendola M, van Steensel B. Easy quantitative assessment of genome editing by sequence trace decomposition. Nucleic Acids Res 2014;42:e168.
295. Gade P, Kalvakolanu DV. Chromatin immunoprecipitation assay as a tool for analyzing transcription factor activity. Methods Mol Biol 2012;809:85-104.
296. Hierholzer JC, Killington RA: 2- Virus isolation and quantitation. In: Mahy BW, Kangro HO, eds. Virological Methods Manual. Elsevier, 1996; 25- 46.
297. Dreos R, Ambrosini G, Groux R, Cavin Perier R, Bucher P. The eukaryotic promoter database in its 30th year: focus on non-vertebrate organisms. Nucleic Acids Res 2017;45:D51-D55.
298. Pringle LM, Young R, Quick L, Riquelme DN, Oliveira AM, May MJ, Chou MM. Atypical mechanism of NF-kappaB activation by TRE17/ubiquitin-specific protease 6 (USP6) oncogene and its requirement in tumorigenesis. Oncogene 2012;31:3525-3535.
299. Han ZQ, Huang T, Deng YZ, Zhu GZ. Expression profile and kinetics of cytokines and chemokines in patients with chronic hepatitis C. Int J Clin Exp Med 2015;8:17995-18003.
300. Murphy PM. Neutrophil receptors for interleukin-8 and related CXC chemokines. Semin Hematol 1997;34:311-318.

301. Tai DI, Tsai SL, Chen TC, Lo SK, Chang YH, Liaw YF. Modulation of tumor necrosis factor receptors 1 and 2 in chronic hepatitis B and C: the differences and implications in pathogenesis. J Biomed Sci 2001;8:321-327.
302. Zhu N, Khoshnan A, Schneider R, Matsumoto M, Dennert G, Ware C, Lai MM. Hepatitis C virus core protein binds to the cytoplasmic domain of tumor necrosis factor (TNF) receptor 1 and enhances TNF-induced apoptosis. J Virol 1998;72:3691-3697.
303. Zhao LJ, Zhang XL, Zhao P, Cao J, Cao MM, Zhu SY, Liu HQ, et al. Up-regulation of ERK and p38 MAPK signaling pathways by hepatitis C virus E2 envelope protein in human T lymphoma cell line. J Leukoc Biol 2006;80:424-432.
304. He Y, Tan SL, Tareen SU, Vijaysri S, Langland JO, Jacobs BL, Katze MG. Regulation of mRNA translation and cellular signaling by hepatitis C virus nonstructural protein NS5A. J Virol 2001;75:5090-5098.
305. Street A, Macdonald A, Crowder K, Harris M. The Hepatitis C virus NS5A protein activates a phosphoinositide 3-kinase-dependent survival signaling cascade. J Biol Chem 2004;279:12232-12241.
306. Waris G, Siddiqui A. Hepatitis C virus stimulates the expression of cyclooxygenase-2 via oxidative stress: role of prostaglandin E2 in RNA replication. J Virol 2005;79:9725-9734.
307. Yoshida H, Kato N, Shiratori Y, Otsuka M, Maeda S, Kato J, Omata M. Hepatitis C virus core protein activates nuclear factor kappa B-dependent signaling through tumor necrosis factor receptor-associated factor. J Biol Chem 2001;276:16399-16405.
308. Joo M, Hahn YS, Kwon M, Sadikot RT, Blackwell TS, Christman JW. Hepatitis C virus core protein suppresses NF-kappaB activation and cyclooxygenase-2 expression by direct interaction with IkappaB kinase beta. J Virol 2005;79:7648-7657.
309. Wang PX, Zhang XJ, Luo P, Jiang X, Zhang P, Guo J, Zhao GN, et al. Hepatocyte TRAF3 promotes liver steatosis and systemic insulin resistance through targeting TAK1-dependent signalling. Nat Commun 2016;7:10592.
310. Hu J, Zhu XH, Zhang XJ, Wang PX, Zhang R, Zhang P, Zhao GN, et al. Targeting TRAF3 signaling protects against hepatic ischemia/reperfusions injury. J Hepatol 2016;64:146-159.
311. Zhou Z, Xu MJ, Gao B. Hepatocytes: a key cell type for innate immunity. Cell Mol Immunol 2016;13:301-315.
312. Van Damme J, Decock B, Lenaerts JP, Conings R, Bertini R, Mantovani A, Billiau A. Identification by sequence analysis of chemotactic factors for monocytes produced by normal and transformed cells stimulated with virus, double-stranded RNA or cytokine. Eur J Immunol 1989;19:2367-2373.
313. Wagoner J, Austin M, Green J, Imaizumi T, Casola A, Brasier A, Khabar KS, et al. Regulation of CXCL-8 (interleukin-8) induction by double-stranded RNA signaling pathways during hepatitis C virus infection. J Virol 2007;81:309-318.
314. Kang HB, Kim YE, Kwon HJ, Sok DE, Lee Y. Enhancement of NF-kappaB expression and activity upon differentiation of human embryonic stem cell line SNUhES3. Stem Cells Dev 2007;16:615-623.
315. Han KQ, Han H, He XQ, Wang L, Guo XD, Zhang XM, Chen J, et al. Chemokine CXCL1 may serve as a potential molecular target for hepatocellular carcinoma. Cancer Med 2016;5:2861-2871.
316. Nischalke HD, Berger C, Luda C, Muller T, Berg T, Coenen M, Kramer B, et al. The CXCL1 rs4074 A allele is associated with enhanced CXCL1 responses to TLR2 ligands and predisposes to cirrhosis in HCV genotype 1-infected Caucasian patients. J Hepatol 2012;56:758-764.
317. Ha J, Lee Y, Kim HH. CXCL2 mediates lipopolysaccharide-induced osteoclastogenesis in RANKL-primed precursors. Cytokine 2011;55:48-55.

318. Kulawik A, Engesser R, Ehlting C, Raue A, Albrecht U, Hahn B, Lehmann WD, et al. IL-1beta-induced and p38(MAPK)-dependent activation of the mitogen-activated protein kinase-activated protein kinase 2 (MK2) in hepatocytes: Signal transduction with robust and concentration-independent signal amplification. J Biol Chem 2017;292:6291-6302.
319. Ehlting C, Rex J, Albrecht U, Deenen R, Tiedje C, Kohrer K, Sawodny O, et al. Cooperative and distinct functions of MK2 and MK3 in the regulation of the macrophage transcriptional response to lipopolysaccharide. Sci Rep 2019;9:11021.
320. Bian ZM, Elner SG, Yoshida A, Kunkel SL, Su J, Elner VM. Activation of p38, ERK1/2 and NIK pathways is required for IL-1beta and TNF-alpha-induced chemokine expression in human retinal pigment epithelial cells. Exp Eye Res 2001;73:111-121.
321. Sasaki CY, Barberi TJ, Ghosh P, Longo DL. Phosphorylation of RelA/p65 on serine 536 defines an I{kappa}B{alpha}-independent NF-{kappa}B pathway. J Biol Chem 2005;280:34538-34547.
322. Ahmed AU, Sarvestani ST, Gantier MP, Williams BR, Hannigan GE. Integrin-linked kinase modulates lipopolysaccharide- and Helicobacter pylori-induced nuclear factor kappaB-activated tumor necrosis factor-alpha production via regulation of p65 serine 536 phosphorylation. J Biol Chem 2014;289:27776-27793.
323. Buss H, Dorrie A, Schmitz ML, Hoffmann E, Resch K, Kracht M. Constitutive and interleukin-1-inducible phosphorylation of p65 NF-{kappa}B at serine 536 is mediated by multiple protein kinases including I{kappa}B kinase (IKK)-{alpha}, IKK{beta}, IKK{epsilon}, TRAF family member-associated (TANK)-binding kinase 1 (TBK1), and an unknown kinase and couples p65 to TATA-binding protein-associated factor II31-mediated interleukin-8 transcription. J Biol Chem 2004;279:55633-55643.
324. Lawrence T, Bebien M, Liu GY, Nizet V, Karin M. IKKalpha limits macrophage NF-kappaB activation and contributes to the resolution of inflammation. Nature 2005;434:1138-1143.
325. Sakurai H, Chiba H, Miyoshi H, Sugita T, Toriumi W. IkappaB kinases phosphorylate NF-kappaB p65 subunit on serine 536 in the transactivation domain. J Biol Chem 1999;274:30353-30356.
326. Sizemore N, Lerner N, Dombrowski N, Sakurai H, Stark GR. Distinct roles of the Ikappa B kinase alpha and beta subunits in liberating nuclear factor kappa B (NF-kappa B) from Ikappa B and in phosphorylating the p65 subunit of NF-kappa B. J Biol Chem 2002;277:3863-3869.
327. Huber AR, Kunkel SL, Todd RF, 3rd, Weiss SJ. Regulation of transendothelial neutrophil migration by endogenous interleukin-8. Science 1991;254:99-102.
328. Hayden MS, Ghosh S. Regulation of NF-kappaB by TNF family cytokines. Semin Immunol 2014;26:253-266.
329. Christian F, Smith EL, Carmody RJ. The Regulation of NF-kappaB Subunits by Phosphorylation. Cells 2016;5.
330. Annibaldi A, Wicky John S, Vanden Berghe T, Swatek KN, Ruan J, Liccardi G, Bianchi K, et al. Ubiquitin-Mediated Regulation of RIPK1 Kinase Activity Independent of IKK and MK2. Mol Cell 2018;69:566-580 e565.
331. Liu Z, Tian Y, Machida K, Lai MM, Luo G, Foung SK, Ou JH. Transient activation of the PI3K-AKT pathway by hepatitis C virus to enhance viral entry. J Biol Chem 2012;287:41922-41930.
332. Chen SJ. Minimizing off-target effects in CRISPR-Cas9 genome editing. Cell Biol Toxicol 2019;35:399-401.
333. Mao Z, Bozzella M, Seluanov A, Gorbunova V. Comparison of nonhomologous end joining and homologous recombination in human cells. DNA Repair (Amst) 2008;7:1765-1771.

334. Shi Q, Hoffman B, Liu Q. PI3K-Akt signaling pathway upregulates hepatitis C virus RNA translation through the activation of SREBPs. Virology 2016;490:99-108.

Danksagung

Für die große Hilfe, welche mir während meiner Doktorarbeit zuteil wurde, möchte ich mich in diesem kurzen Schreiben bedanken.

Ich möchte mich besonders herzlich bei meinem Erstbetreuer, Herrn Prof. Dr. Johannes G. Bode bedanken, welcher es mir ermöglicht hat an diesem spannenden Forschungsprojekt arbeiten zu können. Ich möchte mich für seine Geduld, seine große Hilfe, seine Zeit und sein stets offenes Ohr für mich bedanken. Die Zusammenarbeit hat mir stets viel Freude bereitet und ich konnte in der Zeit meiner Doktorarbeit sehr viel Neues lernen.

Weiters möchte ich mich bei meinem Zweitbetreuer Herrn Prof. Dr. Dieter Willbold für die unkomplizierte Zusammenarbeit und die Mitbetreuung meiner Doktorarbeit bedanken.

Zudem möchte ich mich bei Herrn Prof. Dr. Dieter Häussinger und bei Herrn Prof. Dr. Tom Luedde für die Möglichkeit bedanken, die experimentellen Arbeiten in der Klinik für Gastroenterologie, Hepatologie und Infektiologie durchführen zu können.

Zudem möchte ich mich bei Frau Dr. Sabine Stindt für ihre große Hilfe bedanken, auch sie war stets für mich da und ist mir, auch während ihrer Elternzeit, immer zur Seite gestanden. Ich bin ihr überaus dankbar für ihre konstruktive Kritik und für die freundschaftliche Zusammenarbeit.

Anschließend bedanke ich mich bei der AG Bode, mein besonderer Dank gilt hierbei Herrn Dr. Christian Ehlting, Frau Dr. Stefanie Wolf, Frau Marijana Suzanji und Frau Theresa Ohly, welche mir immer wenn ich Fragen hatte geholfen, mich in die Gruppe aufgenommen, mir alles im Labor gezeigt haben und von welchen ich auch sehr viel lernen konnte. Den Mitarbeitern der experimentellen Hepatologie möchte ich für ihre Bereitschaft mir zu helfen und für die schöne Zeit im Labor danken.

Der Manchot Graduiertenschule (Molecules of Infection III (MOI III)) möchte ich für die Ermöglichung dieser Doktorarbeit durch finanzielle Mittel danken, aber auch für die spannenden Veranstaltungen, welche beruflich, sowie persönlich immer viel Spaß gemacht haben und auf welche ich mich immer gefreut habe.

Ein besonders riesiges Dankeschön möchte ich an meinen Mann Jochen Dobner richten, welcher im wahrsten Sinne des Wortes immer an meiner Seite war, da er selbst Stipendiat der MOI III war. Durch ihn machte mir meine Zeit als Doktorandin noch mehr Spaß. Zudem war er mir persönlich, als auch wissenschaftlich immer eine große Stütze und Hilfe.

Abschließend bedanke ich mich bei meiner Familie. Danke für eure Unterstützung, den Halt, den ihr mir gebt und den Glauben, welchen ihr in mich habt.

Ohne das Mitwirken all dieser Menschen wäre diese Arbeit niemals zustande gekommen.

Eidesstattliche Erklärung

Ich, Frau Kerstin Hermine Rufinatscha, versichere an Eides Statt, dass die vorliegende Dissertation von mir selbständig und ohne unzulässige fremde Hilfe unter Beachtung der „Grundsätze zur Sicherung guter wissenschaftlicher Praxis an der Heinrich-Heine-Universität Düsseldorf" erstellt worden ist.

Düsseldorf, der 14. Januar 2021 _____

Unterschrift